Lecture Notes: Fundamentals of Nonlinear Physics

Victor S. L'vov

The Weizmann Institute of Science, Israel, Rehovot 2014

The lecture course presents in a systematic manner the basic physical ideas in nonlinear dynamics of continuous media in plasma, gases, fluids and solid states, considered from a common background. This approach allows one to reach two goals. First, to clarify the common features of nonlinear phenomena in various areas of physics: in nonlinear wave physics (in plasma, optical crystals and fibers, on a water surface and the atmosphere, etc.), in nonlinear phase transitions (flame propagation and crystal growth), in physics of turbulence. Second: to develop a reasonably simple description of basic nonlinear phenomena, that contains from the very beginning only their essentials, and can serve as a starting point on understanding of the rich nonlinearity of the surrounding world.

Contents

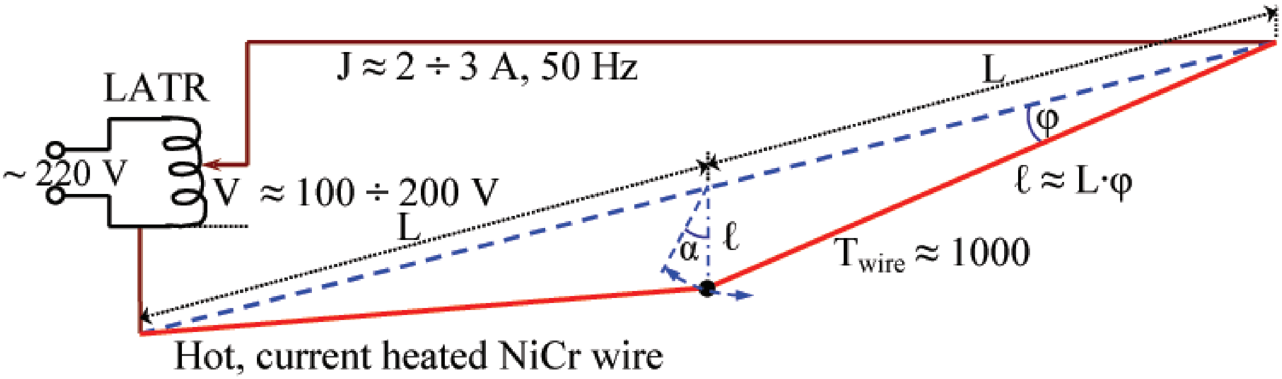

Fig.1.1. Hot-wire quasi-harmonic pendulum

Introductory Lecture 1

Hot-wire quasi-harmonic pendulum & nonlinear phenomena

Questions to answer:

- What is the physical mechanism of this phenomenon (non-decaying oscillations)?
- How to estimate (compute) frequency and amplitude of the oscillations?
- How to estimate transient times (of the amplitude growth and decaying)?
- Why one cannot use, say a copper wire instead of the NiCr wire?
- Why the wire should be so long?, etc.

Basic model: Harmonic oscillator

$$M\ell\,\frac{d^2\alpha}{dt^2} = -M\,g\,\alpha - \left(k\ + k_{\rm NL}\right)\frac{d\alpha}{dt}\ . \tag{1.1a}$$

Neglecting $\quad k_{\rm NL} \quad \Rightarrow \quad \left(\frac{d^2}{dt^2} + 2\gamma\,\frac{d}{dt} + \omega_0^2\right)\alpha \approx 0\,,\quad$ where $\quad$ (1.1b)

$$\omega_0 = \sqrt{\frac{g}{\ell}}\ ,\quad \gamma = \frac{k}{2\,M\,\ell}\ . \tag{1.1c}$$

Solution of this beauty:

$$\alpha(t) = [a\exp(-i\omega t) + \text{c.c.}]\,,\quad \text{with} \tag{1.2a}$$

$$\omega^2 + 2i\gamma\omega - \omega_0^2 = 0\,,\qquad \Rightarrow \tag{1.2b}$$

$$\omega = -i\gamma \pm \omega_1\,,\quad \omega_1 = \sqrt{\omega_0^2 + \gamma^2} \approx \omega_0\,,\Rightarrow \tag{1.2c}$$

$$\alpha(t) \propto \exp(-\gamma\ t)\sin(\omega_1 t + \psi) \tag{1.2d}$$

Hereafter $\psi = 0$. γ – damping decrement, $1/\gamma$ – decay time.

Instability mechanism: parametric excitation

Air cooling for very thin wire $\propto \ell d\alpha/dt$ has maximum at $\alpha = 0$, giving periodic temperature dependence with frequency $2\omega_1$. Due to the thermal expansion:

$$\ell \Rightarrow \ell[1 - \varepsilon\cos(2\,\omega_1 t)]\ . \tag{1.3}$$

With Eq. (1.3) for small $\quad \delta \equiv 4\omega_0\varepsilon \ll \omega_0 \quad$ Equation 1.1b $\Rightarrow$

$$\left\{\frac{d^2}{dt^2} + 2\gamma\,\frac{d}{dt} + \omega_0^2 + 2\delta\omega_0\,[\exp(2i\omega_1 t) + \exp(-2i\omega_1 t)]\right\}\alpha = 0\ . \tag{1.4a}$$

Let $\quad \alpha(t) = [b\exp(i\omega_1 + \nu)t] + b^\dagger\exp(-i\omega_1 + \nu)t] + \text{c.c.} \quad$ (1.4b)

$$\Rightarrow \quad i(\nu + \gamma)b + \delta b^\dagger = 0\,,\quad \delta b - i(\nu + \gamma)b^\dagger = 0$$

$$\Rightarrow \qquad \nu = -\gamma \pm \delta\ . \tag{1.4c}$$

If $\delta > \gamma$ this gives parametric instability with the instability increment $\nu > 0$:

$$\alpha(t) \propto \exp(\nu t)\sin(\omega_0 t)\ . \tag{1.4d}$$

- More about excitation conditions of the hot-wire pendulum:

The length $\ell(T_0 + T') = \ell_0\,(1 + \beta T')$ with the thermal expansion parameter $\beta = d\ln\ell/dT$. The heat balance (C – heat capacity, $v(t)$ -the wire velocity)

$$C\,\frac{dT'(t)}{dt} \propto |v(t)| \approx \ell_0\left|\frac{d\alpha(t)}{dt}\right| \approx \ell_0\alpha_0|\cos(\omega_0 t)| \Rightarrow \ell_0\alpha_0\cos(2\omega_0 t)\ .$$

Thus $\varepsilon \propto \ell_0\,\alpha_0 \Rightarrow \delta \propto \alpha_0$, the pendulum amplitude.
This gives "hard excitation" from the final amplitude α_0.

- Something about stationary state of the hot-wire pendulum:

$k_{\rm NL}$ in Equation 1.1a originates from the force F of turbulent friction of the heavy mass (of diameter D) with air, that can depend on the diameter D, velocity v and the air density ρ: $F \sim D^x v^y \rho^z$. To find $x,\ y,\ z$ consider dimensions

$$[F] = \text{g}\cdot\text{cm}\cdot\text{s}^{-2}\,,\ [D] = \text{cm}\,,\ [v] = \text{cm}\cdot\text{s}^{-1}\,,\ [\rho] = \text{g}\cdot\text{cm}^{-3}\ . \qquad (1.5\text{a})$$

One finds $F \simeq \rho D^2 v^2 \quad\Rightarrow\quad \gamma_{\rm NL} \simeq \rho D^2 \ell\left\langle\frac{d\alpha}{dt}\right\rangle \propto \alpha_0$ balancing δ (1.5b)

- Some nonlinear phenomena, related with the hot-wire oscillator:

- Parametric excitation of waves, nonlinear-wave interactions,..
- Turbulent cooling (of everything: chips in computers, car engines, etc.)
- Turbulent frictions (of cars, aircrafts, ships, etc.)
- Current resistance. Basic mechanisms:
  1. Emission and absorbtion of phonos by conduction electrons. Gives small resistance at $T \to 0$ and $R \propto T$ for large T. Effective in any metal (and semiconductors), except of superconductors.
  2. Electron scattering on static inhomogeneities. Dominates in alloys, like NiCr.
- Thermal expansion of solids (alloys and crystals).

Exercises

Exercise 1.1 Estimate dimensionless ε, its dependence on φ (see Fig. on page 6). Explain, why the hot wire should be so long?

Exercise 1.2 To find the stationary amplitude $\alpha_{\rm st}$ accounting for the next terms in expansions sinα and cosα. subsection 1.3

Lecture 2

Introduction to Classical Hamiltonian Approach

Outline

2.1 Examples of non-linear waves, their frequencies and equations of motion

2.2 Hamiltonian equations of motion for n -degrees of freedom

2.3 Generalization for continuous media.

2.4 Transformation to complex variables

2.5 Canonical transformations

2.6 Exercise

Examples of non-linear waves and equations of motion

Dispersive waves play a crucial role in a vast range of physical applications, from quantum to classical regions, from microscopic to astrophysical scales.
For example:

• Sea waves are important for the momentum and energy transfers from wind to ocean, as well as for navigation conditions;

• Internal waves on density stratifications and inertial waves due to rotation are important in turbulence behavior and mixing in planetary atmospheres and oceans;

• Planetary Rossby waves are important for the weather and climate evolutions;

• Alfven waves are ubiquitous in turbulence of solar wind and interstellar medium;

• Sound waves in plasmas, fluids and solids;

• Electromagnetic waves: microwaves, IR, light, UV, X-rays;

• Spin waves in magnetically ordered solids;

• Kelvin waves propagating on quantized vortex lines provide an essential mechanism of turbulent energy cascades in quantum turbulence in cryogenic Helium;

etc., etc., etc.

Estimates of the dispersion laws (frequency of waves) $\omega(k)$

Wave amplitude: $\eta(\boldsymbol{r}, t) \propto \exp[i\boldsymbol{k} \cdot \boldsymbol{r} - i\omega(k)\, t]\,, \qquad \omega(\boldsymbol{k}) \equiv \omega_k -?$

- Waves on a deep water

– Long gravity waves. Relevant physical parameter – the gravity acceleration g (no fluid density: inertial and gravity masses are the same)

Dimensional reasoning: $[\omega] =$s^{-1}, $\omega(k) = g^x\, k^y$, $[g] =$cm s^{-2}, $[k] =$cm^{-1}.

$$\omega_k = \sqrt{g\, k}\ . \tag{2.1a}$$

Notice that Equation 2.1a is exact.

– Short capillary waves. Relevant parameters: Surface tension (surface energy per unite area): $[\sigma]$ =g s^{-2} and fluid density $[\rho]$ =g cm^{-3}. The only combination is:

$$\omega_k = \sqrt{\frac{\sigma\, k^3}{\rho}}\ . \tag{2.1b}$$

Equation 2.1b is also exact.

– Waves on deep water – General case. In the crossover region ($\rho g \sim \sigma k^2$) dimensional reasoning fails. To find frequency consider

Energy balance: (mean) kinetic energy density (per unite area of the water surface) $E_{\rm K}$ = potential $E_{\rm P}$+ surface $E_{\rm S}$ energies. Accounting that wave motions (with wave amplitude on the surface η_k decay with depth as $\exp(-kz)$ and on the surface the fluid velocity $v = d\eta_k/dt \simeq \omega_k\eta_k$ one gets

$$E_{\rm K} \simeq \frac{\rho}{2\,k}(\eta_k\omega_k)^2\,,\ \ E_{\rm P} \simeq \rho\, g \int_k^\eta z\,\overline{\cos(k\,x)}dz = \frac{\rho}{2}\,g\,\eta_k^2\,,$$

$$E_{\rm S} \simeq \sigma\,\overline{\left(\frac{d\eta_k}{dx}\right)^2} = \frac{\sigma\,(k\eta_k)^2}{2} \ \Rightarrow\ \omega_k = \sqrt{g\,k + \frac{\sigma\,k^3}{\rho}}\ . \tag{2.1c}$$

Equation 2.1c is also exact.

- Waves on a shallow water involves additional parameter, the water depth h. This gives dimensionless parameter $k\,h \ll 1$ and dimensional reasoning fails.

However the energy-balance approach works: Potential and surface energy are h-independent. To find kinetic energy one accounts that continuity equation for water mass requires: horizontal water velocity $v_= \simeq v_\perp/(kh) \gg v_\perp = \eta_k\omega_k$. However, the wave "depth" is not the wave length $2\pi/k$ but only h. These give:

$$E_{\rm K} \simeq \frac{\rho h}{2}\left(\frac{\eta\,\omega_k}{h\,k}\right)^2\,,\ \text{giving}\ \ \omega_k = k\sqrt{h\left(g + \frac{\sigma\,k^2}{\rho}\right)}\ . \tag{2.1d}$$

Equation 2.1d is exact. Together with Equation 2.1d it explain, why near a coast line a wave front is almost parallel to it [independent to its orientation in open sea] and wave amplitude (e.g. near Ceasaria) usually mach larger, then in the open Sea (e.g. near Haifa)

- Acoustic waves (Sound) in solids, fluids and gases:

$$\rho_1\,, v \propto \exp[i\boldsymbol{k}\cdot\boldsymbol{r} - i\omega_k\, t]\ .$$

Relevant parameters:
(adiabatic) compressibility $\beta \equiv \partial\rho/\partial p$, p – pressure and material density ρ

Dimensional analysis: $[\beta] = [\rho/p] =$s^{2}cm^{-2}. Denoting $c_{\rm s} \equiv 1/\sqrt{\beta}$ one has

$$\omega_k = c_{\rm s} k\ . \tag{2.2}$$

- Waves on fluid surface and in stratified fluids: $\Rightarrow$ The Navier-Stokes equations
  Gravity and capillary waves on a deep or shallow water,
  Rossby waves in rotation Atmosphere $\Rightarrow$ Cyclones and Anticyclones
  Intrinsic waves in the Ocean $\Rightarrow$ Long-distance energy trahsfer
- Acoustic waves, Sound: $\Rightarrow$ Material equations
  Acoustic waves in glasses (disordered media), fluids and plasmas
  Optic & Acoustic waves in Crystals
- Electromagnetic waves: $\Rightarrow$ The Maxwell + Material equations
  Radio-frequency & Microwaves, Light, X-rays, etc. in dielectrics,
  Numerous wave types in non-isothermal magnetized plasma
- Spin waves in Magnetics: $\Rightarrow$ The Bloch & Landau-Lifshitz equations

All these equations of motion can be presented in a canonical form as

the Hamiltonian equations of motion

Hamiltonian equations of motion for n -degrees of freedom

- Hamiltonian equations (one degree of freedom)

$$\frac{dq}{dt} = \frac{\partial \mathcal{H}}{\partial p}, \qquad \frac{dp}{dt} = -\frac{\partial \mathcal{H}}{\partial q} \,. \tag{2.3}$$

$\mathcal{H}$ – Hamiltonian function or Hamiltonian ,

$q,\ p$ – Canonical variables: generalized coordinate and momentum.

Simple example: $\mathcal{H} = p^2/2m + U(q) \qquad \Rightarrow$

$$\frac{dq}{dt} = \frac{p}{m}, \qquad \frac{dp}{dt} = -\frac{dU}{dq} \quad \Rightarrow \quad \frac{d^2q}{dt^2} = -\frac{dU}{dq}, \qquad \text{Newtonian equation.}$$

- Hamiltonian equations (n degrees of freedom)

for $q_1, q_2, ...q_n$ and $p_1, p_2, ...p_n$:

$$\frac{dq_i}{dt} = \frac{\partial \mathcal{H}}{\partial p_i}, \quad \frac{dp_i}{dt} = -\frac{\partial \mathcal{H}}{\partial q_i} \,. \tag{2.4}$$

Example 2A: periodical chain of atoms – one dimensional harmonic crystal

$$m - m - m - m \ldots \quad \mathcal{H} = \sum_{j=1}^{n} \left[\frac{p_j^2}{2m} + \frac{\kappa}{2} \left(q_j - q_{j+1} \right)^2 \right] . \tag{2.5}$$

Example 2B: periodical chain of atoms: two atoms in the elementary cell

$$M - m - M - m \quad \mathcal{H} = ? \tag{2.6}$$

Generalization for continuous media

For $q(\boldsymbol{r}, t)$ and $p(\boldsymbol{r}, t)$ at each point $\boldsymbol{r}$:

$$\frac{\partial q(\boldsymbol{r}, t)}{\partial t} = \frac{\delta \mathcal{H}}{\delta p(\boldsymbol{r}, t)}, \quad \frac{\partial p(\boldsymbol{r}, t)}{\partial t} = -\frac{\delta \mathcal{H}}{\delta q(\boldsymbol{r}, t)}, \tag{2.7}$$

– The Hamiltonian $\mathcal{H}$ is a functional of $q(\boldsymbol{r}, t)$, $p(\boldsymbol{r}, t)$, – $\delta/\delta p$ and $\delta/\delta q$ are variational derivatives (generalization of partial derivatives). For more details about variational derivatives see here.

For sound Hamiltonian $$\mathcal{H} = \int \frac{d^3r}{2}\left[\frac{p^2(t,r)}{\rho} + \rho C_\mathrm{s}^2 |\nabla q(t,r)|^2\right] \quad (2.8)$$

Eqs. of motion is $$\partial^2 q(\boldsymbol{r},t)/\partial t^2 = C_\mathrm{s}^2 \Delta q(\boldsymbol{r},t)\ . \quad (2.9)$$

For several type of waves (or polarizations), $j = 1, 2,\ ..n$:

$$\frac{\partial q_j(\boldsymbol{r},t)}{\partial t} = \frac{\delta \mathcal{H}}{\delta p_j(\boldsymbol{r},t)}\,, \quad \frac{\partial p_j(\boldsymbol{r},t)}{\partial t} = -\frac{\delta \mathcal{H}}{\delta q_j(\boldsymbol{r},t)}\ . \quad (2.10)$$

Transformation to complex variables

- Step 1: $Q(\boldsymbol{r}) = \lambda q(\boldsymbol{r})\,,\ P(\boldsymbol{r}) = p(\boldsymbol{r})/\lambda$ (2.11a)

such that P and Q have the same dimension. This is canonical transformation, because:

$$\frac{\partial q(\boldsymbol{r},t)}{\partial t} = \frac{\delta \mathcal{H}}{\delta p(\boldsymbol{r},t)} \Rightarrow \frac{\partial \lambda q(\boldsymbol{r},t)}{\partial t} = \frac{\lambda \delta \mathcal{H}}{\delta p(\boldsymbol{r},t)} \Rightarrow \frac{\partial Q(\boldsymbol{r},t)}{\partial t} = \frac{\delta \mathcal{H}}{\delta P(\boldsymbol{r},t)} \quad (2.11b)$$

$$\frac{\partial p}{\partial t} = -\frac{\delta \mathcal{H}}{\delta q} \Rightarrow \frac{\partial p}{\lambda \partial t} = -\frac{\delta \mathcal{H}}{\delta \lambda q} \Rightarrow \frac{\partial P}{\partial t} = -\frac{\delta \mathcal{H}}{\delta Q}\ . \quad (2.11c)$$

For example, for a harmonic oscillator $\left(\text{with } \lambda^4 \equiv \kappa m \text{ and } \omega \equiv \frac{\lambda^2}{m} = \sqrt{\frac{\kappa}{m}}\right)$:

$$\mathcal{H} = \frac{p^2}{2m} + \frac{\kappa q^2}{2} = \frac{1}{2m}[p^2 + \lambda^4 q^2] = \frac{\lambda^2}{2m}\left[\frac{p^2}{\lambda^2} + \lambda^2 q^2\right] = \frac{\omega}{2}\left[P^2 + Q^2\right]\ . \quad (2.11d)$$

- Step 2: $a_j = (Q_j + iP_j)/\sqrt{2}\,,\quad a_j^* = (Q_j - iP_j)/\sqrt{2}$ (2.12a)

with the equation of motion

$$\sqrt{2}\frac{\partial a_j}{\partial t} = \frac{\delta \mathcal{H}}{\delta P_j} - i\frac{\delta \mathcal{H}}{\delta Q_j}\,, \quad \sqrt{2}\frac{\partial a_j^*}{\partial t} = \frac{\delta \mathcal{H}}{\delta p_j} + i\frac{\delta \mathcal{H}}{\delta Q_j}\ . \quad (2.12b)$$

- Step 3: Substituting $\mathcal{H}(a, a^*)$ $\Rightarrow$ the canonical form of Hamiltonian eq.:

$$\frac{\partial a_j(\boldsymbol{r},t)}{\partial t} = -i\,\frac{\delta \mathcal{H}}{\delta a_j^*(\boldsymbol{r},t)}\,, \quad \frac{\partial a_j^*(\boldsymbol{r},t)}{\partial t} = i\,\frac{\delta \mathcal{H}}{\delta a_j(\boldsymbol{r},t)}\ . \quad (2.12c)$$

For example, for the harmonic oscillator the Hamiltonian takes very simple form:

$$\mathcal{H} = \frac{\omega}{2}\left[P^2 + Q^2\right] = \omega\, aa^* \,, \quad \text{(compare with Eq. (2.11d))}\,, \tag{2.14a}$$

and equation of motion became trivial:

$$\frac{da}{dt} = -i\omega a\,, \quad \Rightarrow \quad a(t) \propto \exp(-i\omega t)\ . \tag{2.14b}$$

Canonical variables $a_j(\boldsymbol{r},t)$ & $a_j(\boldsymbol{r},t)$ are classical analog of the Bose operators of creation and annihilation in quantum mechanics.

General canonical transformations

$$\text{Let } \Big[a_i(\boldsymbol{r},t), a_i^*(\boldsymbol{r},t)\Big] \Rightarrow \Big[b_j(\boldsymbol{r},t), b_j^*(\boldsymbol{r},t)\Big]\,, \quad i,j = 1,2,...N \tag{2.15a}$$

in which b_j & b_j^* are some functionals of a_i & a_i^* (for more details, see Appendix-Lect1-2.

$$b_j(\boldsymbol{r},t) = F\{a_i(\boldsymbol{r},t), a_i^*(\boldsymbol{r},t)\}\,, \quad b_j^*(\boldsymbol{r},t) = F^*\{a_i(\boldsymbol{r},t), a_i^*(\boldsymbol{r},t)\}\ .$$

$$\text{Compute } \frac{\partial b_j}{\partial t} \text{ and require } \frac{\partial b_j(\boldsymbol{r},t)}{\partial t} = -i\,\frac{\delta \mathcal{H}}{\delta b_j^*(\boldsymbol{r},t)}\ . \tag{2.15b}$$

This gives the condition of canonicity, expressed through the Poisson brackets:

$$\{f_i(q), g_j(q')\} = \sum_\ell \int d\boldsymbol{r}'' \left[\frac{\delta f_i(q)}{\delta a_\ell^*(\boldsymbol{r}'')}\frac{\delta g_j(q')}{\delta a_\ell(\boldsymbol{r}'')} - \frac{\delta f_i(q)}{\delta a_\ell(\boldsymbol{r}'')}\frac{\delta g_j(q')}{\delta a_\ell^*(\boldsymbol{r}'')}\right], \tag{2.15c}$$

$$\{b_i(q), b_j(q')\} = 0, \quad \{b(q)_i, b_j^*(q')\} = \delta_{ij}\delta(q - q')\ . \tag{2.15d}$$

In Eq. (2.15c) q runs through a "complete set" of values, e.g., $q = \boldsymbol{r}$ or $q = \boldsymbol{k}$ Eq. (2.15d) – classical analog of the commutation relations for the Bose operators

Exercises

Exercise 2.1 To find for $\mathcal{H}$ of Eq. (2.5) equations of motion and to solve them

Exercise 2.2 To find $\mathcal{H}$ for the model two atoms in the elementary cell, Eq. (2.6), to write equations of motion and to solve. Hint: Use periodical boundary conditions ($p_j = p_{N+j}$) and the Fourier transform.

Exercise 2.3 For sound Hamiltonian, Equation 2.8, derive Equation of motion. Answer: Equation 2.9

Exercise 2.4 To find condition of canonicity for the Fourier transform and for the linear (Bogolubov) $(u\text{-}v)$ transformation: $b = u \cdot a + v \cdot a^*$.

Lecture 3

Hamiltonian structure under small nonlinearity.

Outline

Hamiltonian expansion

Step 1. Let $a\,, a^* = 0$ in the absence of a wave. Assume that $a\,, a^*$ are $small$ in the required sense, for instance, when the elevation of the surface-water waves is smaller then the wavelength.

Step 2. For small $a\,, a^*$ the Hamiltonian $\mathcal{H}$ can be expanded over a, a^*:

$$\mathcal{H} = \mathcal{H}_2 + \mathcal{H}_{\rm int}\,, \quad \mathcal{H}_{\rm int} = \mathcal{H}_3 + \mathcal{H}_4 + \mathcal{H}_5 + \mathcal{H}_6 + \ \dots\,, \tag{3.1}$$

where $\mathcal{H}_j$ is a term proportional to product of j amplitudes a_k and the interaction Hamiltonian $\mathcal{H}_{\rm int}$ describes the wave coupling, as explained below. We omitted here the independent of a_k and a_k^* Hamiltonian of the system at the rest, $\mathcal{H}_0$, because it does not contribute to the motion equation. In the Lectures we consider only waves, exited in the thermodynamically-equilibrium systems, for which $\mathcal{H}$ is minimal at the rest, when $a_k = a_k^* = 0$. Then linear Hamiltonian, $\mathcal{H}_1 = 0$.

Canonical form of free-wave Hamiltonian $\mathcal{H}_2$

$$\mathcal{H}_2 = \sum_{i,j=1}^{n} \int \{A_{ij}(\boldsymbol{r},\boldsymbol{r}')a_i(\boldsymbol{r},t)a_j^*(\boldsymbol{r}',t) \tag{3.2a}$$

$$+\frac{1}{2}[B_{ij}(\boldsymbol{r},\boldsymbol{r}')a_i(\boldsymbol{r},t)a_j(\boldsymbol{r}',t) + \text{c.c}]\}d\boldsymbol{r}d\boldsymbol{r}'\,. \tag{3.2b}$$

"c.c" = complex conjugate.

Consider properties of expansion coefficients of $\mathcal{H}_2$, that follows from:

$\mathcal{H}_2$ is real $\Rightarrow$: $A_{ij}(\boldsymbol{r},\boldsymbol{r}') = A_{ji}^*(\boldsymbol{r}',\boldsymbol{r})$, no restriction on B_{ij};

Hint: Complex conjugate Eq. (3.2a) and relabel $\boldsymbol{r} \leftrightarrow \boldsymbol{r}'$ and $i \leftrightarrow j$. Eq. (3.2b) is real automatically.

Spatial homogeneity $\Rightarrow$ $A_{ij}(\boldsymbol{r},\boldsymbol{r}') = A_{ij}(\boldsymbol{r}-\boldsymbol{r}')\,,\ B_{ij}(\boldsymbol{r},\boldsymbol{r}') = B_{ij}(\boldsymbol{r}-\boldsymbol{r}')$

Inversion symmetry $\Rightarrow$ $\boldsymbol{R} \equiv \boldsymbol{r} - \boldsymbol{r}'$, $A_{ij}(\boldsymbol{R}) = A_{ij}(-\boldsymbol{R})$, $B_{ij}(\boldsymbol{R}) = B_{ij}(-\boldsymbol{R})$

.

$$\mathcal{H}_2 = \sum_{i,j=1}^{n} \int \{A_{ij}(\boldsymbol{R}) a_i(\boldsymbol{r}+\boldsymbol{R},t) a_j^*(\boldsymbol{r},t) \tag{3.3a}$$

$$+\frac{1}{2}\left[B_{ij}^*(\boldsymbol{R}) a_i(\boldsymbol{r}+\boldsymbol{R},t) a_j(\boldsymbol{r},t) + \text{c.c.}\right]\} \, d\boldsymbol{R} d\boldsymbol{r} \ .$$

Step 3. Fourier representation. Define $a(\boldsymbol{k},t) \equiv a_k$ by

$$a_{\boldsymbol{k}} = \frac{1}{V}\int a(\boldsymbol{r},t)\exp(-i\boldsymbol{k}\cdot\boldsymbol{r})\, d\boldsymbol{r} \ , \ a(\boldsymbol{r},t) = \sum_{\boldsymbol{k}} a_{\boldsymbol{k}} \exp(i\boldsymbol{k}\cdot\boldsymbol{r}) \ . \tag{3.4}$$

Hint: $$(2\pi)^d \sum_{\boldsymbol{k}} = V \int d^d k \ .$$

One can show that Eq. (3.4) is canonical, but not unimodal transformation:

$$\frac{\partial a_{\boldsymbol{k}}}{\partial t} = -i\frac{\partial \mathcal{H}(a_{\boldsymbol{k}}, a_{\boldsymbol{k}}^*)}{\partial a_{\boldsymbol{k}}^*}, \quad \mathcal{H}(a_{\boldsymbol{k}}, a_{\boldsymbol{k}}^*) = \mathcal{H}\{a_{\boldsymbol{r}}, a_{\boldsymbol{r}}^*\}/V \ . \tag{3.5}$$

Advantage: because of the spatial homogeneity $\mathcal{H}_2$ is diagonal in $\boldsymbol{k}$, Eq. (3.3a)

$$\Rightarrow \quad \mathcal{H}_2 = \sum_{\boldsymbol{k}} \left\{ A_{\boldsymbol{k}} a_{\boldsymbol{k}} a_{\boldsymbol{k}}^* + \frac{1}{2}[B_{\boldsymbol{k}}^* a_{\boldsymbol{k}} a_{-\boldsymbol{k}} + \text{ c.c.}] \right\} \ , \tag{3.6a}$$

$$A_{\boldsymbol{k}} = \int A(\boldsymbol{R})\exp(i\boldsymbol{k}\cdot\boldsymbol{R})\, d\boldsymbol{R}, \ B_{\boldsymbol{k}} = \int B(\boldsymbol{R})\exp(i\boldsymbol{k}\cdot\boldsymbol{R})\, d\boldsymbol{R} \ .$$

Step 4. Bogolubov u-v diagonalization.

Consider general form $\mathcal{H}_2$ for n types of waves (or wave polarizations):

$$\mathcal{H}_2 = \sum_{ij}^{n} \sum_{\boldsymbol{k}} \left\{ A_{ij}(\boldsymbol{k}) a_i(\boldsymbol{k}) a_j^*(\boldsymbol{k}) + \frac{1}{2}[B_{ij}(\boldsymbol{k}) a_i(\boldsymbol{k}) a_j(-\boldsymbol{k}) + \text{ c.c.}] \right\} . \tag{3.6b}$$

Canonical motion equations

$$\frac{\partial a_i(\boldsymbol{k},t)}{\partial t} = -i\frac{\partial \mathcal{H}(\{a_j, a_j^*\})}{\partial a_i^*(\boldsymbol{k},t)}, \tag{3.7a}$$

with the Hamiltonian, given by Eq. (3.6b), takes the form:

$$i\,\frac{\partial a_i(\boldsymbol{k},t)}{\partial t}=\sum_j^n\left[A_{ij}a_j(\boldsymbol{k},t)+B_{ij}a_j^*(-\boldsymbol{k},t)\right]\ . \tag{3.7b}$$

Eq. (3.7b) becomes algebraic with $a_j(\boldsymbol{k},t),\ a_j^*(-\boldsymbol{k},t)\propto\exp(-i\omega t)$ and have $2n$ non-zero solutions with the $\omega=\pm\omega_j$, that are the roots of:

$$\begin{vmatrix} A_{ij}(\boldsymbol{k})-\omega\delta_{ij}\,, & B_{ij}(\boldsymbol{k}) \\ B_{ij}^*(\boldsymbol{k})\,, & A_{ij}(\boldsymbol{k})+\omega\delta_{ij}\end{vmatrix}=0\ . \tag{3.8}$$

Consider linear canonical transformation (called Bogolubov $\boldsymbol{u}$-$\boldsymbol{v}$ transformation)

$$a_i(\boldsymbol{k},t)=\sum_j^n\left[u_{ij}(k)\,b_j(\boldsymbol{k},t)+v_{ij}(\boldsymbol{k})\,b_j^*(-k,t)\right] \tag{3.9}$$

for which $\mathcal{H}_2(\boldsymbol{b},\boldsymbol{b}^*)$ takes the canonical diagonal form

$$\mathcal{H}_2=\sum_i\int d\boldsymbol{k}\,\omega_i(\boldsymbol{k})b_i(\boldsymbol{k})b_i^*(\boldsymbol{k})\ \Rightarrow\ \dot{b}_i(\boldsymbol{k},t)=-i\omega_i(\boldsymbol{k})b_i(\boldsymbol{k},t)\ . \tag{3.10}$$

$b_i(\boldsymbol{k},t)$ are normal canonical variables.

All physics of non-interacting waves is determined by $\mathcal{H}_2$ and therefore waves in different media differ ONLY in the type of dispersion law $\omega(\boldsymbol{k})$.

ALL information about wave interaction is contained in coefficients of $\mathcal{H}_{\rm int}$

One shows that canonicity condition for the Bogolubov u-v transform, (3.9), (for $n=1$) is

$$u^2(k)-|v(\boldsymbol{k})|^2=1\ . \tag{3.11}$$

For this case:

$$\omega_{\boldsymbol{k}}=\mathrm{sign}\{A_{\boldsymbol{k}}\}\sqrt{A_{\boldsymbol{k}}^2-|B_{\boldsymbol{k}}|^2}\,, \tag{3.12}$$
$$u_{\boldsymbol{k}}=\sqrt{\frac{A_{\boldsymbol{k}}+\omega_{\boldsymbol{k}}}{2\omega_{\boldsymbol{k}}}}\,,\quad v_{\boldsymbol{k}}=-\frac{B_{\boldsymbol{k}}}{|B_{\boldsymbol{k}}|}\sqrt{\frac{A_{\boldsymbol{k}}-\omega_{\boldsymbol{k}}}{2\omega_{\boldsymbol{k}}}}\ .$$

Note: Generally speaking, the frequency ω_k can be negative: Hamiltonian $\mathcal{H}_2$ decreases, if wave amplitudes increase. This is impossible near the thermodynamic equilibrium, but can happens in highly exited media.

Three-wave Interaction Hamiltonian $\mathcal{H}_3$

ALL relevant information about wave interaction (and no extra, unneeded details) is contained in the coefficients of $\mathcal{H}_{\rm int}$

$$\mathcal{H}_{\rm int} = \mathcal{H}_3 + \mathcal{H}_4 + \dots \tag{3.13}$$

Three-wave Interaction Hamiltonian $\mathcal{H}_3$

$$\mathcal{H}_3 = \frac{1}{2} \sum_{\boldsymbol{k}_1=\boldsymbol{k}_2+\boldsymbol{k}_3} \left(V_q b_1^* b_2 b_3 + \text{c.c.}\right) \tag{3.14a}$$

$$+\frac{1}{6} \sum_{\boldsymbol{k}_1+\boldsymbol{k}_2+\boldsymbol{k}_3=0} \left(U_q b_1^* b_2^* b_3^* + \text{c.c.}\right) . \tag{3.14b}$$

describes three-wave processes of interaction.

Terms in Eq. (3.14a) – the decay processes $1 \to 2$ & confluence processes $2 \to 1$.

Terms in Eq. (3.14b) annihilation of three waves $3 \to 0$ & their creation from the vacuum $0 \to 3$

Shorthand notations: $b_j = b(\boldsymbol{k}_j, t)$, $V_q = V_{123} = V(\boldsymbol{k}_1, \boldsymbol{k}_2, \boldsymbol{k}_3)$, etc. Hereafter we are chousing numerical factor in the front of the interaction Hamiltonian as $1/\mathcal{N}$, where $\mathcal{N}$ is the number of elements in the Hamiltonian symmetry group. This simplifies various equations in the problem description.

Four-wave Interaction Hamiltonian $\mathcal{H}_4$

describes processes involving four waves: $2 \leftrightarrow 2$, $1 \leftrightarrow 3$, and $4 \leftrightarrow 0$:

$$\mathcal{H}_4 = \frac{1}{4} \sum_{\boldsymbol{k}_1+\boldsymbol{k}_2=\boldsymbol{k}_3+\boldsymbol{k}_4} W_p\, b_1^* b_2^* b_3 b_4 \tag{3.15a}$$

$$+\frac{1}{3!} \sum_{\boldsymbol{k}_1=\boldsymbol{k}_2+\boldsymbol{k}_3+\boldsymbol{k}_4} \left(G_p\, b_1 b_2^* b_3^* b_4^* + \text{c.c.}\right) \tag{3.15b}$$

$$+\frac{1}{4!} \sum_{\boldsymbol{k}_1+\boldsymbol{k}_2+\boldsymbol{k}_3+\boldsymbol{k}_4=0} \left(R_p^*\, b_1 b_2 b_3 b_4 + \text{c.c}\right). \tag{3.15c}$$

To which order in b, b^* the Hamiltonian $\mathcal{H}$ should be expanded?

Three-wave conservation law : $$\omega(\boldsymbol{k}+\boldsymbol{k}_1)=\omega(\boldsymbol{k})+\omega(\boldsymbol{k}_1)\ . \tag{3.16}$$

3-waves processes can be forbidden. 4-wave scattering ($2 \to 2$) conservation law:

$$\omega(\boldsymbol{k})+\omega(\boldsymbol{k}')=\omega(\boldsymbol{k}+\boldsymbol{\kappa})+\omega(\boldsymbol{k}'-\boldsymbol{\kappa})\ . \tag{3.17}$$

always allowed. Thus, in general,
$\mathcal{H}_5$ and higher-order terms should NOT be taken into account.

Expansion (3.1) utilizes the smallness of the wave amplitudes, therefore, generally speaking,

$$\mathcal{H}_2 > \mathcal{H}_3 > \mathcal{H}_4 > \mathcal{H}_5 > \dots\ . \tag{3.18a}$$

In particular cases, due to specific symmetries of a problem, odd expansion terms vanish (i.g. for spin waves in magnetics with exchange interactions, Kelvin waves in quantum vortex lines). In these cases, instead of (3.18a) one requires:

$$\mathcal{H}_3=\mathcal{H}_5=\mathcal{H}_7=\dots=0\,, \tag{3.18b}$$

$$\mathcal{H}_2 > \mathcal{H}_4 > \mathcal{H}_6 > \mathcal{H}_8 > \dots\ . \tag{3.18c}$$

Therefore, as a rule, three-wave interactions dominate in wave systems with small nonlinearity, e.g. for Rossby waves in the Atmosphere and Ocean, capillary waves on the water surface, drift waves in Plasmas, etc.

On the other hand, if $\mathcal{H}_3=0$, or three-wave processes are forbidden the leading nonlinear processes are four-wave interactions, that are allowed (in the sense that will be clarified below) for all nonlinear systems.

In this Lectures we will discuss only three- and four-wave interactions, that describes vast amount of weakly interacting waves.

Clearly, the physical world cannot be put in the Procrustean bed of any formal scheme. For instance, in one-dimension the system of gravity waves five-wave interactions Hamiltomian $\mathcal{H}_4=0$ an five-wave interactions dominate, whereas six-wave interactions dominate for Kelvin waves in quantum vortex lines. Wave interactions in these and similar systems can be studied along the same lines as the three- and four-wave interacting systems, but this subject lies outside the scope of present Lectures.

Dimensional analysis of the Hamiltonian

For more details, see Sec. 1.2 in my book "Wave Turbulence under Parametric Excitation"

$$\mathcal{H} = \sum_{\boldsymbol{k}} \omega_{\boldsymbol{k}} |b_{\boldsymbol{k}}|^2 + \frac{1}{2} \sum_{\boldsymbol{k}=\boldsymbol{k}'+\boldsymbol{k}''} V_{\boldsymbol{k}\boldsymbol{k}'\boldsymbol{k}''} b^*_{\boldsymbol{k}} b_{k'} b_{\boldsymbol{k}''} \tag{3.19a}$$
$$+\frac{1}{4} \sum_{\boldsymbol{k}+\boldsymbol{k}'=\boldsymbol{k}''+\boldsymbol{k}'''} T_{\boldsymbol{k}\boldsymbol{k}'\boldsymbol{k}''\boldsymbol{k}'''} b^*_{\boldsymbol{k}} b^*_{k'} b_{\boldsymbol{k}''} b_{\boldsymbol{k}'''} \ .$$

$[\mathcal{H}] = \mathsf{g} \cdot \mathsf{cm}^{2-d}\,\mathsf{s}^{-2}$ density of energy, $[\omega_{\boldsymbol{k}}] = \mathsf{s}^{-1}$,
$[b_{\boldsymbol{k}}] = \mathsf{g}^{1/2} \cdot \mathsf{cm}^{1-d/2} \cdot \mathsf{s}^{-1/2}$,

$$[V_{123}] = \left[\frac{\omega_{\boldsymbol{k}}}{b_{\boldsymbol{k}}}\right] = \mathsf{g}^{-1/2} \cdot \mathsf{cm}^{d/2-1}\,\mathsf{s}^{-1/2}\,, \tag{3.19b}$$

$$[T_{1234}] = \left[\frac{\omega_{\boldsymbol{k}}}{b^2_{\boldsymbol{k}}}\right] = \mathsf{g}^{-1} \cdot \mathsf{cm}^{d-2} \ . \tag{3.19c}$$

- Relevant parameters of the problems and results of the dimensional analysis

Sound in Continuous Media

$d=3\,,\ [\rho] = \mathsf{g} \cdot \mathsf{cm}^{-3}$, elasticity coefficient $[\kappa] = \mathsf{g} \cdot \mathsf{cm}^{-1}\,\mathsf{s}^{-2}$ or c_{s}

$$\rho_{\boldsymbol{k}} \simeq b_{\boldsymbol{k}} \sqrt{\frac{k\rho_0}{c_{\mathrm{s}}}}\,, \qquad v_{\boldsymbol{k}} \simeq b_{\boldsymbol{k}} \sqrt{\frac{kc_{\mathrm{s}}}{\rho_0}} \ \Rightarrow \frac{\rho_{\boldsymbol{k}}}{\rho_0} \sim \frac{v_{\boldsymbol{k}}}{c_{\mathrm{s}}}\,, \tag{3.20a}$$
$$V_{123} \simeq \sqrt{\frac{c_{\mathrm{s}}}{\rho_0}} k^3 \ \Rightarrow \ \sqrt{\frac{c_{\mathrm{s}}}{\rho_0}} k_1 k_2 k_3 \ .$$

Gravitational waves on the deep water: $d = 2\,,\ \rho\,,$ gravity acceleration g.

$$\mu_{\boldsymbol k} \simeq b_{\boldsymbol k} \left(\frac{k}{\rho^2 g}\right)^{1/4}, \qquad T_{1234} \simeq \frac{k^3}{\rho}\ . \tag{3.20b}$$

Capillary waves: $d = 2$, ρ, surface tension $[\sigma] = \text{g} \cdot \text{s}^{-2}$

$$\mu_{\boldsymbol k} \simeq b_{\boldsymbol k} \left(\frac{1}{\rho\sigma k}\right)^{1/4}, \qquad V_{123} \simeq \left(\frac{\sigma k^9}{\rho^3}\right)^{1/4}\ . \tag{3.20c}$$

Vortex motion of Incompressible fluid: $d = 3\,,\ [\rho] = \text{g} \cdot \text{cm}^{-3}$.

$$v_k \simeq b_k^2\, k/\rho\,,\ \omega_0 \equiv 0\,,\ V_{123} \equiv 0\,,\ T_{1234} \simeq k^2/\rho\,,\ \mathcal{H} = \mathcal{H}_4\ . \tag{3.20d}$$

Dynamical perturbation theory

⇒ Elimination of the nonresonant terms. Consider simple example:

$$\mathcal{H} = \omega b b^* + \frac{V}{2}(b^2 b^* + b^{*2} b) + \frac{U}{6}(b^3 + b^{*3})\ . \tag{3.21a}$$

Next, consider the weakly nonlinear canonical transformation:

$$b = c + A_1 c^2 + A_2 c c^* + A_3 c^{*2} \tag{3.21b}$$
$$+ B_1 c^3 + B_2 c^* c^2 + B_3 c c^{*2} + B_4 c^{*3} + \dots,$$
$$\{b b^*\} = \frac{\partial b}{\partial c}\frac{\partial b^*}{\partial c^*} - \frac{\partial b^*}{\partial c}\frac{\partial b}{\partial c^*} = 1\ . \tag{3.21c}$$

The canonicity condition, Eq. (3.21c) gives:

$$A_2 = -2A_1,\ B_2 = A_3^2 - A_1^2,\ B_3 + 3B_1 = 2A_2(A_3 - A_1)\ . \tag{3.21d}$$

Demanding that $\mathcal{H} = \omega c c^* + \dfrac{1}{4} T c^2 c^{*2}$ one, in addition to Eq. (3.21d), has

$$A_1 = \frac{V}{2\omega},\ A_2 = -\frac{V}{\omega},\ A_3 = -\frac{U}{6\omega},\ B_1 = \frac{V^2}{4\omega^2} + \frac{VU}{6\omega^2}, \tag{3.21e}$$
$$B_2 = \frac{U^2}{36\omega^2} - \frac{V^2}{4\omega^2}, B_3 = \frac{V^2}{4\omega^2} + \frac{7UV}{12\omega^2}, \quad B_4 = -\frac{UV}{12\omega^2}, \tag{3.21f}$$
$$T = -\frac{3V^2}{\omega} - \frac{U^2}{3\omega}\ . \tag{3.21g}$$

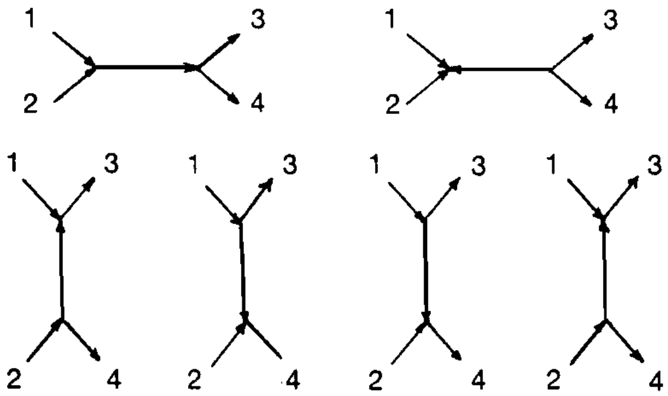

In general, total amplitude of the 4-wave processes

$$T_{12,34} = W_{12,34} + \widetilde{T}_{12,34} \tag{3.22a}$$

$$\begin{aligned}\widetilde{T}_{12,34} = &-\frac{V^*_{(1+2,1,2)}V_{(3+4,3,4)}}{\omega_1+\omega_2-\omega_{1+2}} - \frac{U_{(-1-2,1,2)}U_{(-3-4,3)}}{\omega_3+\omega_4+\omega_{3+4}} \\ &-\frac{V^*_{(1,3,1-3)}V_{(4,2,4-2)}}{\omega_{4-2}+\omega_2-\omega_4} - \frac{V^*_{(2,4,2-4)}V_{(3,1,3-1)}}{\omega_{3-1}+\omega_1-\omega_3} \\ &-\frac{V^*_{(2,3,2-3)}V_{(4,1,4-1)}}{\omega_{4-1}+\omega_1-\omega_4} - \frac{V^*_{(1,4,1-4)}V_{(3,2,3-2)}}{\omega_{3-2}+\omega_2-\omega_3} \,.\end{aligned} \tag{3.22b}$$

Exercises

Exercise 3.1 Prove that Eq. (3.4) is canonical, but not unimodal transformation and derive corresponding canonical equations (in $\boldsymbol{k}$-representation). For answer, see Eq. (5.28c).

Exercise 3.2 Find canonicity condition for the Bogolubov $\boldsymbol{u}$-$\boldsymbol{v}$ transform, given by Eq. (3.9)

Exercise 3.3 For a scale invariant dispersion law

$$\boldsymbol{\omega_k = k^\alpha}$$

find values of $\boldsymbol{\alpha}$ for which 3-wave processes are allowed. For a dispersion law

$$\boldsymbol{\omega_k = \omega_0 \left[1 + (ak)^2\right]}$$

find values of k for which 3-wave processes are allowed.

Exercise 3.4 Using dimensional reasoning find relations between canonical and natural variables and estimate interaction amplitudes for examples, given in Eqs. (3.20)

Exercise 3.5 Using dimensional reasoning find frequency, 4- and 6-wave interaction amplitudes for Kelvin (bending) waves along quantized vortex line in superfluid. The (most important) relevant parameter is $\kappa = \hbar/M$ (M is the atom mass). $[\kappa] = \mathrm{cm}^2/\mathrm{s}$. There is also dimensionless number $\Lambda \simeq \ln(\ell/a) \simeq 12 \div 15$, where ℓ is the mean intervortex distance and $a \sim 10^{-8}$cm (in ^{4}He) is the vortex core radius.

Answer:

$$\begin{aligned}
\omega_k &\sim \kappa k^2 \Rightarrow \frac{\kappa\Lambda\, k^2}{4\pi}\,, \\
T_{12,34} &\sim k^4 \Rightarrow -\Lambda k_1 k_2 k_3 k_4/(4\pi)\,, \\
W_{123,456} &\sim \frac{k^6}{\kappa} \Rightarrow -\frac{3}{4\pi\kappa} k_1 k_2 k_3 k_4 k_5 k_6\,,
\end{aligned} \tag{3.23}$$

see PRB **81** 104526 (2010).

Lecture 4

Linear evolution of wave packages

Outline

4.1 Dynamic equation of motion for weakly nonconservative waves

4.2 Equation for envelopes

4.3 Phase and group velocity

4.4 Dispersion and diffraction of waves

4.5 Exercises

Dynamic equation of motion for weakly nonconservative waves

- Small linear wave damping

If the interaction of the waves with the medium may be neglected:

$$\frac{\partial b(\boldsymbol{k},t)}{\partial t} + i\omega(\boldsymbol{k})b(\boldsymbol{k},t) = -i\frac{\delta \mathcal{H}_{\rm int}}{\delta b^*(\boldsymbol{k},t)} \ . \tag{4.1a}$$

The interaction of the waves with the thermal bath leads to the

exponential damping: $\quad |b(\boldsymbol{k},t)| = |b(\boldsymbol{k},0)|\exp[-\gamma(\boldsymbol{k})t] \ .$ (4.1b)

$\gamma(\boldsymbol{k})$ is the rate of damping. Phenomenologically:

$$\frac{\partial b(\boldsymbol{k},t)}{\partial t} + \big[i\omega(\boldsymbol{k}) + \gamma(\boldsymbol{k})\big]b(\boldsymbol{k},t) = -i\frac{\delta \mathcal{H}_{\rm int}}{\delta b^*(\boldsymbol{k},t)} \ . \tag{4.1c}$$

Region of applicability:

$$\gamma(\boldsymbol{k}) \ll \omega(\boldsymbol{k})\,, \quad \mathcal{H}_{\rm int} \ll \mathcal{H}_2\,, \quad |b(\boldsymbol{k})|^2 \gg |b_0(\boldsymbol{k})|^2 = n_0(\boldsymbol{k}) = T/\omega(\boldsymbol{k}),$$

$n_0(\boldsymbol{k})$ is the Rayleigh–Jeans distribution (classical limit of the Planck distribution).

- Accounting for the thermal noise

$$\frac{\partial b(\boldsymbol{k},t)}{\partial t} + \big[i\omega(\boldsymbol{k}) + \gamma(\boldsymbol{k})\big] b(\boldsymbol{k},t) = -i\frac{\delta \mathcal{H}_{\rm int}}{\delta b^*(\boldsymbol{k},t)} + f(\boldsymbol{k},t)\ . \tag{4.2a}$$

$f(\boldsymbol{k},t)$ is the Langevin force: random, Gaussian, white with the correlation:

$$\langle f(\boldsymbol{k},t) f^*(\boldsymbol{k}',t')\rangle = 2\delta(\boldsymbol{k}-\boldsymbol{k}')\delta(t-t')\gamma(\boldsymbol{k}) n_0(\boldsymbol{k})\ . \tag{4.2b}$$

$f(\boldsymbol{k},t)$ is not correlated at different times and for waves with different $\boldsymbol{k}$.

Derive :

$$\frac{1}{2}\frac{\partial n(\boldsymbol{k},t)}{\partial t} = -\gamma(\boldsymbol{k})[n(\boldsymbol{k},t) - n_0(\boldsymbol{k})]\,, \tag{4.2c}$$

$$\langle b(\boldsymbol{k}) b^*(\boldsymbol{k}')\rangle = n(\boldsymbol{k})\delta(\boldsymbol{k}-\boldsymbol{k}')\ . \tag{4.2d}$$

$n(\boldsymbol{k})$ is the number of waves. At $n(\boldsymbol{k})/\hbar \ll 1$: $n(\boldsymbol{k},t) \Rightarrow \hbar n_{\rm qm}(\boldsymbol{k},t)$.

- Nonlinear damping

$$\gamma[\boldsymbol{k}, n(\boldsymbol{k}')] = \gamma_0(\boldsymbol{k}) + \sum_{\boldsymbol{k}'} \mu(\boldsymbol{k},\boldsymbol{k}') n(\boldsymbol{k}')\ . \tag{4.3}$$

Equation for envelopes

Consider Eq. (4.1c) in linear approximation, taking $\mathcal{H}_{\rm int} = 0$:

$$\frac{\partial b(\boldsymbol{k},t)}{\partial t} + \big[i\omega(\boldsymbol{k}) + \gamma(\boldsymbol{k})\big] b(\boldsymbol{k},t) = 0\ . \tag{4.4}$$

Let $b(\boldsymbol{k},t) \neq 0$ only for $\kappa \ll k_0$, $\boldsymbol{\kappa} \equiv \boldsymbol{k} - \boldsymbol{k}_0$. For

$$c(\boldsymbol{k},t) \equiv b(\boldsymbol{k},t)\exp\big[i\omega(\boldsymbol{k}_0)t\big]\ : \tag{4.5a}$$

$$\frac{\partial c(\boldsymbol{k},t)}{\partial t} + \Big\{i\big[\omega(\boldsymbol{k}) - \omega(\boldsymbol{k}_0)\big] + \gamma(\boldsymbol{k})\Big\} c(\boldsymbol{k},t) = 0\ . \tag{4.5b}$$

Expand the frequency difference

$$\omega(\boldsymbol{k}) - \omega(\boldsymbol{k}_0) = \boldsymbol{v}\cdot\boldsymbol{\kappa} + \Omega_{ij}\kappa_i\kappa_j + \dots \quad \text{Here} \tag{4.6a}$$

$$v = \left(\frac{d\omega}{d\boldsymbol{k}}\right)_{\boldsymbol{k}=\boldsymbol{k}_0} \quad \text{group velocity}\,,\quad \Omega_{ij} \equiv \left(\frac{\partial^2\omega}{2\partial k_i \partial k_j}\right)_{\boldsymbol{k}=\boldsymbol{k}_0}\ . \tag{4.6b}$$

Introduce new variable: Envelope of a narrow wave package $C(r,t)$

$$C(\boldsymbol{r},t)=\frac{1}{(2\pi)^d}\int c(\boldsymbol{k},t)\exp[i(\boldsymbol{k}-\boldsymbol{k}_0)\cdot r]d\boldsymbol{k}\ . \tag{4.7a}$$

$$\left[\frac{\partial}{\partial t}+\boldsymbol{v}\cdot\boldsymbol{\nabla}-i\widehat{L}\right]C(\boldsymbol{r},t)=0\,,\quad \widehat{L}\equiv\Omega_{ij}\frac{\partial^2}{\partial x_i\partial x_j}\ . \tag{4.7b}$$

In an isotropic medium denote:

$$\omega(\boldsymbol{k})=\omega(k)\,,\quad \boldsymbol{v}=\frac{\boldsymbol{k}}{k}v\,,\quad v=\frac{\partial\omega}{\partial k}\,,\quad \omega''=\frac{\partial^2\omega}{\partial k^2}\ .\ \text{This gives} \tag{4.8a}$$

$$\left[\frac{\partial}{\partial t}+\boldsymbol{v}\cdot\nabla-i\left(\frac{\omega''}{2}\frac{\partial^2}{\partial z^2}+\frac{v}{2k}\Delta_\perp\right)\right]C(r,t)=0\ . \tag{4.8b}$$

This is a Hamiltonian equation with the Hamiltonian $\mathcal{H}$

$$i\frac{\partial C}{\partial t}=\frac{\delta\mathcal{H}}{\delta C^*} \tag{4.9}$$

$$\mathcal{H}=\frac{1}{2}\int\left[iv\cdot(C\nabla C^*-C^*\nabla C)+\omega''\left|\frac{\partial C}{\partial z}\right|^2+\frac{v}{k}|\nabla_\perp C|^2\right]d^dr\ .$$

Eq. (4.7b) has an extra integral of motion

$$N=\int|C(r,t)|^2dr \text{ — the total number of particles.} \tag{4.10}$$

Phase and group velocity

Plane wave $C(\boldsymbol{r},t)=C\exp\{i\,[\omega(\boldsymbol{k})t-\boldsymbol{k}\cdot r]\}$ is a solution of Eq. (4.7b). A plane of constant phase propagate with the Phase Velocity

$$V_{\rm ph}(\boldsymbol{k})=\frac{\boldsymbol{k}}{k}\frac{\omega(\boldsymbol{k})}{k}\ . \tag{4.11}$$

Neglect $\widehat{L}$ in Eq. (4.7b). Than one has the family of solutions $(\boldsymbol{r},t)=C(\boldsymbol{r}-\boldsymbol{v}\,t)$ describing a wave package which propagates with the

$$\text{Group Velocity:}\quad \boldsymbol{v}(\boldsymbol{k}_0)=\left(\frac{d\omega}{d\boldsymbol{k}}\right)_{\boldsymbol{k}=\boldsymbol{k}_0} \tag{4.12}$$

Clearly, $\boldsymbol{V}_{\rm ph}(\boldsymbol{k})\neq\boldsymbol{v}(\boldsymbol{k})$.

Dispersion and diffraction of waves

In isotropic media one has

$$\left[\frac{\partial}{\partial t} + \boldsymbol{v}\cdot\boldsymbol{\nabla} - i\left(\frac{\omega''}{2}\frac{\partial^2}{\partial z^2} + \frac{v}{2k}\Delta_\perp\right)\right] C(r,t) = 0\ . \qquad (4.13)$$

Consider stationary diffraction of waves on a half-plane $x > 0\,, \quad -\infty < y < \infty$.

In Eq. (4.13) put $\frac{\partial}{\partial t} = 0\,, \quad \boldsymbol{\nabla} \to \frac{\partial}{\partial z}\,, \quad \frac{\partial^2}{\partial z^2} \to 0\,, \quad \Delta_\perp \to \frac{\partial^2}{\partial x^2}$ (4.14a)

and get $\left(2ik\,\frac{\partial}{\partial z} + \frac{\partial^2}{\partial x^2}\right) C(x,z) = 0\ .$ (4.14b)

Self-similar substitution $C(x,z) = g(\zeta)$ with $\zeta \equiv x\sqrt{k/z}$ yields ordinary differential Eq.:

$$g'' = i\zeta g'\,, \quad g' \equiv h \ \Rightarrow\ \frac{dh}{d\zeta} = i\zeta h \ \Rightarrow\ h(\zeta) = h_0 \exp\frac{i\,\zeta^2}{2}\ . \qquad (4.14c)$$

This describes diffraction of wave package (on the half-plane).

In the co-moving with $\boldsymbol{v}$ reference frame $\boldsymbol{R} = \boldsymbol{r} - \boldsymbol{v}\,t, \quad v\cdot\nabla \to 0$ and:

Eq. (4.13) becomes $\left[\frac{\partial}{\partial t} - i\left(\frac{\omega''}{2}\frac{\partial^2}{\partial z^2} + \frac{v}{2k}\Delta_\perp\right)\right] C(\boldsymbol{R},t) = 0\ .$ (4.15a)

Consider next a $\boldsymbol{r}_\perp$-independent, self-similar solution of Eq. (4.15a):

$C(z,t) = f(\xi)$ with $\xi \equiv \frac{z^2}{\omega'' t}$, giving ordinary differential Eq.: (4.15b)

$$\xi f' - i\,(f' + 2\xi f'') = 0\,, \qquad (4.15c)$$

that describes Dispersion of wave package with $\delta z \simeq \sqrt{\omega'' t}$ (4.15d)

Exercises

Exercise 4.1 Derive Eq. (4.8b) as Hamiltonian equation with $\mathcal{H}$ given by Eq. (4.9)

Exercise 4.2 Find solution $g(\zeta)$ of diffraction Eq. (4.14c) and analyze its asymptotical form for $\zeta \gg 1$.

Exercise 4.3 Find solution $f(\xi)$ of dispersion Eq. (5.35a) and analyze its asymptotical form for $\xi \gg 1$.

Lecture 5

Three–wave processes

5.1 Basic "three-wave equation of motion"

5.2 Confluence of two waves and other induced processes

5.3 Decay instability

5.4 Intraseasonal Oscillations in Earths Atmosphere

5.5 The Bloembergen

5.6 Explosive three-wave instability

5.7 Burgers and Korteweg-de Vries Equations

5.8 Exercise

Basic "three-wave equation of motion"

Substitution $\mathcal{H}_{\text{int}} = \mathcal{H}_3$, Eq. (3.14), into the Eq. (4.1c) of motion yields

$$\frac{\partial b_k}{\partial t} + \left[\omega_k + i\gamma_k\right] b_k \tag{5.1}$$
$$= \frac{-i}{2} \sum_{k=1+2} V^*_{k,12} b_1 b_2 - i \sum_{1=k+2} V_{1,k,2} b_1 b_2^* - \frac{i}{2} \sum_{k+1+2=0} U_{k,12} b_1^* b_2^* ,$$

describing: $k \to k_1 + k_2 \Rightarrow$ Decay Processes, (5.2a)

$k + k_2 \to k_1 \Rightarrow$ Confluence Processes, (5.2b)

$k + k_1 + k_2 \to 0 \Rightarrow$ Annihilation of Waves, (5.2c) and corresponding inverse processes. We used shorthand notations $1 \equiv k_1$, $2 \equiv k_2$, $b_1 \equiv b_{k_1}$, $b_2 \equiv b_{k_2}$, $\sum_{k=1+2} \equiv \sum_{k,1,2} \Delta_{k,1+2}$, etc.

Confluence of two waves and other induced processes

Consider two monochromatic waves with the amplitudes b_1 & b_2:

$$b(k,t) = b_1\Delta(k-k_1)\exp\left[-i\omega(k_1)t\right] + b_2\Delta(k-k_2)\exp\left[-i\omega(k_2)t\right].$$

They excite 4 additional waves: b_3, b_4, $\widetilde{b}_4$ & b_5:

$$\begin{aligned}
b(k,t) &= b_3\delta(k-k_1-k_2)\exp[-i\omega(k_1)t - i\omega(k_2)t] \\
&\quad + b_4\delta(k+k_2-k_1)\exp[-i\omega(k_1)t + i\omega(k_2)t] \\
&\quad + \widetilde{b}_4\delta(k+k_1-k_2)\exp[-i\omega(k_2)t + i\omega(k_1)t] \\
&\quad + b_5\delta(k+k_2+k_1)\exp[i\omega(k_1)t + i\omega(k_2)t]\,, \\
b_3 &= \frac{V^*(k_1+k_2,k_1,k_2)b(k_1)b(k_2)}{[\omega(k_1)+\omega(k_2)-\omega(k_1+k_2)-i\gamma(k_1+k_2)]}\,, \qquad (5.3a) \\
b_4(k_1,k_2) &= \widetilde{b}_4(k_2,k_1) \qquad (5.3b) \\
&= -\frac{V^*(k_1,(k_1-k_2),k_2)b(k_1)b(k_2)}{[\omega(k_1)-\omega(k_2)-\omega(k_1-k_2)-i\gamma(k_1-k_2)]}\,, \\
b_5 &= -\frac{U(-k_1-k_2,k_1,k_2)b^*(k_1)b^*(k_2)}{[\omega(k_1)+\omega(k_2)+\omega(k_1+k_2)-i\gamma(k_1+k_2)]} \qquad (5.3c)
\end{aligned}$$

Resonant Conditions in (5.3a) If

$$\omega(k_1)+\omega(k_2) = \omega(k_1+k_2)\,, \qquad (5.4a)$$

$$\frac{b_3}{b_4} \simeq \frac{b_3}{b_5} \simeq Q \equiv \frac{\omega(k)}{\gamma(k)} \gg 1 :$$ resonance process of confluence of 2 waves.

For "good waves" Q-factor Q is about $10^2 - 10^5$.

Resonant Condition in (5.3b) If

$$\omega(k_1)-\omega(k_2) = \omega(k_1-k_2)\,, \qquad (5.4b)$$

the amplitude $|b_4| \gg |b_{3,5}|$ and one has some strange process.

Consider process (5.3c) near in mechanical/thermodynamic equilibrium

$$\omega(k) \geq 0\,, \quad \text{and} \quad \omega(k_1) + \omega(k_2) + \omega(-k_1 - k_2) \neq 0\ . \tag{5.4c}$$

Thus (5.3c) are non-resonant processes that can neglected for $Q \gg 1$.

Decay instability

is an instability of a finite amplitude B plane monochromatic wave

$$b(k,t) = B\,\delta(k - k_0)\exp\left(-i\omega_0 t\right) \tag{5.5}$$

with respect to decay into two other (secondary) waves:

- Decay of photon into two phonons, two magnons, two plasmons, etc.
- Induced light scattering: photon decaying into a photon and phonon, into a photon and magnon,
- capillary waves (on liquid surface) decaying into two capillary or gravity waves,
- and many others ...

for which in the 3-wave Eq. (5.1) we have to account for (5.2a) terms:

$$\frac{\partial b_i}{\partial t} + \left[\omega_i + i\gamma_i\right] b_i = -\frac{i}{2}\sum_{i=j+l}\left[V^*_{i;j,l} b_j\, b_l\, \dots\right]\ . \tag{5.6}$$

In the presence of finite amplitude plane wave (5.5) in Eq. (5.1) for the secondary waves $b_1\,,\ b_2$, with

$$k = k_1 + k_2 \tag{5.7}$$

we have to account for the confluence terms, (5.2b):

$$\frac{\partial b_1}{\partial t} + [\gamma_1 + i\omega(k_1)]b_1 + iV B\, b_2^* \exp(-i\omega_0 t) = 0\,, \tag{5.8a}$$

$$\frac{\partial b_2^*}{\partial t} + [\gamma_2 + i\omega(k_2)]b_2^* - iV^* B^* b_1 \exp(-i\omega_0 t) = 0\ . \tag{5.8b}$$

Let

$$b_1(t) = b_1 \exp\left[(\nu - i\omega_1)t\right], \quad b_2^*(t) = b_2^* \exp\left[(\nu + i\omega_2)t\right], \tag{5.9a}$$

with the restriction $\omega_1 + \omega_2 = \omega_0\ .$ (5.9b)

We know that Eq. (5.8) has nontrivial solution, $\boldsymbol{b_1}, \boldsymbol{b_2} \neq \boldsymbol{0}$, if:

$$\text{Det} = \begin{vmatrix} \gamma_1 + \nu + i[\omega(k_1) - \omega_1] \ , & iVb \\ -iVb^* & , \ \gamma_2 + \nu - i[\omega(k_2) - \omega_2] \end{vmatrix} = 0 \ , \tag{5.10a}$$

$$\text{Im}\{\text{Det}\} = (\gamma_1 + \nu)[\omega(k_2) - \omega_2] - (\gamma_2 + \nu)[\omega(k_1) - \omega_1] = 0 \ , \tag{5.10b}$$

$$\text{Re}\{\text{Det}\} = \Big[\nu + \frac{\gamma_1 + \gamma_2}{2}\Big]^2 - \frac{(\gamma_1 - \gamma_2)^2}{4} - |V\,b|^2 - [\omega(\boldsymbol{k}_1 - \omega_1)]\,[\omega(\boldsymbol{k}_2) - \omega_2] = 0 \ . \tag{5.10c}$$

Solving Eq. (5.10b) and $\omega_1 + \omega_2 = \omega_0$ with respect to ω_1 and ω_2 and substituting result into Eq. (5.10c) one gets bi-quadratic equation for $\nu + (\gamma_1 + \gamma_2)/2$ with the solution:

$$2\nu = -\gamma_1 - \gamma_2 + \sqrt{B + \sqrt{B^2 + 2(\Delta\gamma\Delta\omega)^2}} \ , \tag{5.10d}$$

$$\Delta\gamma = \gamma_1 - \gamma_2 \ , \quad 2\Delta\omega = \omega(k_1) + \omega(k_2) - \omega(k_0) \ , \tag{5.10e}$$

$$2B = 4|Vb|^2 + (\Delta\gamma)^2 - 4(\Delta\omega)^2 \ . \tag{5.10f}$$

Clearly: $\omega_1 \simeq \omega(k_1)$, and $\omega_2 \simeq \omega(k_2)$. For the simple case $\gamma_1 = \gamma_2 = \gamma$,

$$\nu = -\gamma + \sqrt{|Vb|^2 - (\Delta\omega)^2} \ , \tag{5.11a}$$

$$\omega_1 = \omega(k_1) - \frac{\Delta\omega}{2} \ , \quad \omega_2 = \omega(k_2) + \frac{\Delta\omega}{2} \ . \tag{5.11b}$$

At Re $\nu > 0$ the wave amplitudes exponentially increase. ν is an increment of decay instability.

In general case $(\gamma_1 \neq \gamma_2)$ ν is maximum at the resonance $\Delta\omega = 0$,

$$2\nu_{\max} = -(\gamma_1 + \gamma_2) + \sqrt{4|Vb|^2 + (\Delta\gamma)^2} \ . \tag{5.12a}$$

and $\nu_{\max} = 0$ at the threshold amplitude B_{th}

$$|VB_{\text{th}}| = \sqrt{\gamma_1\gamma_2} \ . \tag{5.12b}$$

At the threshold and in the resonance

$$\sqrt{\gamma_1} b_1 = \sqrt{\gamma_2} b_2 \ . \tag{5.12c}$$

Thus at $\gamma_1 \gg \gamma_2$, $b_1 \ll b_2$.

5.4 Intraseasonal Oscillations in Earths Atmosphere

Intraseasonal Oscillations (IOs) were detected by Madden and Julian in 1971 in their study of tropical wind and later discovered in the atmospheric angular momentum, atmospheric pressure, etc.
Kartashova-L'vov (KL)-model [PRL **98**, 198501 (2007)] considers IOs an intrinsic atmospheric phenomenon, related to a system of resonantly interacting triads of planetary (Rossby) waves with frequencies,

$$\Omega(m,\ell) = 2\Omega m/\ell(\ell+1)\,, \tag{5.13}$$

where Ω is the frequency of the Earth rotation, ℓ and m are longitudinal and latitudinal wave numbers of the j-mode, equal to the number of zeros of the eigen- (spherical-) function along the longitude and latitude.

Due to discreteness of $\Omega(m,\ell)$ there are (only) four isolated triads with

$$\Omega(m_1,\ell_1) = \Omega(m_2,\ell_2) + \Omega(m_3,\ell_3)\,, \quad \text{with } m_j\,,\ \ell_j\ . \tag{5.14}$$

Namely: {[4,12],[4,14],[9,13]}, {[3,14],[1,20],[4,15]}, {[6,18],[7,20],[13,9]}, and {[1,14],[11,21],[12,20]}.

With $\boldsymbol{\gamma_j = 0}$, and $\boldsymbol{a_j = -iB_j}$ their Hamiltonian motion equations are:

$$\dot{\boldsymbol{B}}_1 = -\boldsymbol{V B_2 B_3}, \quad \dot{\boldsymbol{B}}_2 = \boldsymbol{V B_3 B_1^*}\,, \quad \dot{\boldsymbol{B}}_3 = \boldsymbol{V B_1^* B_2}\ . \tag{5.15a}$$

This system has two independent (Manly-Row) conservation laws

$$\boldsymbol{I_1 = |B_1|^2 + |B_2|^2}\,, \quad \boldsymbol{I_2 = |B_1|^2 + |B_3|^2}\,, \tag{5.15b}$$

which allows one to find general solution for $\boldsymbol{B_j}$ expressed in Jacobian elliptic functions

$$\boldsymbol{B_2 = B_{2,0}\mathrm{cn}\,(\tau - \tau_0)}\,, \quad \boldsymbol{B_3 = B_{3,0}\mathrm{sn}\,(\tau - \tau_0)}\,, \boldsymbol{B_1 = B_{1,0}\mathrm{dn}\,(\tau - \tau_0)}\,,$$

where $\boldsymbol{B_{j,0}}\,,\ \boldsymbol{\tau_0}\,,$ are defined by initial conditions and $\boldsymbol{\tau = t/V\sqrt[4]{I_1\,I_2}}$.

Elliptic functions $\mathrm{cn}(\tau)$, $\mathrm{sn}(\tau)$ and $\mathrm{dn}(\tau)$ are periodic and their real periods are equal to $4K, 4K$ and $2K$ correspondingly, with $K(\mu)$ a normalized complete elliptic integral of the first order with modulus μ:

$$K(\mu) = \frac{2}{\pi}\int_0^{\pi/2} \frac{d\theta}{\sqrt{1-\mu\sin^2\theta}}, \ \mu^2 \equiv \min\left\{\frac{I_1}{I_2}, \frac{I_2}{I_1}\right\} \le 1 .$$

Example of time dependence (in days) of B_1 (solid-black), B_2 (dashed-red) and B_3 (blue dotted-dashed) in the first triad is shown below.

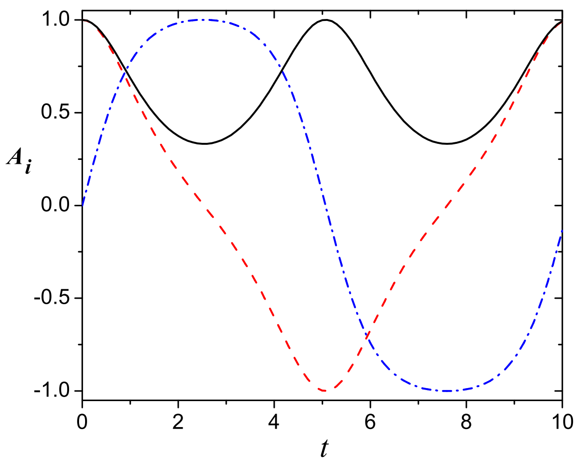

The KL-model is equally applied to the Northern and the Southern Hemispheres, is independent (in the leading order) of Earths topography, naturally has the period of desired order, and allows one to interpret the main observable features of IOs.

5.5 The Bloembergen Problem

Consider 3 narrow packages centered at

k_1, k_2, k_3 and ω_{k_1}, ω_{k_2}, ω_{k_3} such that

$k_1 = k_2 + k_3$, $\omega_{k_1} = \omega_{k_2} + \omega_{k_3}$.

Introduce the envelopes : $a_j(\kappa) = b_j(k_j+\kappa)\exp i[\omega(k_j)t - k_j r]$, (5.16a)

$$a_j(r) = (2\pi)^{-3/2}\int a_j(k)\exp(ikr)\,dk\,, \tag{5.16b}$$

and expand : $\omega(k_j+\kappa) = \omega(k_j) + (\kappa v_j)$. Then (5.16c)

$$\left(\frac{\partial}{\partial t} + \gamma_1 + v_1 \cdot \nabla\right) a_1(r,t) = -iV a_2(r,t) a_3(r,t)\,, \quad (5.17a)$$
$$\left(\frac{\partial}{\partial t} + \gamma_2 + v_2 \cdot \nabla\right) a_2(r,t) = -iV a_1(r,t) a_3^*(r,t)\,, \quad (5.17b)$$
$$\left(\frac{\partial}{\partial t} + \gamma_3 + v_3 \cdot \nabla\right) a_3(r,t) = -iV a_2^*(r,t) a_1(r,t)\,, \quad (5.17c)$$

where $\quad V \equiv (2\pi)^{3/2} V(k_1\,; k_2, k_3)$.

Under $\gamma_i = 0$ Eq. (5.17) are Hamiltonian equations with the Hamiltonian

$$\mathcal{H} = \sum_{j=1}^{3} \frac{v_j}{2i} \int [a_j^*(r) \nabla a_j(r) - \text{c.c}]\, dr + V \int [a_1^* a_2 a_3 + \text{c.c.}]\, dr\ . \quad (5.18a)$$

Under $\gamma_i = 0$ in addition to $\mathcal{H}$, Eq. (5.17) has two other independent (Manly-Row) integrals of motion:

$$N_1 + N_2 = \text{const.}, \quad N_2 + N_3 = \text{const.}, \quad \text{where} \quad (5.18b)$$
$$N_j = \int a_j^*(r,t) a_j(r,t)\, dr \quad (5.18c)$$

is the total number of particles of j type. In particular, Eq. (5.17) describe

Stationary generation of the 2nd harmonic: Let:

$$a_2 = a_3\,, \quad \gamma_j = 0\,, \quad v_j = v\,, \quad a_1(r) = A_1(z)\,, \quad (5.19)$$
$$a_2(r) = a_3(r) = \sqrt{i} A_2(z)\,, \quad A_1, A_2 \text{ real}\ .$$

With (5.19), Eq. (5.17) yields:

$$v \frac{\partial A_1}{\partial z} = V A_2^2\,, \quad v \frac{\partial A_2}{\partial z} = -V A_1 A_2\,, \quad (5.20a)$$

which has integral of motion $A_1^2(z) + A_2^2(z) = A^2$ =const. This gives:

$$v\frac{\partial A_1}{\partial z} = V\left(A^2 - A_1^2\right) , \tag{5.20b}$$

Consider boundary condition at

$$z = 0: \;\; A_1(0) = 0\,, \;\; A_2(0) = B\;. \tag{5.20c}$$

Solution of the problem (5.20):

$$A_1(z) = B \tanh\left(\frac{VBz}{v}\right) , A_2(z) = B \Big/ \cosh\left(\frac{VBz}{v}\right) \;. \tag{5.21}$$

$L = v/(VB)$ is the Interaction Lenght. At $z \gg L$ all the energy of the initial wave is fully transferred into the second harmonics A_1.

Explosive three-wave instability

Waves with negative energy can exist in the active medium! Then the resonance conditions may be satisfied for the Creation of three waves from the vacuum:

$$\omega(k_1) + \omega(k_2) + \omega(k_3) = 0\;, \qquad k_1 + k_2 + k_3 = 0\;. \tag{5.22}$$

Retaining only the last term in Eq. (5.1)

$$\frac{\partial b(k,t)}{\partial t} + \left[\omega(k) + i\gamma(k)\right] b(k,t) = \sum_{k+1+2=0} \frac{1}{2} U(k, k_1, k_2) b_1^* b_2^*\,, \tag{5.23}$$

and assuming

$$b(k,t) = \sum_{j=1}^{3} a_j(t) \Delta(k - k_j) \exp\left[-i\omega(k_j)t\right], \tag{5.24}$$

one has in the resonance

$$
\begin{aligned}
\left[\frac{\partial}{\partial t}+\gamma_1\right] a_1 &= -iU a_2^* a_3^* \,, \\
\left[\frac{\partial}{\partial t}+\gamma_2\right] a_2 &= -iU a_1^* a_3^* \,, \\
\left[\frac{\partial}{\partial t}+\gamma_3\right] a_3 &= -iU a_1^* a_2^* \,.
\end{aligned}
\tag{5.25}
$$

At $\gamma_j = \gamma$ Eqs. (5.25) have a solution $|a_j| = A$ with

$$
A(t) = A_0 \frac{\gamma \exp(-\gamma t)}{\gamma + UA[\exp(-\gamma t) - 1]} \,. \tag{5.26}
$$

This is instability with finite inertial amplitude: If $UA_0 > \gamma$, the amplitude $A(t)$ becomes infinite over a finite time

$$
t = \frac{1}{2UA_0} \,. \tag{5.27}
$$

Burgers and Korteweg-de Vries Equations

- Wave equations for quasi-linear dispersion and hydrodynamic nonlinearity

Consider waves with the quasi-linear dispersion law

$$
\omega_k = c_s k - (c_s a\, k)^3 \,. \tag{5.28a}
$$

Corresponding motion equation for the velocity of that waves, travelling to the right, in one-dimension is

$$
\left(\frac{\partial}{\partial t} + c_s \frac{\partial}{\partial x} + c_s a^2 \frac{\partial^3}{\partial x^3}\right) u(x,t) = 0 \,. \tag{5.28b}
$$

For sound waves in fluids, gravity waves on shallow (of the depth a) water, and in many other systems (of hydrodynamic types) one can account for the quadratic nonlinearity and viscous damping:

$$
\left(\frac{\partial}{\partial t} + c_s \frac{\partial}{\partial x} + \frac{\partial u}{\partial x} + c_s a^2 \frac{\partial^3}{\partial x^3}\right) u = \mu \frac{\partial^2 u}{\partial x^2} \,. \tag{5.28c}
$$

The form of the nonlinear term $u\, u_x$ is determined by the requirement of the Galilei invariance: the form of Eq. (5.28c) must be invariant under the transformation

$$\boldsymbol{r} \to \boldsymbol{r} - \boldsymbol{V}t\,, \quad \boldsymbol{u} \to \boldsymbol{u} + \boldsymbol{V}\ . \tag{5.29}$$

It also can be derived from the sound 3-wave interaction Hamiltonian with the amplitude $V_{1,23} = V\sqrt{k_1 k_2 k_3}$ by the transformations: $\sqrt{k}\, a_k \equiv v_k \to u(x)$.

The 2nd term in the LHS of Eq. (5.28c) disappears in the comoving reference frame

$$x \to x - c_{\rm s} t\,,$$

giving:

$$\left(\frac{\partial}{\partial t} + \frac{\partial u}{\partial x} + c_{\rm s} a^2 \frac{\partial^3}{\partial x^3}\right) u = \mu \frac{\partial^2 u}{\partial x^2}\ . \tag{5.30}$$

– Without viscous term this equation was suggested by Korteweg and his student de Vries in 1895 and is called Korteweg-de Vries (KdV) equation.

– Without dispersion term it was suggested by Burgers in 1940 and is called Burgers equation.

- Burgers equation

$$\frac{\partial u}{\partial t} + u\frac{\partial u}{\partial x} = \mu \frac{\partial^2 u}{\partial x^2} \tag{5.31a}$$

can be solved in general form by the Hopf (1950) substitution

$$u = -2\mu \frac{\partial}{\partial x} \ln \varphi(x, t)\,, \tag{5.31b}$$

which gives for φ linear (thermal-conductivity) equation

$$\frac{\partial \varphi}{\partial t} = \mu \frac{\partial^2 \varphi}{\partial x^2}\ . \tag{5.31c}$$

This allows to find analytical solution of Eq. (5.31a) from any initial condition.

Asymptotically for $t \to \infty$, $\varphi(x,t) \to F(\xi)$, $\xi \equiv \dfrac{x}{\sqrt{4\mu t}}$

$$\boldsymbol{F(\xi) = \frac{1}{\sqrt{\pi}} \left[\text{exp}\left(-\frac{M}{4\mu}\right) \int_{-\infty}^{\xi} d\eta \, \text{exp}\left(-\eta^2\right) + \text{exp}\left(\frac{M}{4\mu}\right) \int_{\xi}^{\infty} d\eta \, \text{exp}\left(-\eta^2\right) \right] ,} \qquad (5.32\text{a})$$

where the only dependence on initial conditions is via the motion integral, mechanical momentum of the system, M :

$$\boldsymbol{M \equiv \int_{-\infty}^{\infty} u(x,t) dx \, .} \qquad (5.32\text{b})$$

In the limit $\mu \to 0$:

$$\boldsymbol{u(x,t) = x/t \, , \text{for} \quad 0 < x < \sqrt{2Mt} \, ,} \qquad (5.32\text{c})$$
$$\boldsymbol{u(x,t) = 0 \, , \quad \text{for} \quad 0 < x \, , \; x > \sqrt{2Mt} \, .}$$

Burgers Eq. (5.31a) has also stationary solutions, propagating "dissipative shock wave"

$$\boldsymbol{u = f(x - W\,t) \, , \quad W = u_0 + \frac{1}{2}\Delta u \, ,} \qquad (5.33\text{a})$$

$$\boldsymbol{f(\xi) = u_0 + \frac{\Delta u}{1 + \text{exp}(\Delta u \xi / 2\mu)} \, ,} \qquad (5.33\text{b})$$

with u_0 and Δu being integration constants. Shock width $\delta = 2\mu/\Delta u$ can be also estimated by the balance of the nonlinear and dissipation term in Eq. (5.31a)

Korteweg-de Vries Equation

• 1834: Observation of solitary waves by a naval architect, John Scott Russell. He was on horseback, riding along the Union Canal between Edinburgh and Glasgow, and he suddenly saw a boat rapidly drawn by a pair of horses, which however stopped suddenly and a rounded, smooth and well defined heap of water loosened from its prow, continuing its course along the channel apparently without change of form and diminution of speed. Russell called these waves solitary waves. Russell performed a number of experiments in wave tanks and was able to gain much empirical knowledge about these waves.

• 1895: Korteweg and de Vries, in the paper "On the change of Form of long Waves advancing in a Rectangular Canal and on a New Type of Long Stationary Waves", suggested the KdV equation:

$$\frac{\partial u}{\partial \tau} + \frac{\partial u}{\partial \xi} + 6u\,\frac{\partial u}{\partial \xi} + \frac{\partial^3 u}{\partial \xi^3} = 0\,. \tag{5.34}$$

This "canonical" choice of constants is reached by proper re-scaling of time, length and amplitude u. The first and second linear terms, describe travelling with velocity $C = 1$ waves. The 2nd term disappear in the co-moving reference frame.

In the linear approximation KdV Eq. (5.34) has the dispersion law:

$$\omega(k) = k - k^3\,. \tag{5.35a}$$

The dispersion term leads to the broadening of the wave profile.

The nonlinear term gives velocity dependence on the wave amplitude:

$$C_{\rm NL} = 1 + 6u\,, \tag{5.35b}$$

and responsible for the the steepening the wave front. The dispersion and front-steepening effects balance each other and give rise to the stationary behavior, solitons. One soliton solution of KdV Eq. (5.34) is

$$u = \frac{2\kappa^2}{\text{ch}[\kappa(\xi - 4\kappa^2 t) + \phi_0]}\,. \tag{5.36}$$

Here free parameter $\sqrt{\kappa}$ describe amplitude of the soliton, related to the non-linear correction of its velocity $4\kappa^2$, and soliton phase, ϕ_0, defines position of its maximum at $t = 0$.

A way to get this solution is as follows:

• In the moving with velocity $1 + c$ reference frame $x = \xi - (1 + c)\tau$ rewrite KdV for $u(x)$

$$\frac{d}{dx}\Big[-cu + 3u^2 + \frac{d^2u}{dx^2}\Big] \Rightarrow \Big[-cu + 3u^2 + \frac{d^2u}{dx^2}\Big] = A \Rightarrow 0\,,$$

with the help of the zero at $\pm\infty$ boundary conditions.

- Multiplying this by du/dx one has similarly:

$$\frac{d}{dx}\Big[-\frac{cu^2}{2}+u^3+\Big(\frac{du}{dx}\Big)^2\Big] \Rightarrow \Big[-\frac{cu^2}{2}+u^3+\frac{1}{2}\Big(\frac{du}{dx}\Big)^2\Big]=B\Rightarrow 0\,,$$

again with the help of the boundary conditions.

- Now one has

$$\frac{du}{dx}=u\sqrt{c-2u}\,,$$

which easily can be integrating to give Eq. (6.16a).

This trick was possible due to two (trivial) integrals of motion, total mechanical momentum

$$I_1 \equiv \int u d\xi\,,$$

and total energy

$$I_2 \equiv \int \frac{u^2}{2} d\xi\ .$$

Indeed, KdV Eq. (5.34) can be identically rewritten as the continuity equations

$$\frac{dI_n}{d\tau}+\frac{dJ_n}{d\xi}=0\,,\quad n=1\,,2 \quad \text{with the fluxes :} \tag{5.37a}$$

$$J_1=\Big(3u^2+\frac{\partial^2 u}{\partial\xi^2}\Big)\,, \tag{5.37b}$$

$$J_2=2u^3+u\,\frac{\partial^2 u}{\partial\xi^2}-\frac{1}{2}\,\Big(\frac{\partial u}{\partial\xi}\Big)^2\ . \tag{5.37c}$$

Later in 1965 Gerald Whitham found a third conservation law :

$$N_3=3u^3-u_\xi\,,\quad u_\xi\equiv\Big(\frac{du}{d\xi}\Big)^2\,, \tag{5.38}$$

$$J_3=3u^4+6u^2(6u)_{\xi\xi}-12uu_\xi^2-2u_\xi\,u_{\xi\xi\xi}+u_{\xi\xi}^2 \tag{5.39}$$

Later up to ten(!) conservation laws were found by Norman Zabusky (currently in Weizmann, Physics Dept.), Kruskal and Miura. This lead to the conjecture that the KdV equation had an infinite number of conservation laws, which was verified explicitly in 1968 by Miura, Gardner and Kruskal. This conjecture was also shown explicitly in 1973 by Whalquist and Estabrook and by Lamb in 1974 using the Auto-Bäcklund transformation.

The KdV equation can support more than one soliton. N-soliton solutions are collisionless. This can be shown using the Hirota direct method, by the inverse-scattering-transform or by the auto-Bäcklund-transform. These derivations are beyond the scope of this course.

Exercises

Exercise 5.1 Derive Hamiltonian of the hot-wire harmonic oscillator (Lect. 1) and consider its parametric instability as a particular case of the decay instability, Sec. 5.2.

Lecture 6

Four–wave processes

Outline

Basic “four-wave equation of motion”

Let 3-wave processes are forbidden. Consider then 4-wave scattering of $2 \Rightarrow 2$ type

$$\omega(\boldsymbol{k}_1) + \omega(\boldsymbol{k}_2) = \omega(\boldsymbol{k}_3) + \omega(\boldsymbol{k}_4)\,, \quad \boldsymbol{k}_1 + \boldsymbol{k}_2 = \boldsymbol{k}_3 + \boldsymbol{k}_4\ . \tag{6.1a}$$

Equation 4.1c in this case are:

$$\frac{\partial c_{\boldsymbol{k}}}{\partial t} + [i\omega_{\boldsymbol{k}} + \gamma_{\boldsymbol{k}}]c_{\boldsymbol{k}} = -\frac{i}{2} \sum_{\boldsymbol{k}+\boldsymbol{k}_1=\boldsymbol{k}_2+\boldsymbol{k}_3} T_{\boldsymbol{k},\boldsymbol{k}_1;\boldsymbol{k}_2,\boldsymbol{k}_3} c^*_{\boldsymbol{k}_1} c_{\boldsymbol{k}_2} c_{\boldsymbol{k}_3} \tag{6.1b}$$

Here $c_{\boldsymbol{k}}$ are canonical variables, in which $\mathcal{H}_2$ is diagonal and all $\mathcal{H}_3$ is eliminated by proper weakly nonlinear canonical transformation, similar to Equation 3.21b. Full 4-wave amplitude of interaction, $T_{\boldsymbol{k},\boldsymbol{k}_1;\boldsymbol{k}_2,\boldsymbol{k}_3}$, is given by Equation 3.22.

Modulation Instability of Plane Waves

Let $b(\boldsymbol{k}) = b_0\,\Delta(\boldsymbol{k}-\boldsymbol{k}_0)$ be a wave of finite amplitude.

Equation 6.1b for b_0 at $\gamma(\boldsymbol{k})=0$ becomes $\dfrac{\partial b_0}{\partial t} + i\Omega_{k_0} b_0 = 0\,,$ (6.2a)

where "Nonlinear" frequency of the wave

$$\Omega_{k_0} \equiv \omega_{\boldsymbol{k}_0} + T_{00}\,|b_0|^2\,,\quad T_{00} \equiv \frac{1}{2} T(\boldsymbol{k}_0,\boldsymbol{k}_0;\boldsymbol{k}_0,\boldsymbol{k}_0)\ . \tag{6.2b}$$

In the presence of b_0 Equation 6.1b for the waves $b_j \equiv b_{\boldsymbol{k}_j} \ll b_0\,, j=1,2$ and under the resonance conditions: $2\omega_{\boldsymbol{k}_0} \simeq \omega_{\boldsymbol{k}_1} + \omega_{\boldsymbol{k}_2}\ ,\ 2\boldsymbol{k}_0 = \boldsymbol{k}_1 + \boldsymbol{k}_2 \Rightarrow$

$$\frac{\partial b_1}{\partial t} + i\Omega_{k_1} b_1 + iS_{12}\, b_0^2 b_2^* = 0\,,\quad S_{12} = \frac{1}{2} T(\boldsymbol{k}_0\boldsymbol{k}_0,\boldsymbol{k}_1\boldsymbol{k}_2), \tag{6.3a}$$

$$\frac{\partial b_2^*}{\partial t} - i\Omega_{k_2} b_2^* - iS_{12}^*\,(b_0^*)^2 b_1 = 0,\quad \Omega_{k_i} = \omega_{\boldsymbol{k}_i} + 2\,T_{i0}|b_0|^2, \tag{6.3b}$$

$$T_{i0} \equiv \frac{1}{2} T(\boldsymbol{k}_i,\boldsymbol{k}_0;\boldsymbol{k}_i,\boldsymbol{k}_0). \quad \text{Attention: } 2 \text{ in } \Omega_{\boldsymbol{k}_i}\ ! \tag{6.3c}$$

- Instability increment in dissipation-less limit

Let $b_1(t) = b_1 \exp\left[(i\omega_1 + \nu\,)\,t\right]\ ,\ \ b_2^*(t) = b_1 \exp\left[(-i\omega_2 + \nu\,)\,t\right]\ ,$ (6.4a)

$$\omega_1 \equiv \Omega_{\boldsymbol{k}_0} + \frac{1}{2}\left(\Omega_{\boldsymbol{k}_1} - \Omega_{\boldsymbol{k}_2}\right)\ ,\ \omega_2 = \Omega_{\boldsymbol{k}_0} + \frac{1}{2}\left(\Omega_{\boldsymbol{k}_2} - \Omega_{\boldsymbol{k}_1}\right). \tag{6.4b}$$

Then Equation 6.3 yields:

$$\nu^2 = |S_{12}\, b_0^2|^2 - \Delta\Omega^2\,, \tag{6.5a}$$

$$\Delta\Omega = \frac{1}{2}\left(\Omega_{\boldsymbol{k}_2} + \Omega_{\boldsymbol{k}_1}\right) - \Omega_{\boldsymbol{k}_0}\ . \tag{6.5b}$$

If $\Delta\Omega = 0,$ then $\nu = |S_{1,2} b_0^2| > 0\ .$ Instability of plane wave!

Consider $\boldsymbol{k}_{1,2} = \boldsymbol{k}_0 \pm \boldsymbol{\kappa}\,,\ \Rightarrow\ \Omega_{\boldsymbol{k}_{1,2}} = \omega(\boldsymbol{k}_0) \mp \boldsymbol{v}\cdot\boldsymbol{\kappa} + \mathcal{L}\kappa^2 + 2S|b_0|^2\ ,$

with $S = S_{12} \simeq T_{i0}\,,\ \ \mathcal{L}\kappa^2 \equiv \dfrac{\kappa_i\kappa_j}{2}\dfrac{\partial^2\omega(\boldsymbol{k})}{\partial k_i \partial k_j}\ .$ Then Eq. (6.5a) yields:

$$\Delta\Omega \simeq S|b_0|^2 + \mathcal{L}\kappa^2\,, \quad \nu^2(\boldsymbol{\kappa}) \simeq -\mathcal{L}\kappa^2(\mathcal{L}\kappa^2 + 2S|b_0|^2)\,. \tag{6.6a}$$

Instability criterion

$$S\,\mathcal{L}\kappa^2 < 0\,, \quad 0 < |\mathcal{L}\kappa^2| < 2|Sb_0^2|\,, \tag{6.6b}$$

The instability is maximum for

$$\mathcal{L}\kappa^2 = -S|b_0|^2\,. \tag{6.6c}$$

Threshold amplitude in a dissipative medium:

$$|Sb_{0,th}^2| = \sqrt{\gamma_1\gamma_2}\,. \tag{6.6d}$$

In isotropic, scale invariant media:

$$\mathcal{L}\kappa^2 \equiv \frac{\kappa_i\kappa_j\partial^2\omega(\boldsymbol{k})}{2\,\partial k_i\partial k_j} \quad \underset{\Longrightarrow}{\omega_{\boldsymbol{k}} = \omega_k} \quad \frac{1}{2}\left[\omega_k''\kappa_\parallel^2 + \frac{\omega_k'}{k}\kappa_\perp^2\right] \tag{6.7a}$$

$$\underset{\Longrightarrow}{\omega_k \propto k^\alpha} \quad \frac{\alpha\,\omega_k}{2\,k^2}\left[(\alpha-1)\kappa_\parallel^2 + \kappa_\perp^2\right]\,. \tag{6.7b}$$

• Nonlinear dielectrics: $\omega_k = \dfrac{kc}{\sqrt{n}}$, n refractive index, and $\dfrac{\partial n}{\partial|E|^2} > 0$.

One has $S < 0$, since $\frac{\partial\omega}{\partial|E|^2} \simeq -\frac{\partial n}{\partial|E|^2}$. For "normal dispersion" $\omega'' > 0$, $S\,\omega'' < 0$. This leads to $S\,\mathcal{L}\kappa^2 < 0$, the modulation instability of light in the nonlinear dielectrics resulting in the self-focusing of light.

• Gravitational waves on a sea: $\omega(\boldsymbol{k}) = \sqrt{gk}\,,\ \alpha = 1/2$.

$$\mathcal{L}\kappa^2 = \frac{\omega(k)}{4k^2}\left(\kappa_\perp^2 - \frac{1}{2}\kappa_\parallel^2\right)\,, \tag{6.8}$$

For $\boldsymbol{\kappa} = \boldsymbol{\kappa}_\perp\,,\ \ \mathcal{L}\kappa^2 > 0$ and for $\boldsymbol{\kappa} = \boldsymbol{\kappa}''\,,\ \mathcal{L}\kappa^2 < 0$. Thus, there is the modulation instability of gravity waves, (whatever the sign of $T_{\boldsymbol{k}_0\,\boldsymbol{k}_0}$), resulting in the phenomenon of a "tenth (or decuman, mountainous) wave":

long-period (with ($\Lambda \approx 9 - 10\lambda$) longitudinal and lateral modulation of the sea-wave amplitudes. Non-linear estimate of $\mathcal{L}/\lambda \simeq 10$, a role of "white horses".

"Decumen wave", Ivan Aivazovskii (1817-1900), Tretyakov galary, Moscow.

Nonlinear Equation for Envelopes

describes nonlinear stage of modulation instability:

$$\left[i\frac{\partial}{\partial t} + i\boldsymbol{v}\cdot\boldsymbol{\nabla} + \mathcal{L} - T|C|^2 \right] C(\boldsymbol{r}, t) = 0 \ , \qquad (6.9a)$$

$$\mathcal{L} = \frac{1}{2}\frac{\partial^2\omega(\boldsymbol{k})}{\partial k_i \partial k_j}\frac{\partial^2}{\partial x_i \partial x_j} \ \Rightarrow [\omega_{\boldsymbol{k}} = \omega_k] \Rightarrow \frac{\omega''}{2}\frac{\partial^2}{\partial z^2} + \frac{v}{2k}\Delta_\perp \ . \qquad (6.9b)$$

T-term describes the nonlinear self-action of the waves in the package.

Optically : dependence of the refractive index of the medium on $|E|^2$.

When (5.4) is treated as a Schrödinger equation,

T-term is self-consistent attraction (at $T < 0$) or repulsive potential (at $T > 0$), that is proportional to the density of particles $N(\boldsymbol{r}, t) = |C(\boldsymbol{r}, t)|^2$.

Equation 13.2 is Hamiltonian

$$\mathcal{H} = \frac{1}{2}\int \Big[i\boldsymbol{v} \cdot (C^*\boldsymbol{\nabla} C - C\boldsymbol{\nabla} C^*) + \omega'' \left(\frac{\partial C}{\partial z}\right)^2 + \frac{v}{k}|\Delta_\perp C|^2 + 2T|C|^4 \Big]\, d^d r\,, \tag{6.10}$$

and has one more integral of motion $N = \int |C|^2 d^d r$, total number of particles.

- Boundary Problem: The wave amplitude is given at a boundary of the medium:

$$\omega'' \frac{\partial^2}{\partial z^2} \ll v\frac{\partial}{\partial z}\,, \quad z \text{ is the } \boldsymbol{v}\text{-direction} \tag{6.11}$$

- Stationary problem: $\partial C/\partial t = 0$. Then

$$\left[iv\frac{\partial}{\partial z} + \frac{v}{2k}\Delta_\perp - T|C|^2 \right] C(\boldsymbol{r}, t) = 0\ . \tag{6.12}$$

Considering $\tau = z/v$ as a new time, Equation 6.12 can be treated as a two-dimensional Schrödinger equation $(\boldsymbol{r} = x, y)$.

Evolution of Wave Packages in Unbounded Media

In the co-moving with a group velocity frame: $(\boldsymbol{v} \cdot \boldsymbol{\nabla})\, C \to 0$; ω'' retains and

$$\text{Eq. (13.2)} \ \Rightarrow \left[i\frac{\partial}{\partial t} + \frac{\omega''}{2}\frac{\partial^2}{\partial z^2} + \frac{v}{2k_0}\Delta_\perp - T|C|^2 \right] C(\boldsymbol{r}, t) = 0\ . \tag{6.13}$$

- Consider $d = 1, 2, 3$ for ω'' >0 and for the "attractive" case $T < 0$.

Let at $t = 0$ ℓ is a characteristic size of the central peak and C is an amplitude in its center. The number of particles at $t = 0$ is

$$N = \int |C|^2 d\boldsymbol{r} \simeq |C|^2 \ell^d\ . \tag{6.14a}$$

N is the integral of motion, dominated by the central peak. Thus:

$$C(t) \simeq \sqrt{N} \ell^{-d}(t) \tag{6.14b}$$

Estimation for the energy of the package:

$$\mathcal{H} \simeq \omega'' N \ell^{-2} - |T| N^2 \ell^{-d} \ . \tag{6.14c}$$

— One dimensional case: Stationary solution with

$$\ell = \ell_0 \simeq \frac{\omega''}{|T|N} \simeq \frac{\omega''}{|TC^2|\ell_0} , \tag{6.15}$$

minimizes the energy of the central peak. The rest of the energy radiates with small amplitude short waves. In this case the pressure of the particles due to their motion in the potential well balances the attractive force.

— Three dimensional case : As $\ell \to 0$ the pressure increases slower than the attractive force which leads to collapse, falling of the particles on the center over finite time. $C(t)$ and $\ell(t)$ are connected by Equation 6.14a with N – the number of the particles involved in collapse. The energy of the collapsing particle decreases (due to a "wave emission").

— Two dimensional case is marginal: the rate of the package of particles is determined by the initial conditions:

At $\omega'' > TN \simeq T|a|^2/\ell$ the minimum given by Eq. (6.15) is achieved as $\ell \to \infty$, i.e. the particles are moved away.

– Under $\omega'' < TN$ part of the package is involved in the collapse process.

- One-dimensional Soliton

Equation 6.13: $$\left[i\frac{\partial}{\partial t} + \frac{\omega''}{2}\frac{\partial^2}{\partial z^2} + \frac{v}{2k_0}\Delta_\perp - T|C|^2 \right] C(\boldsymbol{r}, t) = 0$$

for $d = 1$ (when $\Delta_\perp = 0$) and with $C(z,t) = C(z)\exp(i\lambda^2 t)$ yields

$$\omega'' \frac{d^2C}{dz^2} = 2(\lambda^2 C - |T|C^3) = -\frac{dU}{dC} , \quad U = \frac{1}{2}|T|C^4 - \lambda^2 C^2 , \tag{6.16a}$$

After $z \to t$ this is a Newtonian equation for a "particle" with mass ω'' and coordinate C moving in the field $U(C)$. Equation 6.16a conserves an "Energy":

$$E = \frac{1}{2}\omega'' \left(\frac{dC}{dz}\right)^2 + \frac{1}{2}|T|C^4 - \lambda^2 C^2 \ . \tag{6.16b}$$

– A solution C =const., $\lambda = |T|C^2$ (the particle at rest at the bottom of the well) corresponds to a plane wave. When $E > E_{\rm min}$ it results in periodical oscillations i.e. to periodical modulation of the wave $C(z)$.

– A soliton (at the rest) corresponds

$$E = 0\,,\;\; C(z,t) = \sqrt{\frac{2}{|T|}}\frac{\lambda \exp(i\lambda^2 t)}{\cosh(\sqrt{2}\lambda z/\sqrt{\omega''})}\;. \tag{6.16c}$$

Other solutions: moving solitons, two, three,.. N-soliton solutions.

- Dynamics of N-solitons solutions – inverse scattering problem

- Collapse in d=2, 3.

Let $\omega'' > 0$, $T < 0$ (attractive case).

After proper normalization:

$$i\frac{\partial \Psi}{\partial t} = \frac{\delta \mathcal{H}}{\delta \Psi}\,, \quad \mathcal{H} = \frac{1}{2}\int [|\boldsymbol{\nabla}\Psi|^2 - \frac{1}{2}|\Psi|^4]\, d\boldsymbol{r}, \tag{6.17a}$$

$$i\frac{\partial \Psi}{\partial t} + \Delta\Psi + |\Psi|^2\Psi = 0\;. \tag{6.17b}$$

Calculate:

$$\frac{\partial^2}{\partial t^2}\langle R^2\rangle = \frac{\partial^2}{\partial t^2}\int r^2|\Psi|^2 d\boldsymbol{r} = i\frac{\partial}{\partial t}\int \sum_j x_j^2 \boldsymbol{\nabla}(\Psi^*\boldsymbol{\nabla}\Psi - \Psi\boldsymbol{\nabla}\Psi^*)d\boldsymbol{r}$$

$$= -2i\frac{\partial}{\partial t}\sum_j x_j\left(\Psi\frac{\partial \Psi^*}{\partial x_j} - \Psi^*\frac{\partial \Psi}{\partial x_j}\right) d\boldsymbol{r}\;. \tag{6.18a}$$

Making use the equation of motion, integrating by parts (no terms proportional to x) one get

$$\frac{\partial^2}{\partial t^2}\langle R^2\rangle = 4\int |\boldsymbol{\nabla}\Psi|^2 d\boldsymbol{r} = 8\mathcal{H} + 2(2-d)\int |\Psi|^4 d\boldsymbol{r}\;. \tag{6.18b}$$

At $d > 2$ and $8\mathcal{H} > \partial^2\langle R^2\rangle/\partial t^2$, one has

$$\langle R^2\rangle < 4\mathcal{H}t^2 + C_1 t + C_2\,, \tag{6.18c}$$

i.e. collapse for $\mathcal{H} < 0$ ($R^2 \to 0$ in finite time).

The stationary two-dimensional solution (round wave guide) corresponds to $\mathcal{H} = 0$ with $C_1 = 0$. Unfortunately, this solution is not stable.

Exercises

TO BE PREPARED

Lecture 7.

Statistical description of weakly nonlinear waves

Background: Statistical description of random processes

Let $f_i(t)$ random function, $i = 1, \dots N-$ sample $\#$ in an ensemble.
Ensemble averaging:

$$\langle f(t) f(t') \rangle_{\rm e} \equiv \lim_{N\to\infty} \frac{1}{N} \sum_{i=1}^{N} f_i(t) f_i(t') \,, \tag{7.1a}$$

Stationarity:

$$F_2(t,t') \equiv \langle f(t) f(t') \rangle_{\rm e} \to F_2(t-t') \,, \; F_3(t-t', t-t'') \,, \dots \tag{7.1b}$$

Time averaging in stationary case:

$$\langle f(t) f(t') \rangle_t \equiv \lim_{T\to\infty} \int\limits_0^T f(t) f(t+\tau) dt \,, \tag{7.1c}$$

Ergodicity:

$$\langle ... \rangle_t = \langle ... \rangle_{\rm e} \Rightarrow \langle ... \rangle - \text{“proper averaging”} \,, \tag{7.1d}$$

Fourier transform:

$$\widetilde{f}(\omega) = \int\limits_{-\infty}^{\infty} f(t) \exp(i\omega t) dt \,, \tag{7.1e}$$

$$f(t) = \int\limits_{-\infty}^{\infty} \widetilde{f}(\omega) \exp(-i\omega t) \frac{d\omega}{2\pi} \,, \tag{7.1f}$$

Double correlation functions in t- and ω-representations

$$F_2(t - t') = \int\limits_{-\infty}^{\infty} \left\langle \widetilde{f}(\omega) \widetilde{f}(\omega') \right\rangle \exp[-i\omega t - i\omega' t'] \frac{d\omega \, d\omega'}{(2\pi)^2} \,, \tag{7.1g}$$

$$\int\limits_{-\infty}^{\infty} \exp(i\omega t) dt = 2\pi\delta(\omega) \,, \tag{7.1h}$$

Double correlator in stationary case:

$$\left\langle \widetilde{f}(\omega) \widetilde{f}(\omega') \right\rangle = 2\pi(\omega + \omega') \widetilde{F}_2(\omega) \,, \tag{7.1i}$$

(ω, τ)-relations:

$$F_2(\tau) = \int \widetilde{F}_2(\omega) \exp(-i\omega\tau) \frac{d\omega}{2\pi} , \tag{7.1j}$$

$$\widetilde{F}_2(\omega) = \int F_2(\tau) \exp(i\omega\tau) d\tau \;. \tag{7.1k}$$

Example:

$$F_2(\tau) = F_2 \exp(-\gamma|\tau|) \Leftrightarrow \widetilde{F}_2(\omega) = \frac{2\,\gamma\, F_2}{\omega^2 + \gamma^2} \;. \tag{7.1l}$$

Statistics and evolution of free fields ($\mathcal{H}_{\rm int} = 0$)

Our goal is to go from dynamical description in terms of amplitudes $|c(\boldsymbol{k}, t)|$ and phases of paves $\varphi(\boldsymbol{k}, t)$: $c(\boldsymbol{k}, t) = |c(\boldsymbol{k}, t)| \exp[i\varphi(\boldsymbol{k}, t)]$ to a kinetic description in terms of the correlation function of the wave amplitudes $n(t, \boldsymbol{k}) \equiv n_{\boldsymbol{k}}$ –

classical analog of the occupation numbers

$$n_{\rm class}(t,\boldsymbol{k}) = \hbar n_{\rm quantum}(t,\boldsymbol{k}) \equiv \hbar N_{\boldsymbol{k}},\ \ N_k \gg 1\ . \tag{7.2}$$

At $\mathcal{H}_{\rm int}=0$ $|c(\boldsymbol{k},t)| = \text{const.}$ $\varphi(\boldsymbol{k},t)\equiv\varphi_k=\omega(\boldsymbol{k})t.$ Thus

$$\langle c_k\rangle = \langle |c_k| \exp(i\varphi_k)\rangle = 0\,, \tag{7.3a}$$

$$\langle c_k c_{k'}\rangle = \langle |c_k||c_{k'}| \exp(i\varphi_k + i\varphi_{k'})\rangle = 0\,, \tag{7.3b}$$

$$\langle c_k c^*_{k'}\rangle = \langle |c_k||c_{k'}| \exp(i\varphi_k - i\varphi_{k'})\rangle = n(k)\Delta_{\boldsymbol{k}\boldsymbol{k}'}\,, \tag{7.3c}$$

$$\langle c^*_1 c^*_2 c_3 c_4\rangle = n(\boldsymbol{k}_1)n(\boldsymbol{k}_2)[\Delta_{13}\Delta_{24}+\Delta_{14}\Delta_{23}]\,, \tag{7.3d}$$

$$\langle c^*_1 c^*_2 c^*_3 c_4 c_5 c_6\rangle = n_1 n_2 n_3\big[\Delta_{14}(\Delta_{25}\Delta_{36}+\Delta_{26}\Delta_{35}) \tag{7.3e}$$

$$+\Delta_{15}(\Delta_{24}\Delta_{36}+\Delta_{26}\Delta_{34}) + \Delta_{16}(\Delta_{24}\Delta_{35}+\Delta_{25}\Delta_{34})\big]\,, \dots \tag{7.3f}$$

Gaussian decomposition of high-order correlators "by all possible pairing".

- Kinetic equation for $\mathcal{H}_{\rm int}=0$, Temperature $\Theta\neq 0$

Consider Equation 4.2 with $\mathcal{H}_{\rm int}=0$ and Langevin random force $f_{\boldsymbol{k}}(t)$:

$$\frac{\partial c_{\boldsymbol{k}}(t)}{\partial t} = -(i\omega_{\boldsymbol{k}}+\gamma_{\boldsymbol{k}})c_{\boldsymbol{k}} + f_{\boldsymbol{k}}\,, \tag{7.4a}$$

$$F_{\boldsymbol{k}}(\tau) \equiv \langle f_{\boldsymbol{k}}(\tau) f^*_{\boldsymbol{k}}(0)\rangle = 2\gamma_{\boldsymbol{k}} n_{0\boldsymbol{k}} d(\tau)\,, \tag{7.4b}$$

Here Rayleigh-Jeans (thermodynamic-equilibrium) distribution

$$n_{0\boldsymbol{k}} = \Theta/\omega_{\boldsymbol{k}}\ . \tag{7.4c}$$

Compute:

$$\frac{\partial n_{\boldsymbol{k}}}{\partial t} = 2\text{Re}\left\langle \frac{\partial c_{\boldsymbol{k}}}{\partial t} c^*_k \right\rangle = -2\gamma_{\boldsymbol{k}} n_{\boldsymbol{k}} + 2\text{Re}\langle f_{\boldsymbol{k}}(t) c^*_k(t)\rangle\ , \tag{7.5a}$$

and define different-time correlation function

$$\Psi_{\boldsymbol{k}}(\tau) \equiv \langle f_{\boldsymbol{k}}(\tau) c^*_k(0)\rangle\ = \int \widetilde{\Psi}_{\boldsymbol{k}\omega} \exp(i\omega\tau)\frac{d\omega}{2\pi}\,, \tag{7.5b}$$

(7.5c)

To find $\widetilde{\Psi}_{\boldsymbol{k}\omega}$ consider Equation 7.4a in ω-representation:

$$[i(\omega_{\boldsymbol{k}}-\omega)+\gamma_{\boldsymbol{k}}]\widetilde{c}_{\boldsymbol{k}}(\omega) = \widetilde{f}_{\boldsymbol{k}}(\omega) \tag{7.5d}$$

giving

$$\widetilde{\Psi}_{\boldsymbol{k}\omega} = \frac{\widetilde{F}_{\boldsymbol{k}\omega}}{[i(\omega_{\boldsymbol{k}} - \omega) + \gamma_{\boldsymbol{k}}]}\,, \qquad \widetilde{F}_{\boldsymbol{k}\omega} = 2\gamma_{\boldsymbol{k}} n_{0\boldsymbol{k}}\,, \tag{7.5e}$$

Now in Equation 7.5a

$$\langle f_{\boldsymbol{k}}(t) c_k^*(t)\rangle = \text{Re}\Psi_{\boldsymbol{k}}(0) = \text{Re}\int \widetilde{\Psi}_{\boldsymbol{k}\omega}\frac{d\omega}{2\pi} = \gamma_{\boldsymbol{k}} n_{0\boldsymbol{k}}\ . \tag{7.5f}$$

This gives kinetic equation of free waves, interacting with the thermostat:

$$\frac{\partial n_{\boldsymbol{k}}}{2\partial t} = \gamma_{\boldsymbol{k}}(n_{0\boldsymbol{k}} - n_{\boldsymbol{k}})\ . \tag{7.6a}$$

It describes relaxation to the thermodynamic equilibrium with the relaxation time $1/2\,\gamma_{\boldsymbol{k}}$:

$$n_{\boldsymbol{k}}(t) = [n_{\boldsymbol{k}}(0) - n_{0\boldsymbol{k}}]\ \text{exp}(-2\gamma_k t) + n_{0\boldsymbol{k}}\,, \tag{7.6b}$$

- Space Inhomogeneity, but $\mathcal{H}_{\text{int}} = 0$, and temperature $\Theta = 0$:

  Let

$$\mathcal{H}_2 = \int \Omega_{\boldsymbol{k}\boldsymbol{k}'} c_{\boldsymbol{k}} c^*_{\boldsymbol{k}'} d\boldsymbol{k} d\boldsymbol{k}'\,, \tag{7.7a}$$

Recall: in homogeneous case $\qquad \Omega_{\boldsymbol{k}\boldsymbol{k}'} = \omega_{\boldsymbol{k}}\delta(\boldsymbol{k} - \boldsymbol{k}')$.

With $\mathcal{H}_2$, Eq. (7.7a), motion equation becomes:

$$\left[\frac{\partial}{\partial t} + \gamma_{\boldsymbol{k}}\right] c_{\boldsymbol{k}} + i\int \Omega_{\boldsymbol{k}\boldsymbol{k}'} c_{\boldsymbol{k}'} d\boldsymbol{k}' = 0\,, \tag{7.7b}$$

Define:

$$N_{\boldsymbol{k}\boldsymbol{k}'}(t) \equiv \langle c_{\boldsymbol{k}} c^*_{\boldsymbol{k}'}\rangle\ ,\quad n_{\boldsymbol{k}}(\boldsymbol{r}) \equiv \int N_{\boldsymbol{k}'\boldsymbol{k}''}\ \text{exp}(i\boldsymbol{\kappa}\cdot r) d\boldsymbol{\kappa}\,, \tag{7.7c}$$

$$\boldsymbol{k}' = \boldsymbol{k} + \frac{1}{2}\kappa\,, \quad \boldsymbol{k}'' = \boldsymbol{k} - \frac{1}{2}\boldsymbol{\kappa} \tag{7.7d}$$

and using Equation 7.7b derive

$$\frac{\partial N_{\boldsymbol{k}'\boldsymbol{k}''}}{\partial t} = -(\gamma_{\boldsymbol{k}'} + \gamma_{\boldsymbol{k}''}) N_{\boldsymbol{k}'\boldsymbol{k}''} - i\int (\Omega_{\boldsymbol{k}'1} n_{1\boldsymbol{k}''} - \Omega_{1\boldsymbol{k}''} n_{\boldsymbol{k}'1}) d1 \tag{7.7e}$$

Replacing $\boldsymbol{k}' - \boldsymbol{k}_1 = \kappa'$, $\boldsymbol{k}' - \boldsymbol{k}_1 = \kappa'$ and substituting inverse of Equation 7.7c

$$N_{\boldsymbol{k}'\boldsymbol{k}''} = \int n_{\boldsymbol{k}}(\boldsymbol{r})\ \text{exp}(-i\boldsymbol{\kappa}\cdot r)\frac{d\boldsymbol{r}}{(2\pi)^3}\,, \tag{7.7f}$$

one gets

$$\left(\frac{\partial}{\partial t}+2\gamma_{\boldsymbol{k}}\right)n_{\boldsymbol{k}}(\boldsymbol{r})=-i\int\frac{d\boldsymbol{r}'d\boldsymbol{r}''}{(2\pi)^6}d\kappa'd\kappa'' \tag{7.7g}$$

$$\times\ \exp\left[i\kappa'\cdot(\boldsymbol{r}-\boldsymbol{r}')+i\kappa''\cdot(\boldsymbol{r}-\boldsymbol{r}'')\right]$$

$$\times\left[\omega_{\boldsymbol{k}+\kappa''/2}(\boldsymbol{r}')n_{\boldsymbol{k}-\kappa'/2}(\boldsymbol{r}'')-\omega_{\boldsymbol{k}-\kappa''/2}(\boldsymbol{r}')n_{\boldsymbol{k}+\kappa'/2}(\boldsymbol{r}'')\right]\ ,$$

where $$\omega_{\boldsymbol{k}}(r)\equiv\int\Omega_{\boldsymbol{k}'\boldsymbol{k}''}\exp(i\boldsymbol{\kappa}\cdot r)d\boldsymbol{\kappa}\ . \tag{7.7h}$$

Expanding $$[...]\simeq\left[\frac{\partial\omega_{\boldsymbol{k}}(\boldsymbol{r}')}{\partial\boldsymbol{k}}\cdot\kappa''n_{\boldsymbol{k}}(\boldsymbol{r}'')-\frac{\partial n_{\boldsymbol{k}}(\boldsymbol{r}'')}{\partial\boldsymbol{k}}\cdot\kappa'\omega_{\boldsymbol{k}}(\boldsymbol{r}')\right], \tag{7.7i}$$

and noticing that in r-representation $$i\kappa'\to\frac{\partial}{\partial\boldsymbol{r}'}\,,\ i\kappa''\to\frac{\partial}{\partial\boldsymbol{r}''}\,, \tag{7.7j}$$

one finally gets kinetic equation for $n_k(r)$ in inhomogeneous media

$$\left(\frac{\partial}{\partial t}+2\gamma_{\boldsymbol{k}}\right)n_{\boldsymbol{k}}(\boldsymbol{r})+\left[\frac{\partial\omega_{\boldsymbol{k}}(\boldsymbol{r})}{\partial\boldsymbol{k}}\cdot\frac{\partial n_{\boldsymbol{k}}(\boldsymbol{r})}{\partial\boldsymbol{r}}-\frac{\partial n_{\boldsymbol{k}}(\boldsymbol{r})}{\partial\boldsymbol{k}}\cdot\frac{\partial\omega_{\boldsymbol{k}}(\boldsymbol{r})}{\partial\boldsymbol{r}}\right]=0\ . \tag{7.8}$$

Mean-field approximation (linear in $\mathcal{H}_{\rm int}$)

Consider 4-wave equation of motion in homogeneous media

$$\left[\frac{\partial}{\partial t}+\gamma_{\boldsymbol{k}}\right]c_{\boldsymbol{k}}+i\omega_{\boldsymbol{k}}c_{\boldsymbol{k}}=-\frac{i}{2}\sum_{\boldsymbol{k}+1=\boldsymbol{2}+\boldsymbol{3}}T_{\boldsymbol{k}1,\boldsymbol{23}}\,c_1^*c_{\boldsymbol{2}}c_{\boldsymbol{3}}\,, \tag{7.9a}$$

in which $T_{\boldsymbol{k}1,\boldsymbol{23}}$ has non-hamiltonian part (origin of which will be clarified later):

$$\eta_{\boldsymbol{k}\boldsymbol{k}'}\equiv\frac{i}{2}\left[T((\boldsymbol{k},\boldsymbol{k}';\boldsymbol{k},\boldsymbol{k}')-T^*(\boldsymbol{k},\boldsymbol{k}';\boldsymbol{k},\boldsymbol{k}')\right] \tag{7.9b}$$

and derive straightforwardly:

$$\frac{\partial n_{\boldsymbol{k}}}{\partial t}=-2\gamma_{\boldsymbol{k}}n_{\boldsymbol{k}}-\frac{i}{2}\sum_{\boldsymbol{k}+1=\boldsymbol{2}+\boldsymbol{3}}\left[T_{\boldsymbol{k}1,\boldsymbol{23}}\,\langle c_{\boldsymbol{k}}^*c_1^*c_{\boldsymbol{2}}c_{\boldsymbol{3}}\rangle-T^*_{\boldsymbol{k}1,\boldsymbol{23}}\,\langle c_{\boldsymbol{k}}^*c_1^*c_{\boldsymbol{2}}c_{\boldsymbol{3}}\rangle\right].$$

With the Gaussian decomposition, Equation 7.3d, one finally has

$$\frac{\partial n_{\boldsymbol{k}}}{\partial t}=-2\left(\gamma_{\boldsymbol{k}}+\sum_{\boldsymbol{k}'}\eta_{\boldsymbol{k}\boldsymbol{k}'}n_{\boldsymbol{k}'}\right)n_{\boldsymbol{k}}\ . \tag{7.9c}$$

In general, for slow space inhomogeneity one has

Mean-Field Equation for the "Number" of Quasi-Particles:

$$\frac{\partial n(\boldsymbol{k},r,t)}{\partial t} + 2\Gamma(\boldsymbol{k},r)n(\boldsymbol{k},r,t) \tag{7.10a}$$
$$+\left[\frac{\partial \omega_{_{\rm NL}}(\boldsymbol{k},r)}{\partial \boldsymbol{k}}\cdot\frac{\partial n(\boldsymbol{k},r,t)}{\partial r} - \frac{\partial \omega_{_{\rm NL}}(\boldsymbol{k},r)}{\partial r}\cdot\frac{\partial n(\boldsymbol{k},r,t)}{\partial \boldsymbol{k}}\right] = 0\,,$$

with Self-consistent "nonlinear" frequency

$$\omega_{_{\rm NL}}(\boldsymbol{k},r,t) = \omega(\boldsymbol{k},r) + 2\int T(\boldsymbol{k},\boldsymbol{k}')n(\boldsymbol{k}',r,t)d\boldsymbol{k}'\,, \tag{7.10b}$$

and Self-consistent "nonlinear" damping:

$$\Gamma(\boldsymbol{k},r,t) = \gamma(\boldsymbol{k}) + 2\int \eta(\boldsymbol{k},\boldsymbol{k}')n(\boldsymbol{k}',r,t)d\boldsymbol{k}'\,. \tag{7.10c}$$

Some solutions of these equations and their analysis will be discussed later.

Approximation of kinetic equation (quadratic in $\mathcal{H}_{\rm int}$)

- The three-wave Classical Kinetic Equation (KE)

With the 3-wave interaction Hamiltonian, given by Equation 3.14a, one derives

$$\frac{\partial n_{\boldsymbol{k}}(t)}{\partial t} = \mathrm{Im}\int [\frac{1}{2}V_{\boldsymbol{k},\mathbf{12}}J_{\boldsymbol{k},\mathbf{12}}\delta_{\boldsymbol{k}-\boldsymbol{k}_1-\boldsymbol{k}_2} \tag{7.11a}$$
$$-V_{\mathbf{1},\boldsymbol{k}\mathbf{2}}J_{\mathbf{1},\boldsymbol{k}\mathbf{2}}\delta_{\boldsymbol{k}_1-\boldsymbol{k}-\boldsymbol{k}_2}]\,d\mathbf{1}\,d\mathbf{2}\,,\quad d\boldsymbol{j}\equiv d\boldsymbol{k}_j\,.$$

We replaced $\sum_{\boldsymbol{k}} \Rightarrow \frac{V}{(2\pi)^3}\int d\boldsymbol{k}$, redefined accordingly $V_{\boldsymbol{k},\mathbf{12}}$ and introduced

$$\langle b_{\mathbf{1}}^* b_{\mathbf{2}} b_{\mathbf{3}}\rangle = J_{\mathbf{1},\mathbf{23}}\,\delta(\boldsymbol{k}_1-\boldsymbol{k}_2-\boldsymbol{k}_3)\,,\quad \text{triple correlation function.} \tag{7.11b}$$

$J_{\mathbf{1},\mathbf{23}} = 0$ for a free field. Compute:

$$[i\frac{\partial}{\partial t} + (\omega_{\mathbf{1}}-\omega_{\mathbf{2}}-\omega_{\mathbf{3}})]J_{\mathbf{1},\mathbf{23}} = \int [-\frac{1}{2}V^*_{\mathbf{1},\mathbf{45}}J_{\mathbf{45},\mathbf{23}}\delta_{\boldsymbol{k}_1-\boldsymbol{k}_4-\boldsymbol{k}_5}$$
$$V^*_{\mathbf{4},\mathbf{25}}J_{\mathbf{15},\mathbf{34}}\delta_{\boldsymbol{k}_4-\boldsymbol{k}_2-\boldsymbol{k}_5} + V^*_{4,35}J_{\mathbf{15},\mathbf{24}}\delta_{\boldsymbol{k}_4-\boldsymbol{k}_3-\boldsymbol{k}_5}]\,d\boldsymbol{k}_4 d\boldsymbol{k}_5\,. \tag{7.11c}$$

Here $\langle c_{\mathbf{1}}^* c_{\mathbf{2}}^* c_{\mathbf{3}} c_{\mathbf{4}}\rangle = J_{\mathbf{12},\mathbf{34}}\delta(\boldsymbol{k}_1+\boldsymbol{k}_2-\boldsymbol{k}_3-\boldsymbol{k}_4)$ – quadruple correlator which can be taken for the free field:

$$J_{\mathbf{12},\mathbf{34}} = n_1 n_2[\delta(\boldsymbol{k}_1-\boldsymbol{k}_3)+\delta(\boldsymbol{k}_1-\boldsymbol{k}_4)]\,. \tag{7.11d}$$

This gives: $$\left[i\frac{\partial}{\partial t}+(\omega_1-\omega_2-\omega_3)\right]J_{\mathbf{1,23}}=-V^*_{\mathbf{1,23}}\mathcal{N}_{1,23}\,, \tag{7.11e}$$
$$\mathcal{N}_{1,23}\equiv n_2n_3-n_1(n_3+n_2)\ . \tag{7.11f}$$

In the spirit of perturbational approach one neglects time dependence of $J_{\mathbf{1,23}}$:

$$J_{\mathbf{1,23}}(t)=-\frac{V^*_{\mathbf{123}}\mathcal{N}_{1,23}}{\omega_{\mathbf{1}}-\omega_{\mathbf{2}}-\omega_{\mathbf{3}}+i\delta}\ . \tag{7.11g}$$

The term $i\delta$ specifies how to circumvent the pole. Finally, from Eqs. (7.11a), (7.11g) one has The Three-Wave Classical KE:

$$\frac{\partial n(\boldsymbol{k},t)}{\partial t}=\pi\int\Big[\frac{1}{2}\left|V_{\boldsymbol{k},\mathbf{12}}\right|^2\mathcal{N}_{\boldsymbol{k},\mathbf{12}}\delta(\boldsymbol{k}-\boldsymbol{k}_1-\boldsymbol{k}_2)\delta(\omega_{\boldsymbol{k}}-\omega_{\mathbf{1}}-\omega_2)$$
$$+|V_{1,\boldsymbol{k}2}|^2\mathcal{N}_{\mathbf{1},\boldsymbol{k}\mathbf{2}}\delta(\boldsymbol{k}_1-\boldsymbol{k}-\boldsymbol{k}_2)\delta(\omega_{\mathbf{1}}-\omega_{\boldsymbol{k}}-\omega_{\mathbf{2}})\Big]\,d\boldsymbol{k}_1d\boldsymbol{k}_2\ . \tag{7.12}$$

- The four-wave Classical Kinetic Equation

With the 4-wave Equation 6.1b of motion, which accounts for the contribution of the 3-wave (forbidden) processes into full scattering amplitude $T_{\boldsymbol{k}\mathbf{1},\mathbf{23}}$, one derives

$$\frac{\partial n_{\boldsymbol{k}}(t)}{\partial t}=\mathrm{Im}\int T_{\boldsymbol{k}\mathbf{1},\mathbf{23}}J_{\boldsymbol{k}\mathbf{1},\mathbf{23}}\delta(\boldsymbol{k}+\boldsymbol{k}_1-\boldsymbol{k}_2-\boldsymbol{k}_3)\,d\boldsymbol{k}_1d\boldsymbol{k}_2d\boldsymbol{k}_3\ , \tag{7.13a}$$

where $J_{\boldsymbol{k}\mathbf{1},\mathbf{23}}$ is 4th-order correlator. In 0-th order in $\mathcal{H}_4$ one finds $J^{(0)}_{\boldsymbol{k}\mathbf{1},\mathbf{23}}$ by the Gaussian decomposition, Equation 7.3d:

$$\frac{\partial n(\boldsymbol{k},t)}{\partial t}=n(\boldsymbol{k},t)\mathrm{Im}\int T_{\boldsymbol{k}\boldsymbol{k}'\boldsymbol{k}\boldsymbol{k}'}n(\boldsymbol{k}')\,d\boldsymbol{k}'\ . \tag{7.13b}$$

This is the mean-field approximation. In the 1st order in $\mathcal{H}_4$ one has

$$J^{(1)}_{\boldsymbol{k}\mathbf{1},\mathbf{23}}=\frac{T^*_{\mathbf{1234}}\mathcal{N}_{\boldsymbol{k}\mathbf{1},\mathbf{23}}}{\omega_1+\omega_2-\omega_3-\omega_4+i\delta}\,, \tag{7.13c}$$
$$\mathcal{N}_{\boldsymbol{k}\mathbf{1},\mathbf{23}}\equiv n_{\mathbf{2}}n_{\mathbf{3}}(n_{\mathbf{1}}+n_{\boldsymbol{k}})-n_{\mathbf{1}}n_{\boldsymbol{k}}(n_{\mathbf{2}}+n_{\mathbf{3}})\ . \tag{7.13d}$$

In $J^{(1)}_{\boldsymbol{k}\mathbf{1},\mathbf{23}}$ the 6-th order correlator $J_{\mathbf{123},\mathbf{456}}$ was decomposed to $\mathcal{N}_{\mathbf{12},\mathbf{34}}$ according to Equation 7.3f and we neglected the time derivative of $J^{(1)}_{\mathbf{12},\mathbf{34}}$ like in the 3-wave case. This finally gives The Four-Wave Classical KE:

$$\frac{\partial n(\boldsymbol{k},t)}{\partial t} = \frac{\pi}{2}\int \left|T_{\boldsymbol{k}\mathbf{1},\mathbf{23}}\right|^2 \mathcal{N}_{\boldsymbol{k}\mathbf{1},\mathbf{23}}\,\delta(\boldsymbol{k}+\mathbf{1}-\mathbf{2}-\mathbf{3}) \\ \times\ \delta(\omega_{\boldsymbol{k}}+\omega_1-\omega_2-\omega_3)\,d\mathbf{1}d\mathbf{2}d\mathbf{3}\ . \tag{7.14}$$

Applicability limits for kinetic equations

- Applicability Criterion of the Three-wave kinetic Equation 7.12

– Phase-randomization Estimate:

Consider a broad packet $n(\boldsymbol{k},t)$ with the $\boldsymbol{k}$-width $\Delta k \simeq k$ and $\omega_{\boldsymbol{k}}$-width $\Delta\omega_k$. The characteristic time of $n(\boldsymbol{k},t)$-variation is $\tau_{\boldsymbol{k}} = 1/\gamma_{\boldsymbol{k}}$, where

$$\gamma_{\boldsymbol{k}} \simeq \left|V_{k,kk}\right|^2 \frac{n_k k^d}{\Delta\omega_{\boldsymbol{k}}} \simeq \left|V_{kkk}\right|^2 \frac{N}{\Delta\omega_k}\,,\ \ N \equiv \int n(\boldsymbol{k})\,d\boldsymbol{k} \approx n_k k^d\ . \tag{7.15a}$$

For applicability of the random-phase approximation $\tau_{\boldsymbol{k}} \gg \mathcal{T}_k \approx 1/\Delta\omega_k$, phase randomization time, or $\xi_1(\boldsymbol{k}) \equiv \gamma_k/\Delta\omega_k \ll 1$. It gives

$$\xi_1(\boldsymbol{k}) = \left|V_{kkk}\right|^2 N/(\Delta\omega_{\boldsymbol{k}})^2 \ll 1\ . \tag{7.15b}$$

– Weakness-interaction estimate: Validity of perturbation theory: $\xi_2 \ll 1$.

$$\xi_2(\boldsymbol{k}) \equiv \frac{\langle\mathcal{H}_3\rangle}{\langle\mathcal{H}_2\rangle} = \frac{\mathrm{Re}\int V_{123} J_{123} \delta_{\boldsymbol{k}_1-\boldsymbol{k}_2-\boldsymbol{k}_3}\, d\boldsymbol{k}_1 d\boldsymbol{k}_2 d\boldsymbol{k}_3}{\int \omega(\boldsymbol{k}) n(\boldsymbol{k})\,d\boldsymbol{k}} \tag{7.16a}$$

Using Equation 7.11g one gets:

$$\xi_2(\boldsymbol{k}) = \int \frac{\left|V_{123}\right|^2 \mathcal{N}_{123}}{\omega_1-\omega_2-\omega_3}\,\delta_{\boldsymbol{k}_1-\boldsymbol{k}_2-\boldsymbol{k}_3}\,\frac{d\boldsymbol{k}_1 d\boldsymbol{k}_2 d\boldsymbol{k}_3}{\int \omega(\boldsymbol{k}) n(\boldsymbol{k})\,d\boldsymbol{k}}\ . \tag{7.16b}$$

For the wave packet with $\Delta k \simeq k$ it gives the same estimate: $\xi_1 \simeq \xi_2$.

– Estimate for Narrow Packages:

Consider interaction of 3 narrow packets with amplitudes $c_j \approx c_{\max} \simeq \sqrt{N}$ and the widths $\ell_j \approx \ell \simeq 1/\Delta k$, $j = 1, 2, 3$.

Interaction time (from 3-wave Bloembergen eqs.)

$$\tau_{\rm int} \simeq \left[|V_{123} c_{\max}|\right]^{-1} \tag{7.17a}$$

. Their overlapping or I collision time is

$$\tau_{\rm col} \simeq \ell / v_{123}\,, \quad v_{123} = \max\Big[|\boldsymbol{v}_1 - \boldsymbol{v}_2|, |\boldsymbol{v}_1 - \boldsymbol{v}_3|, |\boldsymbol{v}_2 - \boldsymbol{v}_3|\Big]\,. \tag{7.17b}$$

If $t_{\rm int} \gg t_{\rm col}$, the amplitude and phase of each packet will change only slightly during one collision. The interaction of an ensemble of such packets may be described statistically, i.e by KE. Thus – Applicability criterion of the 3-wave KE for narrow packages

$$\xi_{123} \equiv \frac{\tau_{\rm col}}{\tau_{\rm int}} \ll 1\,, \quad \xi_{123} \sim \frac{\ell \big|V_{123} c_{\max}\big|}{v_{1,23}} \sim \frac{\big|V_{123}\big|\sqrt{N}}{\Delta k \cdot v_{123}} \ll 1\,. \tag{7.17c}$$

For wide packages

$$\Delta k \sim k, \quad v_{123} \sim v \sim \frac{\omega_k}{k} \;\Rightarrow\; \xi_{123} \sim \big|V_{123}\big| \frac{\sqrt{N}}{\omega_k} \sim \sqrt{\xi_1(k)}\,. \tag{7.17d}$$

For acoustic waves

$$\omega(k) = c\, k\,, \boldsymbol{k}_1 \parallel \boldsymbol{k}_2 \parallel \boldsymbol{k}_3\,, \quad \boldsymbol{v}_1 = \boldsymbol{v}_2 = \boldsymbol{v}_3 = c\boldsymbol{k}_j / k_j \tag{7.17e}$$

and $v_{123} = 0$. Therefore

The classical KE isinapplicable at any sound amplitudes.

For applicability of the KE one needs deviations from linear dispersion law:

For $\omega(k) = a k^{1+\varepsilon}$

$$0 < \varepsilon \ll 1\,, \quad \xi_{123} \simeq \frac{|V_{123}\sqrt{N}}{v \Delta k \sqrt{\varepsilon}}\,. \tag{7.17f}$$

For $\omega(k) = C_s k(1 + \boldsymbol{\mu}\, k^2)$

$$\mu\, k^2 \ll 1\,, \quad \xi_{123} \simeq \frac{|V_{123}\sqrt{N}}{C_s \Delta k\, \sqrt{\mu}\, k} \tag{7.17g}$$

- Applicability Criterion of the Four-Wave Kinetic Equation 7.14

Interaction time is

$$\frac{1}{\tau_{\rm int}} \approx |T c_{\rm max}|^2 \simeq TN\ . \tag{7.18a}$$

The most strict applicability criterion is due to self-interaction within one narrow in the $\boldsymbol{k}$-space wave package: the interaction process must be restricted by the diffusion of the package during the time

$$\tau_{\rm dif} \sim \frac{1}{\omega''(\Delta k)^2} \tag{7.18b}$$

For applicability of the Four-Wave Kinetic Equation 7.14 one has

$$\xi_k \simeq \frac{\tau_{\rm dif}}{\tau_{\rm int}} \simeq \frac{TN}{\omega''(\Delta k)^2} \ll 1\ . \tag{7.18c}$$

Quantum kinetic equations

- Three-Wave Quantum Kinetic Equation

$$\frac{\partial N(\boldsymbol{k},t)}{\partial t} = \frac{\pi\hbar}{2}\int \Big[|V_{\boldsymbol{k},\mathbf{12}}|^2 F_{\boldsymbol{k},\mathbf{12}}\delta(\omega_k - \omega_1 - \omega_2)\delta(\boldsymbol{k} - \mathbf{1} - \mathbf{2}) - |V_{\mathbf{1},\boldsymbol{k}\mathbf{2}}|^2 F_{\mathbf{1},\boldsymbol{k}\mathbf{2}}\delta(\omega_{\mathbf{1}} - \omega_{\boldsymbol{k}} - \omega_{\mathbf{2}})\delta(\mathbf{1} - \boldsymbol{k} - \mathbf{2})\Big]\, d\mathbf{1}d\mathbf{2}\ . \tag{7.19a}$$

Here $F_{\boldsymbol{k},\mathbf{12}}$ accounts for a difference between the probability of direct and inverse processes:

$$F_{\boldsymbol{k},\mathbf{12}} = (N_{\mathbf{1}}+1)N_{\mathbf{2}}N_{\mathbf{3}} - N_{\mathbf{1}}(N_{\mathbf{2}}+1)(N_{\mathbf{3}}+1) = N_{\mathbf{2}}N_{\mathbf{3}} - N_{\mathbf{1}}(N_{\mathbf{2}}+N_{\mathbf{3}}+1)\ . \tag{7.19b}$$

If we neglect the unity in this expression and replace $N(k_j)$ by $\hbar n(k_j)$, the quantum KE will turn into the classical Kinetic Equation 7.12.

- Four-Wave Quantum Kinetic Equation

$$\frac{\partial N(\boldsymbol{k},t)}{\partial t} = \frac{\pi\hbar}{2}\int |T_{k123}|^2 F_{\boldsymbol{k}\mathbf{1},\mathbf{23}}\,\delta(\omega_{\boldsymbol{k}}+\omega_{\mathbf{1}}-\omega_{\mathbf{2}}-\omega_{\mathbf{3}}) \times \delta(\boldsymbol{k}+\mathbf{1}-\mathbf{2}-\mathbf{3})\,d\mathbf{1}d\mathbf{2}d\mathbf{3}\,, \tag{7.20a}$$

$$F_{\boldsymbol{k}\mathbf{1},\mathbf{23}} = (N_{\boldsymbol{k}}+1)(N_{\mathbf{1}}+1)N_{\mathbf{2}}N_{\mathbf{3}} - N_{\boldsymbol{k}}N_{\mathbf{1}}(N_{\mathbf{2}}+1)(N_{\mathbf{3}}+1) = N_{\mathbf{2}}N_{\mathbf{3}}(N_{\mathbf{1}}+N_{\boldsymbol{k}}+1) - N_{\mathbf{1}}N_{\boldsymbol{k}}(N_{\mathbf{2}}+N_{\mathbf{3}}+1)\,. \tag{7.20b}$$

As expected, it goes in to the classical Kinetic Equation 7.14 at $N_{\boldsymbol{k}} \gg 1$.

Exercises

TO BE PREPARED

Lecture 8.

Dissipative Self-Consistent Dynamics

Background: Nature of Nonlinear Damping

Consider 3-wave interaction of high- and low- frequency waves, $\omega_{\boldsymbol{k}} \gg \Omega_{\boldsymbol{k}}$ (Light scattering on phonos, Lengmuir wave scattering on ion sound, etc) with

$$\mathcal{H} = \sum_{\boldsymbol{k}} \omega_{\boldsymbol{k}} a_{\boldsymbol{k}} a^*_{\boldsymbol{k}} + \sum_{\boldsymbol{q}} \Omega_{\boldsymbol{q}} b_{\boldsymbol{q}} b^*_{\boldsymbol{q}} + \sum_{\boldsymbol{k}=\boldsymbol{k}'+\boldsymbol{q}} \left[V^*_{\boldsymbol{k};\boldsymbol{k}',\boldsymbol{q}} a^*_{\boldsymbol{k}} a_{\boldsymbol{k}'} b_{\boldsymbol{q}} + \text{c.c} \right] \ . \tag{8.1a}$$

Dynamical motion equations, accounting for damping of waves are

$$\frac{\partial a_{\boldsymbol{k}}}{\partial t} + (\gamma_{\boldsymbol{k}} + i\omega_{\boldsymbol{k}}) a_{\boldsymbol{k}} = -i \sum_{\boldsymbol{k}=\boldsymbol{k}'+\boldsymbol{q}} \left[V^*_{\boldsymbol{k};\boldsymbol{k}',q} b_{\boldsymbol{q}} + V_{\boldsymbol{k}';\boldsymbol{k},-q} b^*_{-\boldsymbol{q}} \right] a_{\boldsymbol{k}'} \ , \tag{8.1b}$$

$$\frac{\partial b_{\boldsymbol{q}}}{\partial t} + (\Gamma_{\boldsymbol{q}} + i\Omega_{\boldsymbol{q}}) b_{\boldsymbol{q}} = -i \sum_{\boldsymbol{k}=\boldsymbol{k}'+\boldsymbol{q}} V_{\boldsymbol{k};\boldsymbol{k}',q} a_{\boldsymbol{k}} a^*_{\boldsymbol{k}'} \Delta_{\boldsymbol{k},\boldsymbol{k}'+\boldsymbol{q}} \ . \tag{8.1c}$$

Our goal is statistical description of high-frequency waves in terms of $n_{\boldsymbol{k}} = \langle a_{\boldsymbol{k}} a^*_{\boldsymbol{k}} \rangle$. Directly from Equation 8.1b one gets

$$\left(\frac{\partial}{\partial t} + 2\gamma_{\boldsymbol{k}}\right) n_{\boldsymbol{k}} = 2 \,\mathrm{Im} \sum_{\boldsymbol{k}=\boldsymbol{k}'+\boldsymbol{q}} \Big[V^*_{\boldsymbol{k};\boldsymbol{k}',q} \langle b_{\boldsymbol{q}} a^*_{\boldsymbol{k}} a_{k'} \rangle + V_{\boldsymbol{k}';\boldsymbol{k},-q} \langle b^*_{-\boldsymbol{q}} a_{\boldsymbol{k}} a_{\boldsymbol{k}'} \rangle \Big] \,. \tag{8.2a}$$

Next step is to compute the triple correlators $\langle \ldots \rangle$, which is convenient to do in the ω-representation:

$$\langle b_{\boldsymbol{q}} a^*_{\boldsymbol{k}} a_{k'} \rangle = \int \frac{d\Omega d\omega d\omega'}{(2\pi)^3} \exp[-i(\Omega - \omega + \omega')t] \langle b_{\boldsymbol{q}\Omega} a^*_{\boldsymbol{k}\omega} a_{k'\omega'} \rangle. \tag{8.2b}$$

Fourier transform $b_{\boldsymbol{q}\,\Omega} \equiv \int b_{\boldsymbol{q}}\,(t) \exp\,(i\Omega t)\, dt$, (7.1e), one finds from Equation 8.1c:

$$b_{\boldsymbol{q}\Omega} = -i \sum_{\boldsymbol{k}=\boldsymbol{k}'+\boldsymbol{q}} V_{\boldsymbol{k};\boldsymbol{k}',q} \int \frac{d\omega_1 d\omega_2 \delta(\Omega + \omega' - \omega) a_{\boldsymbol{k}\omega_1} a^*_{\boldsymbol{k}'\omega_2}}{2\pi[\Gamma_{\boldsymbol{q}} + i(\Omega_{\boldsymbol{q}} - \Omega)]} \tag{8.2c}$$

This allows one to present Equation 8.2b as

$$\langle b_{\boldsymbol{q}} a^*_{\boldsymbol{k}} a_{k'} \rangle = -i \sum_{\boldsymbol{k}=\boldsymbol{k}'+\boldsymbol{q}} V_{\boldsymbol{k};\boldsymbol{k}',q} \int \frac{d\omega_1 d\omega_2 d\omega d\omega' \Big\langle a_{\boldsymbol{k}\omega_1} a^*_{\boldsymbol{k}'\omega_2} a^*_{\boldsymbol{k}\omega} a_{k'\omega'} \Big\rangle}{(2\pi)^4[\Gamma_{\boldsymbol{q}} + i(\Omega_{\boldsymbol{q}} + \omega' - \omega)]} \,. \tag{8.2d}$$

In the spirit of the mean-field approximation, linear in $\mathcal{H}_{\text{int}}$, one should consider in Eq. (8.2d) $\langle \ldots \rangle$ as free-field correlator and can find it by Gaussian decomposition:

$$\langle b_{\boldsymbol{q}} a^*_{\boldsymbol{k}} a_{k'} \rangle \simeq -2i \sum_{\boldsymbol{k}=\boldsymbol{k}'+\boldsymbol{q}} V_{\boldsymbol{k};\boldsymbol{k}',q} \left[\int \frac{d\omega d\omega' n_{\boldsymbol{k}\omega} n_{\boldsymbol{k}'\omega'}}{(2\pi)^2[\Gamma_{\boldsymbol{q}} + i(\Omega_{\boldsymbol{q}} + \omega' - \omega)]} \right] \,. \tag{8.2e}$$

Generalized Fluctuation-Dissipation Theorem (FDT) for weak wave turbulence:

$$n_{\boldsymbol{k}\omega} = \frac{2\gamma_{\boldsymbol{k}}\, n_{\boldsymbol{k}}}{(\omega_{\boldsymbol{k}} - \omega)^2 + \gamma^2_{\boldsymbol{k}}} = 2 n_{\boldsymbol{k}} \,\mathrm{Re}\, \{G_{\boldsymbol{k}\omega}\} \,, \tag{8.3a}$$

$$G_{\boldsymbol{k}\omega} \equiv \frac{1}{i(\omega - \omega_{\boldsymbol{k}}) + \gamma_{\boldsymbol{k}}} \,. \tag{8.3b}$$

Substituting FDT, Equation 8.3, into Equation 8.2e for $\langle b_{\boldsymbol q} a^*_{\boldsymbol k} a_{k'}\rangle$ one gets for

$$[\ldots] = \int \frac{d\omega d\omega' \gamma_{\boldsymbol k}\gamma_{\boldsymbol k'} n_{\boldsymbol k} n_{\boldsymbol k'}}{\pi^2[\Gamma_{\boldsymbol q} + i(\Omega_{\boldsymbol q} + \omega' - \omega)][(\omega_{\boldsymbol k} - \omega)^2 + \gamma^2_{\boldsymbol k}][(\omega_{\boldsymbol k'} - \omega')^2 + \gamma^2_{\boldsymbol k'}]} \tag{8.4}$$

$$= \frac{n_{\boldsymbol k} n_{\boldsymbol k'}}{(2\pi)^2}\int \frac{d\omega d\omega'}{[\Gamma_{\boldsymbol q} + i(\Omega_{\boldsymbol q} + \omega' - \omega)][\gamma_{\boldsymbol k} - i(\omega_{\boldsymbol k} - \omega)][\gamma_{\boldsymbol k'} + i(\omega_{\boldsymbol k'} - \omega')]}$$

$$= \frac{n_{\boldsymbol k} n_{\boldsymbol k'}}{\Gamma_{kk'q} + i(\Omega_{\boldsymbol q} + \omega_{k'} - \omega_{\boldsymbol k})}\,, \tag{8.5}$$

where $1/\Gamma_{kk'q}$ is the triad decay time. Here

$$\Gamma_{kk'q} \equiv \Gamma_{\boldsymbol q} + \gamma_{\boldsymbol k} + \gamma_{\boldsymbol k'}\ . \tag{8.6}$$

Substituting this into Equation 8.2e one gets

$$\langle b_{\boldsymbol q} a^*_{\boldsymbol k} a_{k'}\rangle \simeq -2i \sum_{\boldsymbol k = \boldsymbol k' + \boldsymbol q} \frac{V_{\boldsymbol k;\boldsymbol k',q}\ n_{\boldsymbol k} n_{\boldsymbol k'}}{\Gamma_{kk'q} + i(\Omega_{\boldsymbol q} + \omega_{k'} - \omega_{\boldsymbol k})}\ . \tag{8.7}$$

Now Equation 8.2a can be presented as the Mean-Field Equations:

$$\frac{\partial n_{\boldsymbol k}}{\partial t} = -2\Gamma_{\boldsymbol k} n_{\boldsymbol k}\,, \quad \Gamma_{\boldsymbol k} \equiv \gamma_{\boldsymbol k} + \sum_{\boldsymbol k'} \eta_{\boldsymbol k \boldsymbol k'} n_{\boldsymbol k'}\,, \tag{8.8a}$$

in which $\eta_{\boldsymbol k,\boldsymbol k'} = -\eta_{\boldsymbol k'\boldsymbol k}$

$$= 2\,\mathrm{Im}\left\{\frac{|V_{\boldsymbol k,\boldsymbol k',q}|^2}{\Omega_q + \omega_{\boldsymbol k'} - \omega_{\boldsymbol k} - i\Gamma_{\boldsymbol k\boldsymbol k'q}} + \frac{V_{\boldsymbol k',\boldsymbol k,-q}|^2}{\Omega_q + \omega_{\boldsymbol k} - \omega_{\boldsymbol k'} + i\Gamma_{\boldsymbol k\boldsymbol k'q}}\right\}$$

$$= \frac{2|V_{\boldsymbol k,\boldsymbol k',q}|^2\Gamma_{\boldsymbol k\boldsymbol k'q}}{(\Omega_q + \omega_{\boldsymbol k'} - \omega_{\boldsymbol k})^2 + \Gamma^2_{\boldsymbol k\boldsymbol k'q}} - \frac{2\,|V_{\boldsymbol k',\boldsymbol k,-q}|^2\Gamma_{\boldsymbol k\boldsymbol k'q}}{(\Omega_q + \omega_{\boldsymbol k} - \omega_{\boldsymbol k'})^2 + \widetilde{\Gamma}^2_{\boldsymbol k\boldsymbol k'q}}\,, \tag{8.8b}$$

with $q = \boldsymbol k - \boldsymbol k'$. Equations (8.8) follows from the dynamical Eq. for $a_{\boldsymbol k}$:

$$\frac{\partial a_{\boldsymbol k}}{\partial t} + (\gamma_{\boldsymbol k} + i\omega_{\boldsymbol k})a_{\boldsymbol k} = \frac{-i}{2}\sum_{\boldsymbol k + 1 = \boldsymbol 2 + 3} T_{\boldsymbol k,\boldsymbol 1;\boldsymbol 2,\boldsymbol 3} a^*_{\boldsymbol 1} a_{\boldsymbol 2} a_{\boldsymbol 3} \tag{8.9a}$$

with the effective 4-wave interaction amplitude

$$T_{\boldsymbol k \boldsymbol 1,\boldsymbol 2\boldsymbol 3} = -\frac{V_{\boldsymbol 3;\boldsymbol 1,\boldsymbol 3-\boldsymbol 1} V^*_{\boldsymbol k;\boldsymbol 2,\boldsymbol k-\boldsymbol 2}}{\omega_{\boldsymbol 1} + \Omega_{\boldsymbol 3-\boldsymbol 1} - \omega_{\boldsymbol 3} - i(\gamma_{\boldsymbol 1} + \gamma_{\boldsymbol 2} + \Gamma_{\boldsymbol 3-\boldsymbol 1})} \tag{8.9b}$$

$$- \frac{V_{\boldsymbol 2;\boldsymbol k,\boldsymbol 2-\boldsymbol k} V^*_{\boldsymbol 1,\boldsymbol 3,\boldsymbol 1-\boldsymbol 3}}{\omega_{\boldsymbol 3} + \Omega_{\boldsymbol 1-\boldsymbol 3} - \omega_{\boldsymbol 1} + i(\gamma_{\boldsymbol 1} + \gamma_{\boldsymbol 3} + \Gamma_{\boldsymbol 3-\boldsymbol 1})} + \text{two terms with } \ \boldsymbol k_2 \Leftrightarrow \boldsymbol k_3\ .$$

This vertex has non-hermitian part, originating from the damping in the triads.

Stationary "Jet" Solutions of Eq. (8.8) and their stability

$$\text{Stationarity}\quad \Gamma_{\boldsymbol{k}} n_{\boldsymbol{k}} = 0 \quad \text{requires} \quad n_{\boldsymbol{k}} = 0\,, \ \text{or}\ \Gamma_{\boldsymbol{k}} = 0\,; \tag{8.10a}$$

$$\text{Stability: for } \boldsymbol{k}\,, \quad \text{where} \quad n_{\boldsymbol{k}} = 0 \quad \text{requires} \quad \Gamma_{\boldsymbol{k}} \geq 0\,, \quad \text{giving} \tag{8.10b}$$

$$\text{Stable, stationary solutions:} \quad n_{\boldsymbol{k}} \geq 0\,, \quad \text{where} \quad d\Gamma_{\boldsymbol{k}}/d\boldsymbol{k} = 0\,. \tag{8.10c}$$

Geometrical interpretation of Equation 8.10c produces "jets" distributions in the $\boldsymbol{k}$-space for degenerated kernels $\eta_{\boldsymbol{k}\boldsymbol{k}'}$.

- Differential approximation:

$$[\ \cos\theta \equiv \frac{\boldsymbol{k}\cdot\boldsymbol{k}'}{k\,k'}\ ]$$

$$\text{For} \quad \omega_{\boldsymbol{k}} \gg \Omega_{\boldsymbol{k}} \gg \Gamma_{\boldsymbol{k}\boldsymbol{k}'\kappa} \quad \text{one approximates } \eta_{\boldsymbol{k}\boldsymbol{k}'},\ \text{Equation 8.8b} \tag{8.11a}$$

$$\eta_{\boldsymbol{k}\boldsymbol{k}'} = \frac{2|V_{\boldsymbol{k},\boldsymbol{k}',\kappa}|^2\widetilde{\Gamma}_{\boldsymbol{k}\boldsymbol{k}'\kappa}}{(\Omega_\kappa + \omega_{\boldsymbol{k}'} - \omega_{\boldsymbol{k}})^2 + \Gamma^2_{\boldsymbol{k}\boldsymbol{k}'\kappa}} - \frac{2\,|V_{\boldsymbol{k}',\boldsymbol{k},-\kappa}|^2\Gamma_{\boldsymbol{k}\boldsymbol{k}'\kappa}}{(\Omega_\kappa + \omega_{\boldsymbol{k}} - \omega_{\boldsymbol{k}'})^2 + \Gamma^2_{\boldsymbol{k}\boldsymbol{k}'\kappa}}$$

as follows:

$$\eta_{\boldsymbol{k}\boldsymbol{k}'} \simeq -\eta(k,\theta)\frac{d}{dk}(k-k')\,,\ \ \eta(k,\theta) = 4\pi|V_{\boldsymbol{k},\boldsymbol{k}',\kappa}|^2\frac{\Omega_{\boldsymbol{k}-\boldsymbol{k}'}}{d\omega_{\boldsymbol{k}}/dk}\,, \tag{8.11b}$$

This yields the differential approximation for

$$\Gamma_{\boldsymbol{k}} = \gamma_{\boldsymbol{k}} - \int \frac{d\Omega'}{(2\pi)^3}\eta(k,\theta)\frac{d}{dk}k^2 n(k,\Omega')\,, \tag{8.11c}$$

where $\Omega \equiv \{\theta\,,\phi\}$

- Simple scale-invariant example of the "jet" solution:

Let

$$\gamma_{\boldsymbol{k}} = k^\alpha\,\widetilde{\gamma}(\Omega)\,, \quad \eta(k,\theta) = k^\beta\,\widetilde{\eta}(\theta)\,, \quad n_{\boldsymbol{k}} = k^x\,\widetilde{n}(\Omega)\,, \tag{8.12a}$$

Then

$$\Gamma_{\boldsymbol{k}} = k^\alpha\left[\widetilde{\gamma}(\Omega) - \frac{\alpha - \underline{+}1}{(2\pi)^3}\int d\Omega'\,\widetilde{\eta}(\theta')\,\widetilde{n}(\Omega')\right] \geq 0\,, \tag{8.12b}$$

end $x = \alpha + \pm 1$. $\int \ldots$ is Ω -independent: $\widetilde{n}(\Omega) \neq 0$ at the set $\boldsymbol{\Omega}_j$, where $\widetilde{\gamma}(\Omega_j) = \widetilde{\gamma}_{\max}$. Clearly:

$$g_{\max} = \frac{\alpha - \pm 1}{(2\pi)^3} \int d\Omega\, \widetilde{\eta}(\theta)\, \widetilde{n}(\Omega) \ . \tag{8.12c}$$

For cos $(\theta_j) = \pm 1$ there are 2 jets:

$$\widetilde{n}(\Omega) = N[\delta(\cos\theta - 1) + \delta(\cos\theta + 1)] \,, \tag{8.12d}$$

$$(\alpha - \pm 1)\eta(\theta_j)\, N = 2\pi^2 \gamma_{\max} \ . \tag{8.12e}$$

Integral of motion H and Hidden Hamiltonian Structure

Consider

$$H \equiv \int d\boldsymbol{k} \left[n_{\boldsymbol{k}} + \ln(n_{\boldsymbol{k}}) \int d\boldsymbol{k}' R_{\boldsymbol{k}\boldsymbol{k}'}\, \gamma_{\boldsymbol{k}'} \right] \,, \tag{8.13a}$$

in which $R_{\boldsymbol{k}\boldsymbol{k}'}$ is the matrix, inverse to $\eta_{\boldsymbol{k}'\boldsymbol{k}''}$

$$\int d\boldsymbol{k}' R_{\boldsymbol{k}\boldsymbol{k}'} \eta_{\boldsymbol{k}'\boldsymbol{k}''} \equiv (\boldsymbol{k} - \boldsymbol{k}'') \ . \tag{8.13b}$$

Using Equation 8.8a compute

$$\frac{\partial H}{\partial t} = \int d\boldsymbol{k} \frac{\partial n_{\boldsymbol{k}}}{n_{\boldsymbol{k}} \partial t} \left[n_{\boldsymbol{k}} + \int d\boldsymbol{k}' R_{\boldsymbol{k}\boldsymbol{k}'}\, \gamma_{\boldsymbol{k}'} \right] \tag{8.13c}$$

$$= \int d\boldsymbol{k} \left[\gamma_{\boldsymbol{k}} + \int d\boldsymbol{k}'' \eta_{\boldsymbol{k}\boldsymbol{k}''} n_{\boldsymbol{k}''} \right] \left[n_{\boldsymbol{k}} + \int d\boldsymbol{k}' R_{\boldsymbol{k}\boldsymbol{k}'}\, \gamma_{\boldsymbol{k}'} \right] \tag{8.13d}$$

$$= \int d\boldsymbol{k}\, \gamma_{\boldsymbol{k}} n_{\boldsymbol{k}} - \int d\boldsymbol{k} d\boldsymbol{k}' d\boldsymbol{k}'' \gamma_{\boldsymbol{k}'}\, R_{\boldsymbol{k}'\boldsymbol{k}} \eta_{\boldsymbol{k}\boldsymbol{k}''} n_{\boldsymbol{k}''} \quad \left(= \int d\boldsymbol{k}'\, \gamma_{\boldsymbol{k}'} n_{\boldsymbol{k}'}\right)$$

$$+ \int d\boldsymbol{k} d\boldsymbol{k}' \gamma_{\boldsymbol{k}} R_{\boldsymbol{k}\boldsymbol{k}'} \gamma_{\boldsymbol{k}'} + \int d\boldsymbol{k} d\boldsymbol{k}'' n_{\boldsymbol{k}} \eta_{\boldsymbol{k}\boldsymbol{k}''} n_{\boldsymbol{k}''} = 0 \ . \tag{8.13e}$$

One can show that H is a Hamiltonian of the system, Equation 8.8a.

If $H_{\text{init}} \neq H_{\text{stat}}$ one will not reach the stationary solution within the system, described by Equation 8.8a.

Nonlinear "S-theory" of parametric excitation of waves

WAVE TURBULENCE is a state of a system of many simultaneously excited and interacting waves characterized by an energy distribution which is not in any sense close to thermodynamic equilibrium. Such situations arise, for example, in a choppy sea, in a hot plasma, in dielectrics under a powerful laser beam, in magnetics placed in a strong microwave field, etc. Among the great variety of physical situations in which wave turbulence arises, it is possible to select two large limiting groups which allow a detailed analysis. The first is fully developed wave turbulence arising when energy pumping and dissipation have essentially different space scales. In this case there is a wide power spectrum of turbulence. This type of turbulence will be described in next Lectures within the approximation of Kinetic Equation, explained in subsection 7.4.

In the second limiting case the scales in which energy pumping and dissipation occur are the same. As a rule, in this case a narrow, almost singular spectrum of turbulence appears which is concentrated near surfaces, curves or even points in k-space. One of the most important, widely investigated and instructive examples of this kind of turbulence is parametric wave turbulence appearing as a result of the evolution of a parametric instability of waves in media under strong external periodic modulation (laser beam, microwave electro-magnetic field, etc.). Extremely reach and deeply nontrivial dynamics of wave turbulence under parametric excitation can be described in main details within the mean-field approximation, called " S -theory and described in details in Sec. Sec. 5 of my book "Wave Turbulence Under Parametric Excitation".

Exercises

TO BE PREPARED

Lecture 9.

General properties of wave Kinetic Equation (KE)

9.1 Conservation laws in the 3- and 4-wave KE

9.2 Boltzmann's H-theorem and Thermodynamic Equilibrium in KE

9.3 Stationary Non-equilibrium Distributions in KE

9.4 Exercises

Conservation laws in the 3- and 4-wave KE

Consider Kinetic Equation

$$\frac{\partial n_{\boldsymbol{k}}}{\partial t} = I_{\boldsymbol{k}} \,, \tag{9.1a}$$

with the "collision integral" for the 3-wave KE given by Equation 7.12:

$$\begin{aligned} I_{\boldsymbol{k}} = {} & \pi \sum_{\boldsymbol{k}=\boldsymbol{1}+\boldsymbol{2}} |V_{\boldsymbol{k},\boldsymbol{12}}|^2 \left[n_{\boldsymbol{1}} n_{\boldsymbol{2}} - n_{\boldsymbol{k}}(n_{\boldsymbol{1}} + n_{\boldsymbol{2}})\right] \delta(\omega_{\boldsymbol{k}} - \omega_{\boldsymbol{1}} - \omega_2) \\ & + 2\pi \sum_{\boldsymbol{1}=\boldsymbol{k}+\boldsymbol{2}} |V_{\boldsymbol{1},\boldsymbol{k2}}|^2 \left[n_{\boldsymbol{1}} n_{\boldsymbol{2}} - n_{\boldsymbol{k}}(n_{\boldsymbol{2}} - n_{\boldsymbol{1}})\right])\delta(\omega_{\boldsymbol{1}} - \omega_{\boldsymbol{k}} - \omega_{\boldsymbol{2}}) \,. \end{aligned} \tag{9.1b}$$

For the 4-wave KE the collision integral, Equation 7.14, is

$$\begin{aligned} I_{\boldsymbol{k}} = \pi & \sum_{\boldsymbol{k}+\boldsymbol{1}=\boldsymbol{2}+\boldsymbol{3}} |T_{\boldsymbol{k1},\boldsymbol{23}}|^2 \left[n_{\boldsymbol{2}} n_{\boldsymbol{3}}(n_{\boldsymbol{1}} + n_{\boldsymbol{k}}) - n_{\boldsymbol{1}} n_{\boldsymbol{k}}(n_{\boldsymbol{2}} + n_{\boldsymbol{3}})\right] \\ & \times \delta(\omega_{\boldsymbol{k}} + \omega_{\boldsymbol{1}} - \omega_2 - \omega_3) \,. \end{aligned} \tag{9.1c}$$

- Conservation of Energy

KEs conserve the total energy of non-interacting waves, given by

$$E = \sum_{\boldsymbol{k}} \varepsilon_{\boldsymbol{k}}\,, \quad \text{energy density } \varepsilon_{\boldsymbol{k}} \equiv \omega_{\boldsymbol{k}} n_{\boldsymbol{k}}\ . \tag{9.2}$$

This energy does not include (small) correction to the total energy of the system of interacting waves, described by $\mathcal{H}_{\rm int}$.

Compute $\dfrac{dE}{dt}$ for the 3-wave KE, using $I_{\boldsymbol{k}}$, Equation 10.1b:

$$\begin{aligned}\frac{dE}{dt} = \pi \sum_{\boldsymbol{k}=\boldsymbol{1}+\boldsymbol{2}} |V_{\boldsymbol{k},\boldsymbol{12}}|^2 \left[n_{\boldsymbol{1}} n_{\boldsymbol{2}} - n_{\boldsymbol{k}}(n_{\boldsymbol{1}} + n_{\boldsymbol{2}})\right] \\ \times (\omega_{\boldsymbol{k}} - \omega_{\boldsymbol{1}} - \omega_2)\delta(\omega_{\boldsymbol{k}} - \omega_{\boldsymbol{1}} - \omega_2) = 0\ .\end{aligned} \tag{9.3a}$$

The same calculations for the 4-wave KE with the collision integral Equation 10.1c

$$\begin{aligned}\frac{dE}{dt} = \frac{\pi}{4} \sum_{\boldsymbol{k}+\boldsymbol{1}=\boldsymbol{2}+\boldsymbol{3}} |T_{\boldsymbol{k1},\boldsymbol{23}}|^2 \left[n_{\boldsymbol{2}} n_{\boldsymbol{3}}(n_{\boldsymbol{1}} + n_{\boldsymbol{k}}) - n_{\boldsymbol{1}} n_{\boldsymbol{k}}(n_{\boldsymbol{2}} + n_{\boldsymbol{3}})\right] \\ \times (\omega_{\boldsymbol{k}} + \omega_{\boldsymbol{1}} - \omega_{\boldsymbol{2}} - \omega_{\boldsymbol{3}})\delta(\omega_{\boldsymbol{k}} + \omega_{\boldsymbol{1}} - \omega_{\boldsymbol{2}} - \omega_{\boldsymbol{3}}) = 0\ .\end{aligned} \tag{9.3b}$$

One sees that formally the conservation of energy follows from the $\delta(\omega\ldots)$, that originates from the time-invariance.

Equations (9.3) allows to present the 3- and 4-wave KEs as the continuity Eqs.:

$$\frac{\partial \varepsilon_{\boldsymbol{k}}}{\partial \boldsymbol{k}} = \ \mathrm{div} p_{\boldsymbol{k}}\,, \qquad \text{with the Energy flux } p_{\boldsymbol{k}} : \qquad \mathrm{div} p_{\boldsymbol{k}} = -\omega_{\boldsymbol{k}} I_{\boldsymbol{k}}\ . \tag{9.4}$$

- Conservation of the mechanical moment defined by

$$\boldsymbol{\Pi} \equiv \sum_{\boldsymbol{k}} \boldsymbol{\pi}_{\boldsymbol{k}}\,, \quad \boldsymbol{\pi}_{\boldsymbol{k}} \equiv \boldsymbol{k} n_{\boldsymbol{k}} \tag{9.5}$$

is due to the delta functions $\Delta(\boldsymbol{k} - \boldsymbol{1} - \boldsymbol{2})$ and $\Delta(\boldsymbol{k} - \boldsymbol{1} + \boldsymbol{2})$ in the 3-wave KE and $\Delta(\boldsymbol{k} + \boldsymbol{1} - \boldsymbol{2} - \boldsymbol{3})$ in the 4 wave KE. Corresponding proof is similar to that for the conservation of energy. The momentum conservation allows to present the KEs as the

$$\text{Continuity equation for the density } \boldsymbol{\pi}_{\boldsymbol{k}} : \quad \frac{\partial \boldsymbol{\pi}_{\boldsymbol{k}}}{\partial t} + \operatorname{div}\widehat{R} = 0 \ . \tag{9.6}$$

- Conservation of $N = \sum_{\boldsymbol{k}} n_{\boldsymbol{k}}$ in 4-wave KE can be proven similarly.

- Nontrivial integral of motion in degenerated systems.

From the above discussion it follows: If there exists a function $f(\boldsymbol{k})$ such that

$$f(\boldsymbol{k}_1) + f(\boldsymbol{k}_2) = f(\boldsymbol{k}_1 + \boldsymbol{k}_2)\,, \ f(\boldsymbol{k}) \neq A\,\omega_{\boldsymbol{k}} + B \cdot \boldsymbol{k}\,, \ \omega_{\mathbf{1}} + \omega_{\mathbf{2}} = \omega_{\mathbf{1+2}}\,, \tag{9.7}$$

then there exists additional, independent integral of motion, given by

$$F \equiv \sum_{\boldsymbol{k}} f(\boldsymbol{k}) n_{\boldsymbol{k}} \ . \tag{9.8}$$

Example of the degenerated system, in which one found a function $f(k)$ with the properties (9.7) is Quasi-one-dimensional, $k_x \gg k_y$, shallow-water gravitational-capillary waves with the dispersion law:

$$\omega_{\boldsymbol{k}} = ck\left(1 + \frac{k^2}{2k_*^2}\right) \approx ck_x\left(1 + \frac{k_x^2}{2k_*^2} + \frac{k_y^2}{2k_x^2}\right) \ . \tag{9.9a}$$

To see this introduce $p \equiv 2k_x(c/k_*)^{1/3}$ and $q \equiv k_y c^{2/3}/\sqrt{3}k_*^{1/3}$. Now the RHS of Eq. (9.9a) can be written as

$$\omega_{\boldsymbol{k}} = 2A\,p + \frac{p^3}{16} + \frac{3q^2}{p} \tag{9.9b}$$

with some constant A . With given two wave-vectors k_1 and k_2 introduce three variables ξ_1 , ξ_2 and ξ_3 via p_1 , p_2 and q_1 :

$$p_1 = 2(\xi_1 - \xi_2),\ q_1 = \xi_1^2 - \xi_2^2,\ p_2 = 2(\xi_2 - \xi_3), \tag{9.10a}$$

and let q_2 to be dependent on p_1 , p_2 and q_1 according to

$$q_2 = \xi_2^2 - \xi_3^2 \ . \tag{9.10b}$$

Now we can present

$$\omega(p_1, q_1) = A(\xi_1 - \xi_2) + 2(\xi_1^3 - \xi_2^3)\,, \tag{9.11a}$$

$$\omega(p_2, q_2) = A(\xi_2 - \xi_3) + 2(\xi_2^3 - \xi_3^3)\,, \tag{9.11b}$$

and to see that with our choice of dependence (9.10) the frequencies Eq. (9.11) satisfies the conservation laws:

$$\omega(p_1, q_1) + \omega(p_2, q_2) = \omega(p_1 + p_2, q_1 + q_2)\ . \tag{9.12}$$

Next introduce the function $f(\boldsymbol{k})$

$$f(p_1, q_1) \equiv \varphi(\xi_1) - \varphi(\xi_2) = \varphi\left(\frac{q_2}{p_1} + \frac{p_1}{4}\right) - \varphi\left(\frac{q_1}{p_1} - \frac{p_1}{4}\right)\,, \tag{9.13a}$$

$$f(p_2, q_2) \equiv \varphi(\xi_2) - \varphi(\xi_3) = \varphi\left(\frac{q_2}{p_2} + \frac{p_2}{4}\right) - \varphi\left(\frac{q_2}{p_2} - \frac{p_2}{4}\right)\,, \tag{9.13b}$$

with an arbitrary even function $\varphi(\xi)$.

Then

$$f(p_1 + p_2, q_1 + q_2) = \varphi(\xi_1) - \varphi(\xi_3) = f(p_1, q_1) + f(p_2, q_2)\ . \tag{9.13c}$$

This relation produces an infinite set of independent integrals of motion (9.8), which corresponds to an integrability of Kadomtsev-Petviashvili equation.

Boltzmann's H-theorem and Thermodynamic Equilibrium in KE

Introduce the entropy of the wave system

$$S(t) = \sum_{\boldsymbol{k}} \ln\left[n_{\boldsymbol{k}}\right] \tag{9.14a}$$

and study its evolution, computing with the help of KE (9.15c)

$$\frac{dS}{dt} = \sum_{\boldsymbol{k}} \frac{\partial n_{\boldsymbol{k}}}{n_{\boldsymbol{k}} \partial t} = \sum_{\boldsymbol{k}} \frac{I_{\boldsymbol{k}}}{n_{\boldsymbol{k}}} \tag{9.14b}$$

Using Equation 10.1b for the 3-wave collision integral one gets for the 3-wave KE

$$\frac{dS}{dt} = \pi \sum_{\boldsymbol{k}=\boldsymbol{1}+\boldsymbol{2}} |V_{\boldsymbol{k}\boldsymbol{1}\boldsymbol{2}}|^2 \delta(\omega_{\boldsymbol{k}} - \omega_{\boldsymbol{1}} - \omega_{\boldsymbol{2}}) \frac{(n_{\boldsymbol{1}} n_{\boldsymbol{2}} - n_{\boldsymbol{k}} n_{\boldsymbol{1}} - n_{\boldsymbol{k}} n_{\boldsymbol{2}})^2}{n_{\boldsymbol{k}} n_{\boldsymbol{1}} n_{\boldsymbol{2}}} \geq 0 \quad (9.14c)$$

and, using Equation 10.1b, we have for the 4-wave KE

$$\frac{dS}{dt} = \frac{\pi}{4} \sum_{\boldsymbol{k}+\boldsymbol{1}=\boldsymbol{2}+\boldsymbol{3}} |T_{\boldsymbol{k}\boldsymbol{1},\boldsymbol{2}\boldsymbol{3}}|^2 \delta(\omega_{\boldsymbol{k}} + \omega_{\boldsymbol{1}} - \omega_{\boldsymbol{2}} - \omega_{\boldsymbol{3}}) \quad (9.14d)$$
$$\times \frac{[n_{\boldsymbol{2}} n_{\boldsymbol{3}}(n_{\boldsymbol{1}} + n_{\boldsymbol{k}}) - n_{\boldsymbol{1}} n_{\boldsymbol{k}}(n_{\boldsymbol{2}} + n_{\boldsymbol{3}})]^2}{n_{\boldsymbol{k}} n_{\boldsymbol{1}} n_{\boldsymbol{2}} n_{\boldsymbol{3}}} \geq 0 \,.$$

So, any evolution only increases the entropy. In the state of thermodynamic equilibrium in the 3-wave KE $(..) = 0$. To find the equilibrium transform

$$(..) = n_{\boldsymbol{k}} n_{\boldsymbol{1}} n_{\boldsymbol{2}} \left(n_{\boldsymbol{k}}^{-1} - n_{\boldsymbol{1}}^{-1} - n_{\boldsymbol{2}}^{-1}\right) \,. \quad (9.15a)$$

The equilibrium is the Rayleigh-Jeans distribution

$$n_{\boldsymbol{k}} = \frac{T}{\omega_{\boldsymbol{k}} - \boldsymbol{k} \cdot \boldsymbol{V}} \,, \quad (9.15b)$$

with two free constants, temperature T and velocity V .

In the 4-wave KE one should put $[...] = 0$. Transform

$$[..] = n_{\boldsymbol{k}} n_{\boldsymbol{1}} n_{\boldsymbol{2}} n_{\boldsymbol{3}} \left[n_{\boldsymbol{k}}^{-1} + n_{\boldsymbol{1}}^{-1} - n_{\boldsymbol{2}}^{-1} - n_{\boldsymbol{3}}^{-1}\right] \,, \quad (9.15c)$$

and find: $$n_{\boldsymbol{k}} = \frac{T}{\omega_{\boldsymbol{k}} - \boldsymbol{k} \cdot \boldsymbol{V} - \mu} \,. \quad (9.15d)$$

The conservation law $N =$ const. generate new constant: μ – chemical potential.

Stationary Non-equilibrium Distributions in KE

Introduce $\Gamma(\boldsymbol{k})$ to mimic energy pumping $[\Gamma(\boldsymbol{k}) > 0]$ and damping $[\Gamma(\boldsymbol{k}) < 0]$ in well separated regions of $\boldsymbol{k}$:

$$\frac{\partial n_{\boldsymbol{k}}}{\partial t} = I_{\boldsymbol{k}} + \Gamma_{\boldsymbol{k}} n_{\boldsymbol{k}} \,, \quad \Gamma_{\boldsymbol{k}} = 0 \,, \quad \text{for } k_{\min} \ll k \ll k_{\max} \,. \quad (9.16a)$$

Necessary requirements for the stationarity:

$$\Gamma_{\boldsymbol{k}} n_{\boldsymbol{k}} + I_{\boldsymbol{k}}\{n_{\boldsymbol{k}}\} = 0 \ . \tag{9.17}$$

Notice: Entropy output from the system that produces entropy.
From the H-theorem

$$\sum_{\boldsymbol{k}} \frac{I_{\boldsymbol{k}}}{n_{\boldsymbol{k}}} > 0 \ . \quad \text{Thus:} \ \sum_{\boldsymbol{k}} \Gamma(\boldsymbol{k}) < 0 \ . \tag{9.18a}$$

Conservation of energy, momentum & particle numbers produces three additional constrains

$$\sum_{\boldsymbol{k}} \Gamma(\boldsymbol{k})\omega(\boldsymbol{k})n(\boldsymbol{k}) = 0 \, , \quad \sum_{\boldsymbol{k}} \Gamma(\boldsymbol{k})\boldsymbol{k}\, n(\boldsymbol{k}) = 0 \, , \ \& \sum_{\boldsymbol{k}} \Gamma(\boldsymbol{k})n(\boldsymbol{k}) = 0 \ . \tag{9.18b}$$

Exercises

TO BE PREPARED

Lecture 10

Wave damping and kinetic instability

Wave damping in 3- and 4-wave processes

Consider KEs with the with the the 3- and 4-wave "collision integrals", 7.12, 7.14:

$$\frac{\partial n_{\boldsymbol{k}}}{\partial t} = I_{\boldsymbol{k}} \equiv -\gamma_{\boldsymbol{k}} n_{\boldsymbol{k}} + \Phi_{\boldsymbol{k}} \,, \tag{10.1a}$$

$$I_{\boldsymbol{k}} = \pi \sum_{\boldsymbol{k}=\boldsymbol{1}+\boldsymbol{2}} |V_{\boldsymbol{k},\boldsymbol{12}}|^2 \left[n_1 n_2 - n_{\boldsymbol{k}}(n_{\boldsymbol{1}} + n_{\boldsymbol{2}})\right] \delta(\omega_{\boldsymbol{k}} - \omega_{\boldsymbol{1}} - \omega_2)$$

$$+2\pi \sum_{\boldsymbol{1}=\boldsymbol{k}+\boldsymbol{2}} |V_{\boldsymbol{1},\boldsymbol{k2}}|^2 \left[n_1 n_2 - n_{\boldsymbol{k}}(n_{\boldsymbol{2}} - n_{\boldsymbol{1}})\right])\delta(\omega_{\boldsymbol{1}} - \omega_{\boldsymbol{k}} - \omega_{\boldsymbol{2}}) \,. \tag{10.1b}$$

$$I_{\boldsymbol{k}} = \pi \sum_{\boldsymbol{k}+\boldsymbol{1}=\boldsymbol{2}+\boldsymbol{3}} |T_{\boldsymbol{k1},\boldsymbol{23}}|^2 \left[n_{\boldsymbol{2}} n_{\boldsymbol{3}}(n_1 + n_{\boldsymbol{k}}) - n_{\boldsymbol{k}} n_{\boldsymbol{1}}(n_{\boldsymbol{2}} + n_{\boldsymbol{3}})\right]$$
$$\times \delta(\omega_{\boldsymbol{k}} + \omega_{\boldsymbol{1}} - \omega_2 - \omega_3) \,. \tag{10.1c}$$

Function in the front of $n_{\boldsymbol{k}}$ in the collision integrals can be considered as the wave damping (frequency), in the decay, confluence, and scattering processes:

$$\gamma_{\boldsymbol{k}} = \gamma^{\mathrm{d}}_{\boldsymbol{k}} + \gamma^{\mathrm{c}}_{\boldsymbol{k}} + \gamma^{\mathrm{s}}_{\boldsymbol{k}} \,. \tag{10.2a}$$

Namely

$$\gamma^{\mathrm{d}}_{\boldsymbol{k}} = \pi \int \frac{d\boldsymbol{k}_1 d\boldsymbol{k}_2}{(2\pi)^3} |V_{\boldsymbol{k},\mathbf{12}}|^2 (n_{\mathbf{1}} + n_{\mathbf{2}}) \delta(\omega_{\boldsymbol{k}} - \omega_{\mathbf{1}} - \omega_{\mathbf{2}}) \delta(\boldsymbol{k} - \mathbf{1} - \mathbf{2}) \,, \quad \text{decay} \tag{10.2b}$$

$$\gamma^{\mathrm{c}}_{\boldsymbol{k}} = 2\pi \int \frac{d\boldsymbol{k}_1 d\boldsymbol{k}_2}{(2\pi)^3} |V_{\mathbf{1},\boldsymbol{k}\mathbf{2}}|^2 (n_{\mathbf{2}} - n_{\mathbf{1}}) \delta(\omega_{\mathbf{1}} - \omega_{\boldsymbol{k}} - \omega_{\mathbf{2}}) \delta(\mathbf{1} - \boldsymbol{k} - \mathbf{2}) \,, \quad \text{confluence} \tag{10.2c}$$

$$\gamma^{\mathrm{s}}_{\boldsymbol{k}} = \pi \int \frac{d\boldsymbol{k}_1 d\boldsymbol{k}_2 d\boldsymbol{k}_3}{(2\pi)^6} |T_{\boldsymbol{k}\mathbf{1},\mathbf{23}}|^2 \left[n_{\mathbf{1}}(n_{\mathbf{2}} + n_{\mathbf{3}}) - n_{\mathbf{2}} n_{\mathbf{3}} \right]$$
$$\times \delta(\omega_{\boldsymbol{k}} + \omega_{\mathbf{1}} - \omega_{\mathbf{2}} - \omega_{\mathbf{3}}) \delta(\boldsymbol{k} + \mathbf{1} - \mathbf{2} - \mathbf{3}) \,, \tag{10.2d}$$

scattering

In the thermodynamic equilibrium $I_{\boldsymbol{k}} = 0$ and all $\gamma_{\boldsymbol{k}} > 0$.
In general this is not the case and if $\gamma_{\boldsymbol{k}} < 0$ one has a kinetic instability.

- Example: Damping of sound in solids due to the sound-sound interaction

Recall Debye model of sound in crystals (Peter Joseph Wilhelm Debye, 1884-1966)

$$\omega_k = c_{\mathrm{s}} k \,, \quad \frac{4\pi}{3} k_{\mathrm{D}}^3 = \left(\frac{2\pi}{a} \right)^3 \Rightarrow (a\, k_{\mathrm{D}})^3 = 6\pi^2 \,, \; T_{\mathrm{D}} \equiv \hbar\, c_{\mathrm{s}} k_{\mathrm{D}} \,. \tag{10.3}$$

Usually the Debye temperature in crystals $T_{\mathrm{D}} \sim (100 \div 200)$ K. Our dimensional estimate:

$$V_{\mathbf{1},\mathbf{23}} \simeq V \sqrt{k_1 k_2 k_3} \,, \quad V = \sqrt{c_{\mathrm{s}}/\rho} \,, \quad \rho = M/a^3 \,. \tag{10.4a}$$

Consider first the decay damping, Equation 10.2b:

$$\gamma^{\mathrm{d}}_{\boldsymbol{k}} \simeq \frac{\pi V^2 k}{c_{\mathrm{s}}} \int \frac{d\boldsymbol{k}_1 d\boldsymbol{k}_2}{(2\pi)^3} k_1 k_2 (n_{\mathbf{1}} + n_{\mathbf{2}}) \delta(k - k_1 - k_2) \delta(\boldsymbol{k} - \mathbf{1} - \mathbf{2}) \tag{10.4b}$$

Substitute $n_{\boldsymbol{k}} = \dfrac{T}{c_{\rm s} k}$, $k_2 = \sqrt{k^2 + k_1^2 - 2k\, k_1 \cos\theta} = k - k_1$, $d\Omega_1 d\Omega_2 = 4\pi\, 2\pi d\cos\theta$. This gives:

$$\gamma^{\rm d}_{\boldsymbol{k}} \simeq \frac{T\,V^2 k}{c_{\rm s}^2}\int_0^k dk_1 k_1^3 k_2 \left(\frac{1}{k_1} + \frac{1}{k_2}\right) \int d\cos\theta\, \delta(k - k_1 - k_2) \ . \tag{10.4c}$$

Now we account that:

$$(..) = \frac{k}{k_1 k_2}\,, \quad \text{and} \quad \int .. = \frac{k_2}{k\, k_1} \ .$$

With Eqs. (10.4c) and (10.4a) this gives the following estimates

$$\gamma^{\rm d}_k \simeq \frac{T\,V^2 k}{c_{\rm s}^2}\int_0^k dk_1 k_1 (k - k_1) \simeq \frac{T\,k^4}{\rho c_{\rm s}}\,, \quad \frac{\gamma^{\rm d}_k}{\omega_k} \simeq (a\,k)^3 \frac{T}{M c_{\rm s}^2} \ . \tag{10.4d}$$

Next we estimate the confluence damping:

$$\begin{aligned} \gamma^{\rm c}_{\boldsymbol{k}} &\simeq \frac{V^2 k}{c_{\rm s}} \int \frac{d\boldsymbol{k}_1 d\boldsymbol{k}_2}{(2\pi)^2} k_1 k_2 (n_{\boldsymbol{2}} - n_{\boldsymbol{1}}) \delta(k - k_1 + k_2) \delta(\boldsymbol{k} - \boldsymbol{1} + \boldsymbol{2}) \\ &\simeq \frac{T\,V^2 k}{c_{\rm s}^2} \int_k^{k_{\rm max}} dk_1 k_1 (k - k_1) \simeq \omega_k\, (a\, k_{\rm max})^3 \frac{T}{M c_{\rm s}^2} \ . \end{aligned} \tag{10.5a}$$

For low temperatures, $T \ll T_{\rm D}$ $\hbar c_{\rm s} k_{\rm max} \simeq T$ and (restoring numerical factors):

$$\frac{\gamma^{\rm c}_k}{\omega_k} \approx 160\pi \left(\frac{T}{T_{\rm D}}\right)^3 \frac{T}{M c_{\rm s}^2} \ . \tag{10.5b}$$

For $T \gg T_{\rm D}$ one similarly gets

$$\frac{\gamma^{\rm c}_k}{\omega_k} \approx 9\pi \frac{T}{M c_{\rm s}^2}\,, \quad M c_{\rm s}^2 \simeq 100\, T_{\rm fusion} \ . \tag{10.5c}$$

- Next example: Damping of light due to the light-sound scattering

Consider the Hamiltonian of the problem:

$$\mathcal{H} = \sum_{\boldsymbol{k}} \omega_{\boldsymbol{k}} a_{\boldsymbol{k}} a^*_{\boldsymbol{k}} + \sum_{\boldsymbol{q}} \Omega_{\boldsymbol{q}} b_{\boldsymbol{q}} b^*_{\boldsymbol{q}} + \sum_{\boldsymbol{k},\boldsymbol{k}',\boldsymbol{q}} V_{\boldsymbol{k};\boldsymbol{k}',\boldsymbol{q}} a^*_{\boldsymbol{k}} a_{\boldsymbol{k}'} \left[b_{\boldsymbol{q}} + b^*_{-\boldsymbol{q}} \right] \Delta_{\boldsymbol{k},\boldsymbol{k}'+\boldsymbol{q}} \ . \tag{10.6a}$$

in which $\omega_k = \widetilde{c}\, k$, $\widetilde{c} \equiv \dfrac{c}{\sqrt{\varepsilon}}$, ε is the dielectric constant of the media, $\Omega_q = c_{\rm s} k$, $c_{\rm s}$ is the speed of sound. The light-sound interaction is caused by the sound modulation of the speed of the light via dielectric constant. Therefore

$$V_{\boldsymbol{k};\boldsymbol{k}',\boldsymbol{q}} = V_{\rm ls}\sqrt{k\,k'q}\,,\ V_{\rm ls} \simeq \widetilde{c}\,\frac{\partial \ln \varepsilon}{4\,\partial\rho}\sqrt{\frac{\rho}{\pi^3 c_{\rm s}}}\ . \tag{10.6b}$$

Here ρ is the media density and we used the dimensional estimate of the connection between $\rho_{\boldsymbol{q}}$ and $b_{\boldsymbol{q}}$, given by Equation 3.20a. Now we are ready to compute the Decay and confluence damping:

$$\gamma_{\boldsymbol{k}} \simeq \frac{V_{\rm ls}^2 k}{\widetilde{c}}\int\frac{d\boldsymbol{k}'d\boldsymbol{q}}{(2\pi)^2}k'q(N_q \pm n_{k'})\delta(\boldsymbol{k}-\boldsymbol{k}'\pm\boldsymbol{q})\delta(k-k'\pm\frac{c_{\rm s}}{\widetilde{c}}\,q)\ . \tag{10.6c}$$

Accounting that

$$N_q = \frac{T}{c_{\rm s}q}\ \ \text{and}\ \ n_{k'}\to 0$$

one gets

$$\gamma_{\boldsymbol{k}} \simeq \frac{TV_{\rm ls}^2 k^2}{\widetilde{c}\,c_{\rm s}}\int_0^{2k} qdq\gamma_k \simeq \frac{\widetilde{c}\,k}{32}\left(\frac{\partial\ln\varepsilon}{\partial\rho}\right)^2\frac{k^3\rho T}{c_{\rm s}^2} \simeq \omega_k\left(\frac{\partial\ln\varepsilon}{\partial\ln\rho}\right)^2(\ell k)^3\,, \tag{10.6d}$$

where $\rho\simeq M/\ell^3$ with ℓ being intermolecular distance, M is the molecular mass in gas or fluid and we estimated $Mc_{\rm s}^2\simeq T$.

The conclusion is that

$$\gamma_k \propto \omega_k^4\ . \tag{10.6e}$$

This is why the sky is blue and the sun near the horizon is red.

Linear theory of kinetic instability: 3- and 4-wave interactions

Take a wave distribution $n_{\boldsymbol{k}}$ as the sum of thermodynamic equilibrium $n_{\boldsymbol{k}}^{(0)}$ and intensive "god-given" narrow package with $k=k_0$:

$$n_{\boldsymbol{k}} = n_{\boldsymbol{k}}^{(0)} + \widetilde{n}_{\boldsymbol{k}}\,,\ \widetilde{n}_{\boldsymbol{k}} = \frac{N_0}{4\pi k_0^2}\delta(k-k_0)\,,\ N_0 = \int\widetilde{n}_{\boldsymbol{k}}\,d\boldsymbol{k}\,, \tag{10.7a}$$

and consider confluence, Eq. (10.2c), and scattering, Eq. (10.2d), contributions to damping of all other "secondary" waves in the system, caused by distribution

(10.7a):

$$\widetilde{\gamma}^{\rm c}_{\boldsymbol{k}} = \int \frac{d\boldsymbol{k}_1 d\boldsymbol{k}_2}{(2\pi)^2}|V_{\boldsymbol{1},\boldsymbol{k}\boldsymbol{2}}|^2(n_{\boldsymbol{2}} - n_{\boldsymbol{1}})\delta(\omega_{\boldsymbol{1}} - \omega_{\boldsymbol{k}} - \omega_{\boldsymbol{2}})\delta(\boldsymbol{1} - \boldsymbol{k} - \boldsymbol{2}) \, , \quad (10.7b)$$

$$\widetilde{\gamma}^{\rm s}_{\boldsymbol{k}} = \pi \int \frac{d\boldsymbol{k}_1 d\boldsymbol{k}_2 d\boldsymbol{k}_3}{(2\pi)^6}|T_{\boldsymbol{k}\boldsymbol{1},\boldsymbol{2}\boldsymbol{3}}|^2 \left[n_{\boldsymbol{1}}(n_{\boldsymbol{2}} + n_{\boldsymbol{3}}) - n_{\boldsymbol{2}}n_{\boldsymbol{3}}\right] \quad (10.7c)$$
$$\times\delta(\omega_{\boldsymbol{k}} + \omega_{\boldsymbol{1}} - \omega_{\boldsymbol{2}} - \omega_{\boldsymbol{3}})\delta(\boldsymbol{k} + \boldsymbol{1} - \boldsymbol{2} - \boldsymbol{3}) \, .$$

Evaluate the damping $\gamma^{\rm c}_{\boldsymbol{k}}$ of arbitrary chosen package of secondary waves

$$\widetilde{\gamma}^{\rm c}_{\boldsymbol{k}} = -\frac{N_0}{k_0^2}\int \frac{d\boldsymbol{k}_1 d\boldsymbol{k}_2}{(2\pi)^3}|V^2_{\boldsymbol{1},\boldsymbol{k}\boldsymbol{2}} \quad (10.8a)$$
$$\times\, \delta(k_1 - k_0)\delta(\omega_{\boldsymbol{1}} - \omega_{\boldsymbol{k}} - \omega_{\boldsymbol{2}})\frac{\delta(\boldsymbol{1} - \boldsymbol{k} - \boldsymbol{2})}{2\pi} \, ,$$

where $(\ldots)/2\pi \to 1/kk_1k_2$. Define wave vector $\widetilde{k}$ of the 2nd package of secondary waves, "complementary" to the initial one by

$$\omega_{\widetilde{k}} = \omega_{k_0} - \omega_k \, , \quad \widetilde{v} = \frac{d\omega_{\widetilde{k}}}{d\widetilde{k}} \, . \quad (10.8b)$$

Equations (10.8a) and (10.8b) give

$$\widetilde{\gamma}^{\rm c}_{\boldsymbol{k}} \simeq -\frac{2N_0\widetilde{k}}{\pi k k_0 \widetilde{v}}|V_{k_0,k\widetilde{k}}|^2 \simeq -\frac{N_0|V_{k_0,k\widetilde{k}}|^2}{k\widetilde{v}} < 0 \, . \quad (10.8c)$$

Similarly one finds the scattering contribution to the damping of secondary waves:

$$\widetilde{\gamma}^{\rm s}_{\boldsymbol{k}} \simeq -\frac{N_0^2|T_{k\widetilde{k},k_0k_0}|^2}{k\widetilde{v}} < 0 \, . \quad (10.8d)$$

Negative contributions to the wave damping, caused by the narrow package N ,

$$\widetilde{\gamma}_{\boldsymbol{k}} = \widetilde{\gamma}^{\rm c}_{\boldsymbol{k}} + \widetilde{\gamma}^{\rm s}_{\boldsymbol{k}} \, , \quad (10.9a)$$

($\propto N$, or $\propto N^2$) can exceed the positive contribution γ_k caused by the wide wave thermodynamic-equilibrium distribution n^0_k . This leads to the "kinetic instability". To describe the kinetic instability, consider KEs for the secondary waves:

$$\frac{dn_{\boldsymbol{k}}}{dt} = \gamma_{\boldsymbol{k}}\left[n^{(0)}_{\boldsymbol{k}} - n_{\boldsymbol{k}}\right] - |\widetilde{\gamma}_{\boldsymbol{k}}|n_{\boldsymbol{k}} \, . \quad (10.9b)$$

This equation has the stationary "under-threshold" solution

$$n_{\boldsymbol{k}} = \frac{\gamma_{\boldsymbol{k}} n_{\boldsymbol{k}}^{(0)}}{\gamma_{\boldsymbol{k}} - |\widetilde{\gamma}_{\boldsymbol{k}}|} , \tag{10.9c}$$

which describes the kinetic instability with the threshold

$$\gamma_{\boldsymbol{k}} = |\widetilde{\gamma}_{\boldsymbol{k}}| \ . \tag{10.9d}$$

Nonlinear theory of kinetic instability

- Limitation mechanism by positive nonlinear damping:

$$\Gamma_{\boldsymbol{k}} = \gamma_{\boldsymbol{k}} + \sum_{\boldsymbol{k}'} \eta_{\boldsymbol{k}\boldsymbol{k}'} n_{\boldsymbol{k}'} , \quad \text{with} \quad \eta_{\boldsymbol{k}\boldsymbol{k}'} > 0 \ . \tag{10.10a}$$

Assuming, that the confluence 3-wave processes for the secondary waves are allowed, consider a "confluence" mechanism for positive nonlinear damping. Eq. (10.2c):

$$\gamma_{\boldsymbol{k}}^{\mathrm{c}} = 2\pi \int \frac{d\boldsymbol{k}_1 d\boldsymbol{k}_2}{(2\pi)^3} |V_{1,\boldsymbol{k}\mathbf{2}}|^2 (n_{\mathbf{2}} - n_{\mathbf{1}}) \delta(\omega_{\mathbf{1}} - \omega_{\boldsymbol{k}} - \omega_{\mathbf{2}}) \delta(\mathbf{1} - \boldsymbol{k} - \mathbf{2})$$

immediately gives:

$$\eta_{\boldsymbol{k}\boldsymbol{k}'} = \eta_{\boldsymbol{k}'\boldsymbol{k}} = 2\pi |V_{\boldsymbol{k}+\boldsymbol{k}',\boldsymbol{k}\boldsymbol{k}'}|^2 \delta(\omega_{\boldsymbol{k}+\boldsymbol{k}'} - \omega_{\boldsymbol{k}} - \omega_{\boldsymbol{k}'}) > 0 \ . \tag{10.10b}$$

Nonlinear theory of self-consistent dynamics, described in subsection 9.2 yields Singular wave distributions in the limit $n_{\boldsymbol{k}}^{(0)} \to 0$: $n_{\boldsymbol{k}} \neq 0$ on the set of singular points $\boldsymbol{k}_j$, where

$$\widetilde{\Gamma}_{\boldsymbol{k}_j} \equiv \Gamma_{\boldsymbol{k}} - |\widetilde{\gamma}_{\boldsymbol{k}}| = 0 , \quad d\widetilde{\Gamma}_{\boldsymbol{k}_j}/d\boldsymbol{k}_j = 0 \ . \tag{10.10c}$$

This can happens on

– sphere $|\boldsymbol{k}_j| = k_0$, in case of spherical symmetry, (10.11a)

– circles $|\boldsymbol{k}_j| = k_0$, $\cos\theta_j = \pm\cos\theta_0$ in case of axial symmetry, (10.11b)

– set of points, in case of no symmetry. (10.11c)

In all cases:

$$\Gamma_k = \gamma + \eta N\,, \quad N \equiv \int \frac{n_{\boldsymbol{k}} d\boldsymbol{k}}{(2\pi)^3} = \frac{\widetilde{\gamma} - \gamma}{\eta}\,, \tag{10.12a}$$

where N is the total number of secondary waves, and η is the mean value of $\eta_{k,k'}$ on the manifold, where $n_k \neq 0$. One sees, $N \propto$ super-criticality $\widetilde{\gamma} - \widetilde{\gamma}_{\rm th}$.

Demonstrate a stationary solution with $n_k^{(0)} \neq 0$ for spherical symmetry

$$n_{\boldsymbol{k}} = \frac{\gamma n_{\boldsymbol{k}_0}^{(0)}}{(\delta\widetilde{\Gamma}) + \frac{1}{2}\widetilde{\Gamma}''(k - k_0)^2}\,, \quad N = \frac{\gamma n_{\boldsymbol{k}_0}^{(0)}}{\pi\sqrt{2(\delta\widetilde{\Gamma})\widetilde{\Gamma}''}}\,, \quad \delta k \propto \frac{1}{\widetilde{\gamma} - \widetilde{\gamma}_{\rm th}}\,. \tag{10.12b}$$

- Universal (4-wave) "collision mechanism" of limitation

When 3-wave processes for the secondary waves are forbidden one has to account for their 4-wave scattering. In that case the 4-wave KE is

$$\frac{dn_{\boldsymbol{k}}}{dt} = (\gamma_{\boldsymbol{k}} - \widetilde{\gamma}_{\boldsymbol{k}})n_{\boldsymbol{k}} + \pi \int \frac{d\mathbf{1}d\mathbf{2}d\mathbf{3}}{(2\pi)^6}\,\underset{\cdot}{(}\boldsymbol{k} + \mathbf{1} - \mathbf{2} - \mathbf{3}) \tag{10.13a}$$
$$\times \delta(\omega_{\boldsymbol{k}} + \omega_{\mathbf{1}} - \omega_{\mathbf{2}} - \omega_{\mathbf{3}})|T_{\boldsymbol{k}\mathbf{1},\mathbf{23}}|^2 \left[n_{\mathbf{2}}n_{\mathbf{3}}(n_{\mathbf{1}} + n_{\boldsymbol{k}}) - n_{\mathbf{1}}n_{\boldsymbol{k}}(n_{\mathbf{2}} + n_{\mathbf{3}})\right].$$

In the case of spherical symmetry:

$$n_{\boldsymbol{k}} = \frac{N_\kappa}{4\pi k_{\rm sw}^2}\,, \quad \kappa = k - k_{\rm sw}\,, \quad N \equiv \int N_\kappa d\kappa$$

After the angular integrations Eq. (10.13a) gives:

$$N_\kappa = \frac{F^2}{\widetilde{\Gamma} + \frac{1}{2}\,\gamma''\kappa^2} \int N_{\kappa_1}N_{\kappa_2}N_{\kappa_3}\delta(\kappa + \kappa_1 - \kappa_2 - \kappa_3)\frac{d\kappa_1 d\kappa_2 d\kappa_3}{(2\pi)^2}\,, \tag{10.13b}$$

where

$$F^2 \equiv \frac{\pi}{k_{\rm sw}\,v} \int \frac{d\Omega\,\Omega_{\mathbf{1}}d\Omega_{\mathbf{2}}d\Omega_{\mathbf{3}}}{(4\pi)^4(2\pi)^4}|T_{\boldsymbol{k}\mathbf{1},\mathbf{23}}|^2\,k_{\rm sw}^3\,\underset{\cdot}{(}\boldsymbol{k} + \mathbf{1} - \mathbf{2} - \mathbf{3}) \sim \frac{T^2}{k_{\rm sw}\,v}\,, \tag{10.13c}$$

and additional "scattering" contribution $\widetilde{\gamma}_{k_{\rm sw}}$ to the damping of the secondary waves

$$\widetilde{\Gamma} = \gamma_{k_{\rm sw}} + \gamma^{\rm s}_{k_{\rm sw}} - \widetilde{\gamma}_{\boldsymbol{k}_{\rm sw}}\,, \quad \gamma^{\rm s}_{k_{\rm sw}} = F^2N^2\,. \tag{10.13d}$$

After the substitution $N_\kappa = \displaystyle\int d\tau N_\tau \exp(-i\kappa\tau)$ one has "Newtonian" equation for the material point at "position" N_τ in "time" τ , "mass" $M_{\rm eff}$, in with the “potential energy” $\Pi(N)$ and “total (kinetic plus potential) energy E are:

$$\widetilde{\Gamma} N_\tau - \frac{\gamma''}{2}\frac{d^2 N_\tau}{d\tau^2} = F^2 N_\tau^3 \,, \quad M_{\text{eff}} = \frac{\gamma''}{2}\,, \tag{10.14a}$$

$$\Pi(N) = -\frac{N^2}{2} + \frac{F^2 N^4}{4}\,, \quad E = \frac{\gamma''}{4}\left(\frac{dN}{d\tau}\right)^2 + \Pi(N)\ . \tag{10.14b}$$

A particular solution of Eqs. Eq. (10.14) with zero total energy is:

$$\frac{dN}{d\tau} = \frac{N}{\gamma''}\sqrt{F^2N^2 - 2}\,, \tag{10.15a}$$

$$N_\kappa = \frac{N}{2\kappa_{\text{sw}}}\text{cosh}^{-1}\left(\frac{\pi\kappa}{2\kappa_{\text{sw}}}\right)\ , \ \gamma''\kappa_{\text{sw}}^2 = F^2N^2 = 2\widetilde{\Gamma}\ . \tag{10.15b}$$

The physical mechanism of the “scattering” limitation is the “scattering widening” of the wave package to the region with positive total damping, which allows to balance the energy pumping into a central part of the secondary wave package system, due to the kinetic instability, and the energy damping on the tails of the package.

Exercises

TO BE PREPARED

Lecture 11

Kolmogorov spectra of weak wave turbulence

Self-similarity analysis of the flux-equilibrium spectra

• Amplitudes of interaction. In Lect. 3 we considered dimensions of the interaction amplitudes, and got Eqs. (3.19b) and (3.19c):

$$[V_{123}] = \mathsf{g}^{-1/2} \cdot \mathsf{cm}^{d/2-1} \cdot \mathsf{s}^{-1/2} , \quad [T_{1234}] = \mathsf{g}^{-1} \cdot \mathsf{cm}^{d-2} .$$

Introduce scaling exponents of the frequency α , 3-wave amplitude m , and 4-wave amplitude $\widetilde{m}$ as follows:

$$\omega_k \propto k^{\alpha} , \quad V_{123} \simeq V_0 \, k^{m} , \quad T_{1234} \simeq T_0 \, k^{\widetilde{m}} . \tag{11.1a}$$

For the case of complete self-similarity take as two basic parameters ρ and $\omega_{\boldsymbol{k}}$:

$$V_{123} \simeq \sqrt{\left(\frac{\omega_{\boldsymbol{k}}}{\rho}\right)} k^{(5-d)/2}\,, \quad T_{1234} \simeq \frac{k^{5-d}}{\rho}\;. \tag{11.1b}$$

In this way we found the scaling of the vertices via only one media parameter α :

$$m = \frac{1}{2}(\alpha + 5 - d)\,, \quad \widetilde{m} = (5-d)\;. \tag{11.1c}$$

- Continuity Eq. for energy:

$$\frac{d\omega_{\boldsymbol{k}} n_k}{dt} + \frac{dP_{\boldsymbol{k}}}{d\boldsymbol{k}} = 0\,, \quad \frac{dP_{\boldsymbol{k}}}{d\boldsymbol{k}} = -\omega_{\boldsymbol{k}} I_k\,, \quad \varepsilon_k \equiv 4\pi k^2 P_k\,, \tag{11.2a}$$

where ε_k the energy flux (through the sphere of radius k), in d-dimensions is estimated as

$$\varepsilon_k \simeq k^d \omega_k I_k\;. \tag{11.2b}$$

From the 3-wave KE it follows $\varepsilon = \varepsilon_k \simeq k^{2d} V_0^2 k^{2m} n_k^2$, and therefore:

$$n_k \simeq \frac{\sqrt{\varepsilon}}{V_0\, k^x}\,, \quad x = d + m \Rightarrow \frac{1}{2}(d + 5 + \alpha)\;. \tag{11.3a}$$

In particular, for the 3D acoustic waves we found Zakharov-Sagdeev spectrum

$$\omega_k = c_{\rm s} k\,, \ \ \alpha = 1\,, n_k \simeq \frac{\sqrt{\varepsilon\rho}}{\sqrt{c_{\rm s}}\, k^{9/2}}\,, \tag{11.3b}$$

and for the 2D deep capillary waves – Zakharov-Filonenko spectrum

$$\omega_k = \sqrt{\frac{\sigma k^3}{\rho}}\,, \ \ n_k \simeq \frac{\sqrt{\varepsilon\rho}}{\sqrt{\sigma}\, k^{17/4}}\;. \tag{11.3c}$$

In the case of the 4-wave KE, $\varepsilon = \varepsilon_k \simeq k^{3d} T_0^2 k^{2\widetilde{m}} n_k^3$, and therefore:

$$n_k \simeq \frac{\varepsilon^{1/3}}{T_0^{2/3}\, k^{\widetilde{x}}}\,, \quad \widetilde{x} = d + \frac{2\widetilde{m}}{3} \Rightarrow \frac{d+10}{3}\;. \tag{11.4a}$$

In particular, for the 2D deep gravity waves we found Zakharov-Filonenko spectrum

$$\omega_k = \sqrt{g\, k}\,, \quad n_k = \frac{(\varepsilon\rho^2)^{1/3}}{k^4}\,, \tag{11.4b}$$

and for the physically very different cases of the Langmuir wave in plasmas and spin waves in magnetically ordered dielectrics, for which $\alpha = 2$, it follows

$$\widetilde{m} = 0\,, \ \ \widetilde{x} = d\,. \tag{11.4c}$$

- Constant Particle-flux ($\mu_k = \mu$) spectra in 4-w KE. Replacing in Equation 11.4a

$\varepsilon \Rightarrow \omega_k\,\mu$ one has

$$n_k \simeq \frac{\mu^{1/3}\,\omega_k^{1/3}}{T_0^{2/3}\,k^{\widetilde{x}}} \propto \frac{1}{k^y}\,, \quad y = d + \frac{2\widetilde{m} - \alpha}{3}\;. \tag{11.4d}$$

- Simplification for full self-similarity:

– Constant energy flux spectra:

$$n_k = \frac{\rho\omega_k}{k^5} F\left(\frac{\varepsilon\, k^{5-d}}{\rho\omega_k^3}\right)\,, \tag{11.5a}$$

in the 3-wave KE

$$F(x) \simeq \sqrt{x}\,, \quad n_k \simeq \sqrt{\frac{\varepsilon\,\rho}{\omega_k\,k^{5+d}}}\,; \tag{11.5b}$$

and in the 3-wave KE

$$F(x) \simeq x^{1/3}\,, \quad n_k \simeq \left(\frac{\varepsilon\,\rho^2}{k^{10+d}}\right)^{1/3}\;. \tag{11.5c}$$

– Constant Particle-flux spectra in 4-w KE:

$$n_k \simeq \left(\frac{\mu\,\omega_k\,\rho^2}{k^{10+d}}\right)^{1/3}\;. \tag{11.5d}$$

Direction of fluxes

- Direct energy cascade in the 3-w KE:

From one side, in Equation 11.3a we showed:

$$n_k \propto k^{-x}\,, \quad x = d + m = \frac{1}{2}(d + 5 + \alpha)\;.$$

From other side, in the thermodynamic equilibrium $n_k = \dfrac{T}{\omega_k} \propto k^{-\alpha}$. Because $d + 5 > \alpha$ and $x > \alpha$ energy goes toward toward equilibrium distribution, i.e. to large k. Therefore we have "Direct energy cascade" (toward large k).

- Direct energy and inverse "particle" cascade in the 4-w KE:

Following Bob Kraichnan consider energy and particle-number influxes, ε^+ and μ^+ at some $k \approx k_0$. Denote as
$\omega_\pm$, and $\gamma_\pm$ – the wave frequencies and dampings at $k_+ \gg k_0$ and $k_- \ll k_0$,
$n_\pm = n(k_\pm)$ – particle numbers at $k = k_\pm$.
Then in the $k_\pm$ areas the rates of particle-number dissipations are

$$\mu_\pm \simeq n_\pm \gamma_\pm \,,$$

and the rates of energy dissipation:

$$\varepsilon_\pm \simeq \omega_\pm \mu_\pm \ .$$

Clearly the total dissipations:

$$\mu \equiv \mu_+ + \mu_- \,, \quad \varepsilon \equiv \varepsilon_+ + \varepsilon_- = \omega_+ \mu_+ + \omega_- \mu_- \ . \tag{11.6a}$$

Solving these two equations in the limit $\omega_- \to 0$, and $\omega_+ \to \infty$ one has:

$$\mu = \mu_- + \frac{\varepsilon}{\omega_+} \to \mu^- \,, \quad \varepsilon {=} \varepsilon_+ + \omega_- \mu^+ \to \varepsilon_+ \ . \tag{11.6b}$$

This mean that the energy mainly dissipates at large k and we have

Direct energy cascade,

whereas the particle number mainly dissipates at small k and one has

Inverse particle cascade.

Many-flux Kolmogorov spectra

– Anisotropic corrections due to a small additional momentum-flux $\delta\pi$:

$$n_k = n_k^{(0)} \Psi_{\rm m} \left[\frac{(\boldsymbol{k} \cdot \delta\pi)\omega_k}{\varepsilon k^2} \right] \simeq n_k^{(0)} \left[C_1 + C_2 \cos(\theta_k) \frac{\omega_k}{k} \frac{\delta\pi}{\varepsilon} \right] \,, \tag{11.7a}$$

where $n_k^{(0)}$ is the constant energy-flux spectrum.
In the decay case ($\omega_k \propto k^\alpha$, $\alpha > 1$), when the 3-wave processes are allowed,

one sees the increase of the anisotropy toward large k, i.e. "structural instability".

– Isotropic corrections due to a small additional particle-flux $\delta\mu$:

$$n_k = n_k^{(0)}\Psi_{\rm p}\left[\frac{\delta\mu\,\omega_k}{\varepsilon}\right] \simeq n_k^{(0)}\left[C_1 + C_3\frac{\delta\mu\,\omega_k}{\varepsilon}\right] . \tag{11.7b}$$

Again, correction increases toward large k, now as ω_k.

– Correction to the particle-flux spectrum due to a small energy flux can be found similarly.

Exact flux solutions of the 3-wave & 4-wave KEs

- Exact flux solutions of the 3-wave KE (Kraichnan, Zakharov, Kats, Kontorovich)

Consider 3-wave collision integral (7.12), written in the form:

$$\begin{aligned} I_{\boldsymbol k} = \ & \pi\int\frac{d\boldsymbol k_1 d\boldsymbol k_2}{(2\pi)^d}\Big\{|V_{\boldsymbol k,\mathbf{12}}|^2\,[n_{\mathbf 1}n_{\mathbf 2} - n_{\boldsymbol k}(n_{\mathbf 1}+n_{\mathbf 2})] \\ & \times(\boldsymbol k - \mathbf 1 - \mathbf 2)\delta(\omega_{\boldsymbol k} - \omega_{\mathbf 1} - \omega_2) \\ & +|V_{\mathbf 1,\boldsymbol k\mathbf 2}|^2[n_{\mathbf 1}n_{\mathbf 2} - n_{\boldsymbol k}(n_{\mathbf 2}-n_{\mathbf 1})](\mathbf 1 - \boldsymbol k - \mathbf 2)\delta(\omega_{\mathbf 1} - \omega_{\boldsymbol k} - \omega_{\mathbf 2}) \\ & +|V_{\mathbf 2,\boldsymbol k\mathbf 1}|^2\,[n_{\mathbf 1}n_{\mathbf 2} - n_{\boldsymbol k}(n_{\mathbf 1}-n_{\mathbf 2})])(\mathbf 2 - \boldsymbol k - \mathbf 1)\delta(\omega_{\mathbf 2} - \omega_{\boldsymbol k} - \omega_{\mathbf 1})\Big\} . \end{aligned} \tag{11.8}$$

Kats-Kontorovich version of the Kraichnan-Zakharov transformation:

In red marked term: Rotate the $(\boldsymbol k,\ \boldsymbol k_1,\ \boldsymbol k_2)$ -triangle on angle ϕ_1 from $\boldsymbol k_1$ to $\boldsymbol k$ in the $(\boldsymbol k,\ \boldsymbol k_1,\ \boldsymbol k_2)$-plane (denote this transformation by $\widehat P_1$) and elongate the triangle in $\lambda_1 = k/k_1$ times. This gives $\lambda_1\widehat P_1\boldsymbol k_1 = \boldsymbol k\,;\ \lambda_1\widehat P_1\boldsymbol k = \boldsymbol k' \Rightarrow \boldsymbol k_1\,,$ and

$$k' = \frac{k^2}{k_1};\ \lambda_1\widehat P_1\boldsymbol k_2 = \boldsymbol k'' \Rightarrow \boldsymbol k_2\,,\ \ k'' = \frac{kk_2}{k_1}\ . \tag{11.9a}$$

As a result the [red marked term] $=-$[grey marked term] $\times{\lambda_1}^{\zeta}$ where

$$\zeta = 2m\ -\ d\ \ -\alpha\ -2x\ +\ 3d\ . \tag{11.9b}$$

The origin of five contributions to ζ in their ordering in Eq. (11.9a) is as follows:

$$|V|^2,\ (\boldsymbol{k}),\ (\omega),\quad n^2,\quad \frac{D(\boldsymbol{k}_1,\boldsymbol{k}_2)}{D(\boldsymbol{k}',\boldsymbol{k}'')}\ . \tag{11.9c}$$

Transform also the [green marked term] as follows:

$$\lambda_2\widehat{P}_2\boldsymbol{k}_2=\boldsymbol{k}\,;\,\lambda_2\widehat{P}_2\boldsymbol{k}=\boldsymbol{k}''\Rightarrow\boldsymbol{k}_2\,,\,\lambda_2\widehat{P}_2\boldsymbol{k}_1=\boldsymbol{k}'\Rightarrow\boldsymbol{k}_1\,,\,\lambda_2=\frac{k}{k_2}\ . \tag{11.9d}$$

As a result the [green marked term]$=-$[grey marked term] $\times\lambda_2{}^{\zeta}$. Now the sum

$$\text{[grey]+[red]+[green]=[grey]}\left[1-\left(\frac{k}{k_1}\right)^{\zeta}-\left(\frac{k}{k_2}\right)^{\zeta}\right]\ . \tag{11.9e}$$

Clearly, at $\zeta=-\alpha$, the collision integral (11.8) vanishes due to the factor

$$\left[1-\left(\frac{k}{k_1}\right)^{\zeta}-\left(\frac{k}{k_2}\right)^{\zeta}\right]\ (\omega_k-\omega_1-\omega_2)=0\ . \tag{11.9f}$$

Equation 11.9c with $\zeta=-\alpha$ gives

$$x=(m+d)\,, \tag{11.10}$$

in full agreement with our preliminary result (11.3a), which now gets the status of Exact solution of the 3-wave KE in the "inertial interval of scales".

- Exact flux solutions of the 4-wave KE

Consider the 4-wave collision integral (7.14)

$$I_{\boldsymbol{k}}=\frac{\pi}{2}\int\left|T_{\boldsymbol{k}1,23}\right|^2\mathcal{N}_{\boldsymbol{k}1,23}\delta(\boldsymbol{k}+\mathbf{1}-\mathbf{2}-\mathbf{3}) \tag{11.11a}$$
$$\times\delta(\omega_{\boldsymbol{k}}+\omega_1-\omega_2-\omega_3)\,d\mathbf{1}d\mathbf{2}d\mathbf{3}\,,$$
$$\mathcal{N}_{\boldsymbol{k}1,23}\equiv n_2n_3(n_1+n_{\boldsymbol{k}})-n_1n_{\boldsymbol{k}}(n_2+n_3)$$

and mark in grey, red, blue and green each one quarter of it:

$$I_{\boldsymbol{k}}=\frac{1}{4}\left[I_{\boldsymbol{k}}+I_{\boldsymbol{k}}+I_{\boldsymbol{k}}+I_{\boldsymbol{k}}\right]\ . \tag{11.11b}$$

Let $\widehat{P}_j$ - rotation operator from $\boldsymbol{k}_j$ to $\boldsymbol{k}$ and $\boldsymbol{\lambda_j = k/k_j}$. Anzats in $I_{\boldsymbol{k}}$, $I_{\boldsymbol{k}}$ &$I_{\boldsymbol{k}}$:

$$\lambda_1\widehat{P}_1\boldsymbol{k}_1 = \boldsymbol{k},\ \lambda_1\widehat{P}_1\boldsymbol{k} = \boldsymbol{k}' \Rightarrow \boldsymbol{k}_1,\ \lambda_1\widehat{P}_1\boldsymbol{k}_2 = \boldsymbol{k}'' \Rightarrow \boldsymbol{k}_2, \qquad (11.11c)$$

$$\lambda_1\widehat{P}_1\boldsymbol{k}_3 = \boldsymbol{k}''' \Rightarrow \boldsymbol{k}_3;$$

$$\lambda_2\widehat{P}_2\boldsymbol{k}_2 = \boldsymbol{k},\ \lambda_2\widehat{P}_2\boldsymbol{k} = \boldsymbol{k}' \Rightarrow \boldsymbol{k}_2,\ \lambda_2\widehat{P}_2\boldsymbol{k}_1 = \boldsymbol{k}'' \Rightarrow \boldsymbol{k}_3, \qquad (11.11d)$$

$$\lambda_2\widehat{P}_2\boldsymbol{k}_3 = \boldsymbol{k}''' \Rightarrow \boldsymbol{k}_1;$$

$$\lambda_3\widehat{P}_3\boldsymbol{k}_3 = \boldsymbol{k},\ \lambda_3\widehat{P}_3\boldsymbol{k} = \boldsymbol{k}' \Rightarrow \boldsymbol{k}_3,\ \lambda_3\widehat{P}_3\boldsymbol{k}_1 = \boldsymbol{k}'' \Rightarrow \boldsymbol{k}_2, \qquad (11.11e)$$

$$\lambda_3\widehat{P}_3\boldsymbol{k}_2 = \boldsymbol{k}''' \Rightarrow \boldsymbol{k}_3$$

replaced $\boldsymbol{k} \Leftrightarrow \boldsymbol{k}_1$ in $I_{\boldsymbol{k}}$, $\boldsymbol{k} \Leftrightarrow \boldsymbol{k}_2$ & $\boldsymbol{k}_1 \Leftrightarrow \boldsymbol{k}_3$ in $I_{\boldsymbol{k}}$ and $\boldsymbol{k} \Leftrightarrow \boldsymbol{k}_3$ in $I_{\boldsymbol{k}}$ & $\boldsymbol{k}_1 \Leftrightarrow \boldsymbol{k}_2$ giving factor

$$\frac{1}{4}\left[1+\left(\frac{k}{k_1}\right)^{\widetilde{\zeta}}-\left(\frac{k}{k_2}\right)^{\widetilde{\zeta}}-\left(\frac{k}{k_3}\right)^{\widetilde{\zeta}}\right],$$

where

$$\widetilde{\zeta} = 2\widetilde{m} - 3\widetilde{x} - \alpha + 3d\ . \qquad (11.11f)$$

In this ordering, the contributions to $\widetilde{\zeta}$ originated from $|T|^2$, $\mathcal{N}$, $(\boldsymbol{k}..)$, $(\varnothing..)$ and from the Jacobian.

As before, due to $(\omega...)$ the collision integral vanishes at $\widetilde{\zeta} = -\alpha$, giving

$$\widetilde{x} = d + \frac{2}{3}\widetilde{m}\ . \qquad (11.12a)$$

This in agreement with the preliminary Eq. (11.4a) for the energy flux spectrum.

The second exact solution of the 4-wave KE in the inertial interval of scales one gets, putting $\widetilde{\zeta} = 0$. With Equation 11.11f this gives

$$\widetilde{x} = d + \frac{2\,\widetilde{m} - \alpha}{3}, \qquad (11.12b)$$

and agrees with Eq. (11.4d) for the exponent of the particle flux spectrum.

- Locality of the interaction $\Rightarrow$ Convergence of the collision integral

Consider again the 3-wave collision integral in the form (11.8):

$$I_{\boldsymbol{k}} = \pi \int \frac{d\boldsymbol{k}_1 d\boldsymbol{k}_2}{(2\pi)^d} \Big\{ |V_{\boldsymbol{k},\mathbf{12}}|^2 \left[n_{\mathbf{1}} n_{\mathbf{2}} - n_{\boldsymbol{k}}(n_{\mathbf{1}} + n_{\mathbf{2}}) \right] \tag{11.13a}$$
$$\times (\boldsymbol{k} - \mathbf{1} - \mathbf{2}) \delta(\omega_{\boldsymbol{k}} - \omega_1 - \omega_2)$$
$$+ |V_{\mathbf{1},\boldsymbol{k}\mathbf{2}}|^2 [n_{\mathbf{1}} n_{\mathbf{2}} - n_{\boldsymbol{k}}(n_{\mathbf{2}} - n_{\mathbf{1}})] (\mathbf{1} - \boldsymbol{k} - \mathbf{2}) \delta(\omega_{\mathbf{1}} - \omega_{\boldsymbol{k}} - \omega_{\mathbf{2}})$$
$$+ |V_{\mathbf{2},\boldsymbol{k}\mathbf{1}}|^2 [n_{\mathbf{1}} n_{\mathbf{2}} - n_{\boldsymbol{k}}(n_{\mathbf{1}} - n_{\mathbf{2}})]) (\mathbf{2} - \boldsymbol{k} - \mathbf{1}) \delta(\omega_{\mathbf{2}} - \omega_{\boldsymbol{k}} - \omega_{\mathbf{1}}) \Big\} .$$

– Infrared locality: Region $k_1 \ll k \simeq k_2$: $\boldsymbol{\kappa} \equiv \boldsymbol{k}_1$,, where [grey]$\simeq$[green]$\gg$[red]. Ignoring red term, present the sum of the grey and green ones as follows

$$I_{\boldsymbol{k}} \sim \int d\boldsymbol{\kappa} |V_{\boldsymbol{k},\boldsymbol{\kappa}\boldsymbol{k}}|^2 n_\kappa \left[(n_{\boldsymbol{k}-\boldsymbol{\kappa}} - n_{\boldsymbol{k}}) \delta(\omega_{\boldsymbol{k}} - \omega_{\boldsymbol{k}-\boldsymbol{\kappa}}) + \text{term } \boldsymbol{\kappa} \to -\boldsymbol{\kappa} \right]$$

Expanding $(\dots)$ and $(\dots)$ in $\boldsymbol{\kappa}$ up to κ^2 one finds a Double cancellation in the collision integral (11.13a) (of the zero-order and linear in $\boldsymbol{\kappa}$ terms):

$$(\dots) + (\dots) = \frac{dn_k}{d\boldsymbol{k}} \cdot (\boldsymbol{\kappa} - \boldsymbol{\kappa}) + n_k'' \kappa^2 \left(\frac{1}{2} + \frac{1}{2} \right) + \dots$$

The resulting estimate of the collision integral in the infrared regime is as follows

$$I_k \sim \int \frac{d^d \kappa}{\kappa v_k} \kappa^{2m_1 - x} n_k'' \kappa^2 \propto \int_0^k d\kappa \, \kappa^{z-1} \,, \tag{11.13b}$$

Here m_1 is the κ-scaling exponent of the $(\kappa \ll k)$-asymptotic of the vertex

$$V_{\boldsymbol{k},\boldsymbol{\kappa}\boldsymbol{k}} \propto \kappa^{m_1} k^{m-m_1} \,, \quad \text{and} \tag{11.13c}$$
$$z = d + 2m_1 - x + 1 = 2m_1 - m + 1 \,, \tag{11.13d}$$

where x , the scaling exponent of n_k is taken from Equation 11.10. Integral (11.13b) converges in the infrared region $\kappa \to 0$ at $z > 0$, which gives the condition of

$$\text{Infrared locality of 3-wave interaction:} \quad z = 2\,m_1 - m + 1 > 0 \,. \tag{11.14}$$

– Ultraviolet Locality: Region $k_1 \simeq k_2 \gg k$, in which [red] $\simeq$ [green] $\gg$ [grey]. In both terms the leading contribution $\propto n_k$ and one has only one cancellation in the $n_{\boldsymbol{k}}$-expansion. In particular, in the red term:

$$(n_1 - n_2) = \frac{dn_1}{d\boldsymbol{k}_1} \cdot \boldsymbol{k} \simeq n_1 \frac{k}{k_1} \ll n_1$$

The resulting estimate of the collision integral in the infrared regime is as follows

$$I_k \propto n_k \int_k^\infty dk_1 k_1^{d-1} |V_{\mathbf{1},\boldsymbol{k},\mathbf{1}}|^2 \frac{n_1\, k}{k_1} \frac{1}{k v_1} \propto n_k \int_k^\infty dk_1 k_1^{\widetilde{z}-1} \,, \qquad (11.15a)$$

$$\widetilde{z} = d + 2(m - m_1) - x - \alpha = m - 2m_1 - \alpha. \qquad (11.15b)$$

Clearly, for convergence of integral (11.15a) one needs $\widetilde{z} < 0$, i.e. the condition of

Ultraviolet Locality of the 3-wave interaction: $2m_1 - m + \alpha > 0 \qquad (11.16)$

Only fully (IR and UV) local flux spectra of weak wave turbulence (found by the dimensional estimate or as exact solution of KE with the help of Kraichnan-Zakharov conformal transformation) can be realized. The most of known flux-spectra are local indeed.

Example: For acoustic turbulence $\alpha = 1$, $m_1 = \frac{1}{2}$, $m = \frac{3}{2}$ and Zakharov-Sagdeev spectrum is local (with equal IR and UV gap of locality).

Non-local spectra of turbulence require separate study and were found for some physical systems, for example, surface roughening within the 2D Kardar-Parisi-Zhang model and some others.

Exercises

TO BE PREPARED

Lecture 12

Kolmogorov spectra of strong wave turbulence

Universal spectra of strong wave turbulence

For large enough wave amplitudes, the theory of weak wave turbulence, based on the random-phase approximation, leading to the KE, no longer valid. At this condition there is a possibility for strong phase correlations of waves with different $\boldsymbol{k}$, corresponding to creation singularities of the wave profile (in $\boldsymbol{r}$ -space). In the $\boldsymbol{k}$ -representation this reflects in new universal spectra of strong wave turbulence, independent of the (energy or whatever) fluxes, and depending only on a wave profile near the singularity.

Remarkably, in the case of Full self-similarity one finds these spectra by dimensional reasoning, as follows. Generalizing Equation 11.5a

$$n_k = \frac{\rho\omega_k}{k^5} F\left(\frac{\varepsilon\, k^{5-d}}{\rho\omega_k^3}, \text{...other possible fluxes}\right), \tag{12.1a}$$

we have to assume $F(\infty, \infty, ...) \to F$, flux independent dimensionless constant:

$$n_k \simeq \frac{\rho\omega_k}{k^5}\,, \qquad E_k \equiv \omega_k k^{d-1}\, n_k \simeq \frac{\rho\,\omega_k^2}{k^{6-d}}\,, \tag{12.1b}$$

where E_k is the so called one-dimensional energy spectrum.

– Gravity surface waves [with $d=2$ and $\omega_k = \sqrt{g\,k}$]:

When acceleration on the top of waves exceed the gravity acceleration there are discontinuity of the first derivative of the wave profile (creation of "white horses"). In the $\boldsymbol{k}$ -representation this corresponds to universal

$$\text{Fillips' spectrum of the surface gravity waves:} \qquad E_k \simeq \frac{\rho\, g}{k^3}\,, \tag{12.2a}$$

$$\text{or in terms of "occupation numbers"} \qquad n_k \simeq \frac{\rho\sqrt{g}}{k^{9/2}}\,, \tag{12.2b}$$

which agrees with Eq. (12.1b) and is confirmed in experiments.

– Capillary surface waves with $d=2$ and $\omega_k = \sqrt{\dfrac{\sigma\, k^3}{\rho}}$ one finds from Eq. (12.1b)

$$\text{Hix's spectrum of the capillary waves:} \quad E_k \simeq \frac{\sigma}{k}\,, \; n_k \simeq \sqrt{\frac{\sigma}{\rho}}\,\frac{1}{k^{7/2}}\,. \tag{12.3}$$

– Plasma Langmuir waves Collapse ⇒ Point-singularities ⇒ Universal spectrum.

Matching of spectra of the weak and strong wave turbulence

Presenting applicability parameter ξ_1 of the 3-wave KE, Equation 7.15b, as

$$1 \gg \xi_k \simeq \frac{\gamma_k}{\omega_k} \simeq \frac{|V_{kkk}|^2 n_k k^d}{\omega_k^2}\,, \tag{12.4a}$$

and substituting n_k for the constant-energy flux $n_k \simeq \dfrac{\sqrt{\varepsilon}}{|V_{kkk}|k^d}$ one gets

$$\xi_k \simeq \frac{\sqrt{\varepsilon}\,|V_{kkk}|}{\omega_k^2} \tag{12.4b}$$

In the case of full self-similarity, when $V_{kkk} \simeq \dfrac{\sqrt{\omega_k k^{5-d}}}{\sqrt{\rho}}$, ξ_k^2 becomes

$$\xi_k^2 \simeq \frac{\varepsilon\, k^{5-d}}{\rho\, \omega_k^3} \ . \tag{12.4c}$$

This allows to rewrite Eq. (12.1a) for the energy-flux spectra in 3-wave KE as

$$n_k = \frac{\rho \omega_k}{k^5} F\left(\xi_k^2\right) \ . \tag{12.5}$$

Repeat the same job for the energy-flux spectrum in the 4-wave KE. Defining:

$$\widetilde{\xi}_k \simeq \frac{\gamma_k}{\omega_k} \simeq \frac{|T_{k\dots}|^2 n_k^2 k^{2d}}{\omega_k^2} , \tag{12.6a}$$

and taking n_k for the energy spectrum in 4-wave KE, $n_k \simeq \dfrac{\varepsilon^{1/3}}{|T_{k\dots}|^{2/3} k^d}$ one gets

$$\widetilde{\xi}_k \simeq \frac{\varepsilon^{2/3}\, |T_{k..}|^{2/3}}{\omega_k^2}$$

In the case of full self-similarity, when $T_{k\dots} \simeq \dfrac{k^{5-d}}{\rho}$, parameter $\widetilde{\xi}_k^{3/2}$ becomes the same as ξ_k^2 , Eq. (12.4c):

$$\widetilde{\xi}_k^{3/2} \simeq \frac{\varepsilon\, k^{5-d}}{\rho\, \omega_k^3} \ . \tag{12.6b}$$

Now, we can rewrite Eq. (12.1a) for the energy-flux spectra in 4-wave KE in the way, similar to Eq. (12.5):

$$n_k = \frac{\rho \omega_k}{k^5} F\left(\xi_k^{3/2}\right) \ . \tag{12.7}$$

Thus, The crossover scale between weak and strong turbulence, $k_{\rm ws}$ is given by

$$\xi_{k_{\rm ws}}^2 \simeq \widetilde{\xi}_{k_{\rm ws}}^{3/2} \simeq \frac{\varepsilon\, {k_{\rm ws}}^{5-d}}{\rho\, \omega_{k_{\rm ws}}^3} \simeq 1 \,, \quad \Rightarrow \quad \varepsilon\, {k_{\rm ws}}^{5-d} \simeq \rho\, \omega_{k_{\rm ws}}^3 \ . \tag{12.8}$$

For $\omega_k \propto k^\alpha$ and $\alpha < \frac{1}{3}(5-d)$ wave turbulence in the small k region, $k < k_{\rm ws}$, is weak and in the region $k > k_{\rm ws}$ is strong.

This is the case for the deep gravity waves with $\alpha = \frac{1}{2} < \frac{1}{3}(5-d) = 1$. Thus

"Weak" Zakharov-Filonenko sp. (11.4b): $n_k \propto k^{-4}, \quad k < k_{\rm ws}$; (12.9a)

"Strong" (& deeper) Fillips sp. (12.3): $n_k \propto k^{-9/2}, \quad k > k_{\rm ws}$.

For $\alpha > \frac{1}{3}(5-d)$ the picture is opposite: strong wave turbulence for $k < k_{\rm ws}$, and weak turbulence for $k > k_{\rm ws}$. For example, for deep capillary waves with $\alpha = \frac{3}{2} > \frac{1}{3}(5-d) = 1$ one has

"Strong" Hix's sp. (12.3): $n_k \propto k^{-7/2}, \quad k < k_{\rm ws}$; (12.9b)

"Weak" (& deeper) Zakh.-Fil. sp. (11.3c): $n_k \propto k^{-17/4}, \quad k < k_{\rm ws}$;

Summary for surface waves. When k increases:

Small $k \Rightarrow$ Weak Zakharov-Filonenko: $k^{-4} \Rightarrow$ Strong Fillips: $k^{-9/2} \Rightarrow$ Strong Hix: $k^{-7/2} \Rightarrow$ Weak Zakharov-Filonenko: $k^{-17/4} \Rightarrow$ Large k

Real life even more complicated: particle-flux spectrum, wind–wave interaction, gravity-capillary wave interaction, anizotropy of spectra...

Spectrum of acoustic turbulence

Recall "Weak" Zakharov–Sagdeev spectrum, Equation 11.3b:

$$n_k \simeq \frac{\sqrt{\varepsilon\rho}}{\sqrt{c_{\rm s}}\, k^{3/2+d}}\,, \quad E_k \simeq \frac{\sqrt{\varepsilon\rho\, c_{\rm s}}}{k^{3/2}}\,, \tag{12.10a}$$

and derive "Strong", non-universal, Kadomtsev-Petviashvili spectrum:

$$E_k \simeq \frac{2\pi\, E}{L\, k^2}\,, \quad E \equiv \int_{2\pi/L} E_k dk\,, \ \text{with } L \text{ – outer scale of turbulence.} \tag{12.10b}$$

In 1D sound waves with $\omega_k = c_{\rm s} k$ is described by the Burgers Equation 5.31a

$$u_t + (c_{\rm s} + u) u_x - \nu\, u_{xx} = 0\,, \tag{12.11a}$$

for the fluid velocity u . Sound propagation with an effective nonlinear velocity $(c_{\rm s}+u)$ leads to creation of shock waves during Creation time $\tau_{\rm sh} \simeq L/u$.

Front width of the dissipative shock ℓ cab be estimated by balancing $uu_x \simeq \nu u_{xx}$ leading to

$$\ell \simeq \nu/u \ . \tag{12.12}$$

To find One-dimensional spectrum of random shocks consider randomly distributed shocks at $x = x_j$ with the amplitudes v_j of the order of the rms velocity v, separated in mean by L and placed in periodical box of length $\mathcal{L} \gg L$.

Define mean energy density of the system and model for the velocity derivative $v'(x) = dv/dx$ as:

$$E = \frac{\rho}{2}\left\langle v^2 \right\rangle \ , \quad \left\langle v_j \right\rangle \simeq v^2 \ , \tag{12.13a}$$

$$v'(x) \simeq \frac{v}{L} + \sum_j v_j\, \delta(x - x_j) \ , \tag{12.13b}$$

Define k-representation:

$$v'(x) = \sum_k v'_k \exp(ikx) \ , \quad v'_k = ikv_k = \frac{2\pi}{\mathcal{L}} \int v'(x) \exp(-ik\,x) \ . \tag{12.13c}$$

For $k \neq 0$, Eq. (12.13b) results in:

$$v_k = \frac{2\pi}{ik\mathcal{L}} \sum_j v_j \exp(ikx_j) \tag{12.13d}$$

The total (in k-space) energy density (in x-space) is

$$E = \frac{\rho}{2} \int_0^{\mathcal{L}} \frac{dx}{\mathcal{L}} v^2(x) = \frac{\rho}{2} \int_0^{\mathcal{L}} \frac{dx}{\mathcal{L}} \sum_{k,k'} \left\langle v_k v_{k'} \right\rangle \exp[i(k+k')x] \tag{12.14a}$$

$$= \frac{\rho}{2} \sum_k |v_k|^2 = \frac{\rho}{2}\frac{\mathcal{L}}{2\pi} \int dk\ \left\langle |v_k|^2 \right\rangle \implies E_k = \frac{\rho}{2}\frac{\mathcal{L}}{2\pi} \left\langle |v_k|^2 \right\rangle \tag{12.14b}$$

Substituting v_k from Equation 12.13d one gets

$$E_k \simeq \frac{\pi\,\rho}{k^2\mathcal{L}} \sum_{j\ell} v_j v_\ell \exp[ik(x_j - x_\ell)] = \frac{\pi\,\rho v^2}{k^2 L} \simeq \frac{2\pi\,E}{2\pi k^2 L} \ , \tag{12.14c}$$

in agreement with the Kadomtsev-Petviashvili spectrum of random shocks, Eq. (12.12
This spectrum is non-local in k-space due to the phase correlations in the shocks.

–Unsolved problem of acoustic turbulence:

Zakharov-Sagdeev vs Kadomtsev-Petviashvili spectra

Exercises

TO BE PREPARED

Lecture 13

Introduction to Hydrodynamic Turbulence

"I am an old man now, and when I die and go to Heaven there are two matters on which I hope enlightenment. One is quantum electro-dynamics and the other is turbulence of fluids. About the former, I am really rather optimistic"

Sir Horace Lamb (1932)

Turbulence in the Universe: from spiral galaxies to cars

– Hydrodynamic turbulence at galactic distances $\sim 10^{21} - 10^{19}$ m.

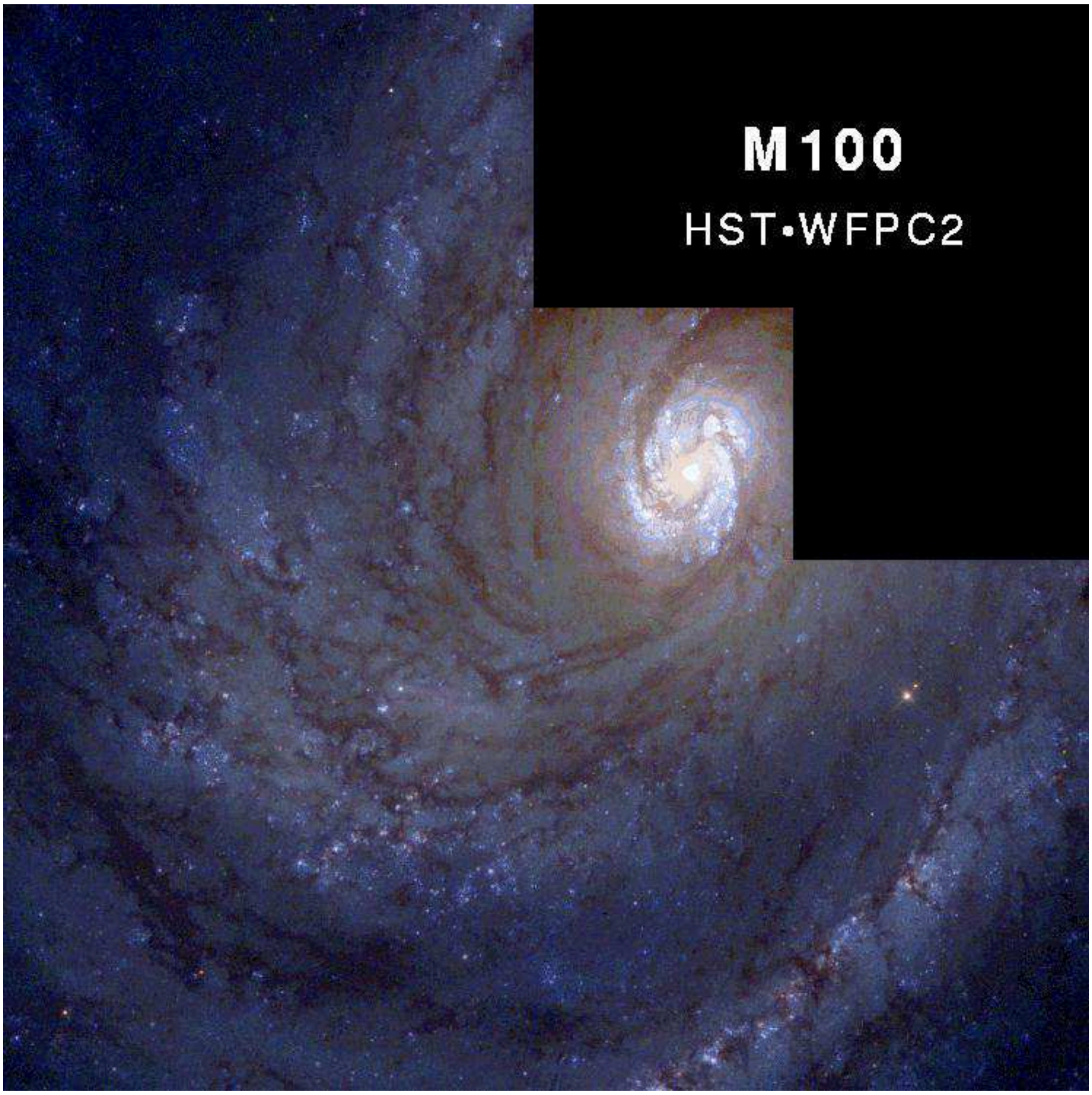

Rayleigh-Taylor instability (of heavy fluid above the light one) played an important role in the Universe evolution on the fluid stage.

Later the Taylor instability in the planar Couette flow lead to creation of spiral galaxies:

Spiral Galaxy M-100 in Coma Benerices. Distance $\sim 6 \cdot 10^7$ light years

– Hydrodynamic turbulence at interstellar scales $\sim 10^{17} - 10^{16}$ km.

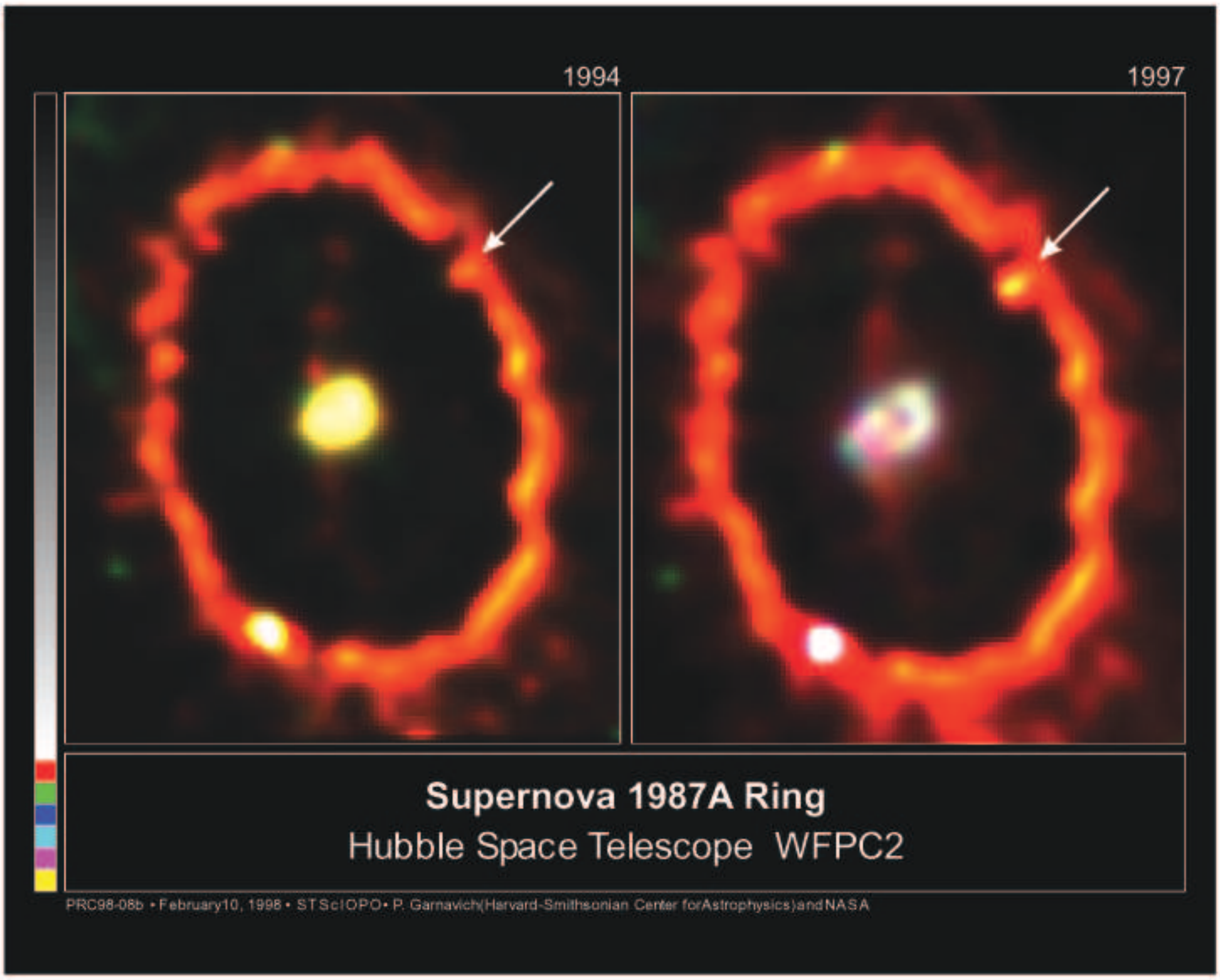

Growing turbulent gas ring around Supernova 1987a. Bright knot – collision heat with the innermost part of the circum-stellar ring

– More turbulent details on $\sim 10^{17} - 10^{16}$ m.

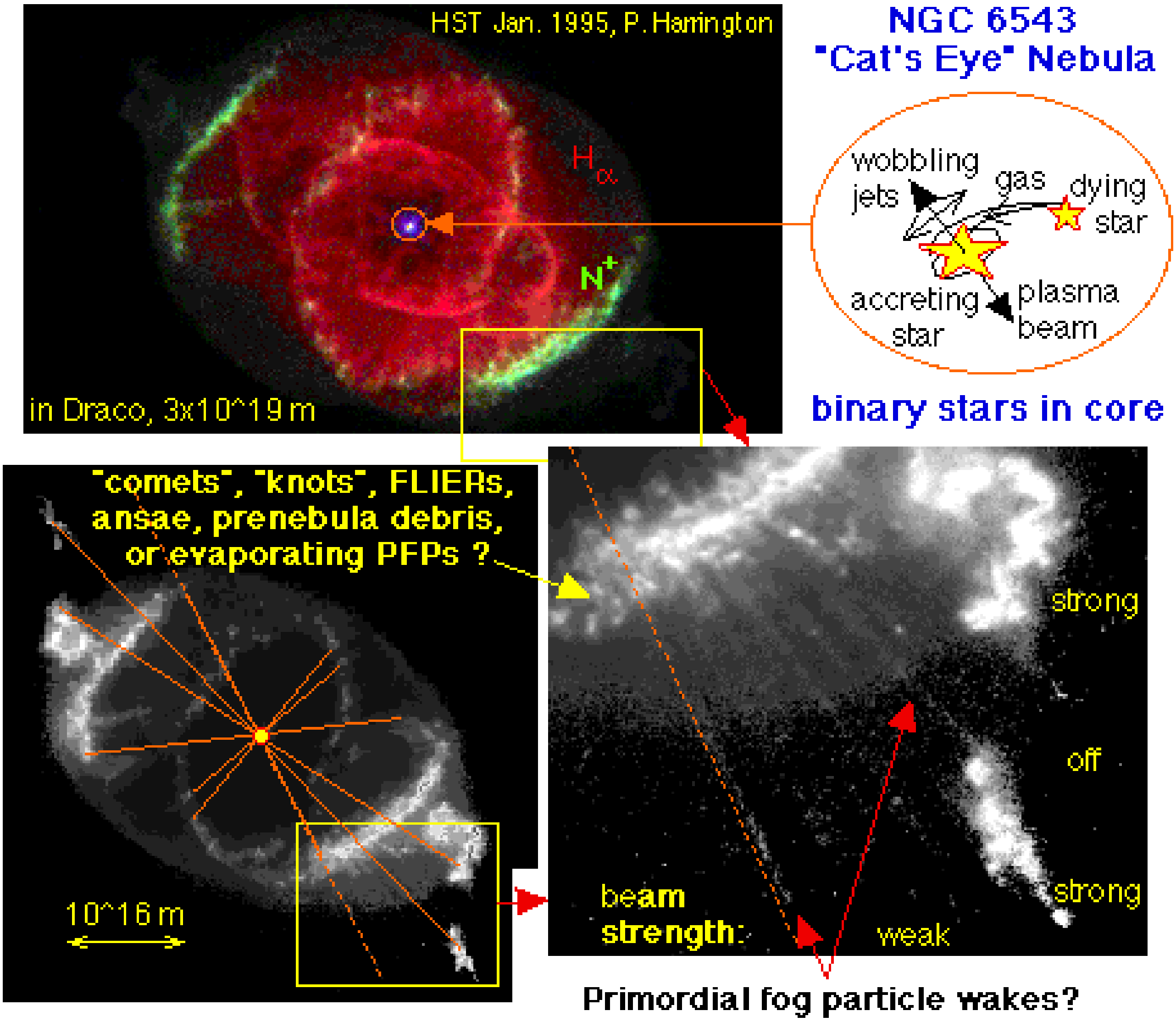

Accretion in binary starts, controlled by the turbulent diffusion of angular momenta, defines their life-time

– Planetary turbulence, scales $\sim 10^7 - 10^6$ m.

Storm on Jupiter

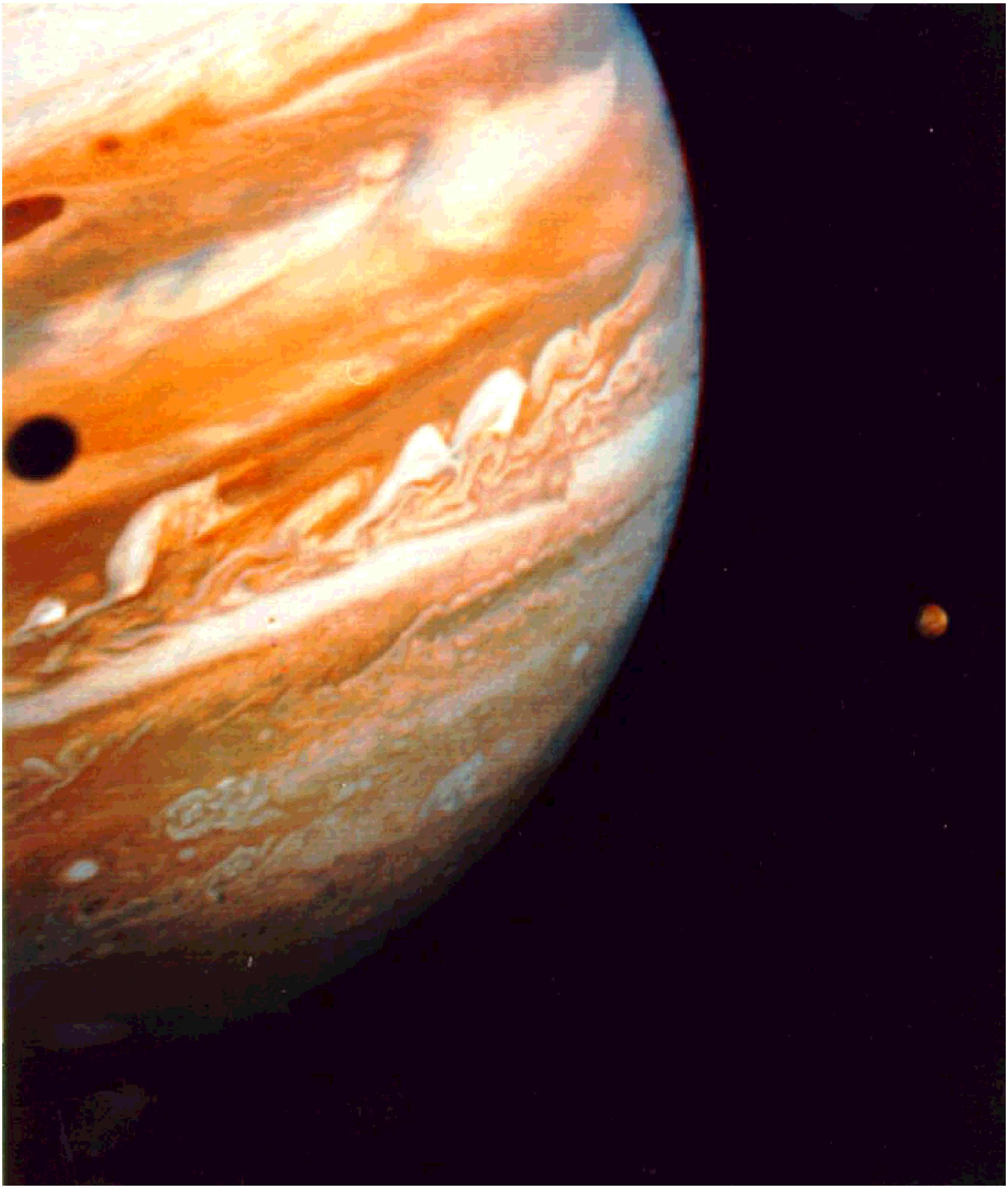

Tropical Hurricane Gladis, Oct. 68

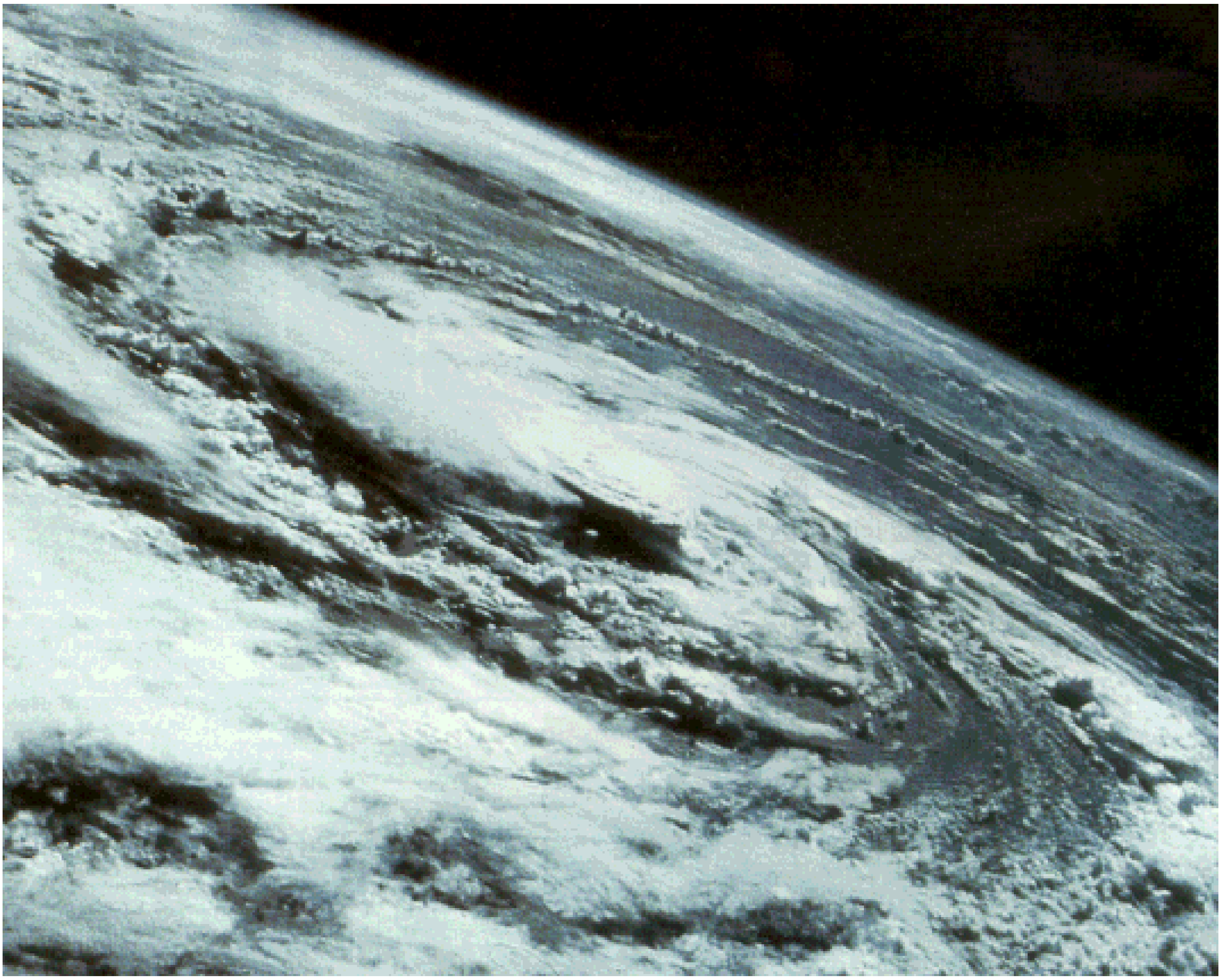

•– Turbulence on human scales (meters): Ottadalen, Sweden, Aug.2003

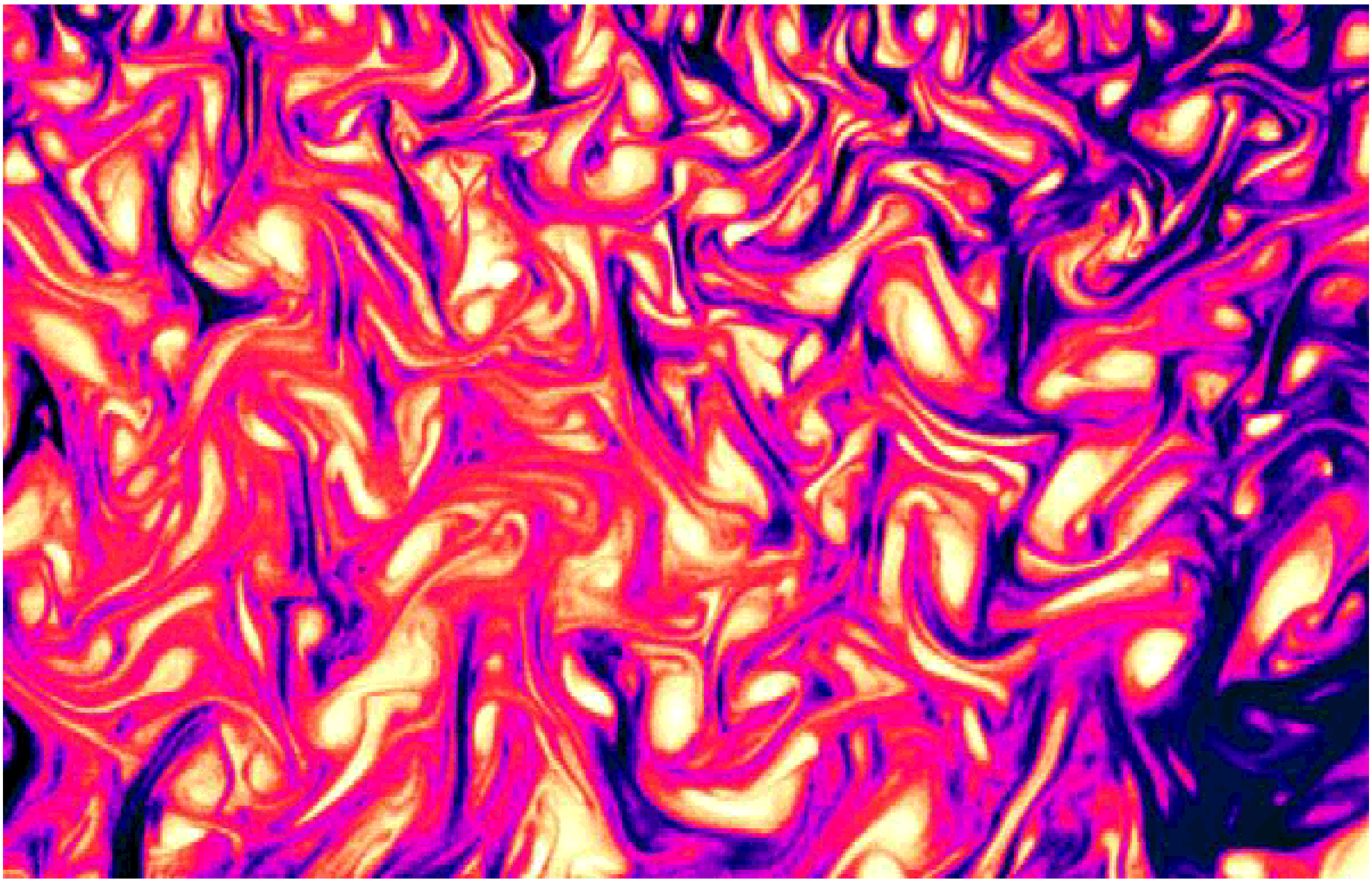

– Some engineering aspects of turbulence

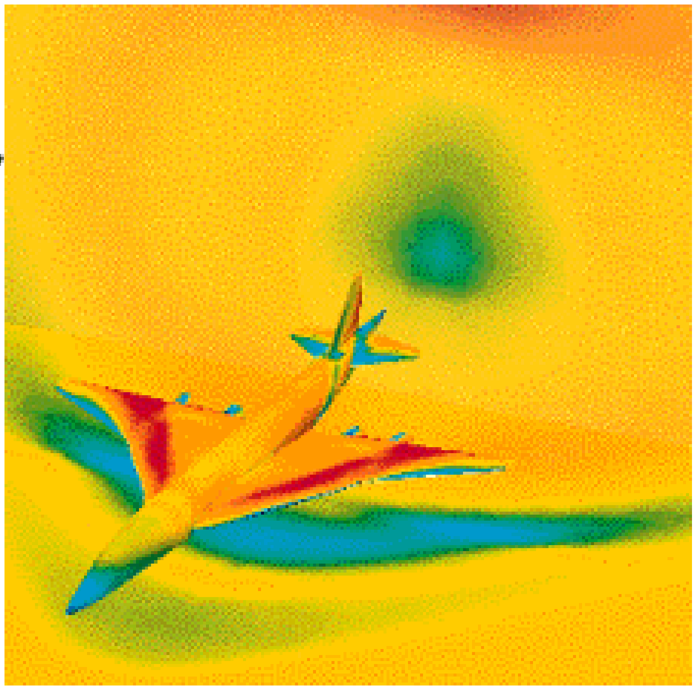

Computer simulated turbulent air pressure: sonic boom behind supersonic aircraft Lockhid 3A

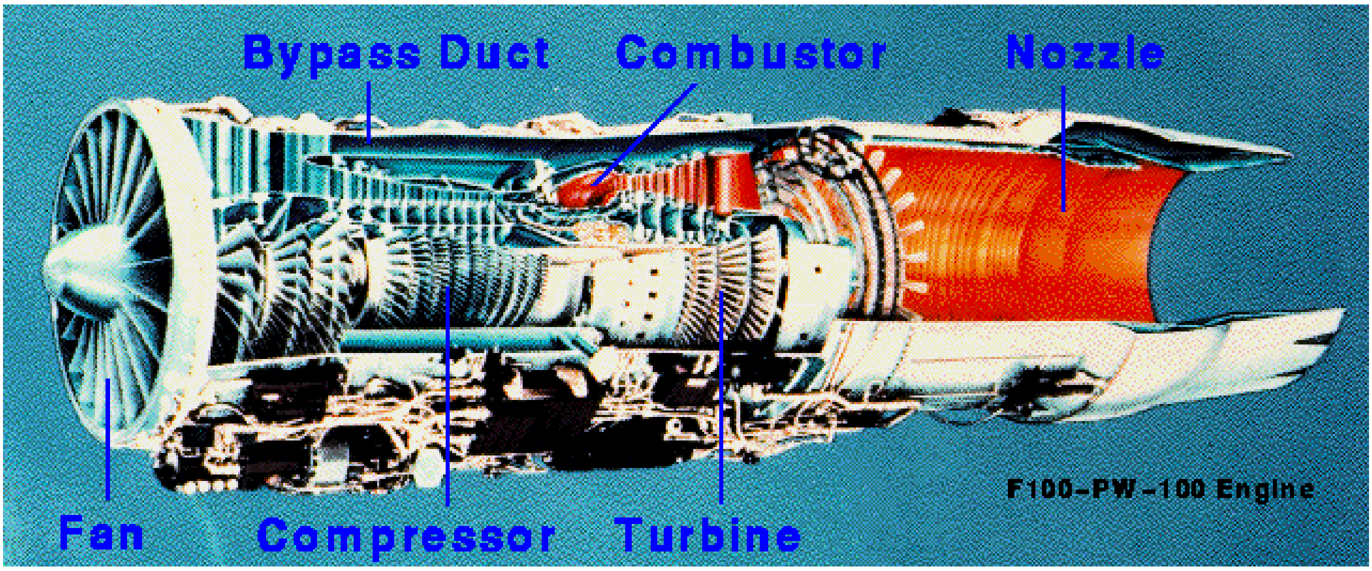

Turbulent fuel combustion in an aircraft engine

Euler and Navier Stokes equations, Reynolds number

The Euler equation for $\boldsymbol{v}(\boldsymbol{r},t)$ is the 2nd Newton's law for the fluid particle:

$$\rho\Big[\overbrace{\frac{\partial \boldsymbol{v}(\boldsymbol{r},t)}{\partial t}+(\boldsymbol{v}\cdot\boldsymbol{\nabla})\boldsymbol{v}}^{\text{Fluid particle Acceleration}}\Big] - \underbrace{(-\boldsymbol{\nabla} p)}_{\text{Pressure Force}} = 0\,, \quad \text{Leonard Euler, 1741.} \tag{13.1}$$

The Navier-Stokes equation accounts for the viscous friction:

$$\Big[\frac{\partial \boldsymbol{v}(\boldsymbol{r},t)}{\partial t} + \underbrace{(\boldsymbol{v}\cdot\boldsymbol{\nabla})\boldsymbol{v}\Big]}_{\text{Nonlinear interaction}} + \boldsymbol{\nabla} p/\rho = \underbrace{\nu\Delta\boldsymbol{v}}_{\text{viscous friction}}\,, \tag{13.2}$$

Claude L.M.H. Navier, 1827,
George Gabriel Stokes, 1845.

Osborne Reynolds (1894) introduced "Reynolds number" $\mathcal{R}e$

$$\mathcal{R}e = \frac{\blacksquare}{\blacksquare} \simeq \frac{u\nabla v}{\nu\Delta v} \simeq \frac{LV}{\nu} \quad \text{as a measure of the nonlinearity of the NSE.} \tag{13.3}$$

Turbulence in the Jordan River

– Simplest model of the Jordan river : a water flow on an incline plane

JORDAN RIVER

Stationary

NSE: $g \sin\alpha = \nu \dfrac{d^2 v(z)}{dz^2}$

gravity acceleration: $g \simeq 980\,\text{cm}\,\text{s}^{-2}$,

Mean inclination angle for Jordan: $\alpha \simeq H/L$,

$H =$ 725 m, $L =$ 325 km,

$\alpha \simeq 2.2 \cdot 10^{-3}$,

Kinematic viscosity for water $\nu \simeq 10^{-2}$ cm ^{2} s $^{-1}$, Estimate mean Jordan depth: $h \simeq 100$ cm,

Boundary condition at the bottom, $v(0) = 0$,

At the surface, at $z = h$: $dv/dz = 0$.

Solution of NSE:

$$v(z) = \frac{V_\ell z}{h}\left(\frac{z}{h} - 2\right) ,$$

$V_\ell = \dfrac{g\,\alpha\,h^2}{2\,\nu} \Rightarrow$ for Jordan $V_\ell \simeq 10^6\,\frac{\text{cm}}{s}$

.

Jordan velocity is much larger than the sound speed in Israel

$$c_\text{s} \simeq 3.4 \cdot 10^4\,\text{cm}\,\text{s}^{-1} .$$

Conservation of energy gives $V_\ell \sim c_\text{s}$, namely:

$$V_\ell = \sqrt{2gH} \simeq 1.2 \cdot 10^4\,\text{cm}\,\text{s}^{-1} ,$$

while experimental value $V_\ell \simeq 300\,\text{cm}\,\text{s}^{-1} \simeq 10\,\text{Km}\,\text{h}^{-1}$.

Reynolds number $\mathcal{R}e = \dfrac{hV_\ell}{\nu} \simeq 10^{10} \gg 1$,
however the nonlinear term $\blacksquare = 0$ in the above solution.

Reynolds conjecture: laminar flows unstable for $\mathcal{R}e > \mathcal{R}e_{\rm cr} \simeq 10 \div 1000$ resulting in Hydrodynamic turbulence !!!

Before "turbulent" estimate for V_ℓ consider related problem of air turbulence behind a car.

Simple model of turbulence behind my car

During time τ a car produces turbulence with the typical turbulent velocity $V_{\rm turb} \simeq V_{\rm max}$ in the volume $\simeq V_{\rm max}\,\tau S_\times$, $S_\times$ – the car $\times$-section area. Resulting turbulent kinetic energy ($\rho_{\rm air} \simeq 1.2 \cdot 10^{-3}$ g cm $^{-3}$) is

$$E_{\rm turb} \simeq \frac{1}{2}\,\rho_{\rm air} V_{\rm turb}^2 V_{\rm max}\,\tau S_\times$$

$\simeq \tau W_{\rm car}$, power of a car engine $V_{\max} \simeq \left[\frac{2\, W_{\rm car}}{\rho_{\rm air}\, S_{\times}}\right]^{1/3}$ $\Rightarrow$ Evaluation for Hyndai Lantra: $S_{\times} \simeq 2 \cdot 10^4\, \mathrm{cm}^2$,

$$W_{\rm car} = 116\, \mathrm{HP} = 8.7 \cdot 10^{11}\, \frac{\mathrm{g\ cm}^2}{\mathrm{s}^3}, \quad V_{\max} \simeq 4.2 \cdot 10^3\, \frac{\mathrm{cm}}{\mathrm{s}} \simeq 150\, \frac{\mathrm{km}}{\mathrm{h}}\ .$$

Richardson cascade picture of developed turbulence

"Big whirls have little whirls
That feed on their velocity
And little whirls have lesser whirls
And so on to viscosity"

Lewis Fry Richardson, paraphrase of J. Swift , 1920

Hurricane Bonnie, $V_{\rm T} \simeq 300 \frac{\rm m}{\rm s}$,

Reynolds number at $H \simeq 500$ m $\mathcal{R}e = \frac{V_{\rm T} H}{\nu} \simeq 10^{10} \gg \mathcal{R}e_{\rm cr}$

Unstable H, V_{T} -eddies create smaller H_1, V_1 -eddies with $\mathcal{R}e > \mathcal{R}e_1 \gg \mathcal{R}e_{\mathrm{cr}}$. Their instability creates H_2, V_2 -eddies of the second generation, end so on, until $\mathcal{R}e_n$ of the n -th generation eddies reaches R_{cr} and will be dissipated by viscosity: $\mathcal{R}e > \mathcal{R}e_1 > \mathcal{R}e_2 > \ \ldots \ > \mathcal{R}e_{n-1} > \mathcal{R}e_n > \mathcal{R}e_{\mathrm{cr}}.$

– Simplest "turbulent" model of the water flow in rivers

Rate of energy dissipation=Rate of energy production:

$$\frac{dE_{\rm turb}}{dt} \simeq \rho_{\rm water} h^3 \frac{V_{\rm t}^2}{2}\,\frac{V_{\rm t}}{2\,h} \tag{13.4a}$$
$$= F_{\rm grav} V_{\rm t} \simeq \rho_{\rm water} h^3 g\alpha\, V_{\rm t} \tag{13.4b}$$

h – depth, α – mean inclination angle. This gives

$$V_{\rm t} \simeq 2\sqrt{g\,h\,\alpha}\ . \tag{13.5}$$

This "turbulent" evaluation for Jordan river gives

$$V_{\rm t} \simeq 30\frac{\rm cm}{\rm s} \simeq 1\,\frac{\rm Km}{\rm h}\,, \tag{13.6a}$$

which is much more reasonable than our "laminar" evaluation,

$$V_\ell \simeq 36,000\,{\rm Km/h}\ . \tag{13.6b}$$

A.N. Kolmogorov-1941 universal picture of developed turbulence

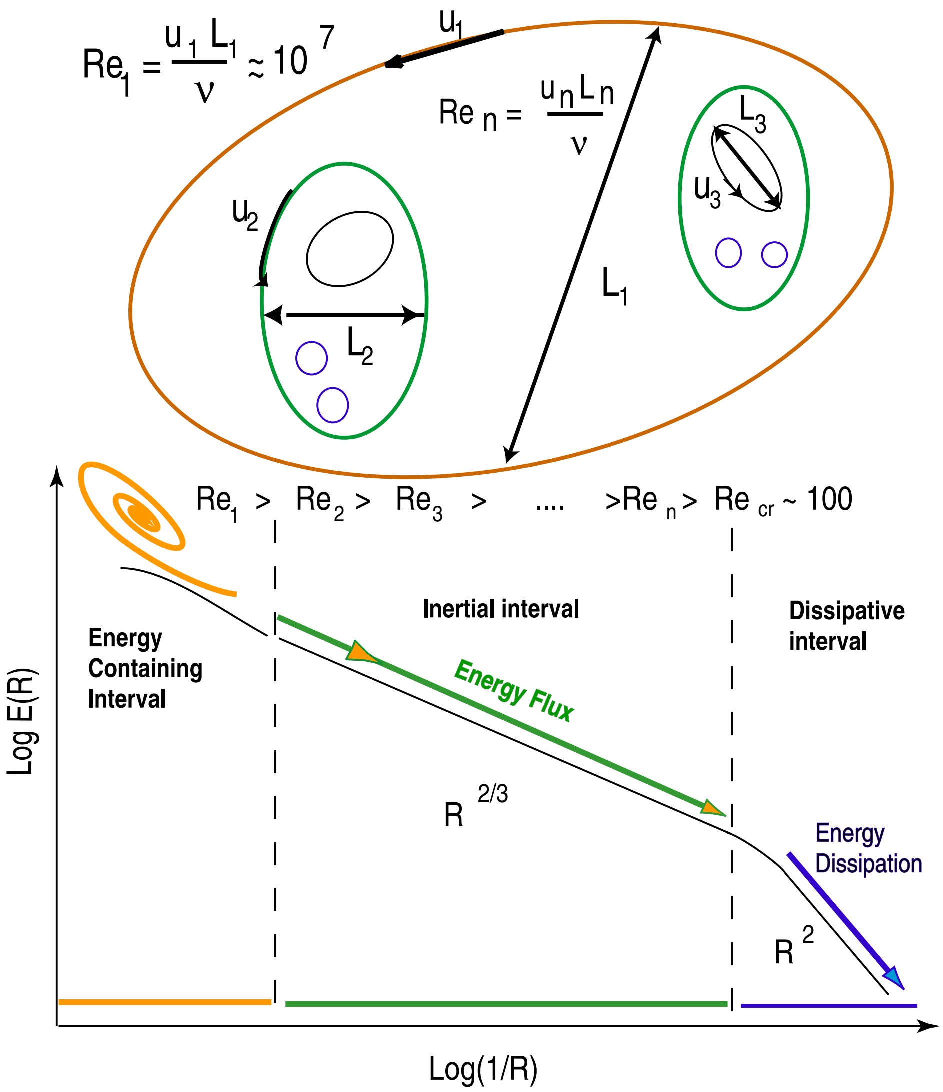

I. Universality of small scale statistics, isotropy, homogeneity;

II. Scale-by-scale "locality" of the energy transfer;

III. In the inertial interval of scales the only relevant parameter is mean energy flux ε . $\Rightarrow$ dimensional reasoning $\Rightarrow$

1. Turbulent energy of scale ℓ in inertial interval $E_\ell \simeq \rho\, \varepsilon^{2/3}\, \ell^{2/3}$,
2. Turnover and life time of ℓ -eddies: $\tau_\ell \simeq \varepsilon^{-1/3}\, \ell^{2/3}$
3. Viscous crossover scale η

and Number degrees of freedom, N $\eta \simeq \varepsilon^{-1/4}\, \nu^{3/4}$, $N \sim \mathcal{R}e^{3/4}$...

Exercises

Lecture 14

Quantum and Quasi-classical turbulence in superfluids

?? To be prepared

?? To be prepared

?? To be prepared

?? To be prepared

?? To be prepared
13.7 Exercises

To be prepared

Lecture 15

Intermittency and Anomalous Scaling

15.1 Structure functions, intermittency & multiscaling

15.2 Dissipative scaling exponents μ_n, dissipative and temporal bridges

15.3 Phenomenological models of multi-scaling

15.4 Dynamical "shell models" of multiscaling: GOY, Sabra and others

15.5 Toward analytical theory of multiscaling

Structure functions, intermittency and multiscaling

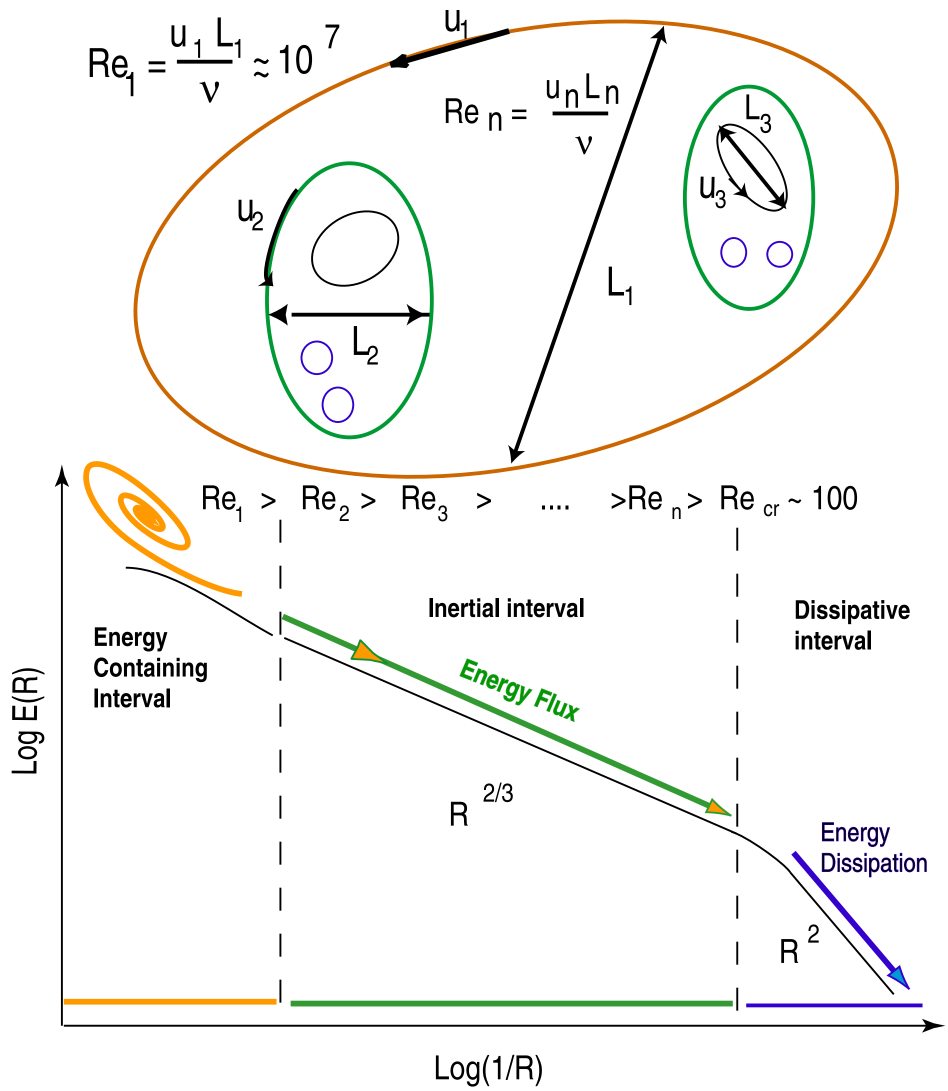

I. Universality of small scale statistics, isotropy, homogeneity;

II. Scale-by-scale "locality" of the energy transfer;

III. In the inertial interval of scales the only relevant parameter is mean energy flux ε . $\Rightarrow$ dimensional reasoning $\Rightarrow$

1. Turbulent energy of scale ℓ in inertial interval $E_\ell \simeq \rho\, \varepsilon^{2/3}\, \ell^{2/3}$,

2. Turnover and life time of ℓ -eddies: $\tau_\ell \simeq \varepsilon^{-1/3}\, \ell^{2/3}$

3. Viscous crossover scale η

and Number degrees of freedom, N $\eta \simeq \varepsilon^{-1/4}\, \nu^{3/4}$, $N \sim \mathcal{R}e^{3/4}$...

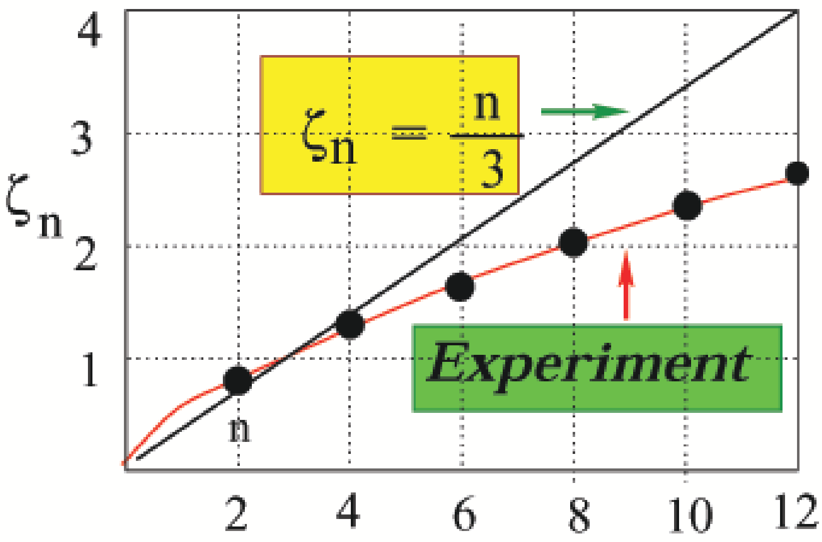

n	n/3	ζ_n
2	0.67	0.70
4	1.33	1.20
6	2.00	1.62
8	2.67	2.00
10	3.33	2.36
12	4.00	2.68

Velocity difference across separation $\boldsymbol{r}$ gives velocity of "$\boldsymbol{r}$-eddies:"

$\vec{W}_{\vec{r}} = \vec{v}(\vec{r},t) - \vec{v}(0,t)$, – Longitudinal velocity: $W^{\ell}_{\vec{r}} = \vec{W}_{\vec{r}} \cdot \vec{r}/r$

Longitudinal velocity structure functions $S^{\ell}_{n}(\vec{r}) = \langle (W^{\ell}_{\vec{r}})^n \rangle \propto r^{\zeta_n}$.

In particular: $S_2(\vec{r})$ – Energy of $\vec{r}$ -eddies,

$S_3(r) = -\frac{4}{5}\, r$ (Kolmogorov-41) – Energy flux on scale r,

$S_4(r) - 3\, S_2^2(r)$ – Deviation from the Gaussian statistics,

...

$S_{2n}(\vec{r})/S_2^n(r)$ – Statistics of very rare events

$$S^{\ell}_{n}(r) = C_n\, (\vec{r})^{n/3} \left(\frac{r}{L}\right)^{\zeta_n - n/3}, \quad L \text{ — renormalization length} .$$

Dissipative scaling exponents μ_n and "bridges"

$$K_{n\varepsilon}(\vec{R}_{ij}) = \langle \varepsilon_{11'}\varepsilon_{22'} \dots \varepsilon_{nn'} \rangle \propto R^{-\mu_n}, \quad \varepsilon_{ij} \equiv \varepsilon(r_i) - \varepsilon(r_j),$$

$\vec{R}_{ij} \equiv \vec{r}_i - \vec{r}_j$. Straightforward K41 phenomenology predicts $\mu_2 = \frac{8}{3}$.

Experiment: $\mu_2 \simeq 0.3$? $\Rightarrow$ **Viscous anomaly:**

To explain this phenomenon, introduce pair velocity correlations

$$\left\langle v^{\alpha}_{\vec{k}} v^{\beta}_{\vec{k}'} \right\rangle = (2\pi)^3 (\vec{k} + \vec{k}') F_2^{\alpha\beta}(\vec{k}), \ \Rightarrow \text{K41} \ \Rightarrow \ \vec{F}_2(\vec{k}) \simeq \frac{\varepsilon^{2/3}}{k^{11/3}} .$$

$$S_2^\ell(R) = \int \frac{d\vec{k}}{(2\pi)^3}|1-\exp(i\vec{k}\cdot\vec{R})|^2 F_2^{\ell\ell}(\vec{k}) \simeq \varepsilon^{2/3}\int_0^\infty \frac{k^2\,d\,k}{k^{11/3}}\int_{-1}^1 \frac{d\,x}{\pi^2}\sin^2\left(\frac{k\,R\,x}{2}\right) \quad (15.1)$$

$$\simeq (\varepsilon\,R)^{2/3} \quad \text{due to UV \& IR convergence of the integral .} \quad (15.2)$$

From other side:

$$\langle \varepsilon\vec{r})\rangle \simeq \int \frac{\nu\,d\vec{k}}{(2\pi)^3}k^2 F_2(\vec{k}) \simeq \nu\,\varepsilon^{2/3}\int_0^{1/\eta}\frac{k^4\,d\,k}{k^{11/3}} \simeq \nu\varepsilon^{2/3}\int_0^{1/\eta}k^{1/3}dk \simeq \frac{\nu\varepsilon^{2/3}}{\eta^{4/3}} \quad (15.3)$$

$$\Rightarrow \quad \left[\eta \simeq \varepsilon^{-1/4}\nu^{4/3}\right] \Rightarrow \quad (15.4)$$

ε , ν . As a result ε is μ independent $\Rightarrow$ the viscous anomaly!

$\varepsilon\vec{r})$ is the viscous scale object and $K_{n\varepsilon}(\vec{R}_{ij})$ cannot be evaluated in the K41 manner via inertial-interval parameters! Instead one can use

- **Exact "Dissipative-bridge" relationships**, (L'vov-Procaccia-96)

Consider the NSE:

$$\frac{\partial\vec{v}}{\partial t} + (\vec{v}\cdot\vec{\nabla})\vec{v} + \vec{\nabla}p = \nu\,\Delta\vec{v} \quad \Rightarrow \quad \frac{\partial\vec{v}}{\partial t} + \widehat{P}\left[(\vec{v}\cdot\vec{\nabla})\vec{v}\right] = \nu\,\Delta\vec{v}\,,$$

where $\widehat{P}$: transversal projector. Introduce $\vec{W}_{\vec{r}}$, $\vec{r}$-separated velocity increment for which NSE can be schematically written as

$$\frac{\partial\vec{W}_{\vec{r}}}{\partial t} + \widehat{P}\left[(\vec{W}_{\vec{r}}\cdot\vec{\nabla})\vec{W}_{\vec{r}}\right] = \nu\,\Delta\vec{W}_{\vec{r}} \Rightarrow$$

$$\vec{W}_{\vec{r}}\frac{\partial\vec{W}_{\vec{r}}}{\partial t} + \vec{W}_{\vec{r}}\widehat{P}\left[(\vec{W}_{\vec{r}}\cdot\vec{\nabla})\vec{W}_{\vec{r}}\right] = \vec{W}_{\vec{r}}\nu\,\Delta\vec{W}_{\vec{r}} \Rightarrow -\nu(\nabla\vec{W}_{\vec{r}})\cdot(\nabla\vec{W}_{\vec{r}}) \simeq -\varepsilon\vec{r})\ .$$

Thus, inside of the average operator, $\langle\ldots\rangle$, the viscous range object $\varepsilon\vec{r})$ can be evaluated as the inertial range object $\vec{W}_{\vec{r}}\widehat{P}\left[(\vec{W}_{\vec{r}}\cdot\vec{\nabla})\vec{W}_{\vec{r}}\right] \simeq W_{\vec{r}}^3/r$:

$$\varepsilon\vec{r}) \Rightarrow \frac{W_r^3}{r} \quad \Rightarrow \quad \mu_n = n - \zeta_{3n} \quad \Rightarrow \quad \mu_2 = 2 - \zeta_6 \simeq 0.3 \div 0.4$$

Exact "dissipative-bridge" relations $\mu_n = n - \zeta_{3n}$ are known in literature as a consequence of Kolmogorov "Refined Similarity" hypothesis.

To proof it one needs to proof K41 hypothesis on "interaction locality" which actually is the proof of convergence of many-point, one time "fully unfused" correlation function

$$\left\langle \vec{W}_{\vec{1}}\vec{W}_{\vec{2}}\dots\vec{W}_{\vec{n}}\widehat{P}\Big[(\vec{W}_{\vec{r}}\cdot\vec{\nabla})\vec{W}_{\vec{r}}\Big]\right\rangle$$

that contains non-local transversal projector (with inverse of the Laplacian operator). This was done by LP in 96 with the help of their 1996-

- Fusion rules for the systems with flux equilibrium

which roughly can be written as:

$$\left\langle (W_r)^n(W_R)^m\right\rangle \propto r^{\zeta_n}R^{\zeta_{n+m}-\zeta_n} \quad \text{for} \quad L\gg R\gg r\gg\eta$$

LP-fusion rules later was confirmed in the field and laboratory experiments.

Similarly to dissipative bridge LP derived in 97 exact temporal bridge relations for correlation functions, that involve time-derivative and tile integrations. As a result

Three infinite sets of anomalous scaling exponents (static, dissipative and temporal) can be expressed in terms of just one set of the static exponents ζ_n .

Phenomenological models of multi-scaling

– Kolmogorov-62 **log-normal model:** $\Rightarrow$ K62 conjecture by analogy of random breaking of stones with that of eddies: $\ln\varepsilon(\vec{r})$ is normally distributed (i.e. Gaussian statistics). This gives:

$$\mu_n=\frac{\mu_2}{2}n(n-1)\,,\quad \zeta_n=\frac{n}{3}-\frac{\mu_2}{18}n(n-3)\,,\quad [\mu_n=n-\zeta_{3n}]\ . \qquad \text{(K62)}$$

Experimentally reasonable for $n\le 6\div 8$ $\Rightarrow$ "small n" expansion.
For large n: wrong, in particular, contradicts to exact statement $d\zeta_n/dn\ge 0$.

– **β-model of anomalous scaling**: Frisch-Sulem-Nelkin-78 conjecture: Volume fraction $\mathcal{V}_r$, occupied by r-eddies scales: $\mathcal{V}_r\simeq\left(\frac{r}{L}\right)^\beta$.

Energy flux (at r-scale)

$$\varepsilon_{\vec{r}} \simeq \frac{v_r^2}{\tau_r}\mathcal{V}_r \simeq \frac{v_r^3}{r}\left(\frac{r}{L}\right)^{\beta} = \varepsilon \;\Rightarrow\; v_r \simeq (\varepsilon\, r)^{1/3}\left(\frac{L}{r}\right)^{\beta/3} .$$

Structure functions: $S_n(r) \simeq v_r^n \mathcal{V}_r = (\varepsilon\, r)^{n/3}\left(\frac{r}{L}\right)^{\beta(1-n/3)} \Rightarrow$

$$\zeta_n = \frac{n}{3} + \frac{\beta}{3}(n-3) \quad \beta - \text{co-dimension} \quad (\beta - \text{model})$$

– Multifractal model (Parisi-Frisch-85)

The Euler equation: $\dfrac{\partial \vec{v}}{\partial t} + \widehat{P}\left[(\vec{v}\cdot\vec{\nabla})\vec{v}\right] = 0$ has the rescaling symmetry

$\mathcal{R}(\lambda,h)r = \lambda r\,,\ \mathcal{R}(\lambda,h)t = \lambda^{1-h}t\,,\ \mathcal{R}(\lambda,h)v = \lambda^{h}v\,,$ h – scaling of velocity: Let "ℓ-eddy" $\vec{v}_\ell(\vec{r},t)$ be a solution of EE with characteristic scale ℓ. Then

$$\vec{v}_{\lambda\ell}(\vec{r},t) \equiv \mathcal{R}(\lambda,h)\vec{v}_\ell(\vec{r},t) = \lambda^h \vec{v}_\ell(\lambda\vec{r},\lambda^{1-h}t)$$

is " $\lambda\,\ell$- eddy", an EE solution with scale $\lambda\ell$. Denote as $\mathcal{P}(\ell)$ the probability to meet ℓ-eddy in the turbulent ensemble. One expects, that

$$\mathcal{P}(\ell) \text{ is scale invariant: } CR(\lambda,h)\mathcal{P}(\ell) \equiv \mathcal{P}(\lambda\ell) = \mathcal{P}(\ell)\lambda^{\beta(h)}$$

with $\beta(h)$ being the "probability scaling index", that depends on h. Now

$$S_n(r) \simeq V_L^n \int_{h_{\min}}^{h_{\max}} dh \left(\frac{r}{L}\right)^{nh+\beta(h)} \Rightarrow [\text{steepest decent}] \simeq V_L^n\left(\frac{r}{L}\right)^{\zeta_n}$$

$\zeta_n = \min\limits_h[n\,h + \beta(h)]$. Geometrically: $\beta(h) \Rightarrow 3 - D(h)$, $D(h)$ - co-dimension of the "fractal support" of "h-turbulent cascade".

Dynamical "shell models" of multiscaling

GOY model (Gledzer-73, Ohkinani-Yamada-89), and (born in Israel) **Sabra** model (L'vov-Podivilov-Pomyalov-Procaccia-Vandembroucq-98) and many others

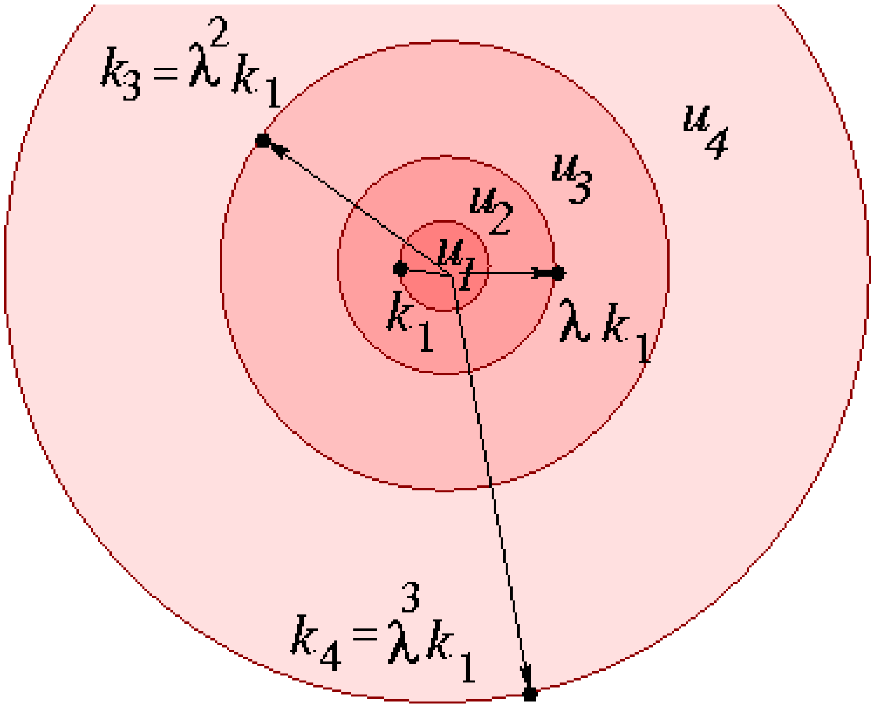

The model equation of motion mimics NSE nonlinearity & "interaction locality":

$$\text{Sabra model:} \quad \frac{du_n}{dt} = i\big(ak_{n+1}u_{n+2}u^*_{n+1} + bk_n u_{n+1}u^*_{n-1} \\ -ck_{n-1}u_{n-1}u_{n-2}\big) - \nu k_n^2 u_n + f_n \,, \tag{15.5}$$

Conservation of energy $E = \sum_n |u_n|^2$ requires

$a + b + c = 0 \;\Rightarrow$ conservation of "helicity" $\mathcal{H} = \sum_n \left(\frac{a}{c}\right)^n |u_n|^2$.

Kolmogorov-41 fixed point

$$\bar{v}_n = \frac{1}{[2(a-c)]^{1/3}\lambda^{n/3}}$$

is unstable, giving a random evolution of the "shell velocities"

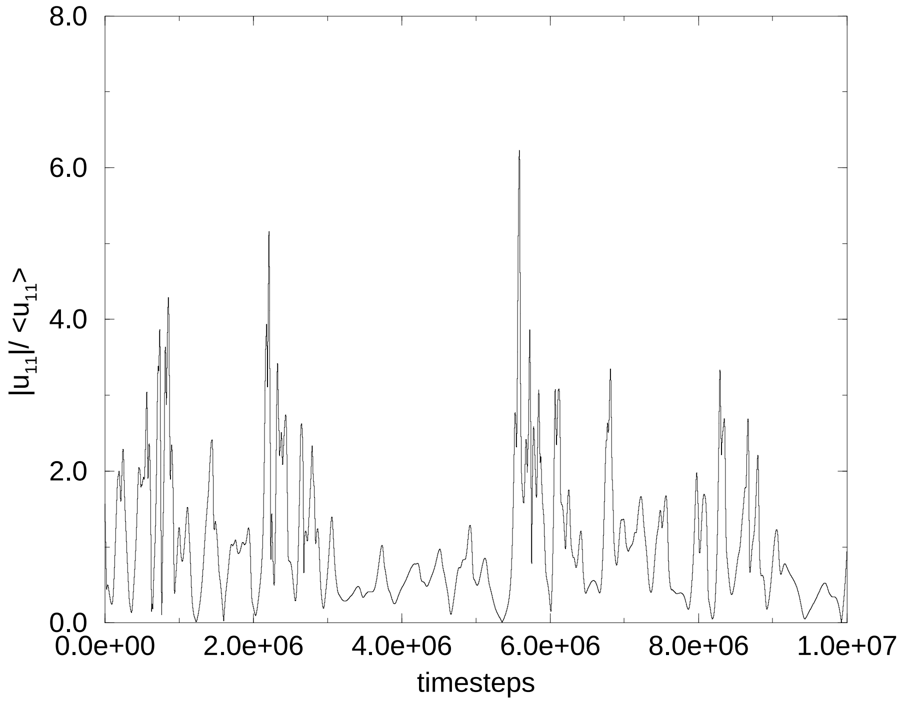

,

one finds odel:

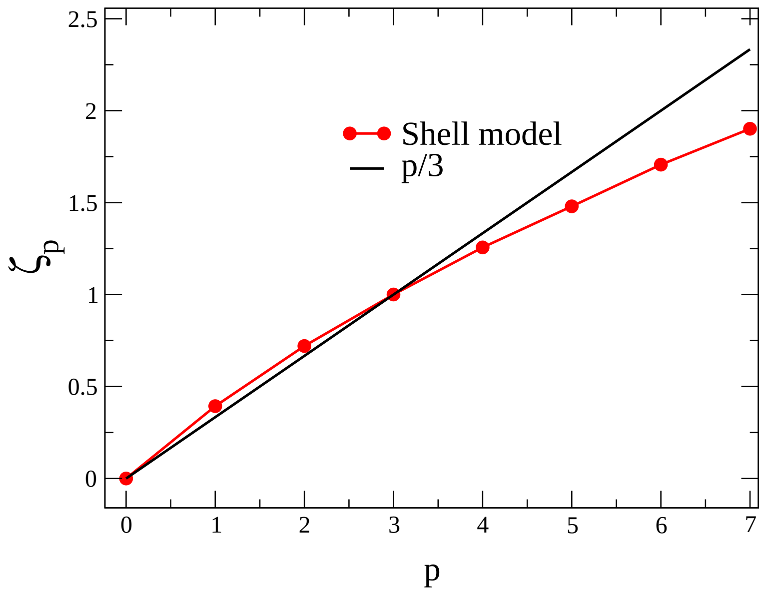

which, with a proper choice of one fitting parameter a , are in good agreement with those for NSE turbulence.

In particular, for $S_3(k_n) \equiv \text{Im}\{\langle u_{n-1}u_nu_{n+1^*}\rangle\}$ one has exact relation:

$$S_3(k_n) = \frac{1}{2k_n(a-c)}\left[-\bar{\epsilon}+\bar{\delta}\left(\frac{c}{a}\right)^n\right], \quad \zeta_3 = 1 .$$

• "Euler" rescaling symmetry and "self-similar" propagation of "solitons"

Sabra (and others) shell-model equations allow self-similar substitution:

$$u_n(t) \approx v\lambda^{-hn} f\left[(t-t_n)vk_0\lambda^{(1-h)n}\right], \qquad (15.6)$$

in which λ is the rescaling of $k_n = k_0\lambda^n$ and $\lambda^{h\,n}$ is the rescaling of the velocity: $u_n = v\lambda^{h\,n}$. Here free parameter h is the velocity scaling index (the same as in the multifractal models of intermittency).

Equation (15.6) describes self-similar "solitonic" propagation of pulses over shells, that was found in numerics by LPP in PRE **61**, 056118, (2001):

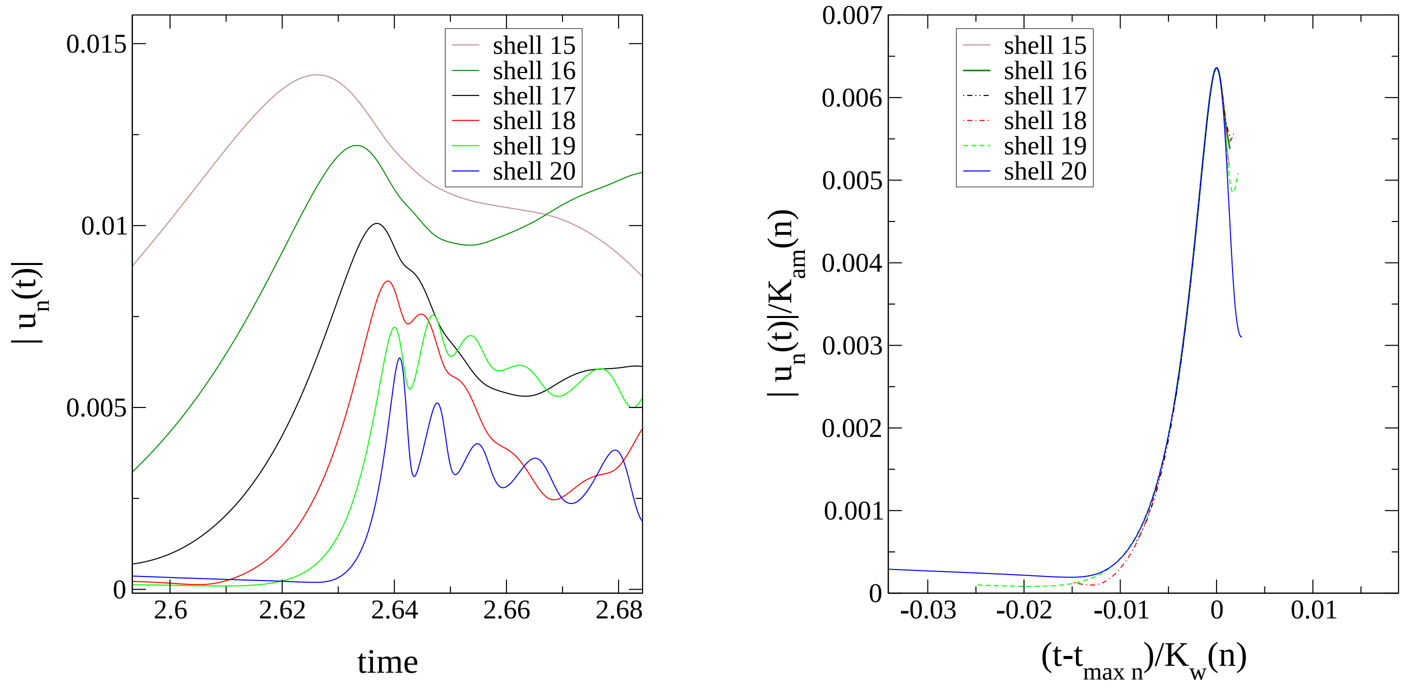

In 2002 L'vov analytically demonstrated stability of solitons in some region $[h_{\text{mix}} < h < h_{\text{max}}]$. Solitons with different h contribute to different (high) order structure functions, giving birth to asymptotical multiscaling.

Toward analytical theory of multiscaling

Kraichnan-59 DIA: Direct Interaction Approximation $\zeta_2 = \frac{2}{3} + \frac{1}{6} \simeq 0.83$

Kraichnan-62 "Lagrangian-History" DIA: $\zeta_2 = \frac{2}{3} < \zeta_{2,\mathrm{exp}} \simeq 0.701$

Belinicher-L'vov-87 sweeping-free approach: K41 is an "order-by-order" perturbation solution and intermittency is not perturbation phenomenon.

Lebedev-L'vov-94 Telescopic Multi-Step Eddy-Interaction: non-perturbation mechanism of multiscaling $\Rightarrow$ infinite re-summation of ladder diagrams.

Yakhot-Orszag-86-90 Straightforward Renormalization Group (RG) approach (for car design, etc.) reproduces K41 scaling

Anjemyan-Antonov-Vasil'ev-89-now: modern RG $\Rightarrow$ principal possibility of anomalous scaling

Belinicher-L'vov-Pomyalov-Procaccia-98: Standard Gaussian decomposition, like $F_4 \Rightarrow F_2^2$, destroys Euler rescaling symmetry and fixes $h = \frac{1}{3}$, (K41). Suggested h-invariant decompositions, like $F_4 \Rightarrow F_3^2/F_2$, preserve the rescaling symmetry, leave h free, and demonstrate multiscaling in an analytical, NS based theory (in the BL-87 sweeping-free representation)

L'vov-Procaccia-2000 Analytic calculation of anomalous exps. ζ_n in NS turbulence: Using the (LP-96) fusing rules to flush out a small parameter $\doteq \zeta_2 - \frac{2}{3} \simeq 0.03$ in "4–eddy interaction amplitude" in the ladder diagrams for exps. $\Rightarrow$
$DS\zeta_n = \frac{n}{3} - \delta \frac{n(n-3)}{2} \left[1 + 2\,\delta\, b\,(n-2)\right],$
$green\delta\, n < 1\,, \quad n \le 12\ .$

Benzi-Bifferale-Sbragaglia-Toschi-03: Anomalous scaling in shell models: Using Fusion Rules and "time-dependent random multiplicative process" for closure of correlation function $\Rightarrow$ calculation (without free parameters) of the anomalous scaling exps. in shell models.

TO BE CONTINUED

Lecture 16

Phenomenology of wall bounded turbulence

Introduction

In contrast to free shear flows, most turbulent flows are bounded (at least in part) by one or more solid surfaces. Examples include *internal flows* such as the flow through pipes and ducts; *external flows* such as the flow around aircraft and ships' hulls; and flows in the environment such as the atmospheric boundary layer (BL), and flow of rivers.

The simplest examples of these flows are: fully developed channel flow; fully developed pipe flow; and the flat-plate boundary layer. In each of these flows the mean velocity vector is (or is nearly) parallel to the wall, and the near-wall behaviors in each of these cases are very similar. These simple flows are of practical importance and played a prominent role in the historical development of the study of turbulent flows.

Description of the channel flow

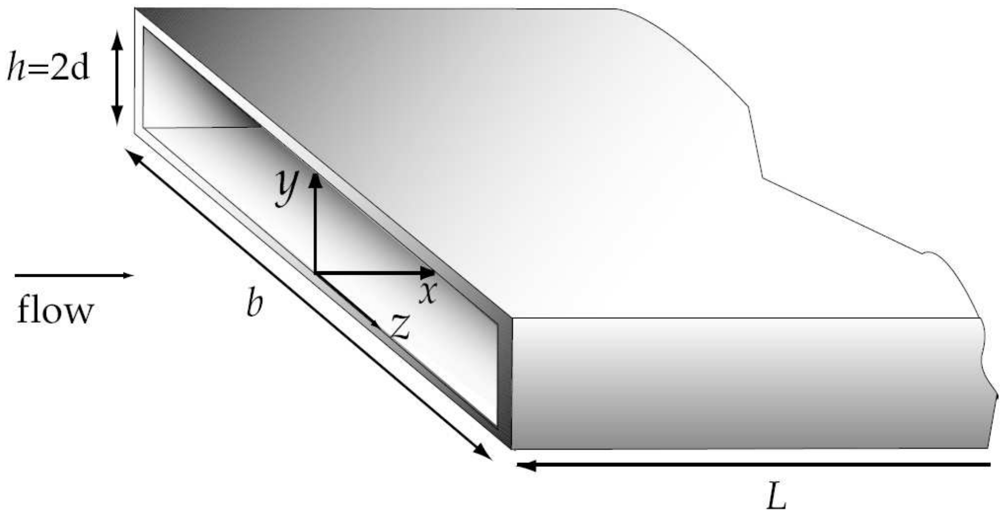

The flow through a rectangular duct of hight $h = 2\delta$, length $L \gg \delta$ and width $b \gg \delta$. The mean flow is in axial x direction, with the mean velocity varying in the cross-stream direction y . The bottom and top walls are at $y = 0$ and $y = 2\delta$. Due to $b \gg \delta$ the flow (remote from the walls) is statistically independent of z . The centerline is at $y = \delta$, $z = 0$. The velocities in the three coordinate directions are (U_x, U_y, U_z) with fluctuations (u_x, u_y, u_z) . And $\langle U_z \rangle = 0$.

We consider *fully developed* region (large x), in which velocity statistics no longer vary with x . Hence we have statistically stationary and statistically one-dimensional flow which velocity statistics depending only on y , and which is statistically symmetric about the mid-plane $y = \delta$.

Reynolds numbers:

$$\mathbf{Re} \equiv \frac{2\delta\,\overline{U}}{\nu}, \qquad \mathbf{Re}_0 \equiv \frac{U_0\,\delta}{\nu}, \tag{16.1a}$$

$$\overline{U} \equiv \frac{1}{\delta}\int_0^\delta \langle U_x \rangle\, dy\,, \quad U_0 \equiv \langle U_x \rangle_{y=\delta}\,. \tag{16.1b}$$

- The balance of mean forces

Reynolds decomposition:

$$\vec{U}(\vec{r},t) = \left\langle \vec{U}(y) \right\rangle + \vec{u}(\vec{r},t) \tag{16.2}$$

The continuity eq.

$$\vec{\nabla} \cdot \vec{U} = 0 \;\Rightarrow\; \frac{d\,\langle U_y\rangle}{dy} = 0\,,\; \langle U_y\rangle_{y=0} = 0 \;\Rightarrow\; \langle U_y\rangle = 0\,. \tag{16.3}$$

The mean-momentum eq. (in the wall-normal direction)

$$\nu\,\frac{d^2}{dy^2}\,\langle U_x\rangle - \frac{d}{dy}\,\langle u_x u_y\rangle = \frac{1}{\rho}\frac{\partial}{\partial x}\,\langle p\rangle\,, \;\Rightarrow\; \frac{d}{dy}\,\tau = \frac{dp_{\mathrm{w}}}{dx}\,, \tag{16.4}$$

where the total shear stress is the sum of the viscous and Reynolds stresses

$$\boldsymbol{\tau(y) \equiv \rho\,\nu\,S - \rho\,W_{xy}\,, \quad S(y) \equiv \frac{d}{dy}\,\langle U_x\rangle\,,\; W_{ij} \equiv \langle u_i u_j\rangle\;.} \tag{16.5}$$

Introduce *wall shear stress* $\tau_{\mathrm{w}} \equiv \tau(0)$. The solution to Eq. (16.4) then

$$\tau(y) = \tau_{\mathrm{w}}\left(1 - \frac{y}{\delta}\right), \qquad -\frac{dp_{\mathrm{w}}}{dx} = \frac{\tau_{\mathrm{w}}}{\delta}\,. \tag{16.6}$$

To summarize: the flow is driven by the drop in pressure between the entrance and the exit of the channel. In the fully developed region there is a constant (negative) pressure gradient (??), which is balanced by the shear stress gradient (16.4). For a given pressure gradient dp_{w}/dx and channel half-width δ , the linear shear-stress profile is given by (16.6) – independent of the fluid properties (i.g. ρ or ν), and state of fluid motion (i.e., laminar or turbulent).

- The near-wall shear stress

At the wall $\vec{U} = 0 \Rightarrow \langle u_i u_j\rangle = 0 \Rightarrow$

$$\tau_{\mathrm{w}} \equiv \rho\,\nu\left(\frac{d\,\langle U_x\rangle}{dy}\right)_{y=0}\,. \tag{16.7}$$

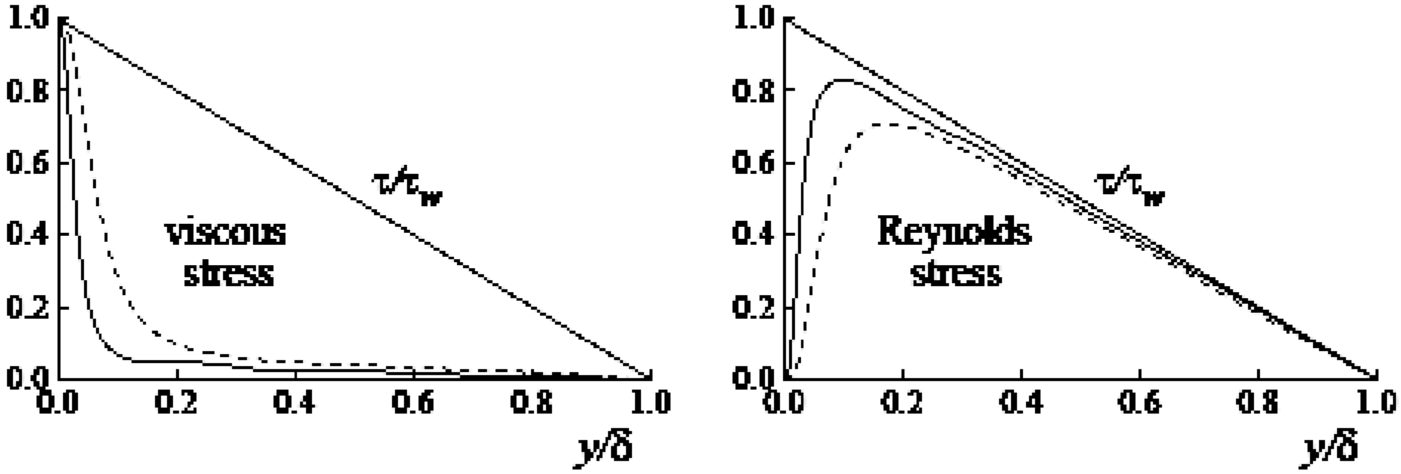

DNS: - - - - Re $=$ 5600 (Re_τ $=$ 180), —— Re $=$ 13750 (Re_τ $=$ 395).

The viscous stress dominates at the wall in contrast to the situation in free shear flows, there, at high Re, $|\rho\nu\nabla_i \langle U_j \rangle| \ll |\rho \langle u_i u_j \rangle|$. Also, since ν is important near the wall, the velocity profile depends on Re.

- Viscous scales

$$u_\tau \equiv \sqrt{\frac{\tau_{\mathrm{w}}}{\rho}}, \quad \textit{friction velocity}; \qquad \ell_\tau \equiv \frac{\nu}{u_\tau}, \quad \textit{viscous lengthscale}. \tag{16.8}$$

The *friction Reynolds number*

$$\mathbf{Re}_\tau \equiv \frac{u_\tau \delta}{\nu} = \frac{\delta}{\ell_\tau}. \tag{16.9}$$

The velocity and the distance from the wall measured in *wall units*

$$u^+ \equiv \frac{u}{u_\tau}, \qquad y^+ \equiv \frac{y}{\ell_\tau} = \frac{u_\tau y}{\nu}, \quad \Rightarrow \quad y = \frac{y^+ \delta}{\mathrm{Re}_\tau}, \tag{16.10}$$

which is similar to a local Reynolds number, so its magnitude can be expected to determine the relative importance of viscous and turbulent processes.

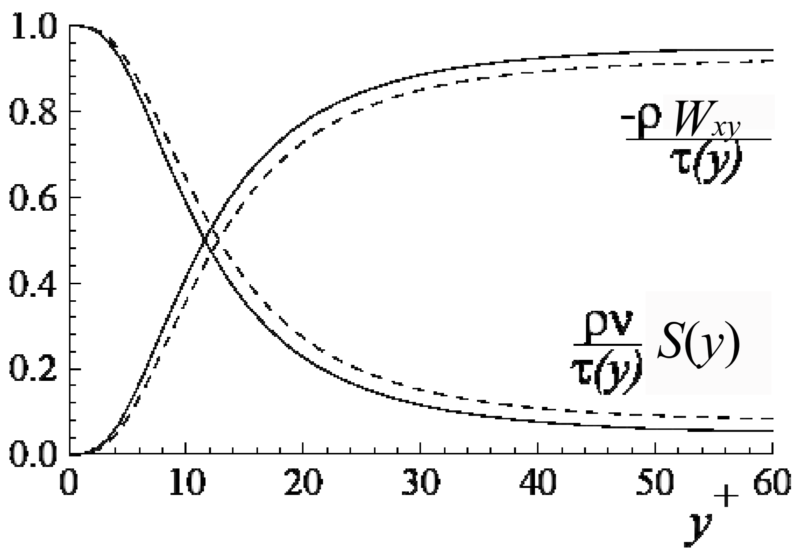

Relative importance of the viscous and turbulent fluxes of mechanical moments toward the wall:

- Viscous wall region $y^+ < 50$: direct effect of viscosity on the shear stress;
  - Outer layer $y^+ > 50$: direct effect of viscosity is negligible;
  - Viscous sublayer $y^+ < 5$: $W_{xy} \ll \mu S$.

As Re of the flow increases, the fraction of the channel occupied by the viscous wall region decreases, see Eq. (16.10), centerline in wall unites: $\boldsymbol{\delta}^+ = \text{Re}_\tau$.

Mean velocity profiles

Fully developed channel flow is completely specified by ρ , ν , δ and u_τ . There are just two non-dimensional groups that can be formed from them: y/δ and Re_τ . Hence,

$$\boldsymbol{S = \frac{d\,\langle U_x\rangle}{dy} = \frac{u_\tau}{y}\ \Phi\left(\frac{y}{\ell_\tau}, \frac{y}{\delta}\right)}. \qquad (16.11)$$

where Φ is a universal non-dimensional function. Here ℓ_τ is the appropriate lengthscale in the viscous wall region $y^+ < 50$, while δ is the appropriate length-scale in the outer layer $y^+ > 50$.

- The law of the wall

Prandtl (1925): at high Re, close to the wall $(y/\delta \ll 1)$ there is an *inner layer* in which $\langle U_x \rangle$ is determined by the viscous scales, independent of δ and U_0 .

$$\frac{d\langle \boldsymbol{U_x} \rangle}{dy} = \frac{\boldsymbol{u_\tau}}{\boldsymbol{y}} \; \boldsymbol{\Phi}_{\mathrm{I}}\left(\frac{\boldsymbol{y}}{\boldsymbol{\ell_\tau}}\right), \quad \text{for } \frac{y}{\delta} \ll 1\,,$$

$$S^+ = \frac{d\langle U_x\rangle^+}{dy^+} = \frac{1}{y^+}\,\Phi_{\mathrm{I}}(y^+)\;. \tag{16.12}$$

$$\langle U_x\rangle^+ = f_{\mathrm{w}}(y^+) \equiv \int_0^{y^+} \frac{1}{x}\,\Phi_{\mathrm{I}}(x)dx\;. \tag{16.13}$$

The no-slip condition $\langle U_x\rangle_{y=0} = 0$ corresponds to $f_{\mathrm{w}}(0) = 0$, while the viscous stress law at the wall (Eq. (16.7)) yields $f'_{\mathrm{w}}(0) = 1$. (This is the result of normalization). Therefore

$$\langle \boldsymbol{U_x}\rangle^+ = \boldsymbol{y}^+ + \boldsymbol{\mathcal{O}}\left((\boldsymbol{y}^+)^2\right), \quad \text{for } y^+ < 5\;. \tag{16.14}$$

The leading term in the RHS is direct consequence of the NSE, in which the nonlinear term is neglected. DNS show that the departures from the linear dependance are negligible in the viscous sublayer $(y^+ < 5)$ but are significant for $y^+ > 12$.

- The log-law

The inner layer is defined as $y/\delta < 0.1$. At high Reynolds numbers, the *outer part* of the *inner layer* corresponds to large $y^+ \approx 0.1\,\delta/\ell_\tau = 0.1\,\mathrm{Re}_\tau \gg 1$, where the viscosity has little effect and one expects that Φ has to be viscosity independent, i.e. saturate at some constant level (denoted as $1/\kappa$). Hence

$$\Phi_{\mathrm{I}}(y^+) = \frac{1}{\kappa}\,,$$

$$\langle \boldsymbol{U_x}\rangle^+ = \frac{\boldsymbol{1}}{\boldsymbol{\kappa}}\ln(\boldsymbol{y}^+) + \boldsymbol{B}, \quad \text{for } \frac{y}{\delta} \ll 1 \text{ and } y^+ \gg 1, \tag{16.15}$$

where $\kappa \approx 0.41$ is the von Kámán constant (1930) and $B \approx 5.2$.

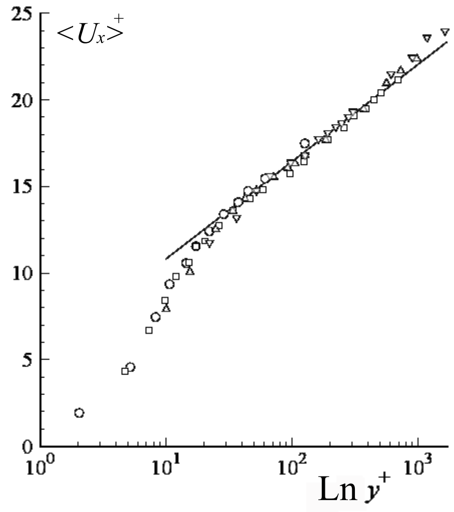

Experiments for $\mathrm{Re}_0 = 3000 \div 40000$; —— theory.

- Wall regions and layers and their defining properties

Region	Location	Defining property
Inner layer	$y/\delta < 0.1$	$\langle U_x \rangle$ determined by u_τ and y^+, independent of U_0 and δ
Viscous wall region	$y^+ < 50$	The viscous contribution to the shear stress is significant
Viscous sublayer	$y^+ < 5$	Reynolds shear stress is negligible compared to the viscous stress
Outer layer	$y^+ > 50$	Direct effects of viscosity on $\langle U_x \rangle$ are negligible
Overlap region	$y^+ > 50, y/\delta < 0.1$	Region of overlap between inner and outer layers (at large Re)
Log-law region	$y^+ > 30, y/\delta < 0.3$	The log-law holds
Buffer layer	$5 < y^+ < 30$	The region between the *viscous sublayer* and *log-law region*

"Minimal Model" of Turbulent Boundary Layer (TBL)

Suggested by LPPZ in 2006 **Minimal Model** is a version of algebraic Reynolds stress models, designed to describe in the plain geometry the mean flow and statistics of turbulence on the level of simultaneous, one-point second-order velocity correlation functions, which is the Reynolds-stress tensor $\boldsymbol{W_{ij}}$.

The exact equation for the mechanical balance (the same as (16.4)) reads:

$$-\boldsymbol{W_{xy}(y)}+\boldsymbol{\nu S(y)}=\boldsymbol{P(y)}\,, \tag{16.16}$$

where $P(y)=p'(L-y)$ for a channel flow.

Balance equation for the Reynolds stress tensor:

$$\frac{\boldsymbol{dW_{ij}}}{\boldsymbol{d\,t}}+\boldsymbol{\epsilon_{ij}}+\boldsymbol{I_{ij}}=-\boldsymbol{S(W_{iy}\delta_{jx}+W_{jy}\delta_{ix})}\,, \tag{16.17}$$

is obtained by applying the Reynolds decomposition (16.2) to NSE; writing the equation for fluctuating velocity $\overrightarrow{u}$ in the operator form $\mathcal{L}\overrightarrow{u}=0$; constructing the object $\langle u_i\mathcal{L}u_j+u_j\mathcal{L}u_i\rangle=0$ and ignoring the term $\overrightarrow{\nabla}\cdot(..)$.

The RHS of Eq. (16.17) is exact. It describes the energy flux from the mean flow to the turbulent subsystem.

In the LHS of Eq. (16.17) the energy dissipation rate $\boldsymbol{\epsilon_{ij}}$ is dominated by the smallest, microscale eddies (of scales $\sim\eta$), while $\boldsymbol{W_{ij}}$ is dominated by the largest, outer scale eddies.

The traceless (due to conservation of energy in the Euler equation), so-called "Return to isotropy tensor $\boldsymbol{I_{ij}}$ " originates from the nonlinear term in the NSE and proportional to the triple-velocity correlations. Therefore

Balance Eq. (16.17) does not close the problem, it requires modeling, using physical intuitions, laboratory and numerical experiments, etc.:

• Far away from the wall and for large Re the energy dissipation tensor dominates by the Kolmogorov viscous microscale motions at which turbulence can be considered as isotropic. On the other hand, in the viscous sublayer there is a direct viscous contribution of the dissipation of the largest eddies in the system (of scale z).

$$\epsilon_{ij} \approx \Gamma\, W \delta_{ij} + \widetilde{\Gamma}\, W_{ij}\, (1-\delta_{ij}) \ , \tag{16.18}$$

$$\Gamma = \nu \left(\frac{a}{y}\right)^2 + \frac{b\sqrt{W}}{y} , \quad \widetilde{\Gamma} = \nu \left(\frac{\widetilde{a}}{y}\right)^2 + \frac{\widetilde{b}\sqrt{W}}{y} \ . \tag{16.19}$$

The parameters $a = 1, \widetilde{a} = 10.7$ are responsible for the *viscous dissipation* of the diagonal, W_{ii} , and off-diagonal, W_{xy} , components of the Reynolds-stress tensor. They are chosen to describe the observed values of the intersection B of the log-law (16.15) and the pick of kinetic energy in the buffer sublayer.

- The "Return to isotropy" tensor is modelled by the simplest Rotta's form:

$$I_{ij} \approx \gamma\, (3\, W_{ii} - W)\, \delta_{ij} + \widetilde{\gamma}\, W_{ij}\, (1-\delta_{ij}) \ , \tag{16.20}$$

$$\gamma(y) \equiv b\, \frac{\sqrt{W(y)}}{y} , \quad \widetilde{\gamma} \equiv \widetilde{b}\, \frac{\sqrt{W}}{y} \ . \tag{16.21}$$

The *outer layer* parameters $b = 0.25, \widetilde{b}b = 0.50$ are chosen to describe the observed constant values of von-Kàrmàn in the log-law and the asymptotic level of the density of kinetic energy, $W/2$.

• Summary of the minimal model

$$\begin{aligned} -W_{xy}(y) + \nu S(y) &= P(y) \,, \\ [\Gamma + 3\gamma]\, W_{xx} &= \gamma\, W - 2\, S\, W_{xy}, \\ [\Gamma + 3\gamma]\, W_{yy} &= \gamma\, W \,, \\ [\Gamma + 3\gamma]\, W_{zz} &= \gamma\, W \,, \\ \left[\widetilde{\Gamma} + 3\widetilde{\gamma}\right] W_{xy} &= -S\, W_{yy} \ . \end{aligned} \tag{16.22}$$

- **General solution of the Minimal Model Equations**

Define dimensionless "near-wall, double-dagger" objects

$$S^\ddagger \equiv \frac{\nu S}{P(y)}\,, \quad W^\ddagger \equiv \frac{W}{P(y)}\,, \quad y^\ddagger \equiv \frac{y\sqrt{P(y)}}{\nu}\,, \tag{16.23}$$

in which

$$W^\ddagger_{yy} = W^\ddagger_{zz} = \frac{v^\ddagger}{4\,v_4}W^\ddagger\,, \quad W^\ddagger_{xx} = \frac{v_2}{2\,v_4}W^\ddagger\,,$$

$$W^\ddagger_{xy} = -\frac{W^\ddagger}{2}\sqrt{\frac{b\,v^\ddagger v_1}{6\,\widetilde{b}\,v_3 v_4}}\,, \quad S^\ddagger = \frac{1}{y^\ddagger}\sqrt{\frac{6\,b\,\widetilde{b}\,v_1 v_3 v_4}{v^\ddagger}}\,. \tag{16.24}$$

General solution of the Minimal Model via $W^\ddagger$. Here:

$$v_1 \equiv v^\ddagger + \frac{a^2}{b\,y^\ddagger}\,, \quad v_2 \equiv v^\ddagger + \frac{a^2}{2\,b\,y^\ddagger}\,, v_3 \equiv v^\ddagger + \frac{\widetilde{a}^2}{3\,\widetilde{b}\,y^\ddagger}\,, \quad v_4 \equiv v^\ddagger + \frac{a^2}{4\,b\,y^\ddagger}\,,$$

with an Eq. for $W^\ddagger \equiv {v^\ddagger}^2$:

$$\frac{b}{24\,\widetilde{b}}{v^\ddagger}^6 v_1 + v^\ddagger v_3 v_4\left[\frac{b}{y}{v^\ddagger}^2 v_1 - 1\right] + \frac{6\,b\,\widetilde{b}}{y^2}\,v_1 v_3^2 v_4^2 = 0\,. \tag{16.25}$$

- **DNS, LES & Experiment in comparison with the Min.-Mod.**

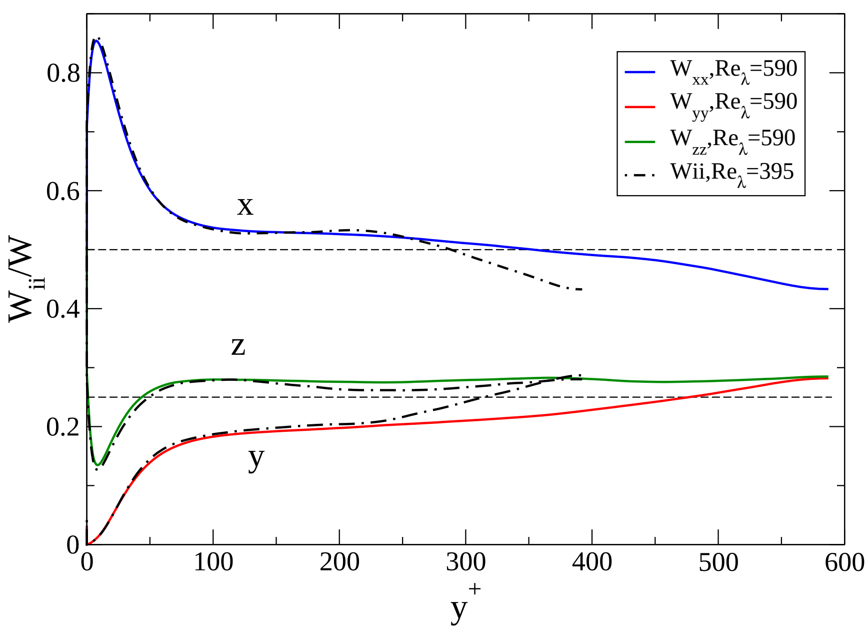

DNS profiles of the relative kinetic energies in turbulent channel flow

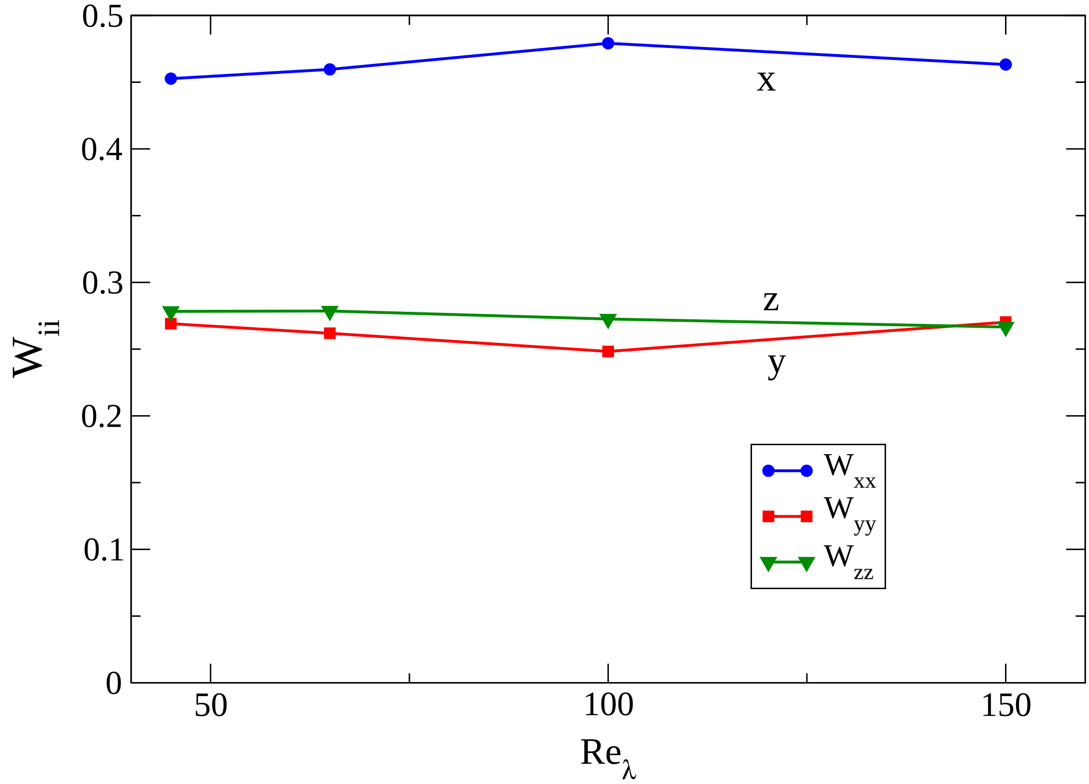

LES for the relative kinetic energies in turbulent channel flow

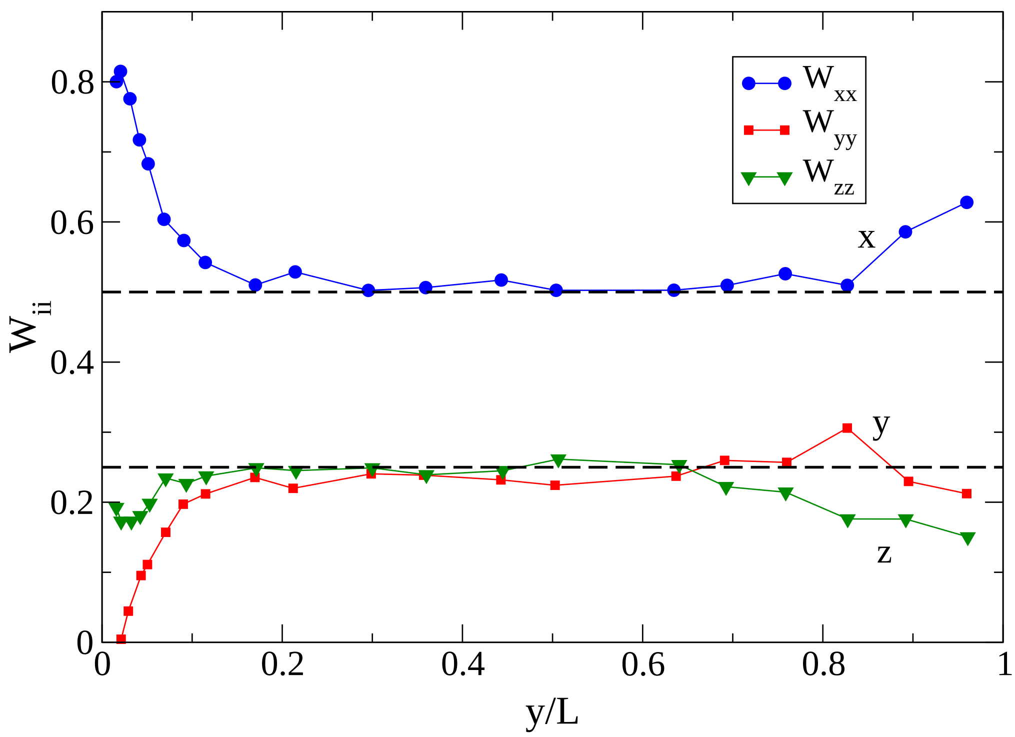

Profiles of relative kinetic energies in vertical water channel, $\mathrm{Re}_\tau = 10^3$.

$\widetilde{W}_{ii,\infty}$, $\downarrow ii \downarrow$	DNS	LES	Water channel	Minimal Model
xx	≈ 0.53	≈ 0.46	0.50 ± 0.01	1/2
yy	≈ 0.22	≈ 0.27	0.25 ± 0.02	1/4
zz	≈ 0.27	≈ 0.27	0.25 ± 0.02	1/4

Table. Anisotropy of the outer layer. Asymptotic values of the relative kinetic energies $\widetilde{W}_{ii}$ in the log-law region (where $y^\ddagger > 200$) taken from DNS by Moser, R. G., Kim, J., and Mansour, N. N.: (1999) with $\mathrm{Re}_\tau = 395, 590$) LES by Carlo M. Casciola (2004) and experiment by A. Agrawal, L. Djenidi and R.A. Antonia (2004), in a water channel with $\mathrm{Re}_\tau = 10^3$.
The last column presents the predictions of the *minimal model*.

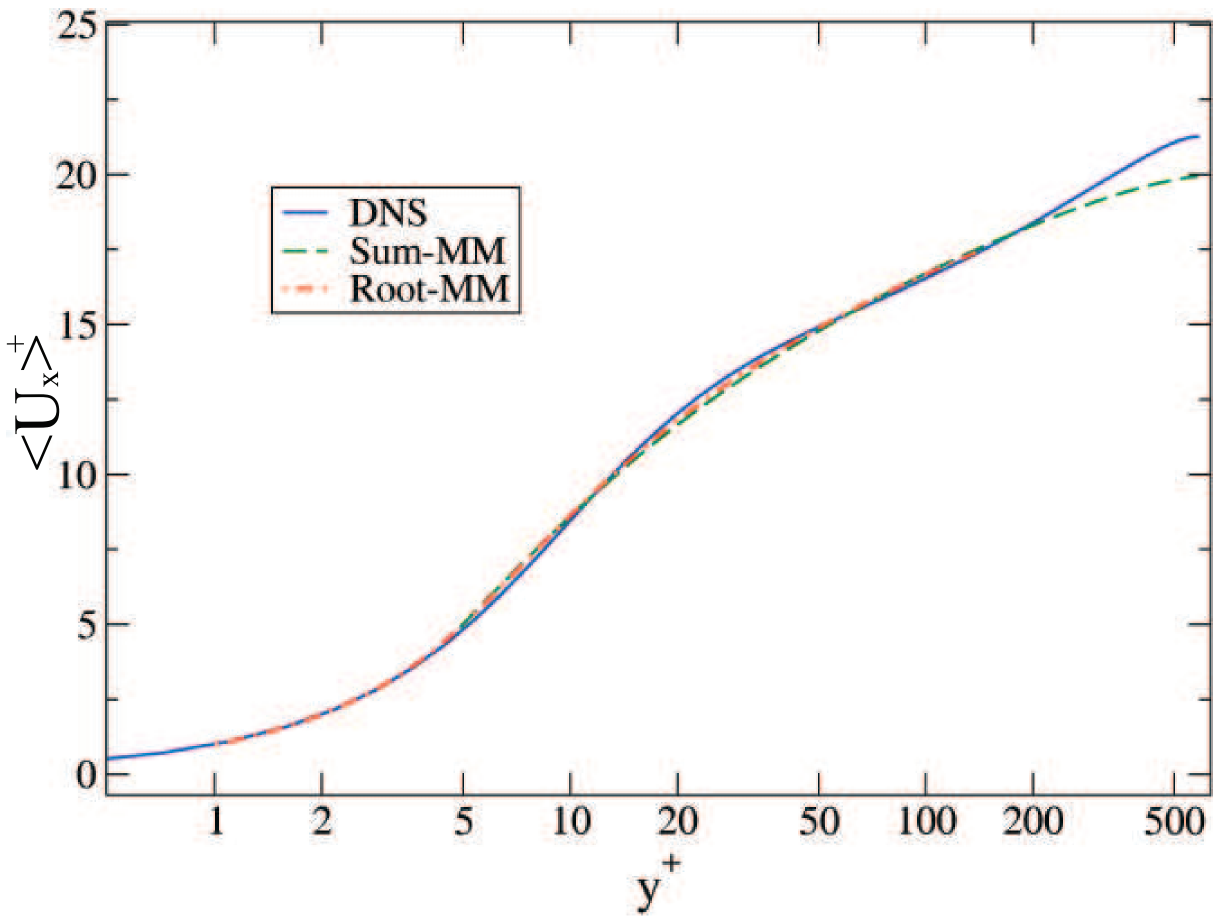

Min.-Mod. comparison with DNS for the Mean velocity profile, $\mathrm{Re}_\tau = 590$

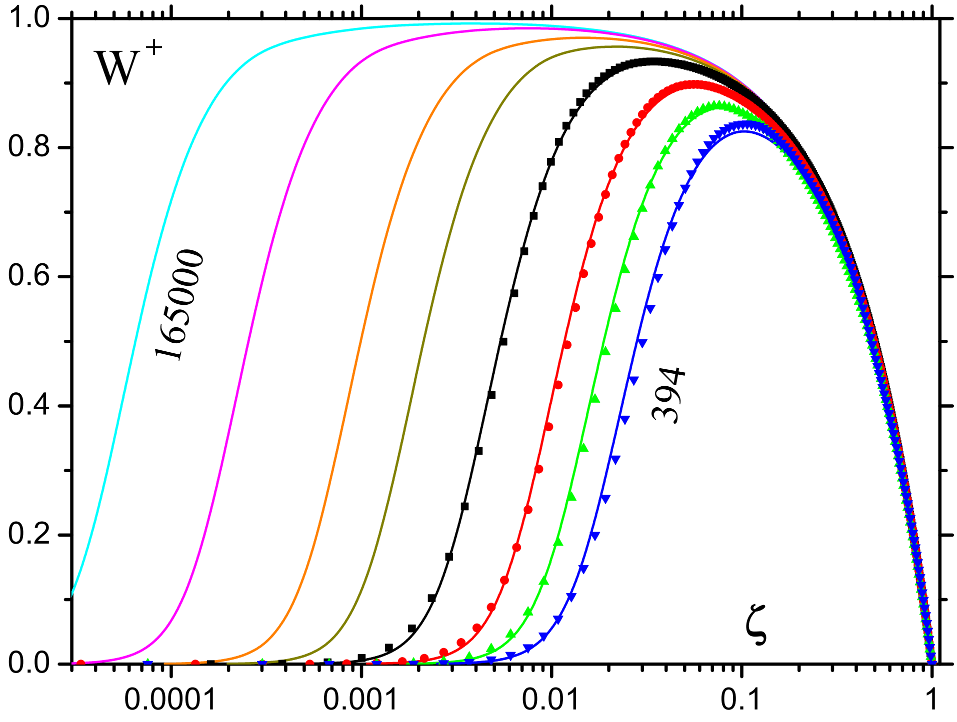

Reynolds shear stress $W^+ = \langle u_x u_z \rangle$ *vs.* $\zeta = z^+/\mathrm{Re}_\tau$. Dots – direct numerical simulations for $\mathrm{Re}_\tau = 395,\ 590,\ 1000$ and 2009. Lines – the Min-Mod. predictions.

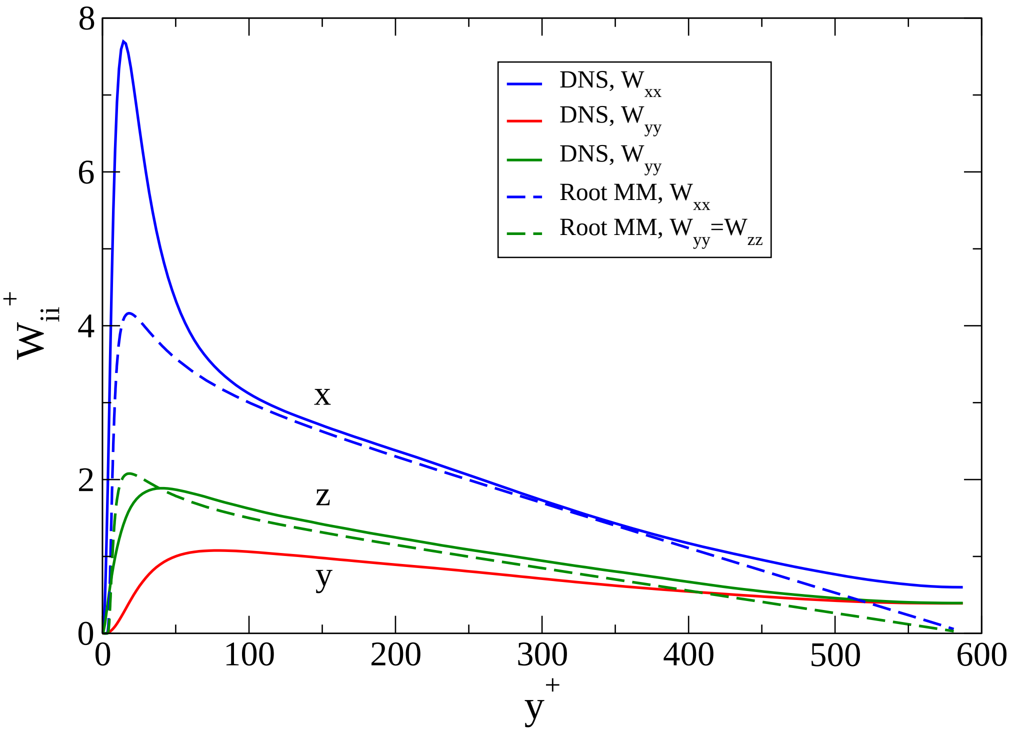

Min.-Mod. comparison with DNS for the diagonal W_{ii}^+ , $\mathrm{Re}_\tau = 590$

- Modification of the Min.-Mod. for the turbulent core:

Scaling function approach instead of simple distance to the wall:
When distance to the wall y is compatible with the channel width δ the turbulent eddies "fill" the second wall and their characteristic scale ℓ is no longer $\propto y$. From symmetry reasoning one expects that ℓ/δ depends on

$$\zeta = \frac{y}{\delta}\Big(1 - \frac{y}{2\,\delta}\Big)\,, \tag{16.26}$$

that $\to y/\delta$ near the wall $y = 0$ (as it was) and $\to (2\delta - y)/\delta$ as it expected. This function has maximum $\delta/2$ at the centerline. 2007-LPR analysis of DNS data gives maximal value of the eddy-scale $\ell_{\rm s} \approx 0.311\delta$. Suggested analytical form of the scaling function

$$\frac{\ell^+(\zeta)}{\mathrm{Re}_\tau} = \ell_{\rm s}\Big\{1 - \exp\Big[-\frac{\zeta}{\ell_s}\Big(1 + \frac{\zeta}{2\ell_s}\Big)\Big]\Big\} \tag{16.27}$$

with one fitting parameter $\ell_{\rm s} = 0.311\delta$ allows to describe the mean velocity profiles in the entire channel and tube flows (including the "wake region") in wide region of Re_τ with just three Re_τ-independent fitting parameters:

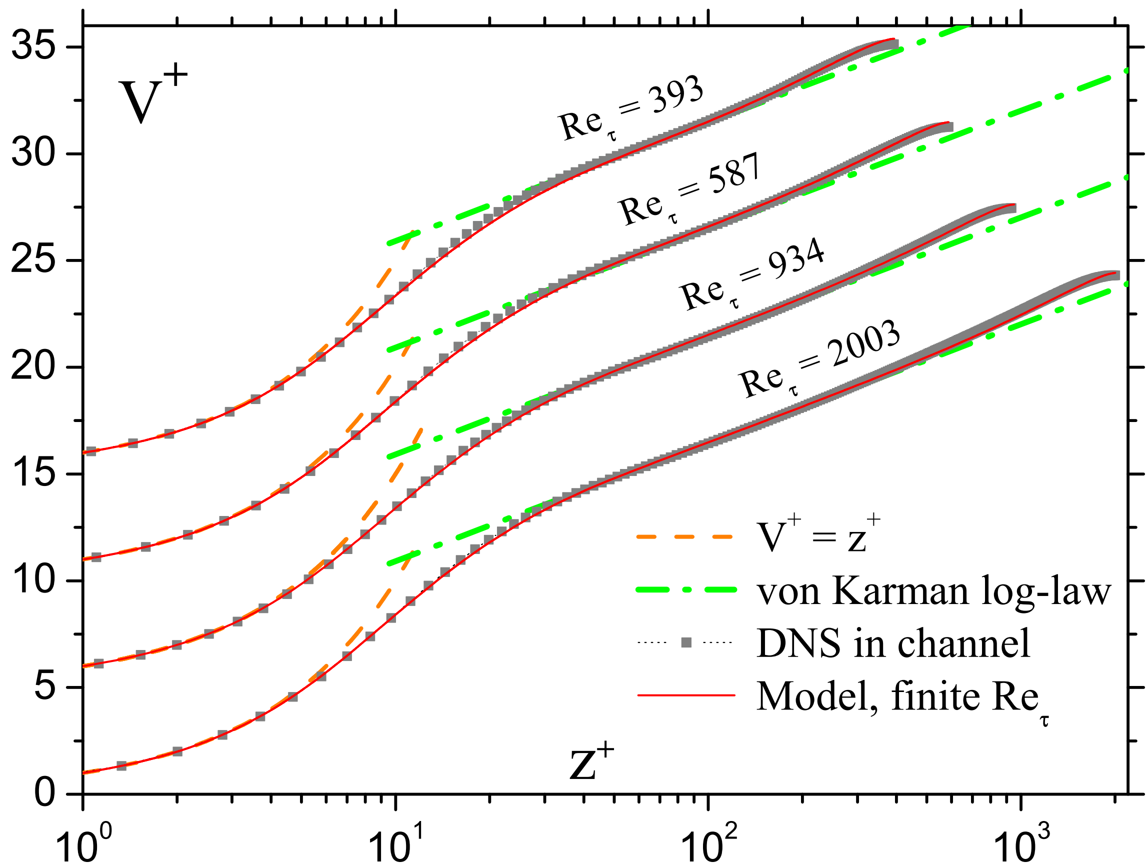

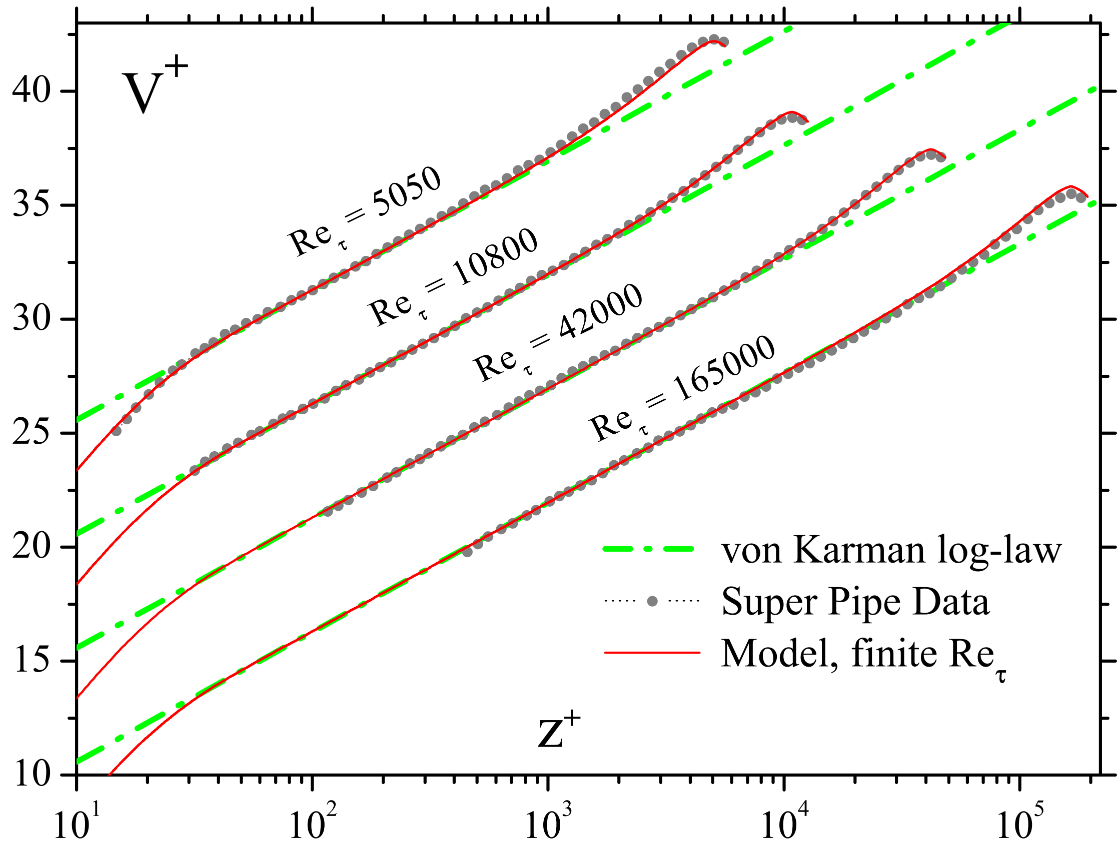

- Summary: Strength and Limitations of the Minimal Model

Min.-Mod. with the given set of four parameters describes five profiles:

- $V(y)$ – with accuracy of $\simeq 1\%$ – throughout the channel
- the Reynolds stress $W_{xy}(y)$ – with accuracy of few percents
- the kinetic energy $\frac{1}{2}W(y)$ – with reasonable, semi-quantitative accuracy, including the position and width of its peak in the buffer sub-layer
- The profiles of $W_{xx}(y)$, $W_{yy}(y)$ and $W_{zz}(y)$, including $\frac{1}{2}$ - $\frac{1}{4}$ - $\frac{1}{4}$ distribution.

Min.-Mod. cannot pretend to describe all the aspects of the turbulent statistics: The Min.-Mod. ignores the quasi-two dimensional character of turbulence, coherent structures in the very vicinity of the wall, etc.

Conclusion: The Min.-Mod. takes into account the essential physics of wall-bounded turbulence almost throughout the channel flow. With a proper generalization, the Min.-Mod. will be useful in studies of more complicated turbulent flows, laden with heavy particles, bubbles.

Lecture 16

Drag Reduction by Polymers in Wall Bounded Turbulence

History: experiments, engineering developments and ideas

– B.A.Toms, 1949: An addition of $\sim 10^{-4}$ weight parts of long-chain polymers can suppress the turbulent friction drag up to 80%.
– This phenomenon of "drag reduction" is intensively studied (by 1995 there were about 2500 papers, now we have many more) and reviewed by Lumley (1969), Hoyt (1972), Landhal (1973), Virk (1975), McComb (1990), de Gennes (1990), Sreenivasan & White (2000), and others.
– In spite of the extensive – and continuing – activity the fundamental mechanism has remained under debate for a long time, oscillating between Lumley's suggestion of importance of the polymeric contribution to the fluid viscosity and de Gennes's idea of importance of the polymeric elasticity.
Some researches tried to satisfy simultaneously both respectable.
– Nevertheless, the phenomenon of drag reduction has various technological applications from fire engines (allowing a water jet to reach high floors) to oil pipelines, starting from its first and impressive application in the Trans-Alaska Pipeline System.

Trans-Alaska Pipeline System $L \approx 800$ Miles, $\oslash = 48$ inches
$\Rightarrow$ TAPS was designed with 12 pump stations (PS) and a throughput capacity of 2.00 million barrels per day (BPD). Now TAPS operates with only 10 PS (final 2 were never build) with throughput 2.1 BPD, with a total injection of ≈ 250 wppm of polymer "PEO" **drag reduction additive** $\Rightarrow$ (wppm $\equiv$ weight parts per million, 250 wppm $= 2.5 \cdot 10^{-4}$)

• **INFO PEO page:** Typical parameters of polymeric molecules PEO – Polyethylene oxide ($N \times [- CH_2 - CH_2 - O]$) and their solutions in water:

- degree of polymerization $N \approx (1.2 - 12) \times 10^4$,
- molecular weight $M \approx (0.5 - 8) \times 10^6$,
- equilibrium end-to-end distance $R_0 \approx (7 - 20) \times 10^{-8}$ m,
- maximal end-to-end distance $R_{\max} \sim \sqrt{N} R_0 \approx 6 \times 10^{-6}$ m;
- typical mass loading $\psi = 10^{-5} - 10^{-3}$.

For $\psi = 2.8 \times 10^{-4}$ of PEO: $\nu_{\rm pol} \approx \nu_0$.
PEO solutions are dilute up to $\psi = 5.5 \times 10^{-4}$.

Essentials of the phenomenon: MDR asymptote and ×-over

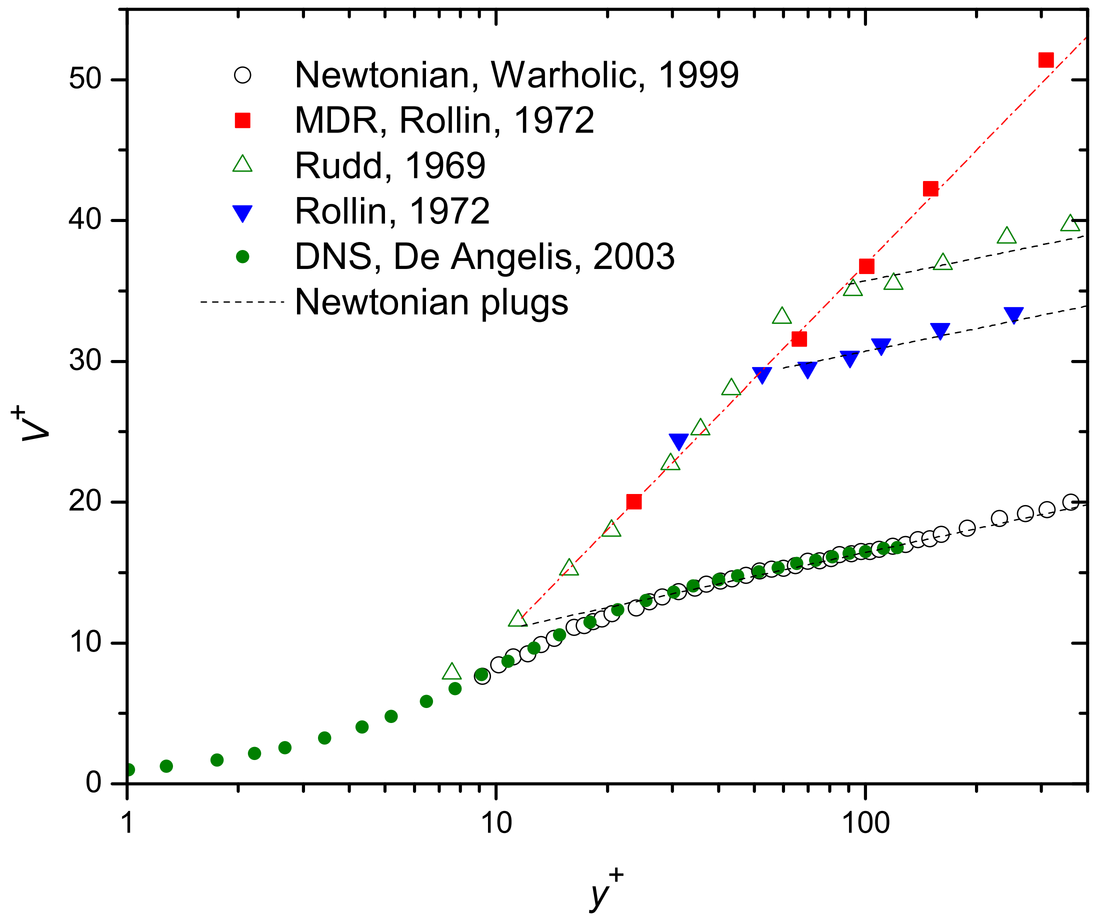

Normalized mean velocity profiles V^+ vs. normalized distance from the wall y^+

Green circles – DNS for Newtonian channel flow, open circles – experiment.

The Prandtl-Karman log-profile :

$$V^+ = 2.5 \ln y^+ + 5.5$$

Red squares – experiment, universal Virk's MDR asymptote

$$V^+ = 11.7 \ln y^+ - 17.0$$

Blue triangles and green open triangles – $\times$ -over, for intermediate concentrations of the polymer, from the MDR asymptote to the Newtonian plug.

Wall normalization: $\mathcal{R}e \equiv \frac{L\sqrt{p'L}}{\nu_0}$, $y^+ \equiv \frac{y\mathcal{R}e}{L}$, $V^+ \equiv \frac{V}{\sqrt{p'L}}$.

Simple theory of basic phenomena in drag reduction

is based on:

– An approximation of effective polymeric viscosity for visco-elastic flows,

– An algebraic Reynolds-stress model for visco-elastic wall turbulence.

• An approximation of effective polymeric viscosity accounts for the effective polymeric viscosity (according to Lumley) and neglects elasticity (accounting for the elasticity effects was the main point of the de Gennes' approach)

We stress: the polymeric viscosity is $\vec{r}$ -dependent, Lumley's $\nu_p \Rightarrow \nu_p(\vec{r})$

• Algebraic Reynolds-stress model for a channel (of width $2L$):

– Exact (standard) equation for the flux of mechanical momentum:

$$\nu(y)S(y) + W(y) = p'L\,, \qquad \nu(y) \equiv \nu_0 + \nu_p(y)\,. \tag{17.1}$$

Hereafter: x & y streamwise & wall-normal directions, $p' \equiv -dp/dx$

Mean shear: $S(y) \equiv \dfrac{d\,V_x(y)}{dy}$, Reynolds stress: $W(y) \equiv -\langle v_x v_y \rangle$.

– Balance Eq. for the density of the turbulent kinetic energy $K \equiv \langle |\vec{v}|^2 \rangle /2$:

$$\left[\, \nu(y)\, (a/y)^2 + b\,\sqrt{K(y)}/y \,\right] K(y) = W(y)S(y)\,, \tag{17.2a}$$

– Simple TBL closure:
$$\frac{W(y)}{K(y)} = \begin{cases} c_{\rm N}^2\,, & \text{for Newtonian flow,} \\ c_{\rm V}^2\,, & \text{for viscoelastic flow.} \end{cases} \tag{17.2b}$$

– Dynamics of polymers (in harmonic approximation, with $\tau_{\rm p}$ – polymeric relaxation time) restricts the level of turbulent activity, (consuming kinetic energy) at the threshold level:

$$1 \simeq \tau_{\rm p} \sqrt{\left\langle \frac{\partial u_i}{\partial r_j}\frac{\partial u_i}{\partial r_j} \right\rangle} \simeq \tau_{\rm p}\, \frac{\sqrt{W(y)}}{y}\,. \tag{17.3}$$

- Algebraic Reynolds-stress model in wall units:

$$\mathcal{R}e \equiv \frac{L\sqrt{p'L}}{\nu_0}, \quad y^+ \equiv \frac{y\mathcal{R}e}{L}, \quad V^+ \equiv \frac{V}{\sqrt{p'L}}, \quad \nu^+ = \left[1 + \nu_\mathrm{p}^+\right] \ . \tag{17.4a}$$

Mechanical balance: $$\nu^+ S^+ + W^+ = 1\,, \tag{17.4b}$$

Energy balance: $$\nu^+ \left(\delta/y^+\right)^2 + \sqrt{W^+}/\kappa_\mathrm{K} y^+ = S^+, \tag{17.4c}$$

Polymer dynamics: $$\sqrt{W^+} = L^2\,\nu_0\,y^+/\tau_\mathrm{p}\,\mathcal{R}e^2 \ . \tag{17.4d}$$

- Test case: Newtonian turbulence:

Disregard polymeric terms: $\nu^+ \to 1$ & solve quadratic Eqs. (1)-(2) for $S^+(y^+)$ & integrate. The result :

For $y^+ \le \delta$: $$V^+ = y^+, \tag{17.5a}$$

For $y^+ \ge \delta$: $$V^+(y^+) = \frac{1}{\kappa_\mathrm{K}} \ln Y(y^+) + B - \Delta(y^+)\,, \tag{17.5b}$$

$$B = 2\delta - \frac{1}{\kappa_\mathrm{K}} \ln \left[\frac{e\,(1 + 2\,\kappa_\mathrm{K}\delta)}{4\kappa_\mathrm{K}}\right]\,, \tag{17.5c}$$

$$Y(y^+) = \frac{1}{2}\left[y^+ + \sqrt{y^{+2} - \delta^2 + \left(2\kappa_\mathrm{K}\right)^{-2}}\right], \tag{17.5d}$$

$$\Delta(y^+) = \frac{2\,\kappa_\mathrm{K}^2\delta^2 + 4\kappa_\mathrm{K}\left[Y(y^+) - y^+\right] + 1}{2\kappa_\mathrm{K}^2 y^+}\ . \tag{17.5e}$$

Two fit parameters: κ_N & δ .

• **Comparison of analytical profile with experiment & numerics** using $\kappa_{\rm K}^{-1}=0.4$ and $\delta_{\rm N}=6$.

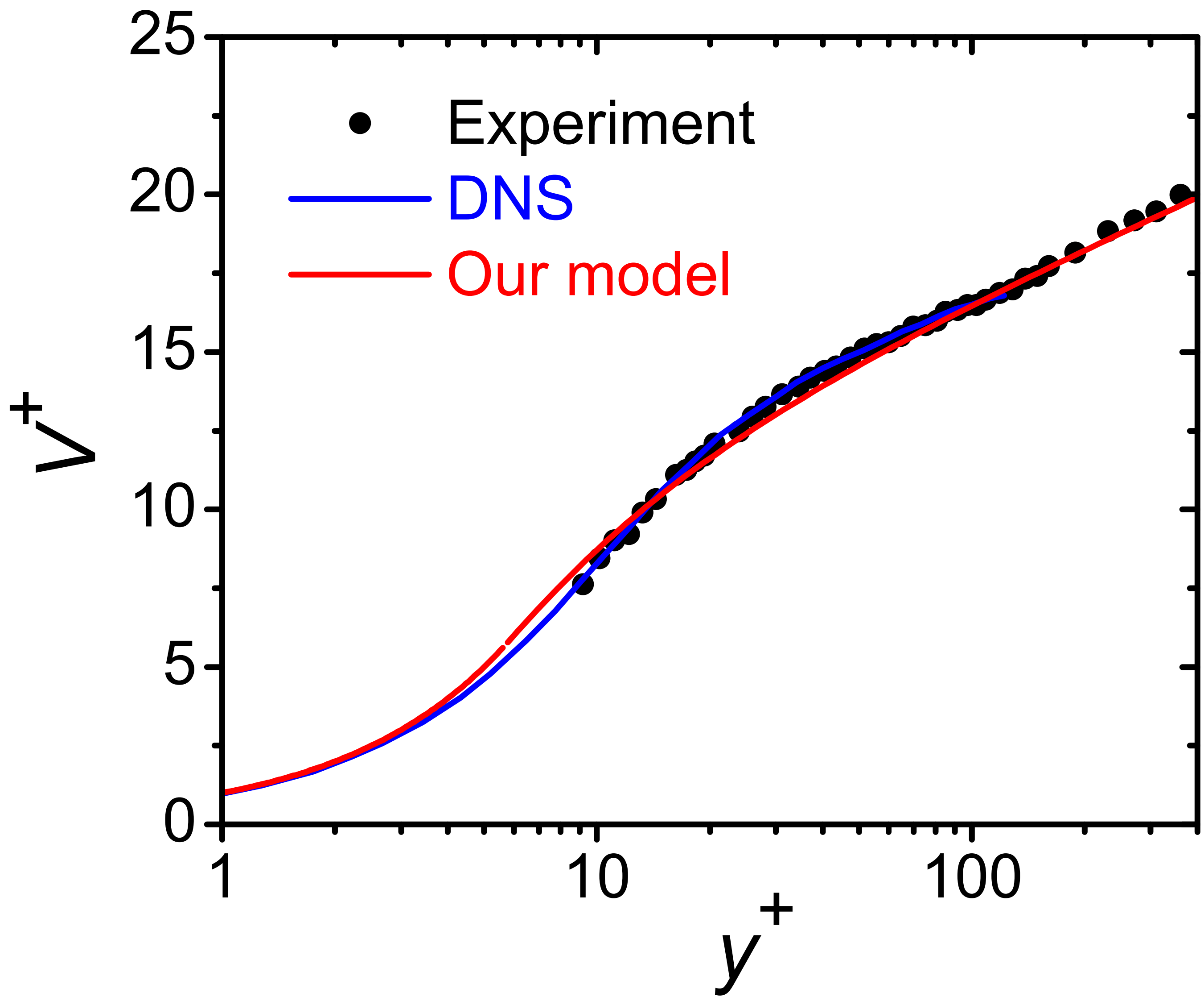

Summary: Our simple Algebraic Reynolds-stress model, based on the *exact* balance of mechanical momentum and K41 inspired *model equation* for the local energy balance, gives physically transparent, analytical, semi-quantitative description of turbulent boundary layer

- Viscoelastic turbulent flow & Universal MDR asymptote:

$$\text{Mechanical balance:}\quad \nu^+ S^+ + W^+ = 1\,, \tag{17.6a}$$

$$\text{Energy balance:}\quad \nu^+\left(\frac{\delta_{\rm N,V}}{y^+}\right)^2 + \frac{\sqrt{W^+}}{\kappa_{\rm K} y^+} = S^+, \tag{17.6b}$$

$$\text{Polymer dynamics:}\quad \sqrt{W^+} = \frac{L^2\nu_0}{\tau_{\rm p}}\,\frac{y^+}{\mathcal{R}e^2} \to 0 \tag{17.6c}$$

at fixed y^+ & $\mathcal{R}e \to \infty$.

Equation (17.6c) dictates:

Maximum Drag Reduction (**MDR**) asymptote $\Rightarrow \quad \mathcal{R}e \to \infty\,,\ W^+ = 0$.

We have learned that in the MDR regime:

— normalized (by wall units) turbulent kinetic energy [Eq.(17.6c)] $K^+ \propto W^+ \to 0$;

— the mechanical balance [Eq.(17.6a)] and the balance of kinetic energy [Eq.(17.6b)] are dominated by the polymeric contribution $\propto \nu^+$.

In the MDR regime Eqs. (1,2) become $\Rightarrow \quad \nu^+ S^+ = 1\,,\ \nu^+\delta_{\rm V}^2 = S^+ y^{+2}$

and have solution: $\quad S^+ = \delta_{\rm V}/y^+\,,\quad \nu^+ = y^+/\delta_{\rm V}$

for $y^+ \geq \delta_{\rm V}$, $\quad$ because $\nu^+(y^+) \geq \nu_0^+ = 1$.

For $y^+ \leq \delta_{\rm V}\,,\ S^+ = 1\,,\ \nu^+ = 1;\ V^+(y^+) = \delta_{\rm V}\displaystyle\int_{\delta_{\rm V}}^{y^+} S^+(\xi)d\xi \ \Rightarrow$

$$\text{Universal MDR asymptote:}\quad V^+(y^+) = \delta_{\rm V}\ln\left(e\,y^+/\delta_{\rm V}\right)\ . \tag{17.7}$$

Summary:

— In the MDR regime normalized (by wall units) turbulent kinetic energy $K^+ \to 0$;

— MDR regime is the edge of turbulent solution of the Navier-Stokes Eq. (NSE) with the largest possible effective viscosity $\nu(y)$, at which the turbulence still exists!

— MDR profiles of $\nu(y)$ & $S(y)$ are determined by the NSE itself and **are universal, independent of parameters of polymeric additives.**

- Calculation of $\delta_{\rm V}$ in the MDR asymptote:

$$V^+(y^+) = \delta_{\rm V} \ln(e\ y^+/\delta_{\rm V})\,. \tag{17.8}$$

Consider $\nu^+ S^+ + W^+ = 1\,, \quad \nu^+ \dfrac{\delta^2_{\rm N,V}}{{y^+}^2} + \dfrac{\sqrt{W^+}}{\kappa_{\rm K} y^+} = S^+$ with prescribed $\nu^+ = 1 + \alpha(y^+ - \delta_{\rm N})$ and replace flow dependent $\delta_{\rm N,V} \to \Delta(\alpha)$ with yet arbitral α :

$$[1 + \alpha(y^+ - \delta_{\rm N})]S^+ + W^+ = 1\,, \tag{17.9a}$$

$$[1 + \alpha(y^+ - \delta_{\rm N})]\frac{\Delta^2(\alpha)}{{y^+}^2} + \frac{\sqrt{W^+}}{\kappa_{\rm K} y^+} = S^+\,. \tag{17.9b}$$

Clearly, $\delta_{\rm N} = \Delta(0)$ (Newtonian flow) and $\delta_{\rm V} = \Delta(\alpha_{\rm V})$, where $\Delta(\alpha_{\rm V})$ is the MDR solution of (17.9) in asymptotical region $y^+ \gg 1$ with $W = 0$:

$$\alpha_{\rm V}\,\Delta(\alpha_{\rm V}) = 1\,, \quad \Delta(\alpha) = \frac{\delta_{\rm N}}{1 - \alpha\delta_{\rm N}}\,, \Rightarrow\ \alpha_{\rm V} = \frac{1}{2\delta_{\rm N}}\,, \Rightarrow\ \delta_{\rm V} = 2\,\delta_{\rm N}\,. \tag{17.10}$$

$\Delta(\alpha)$ follows from the requirement of the rescaling symmetry of Eq. (17.9):

$$y^+ \to y^\ddagger \equiv \tfrac{y^+}{g(\widetilde{\delta})}\,,\ g(\widetilde{\delta}) \equiv 1 + \alpha(\widetilde{\delta} - \delta_{\rm N})\,,$$
$$\widetilde{\delta} \to \delta^\ddagger \tfrac{\widetilde{\delta}}{g(\widetilde{\delta})}\,,\ S^+ \to S^\ddagger \equiv S^+ g(\widetilde{\delta})\,.$$

Finally our theory gives

$$V^+(y^+) = 2\delta_{\rm N} \ln\left(\frac{e\ y^+}{2\,\delta_{\rm N}}\right), \tag{17.11}$$

with Newtonian constant $\delta_{\rm N} \approx 6$ (†)

- Virk's MDR asymptote: experiment (‡) *vs* our equation (†)

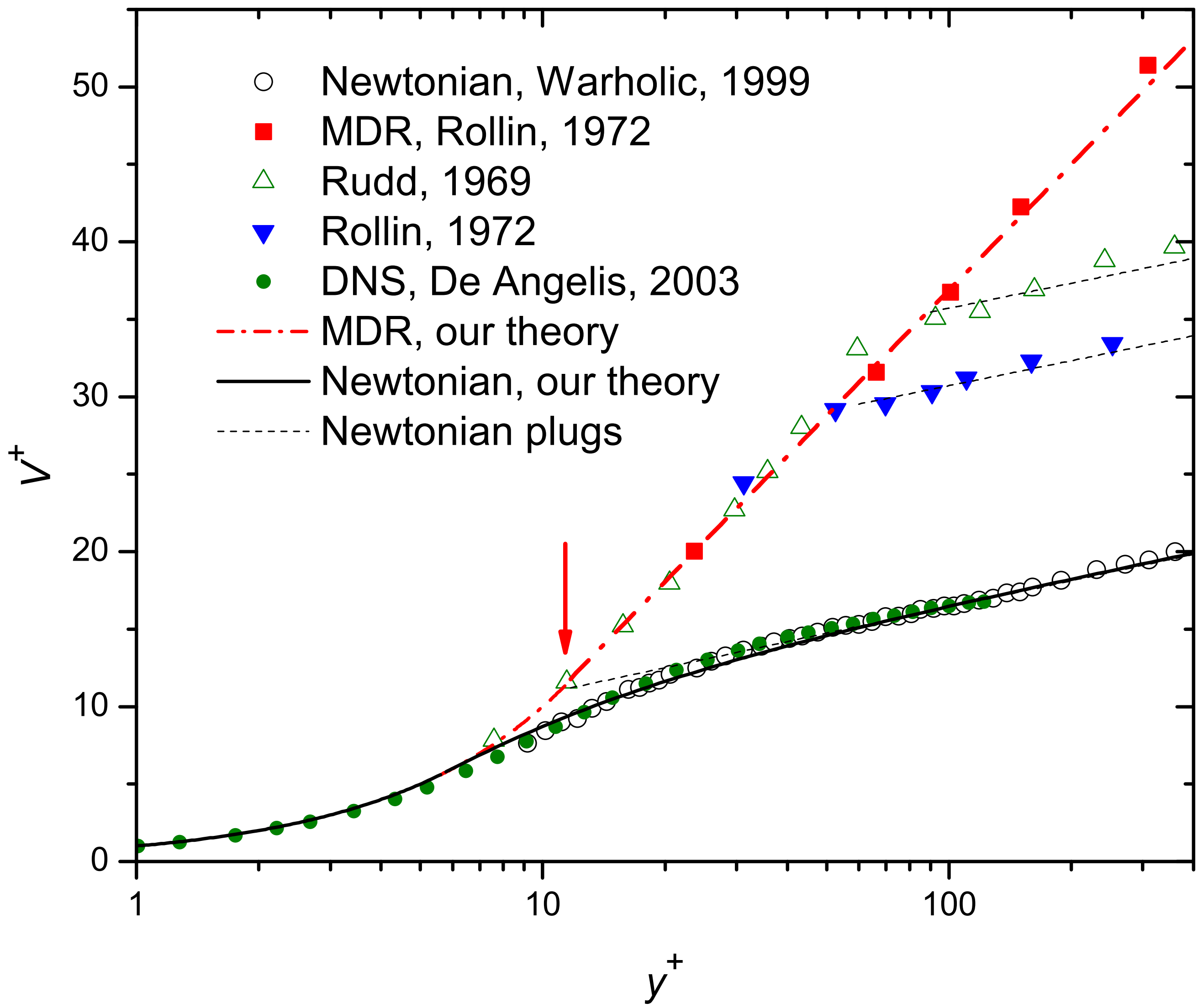

Red squares – experiment,
MDR:

$$V^+ = 11.7 \ln y^+ - 17.0\,. \quad (\ddagger)$$

$$V^+ = 2\delta_{\rm N} \ln(e\, y^+/2\delta_{\rm N})\,. \quad (\dagger)$$

Taking $\delta_{\rm N} \approx 6$ from Newtonian data one has slope $2\delta_{\rm N} \approx 12$, close to 11.7 in (‡) and intercept
$2\delta_{\rm N} \ln(e/2\delta_{\rm N}) \approx -17.8$, close to -17.0 in (‡).

Summary: Maximum possible drag reduction (MDR asymptote) corresponds to the maximum possible viscosity profile at the edge of existence of turbulent solution and thus is universal, i.e. independent of polymer parameters, if polymers are able to provide required viscosity profile.

el

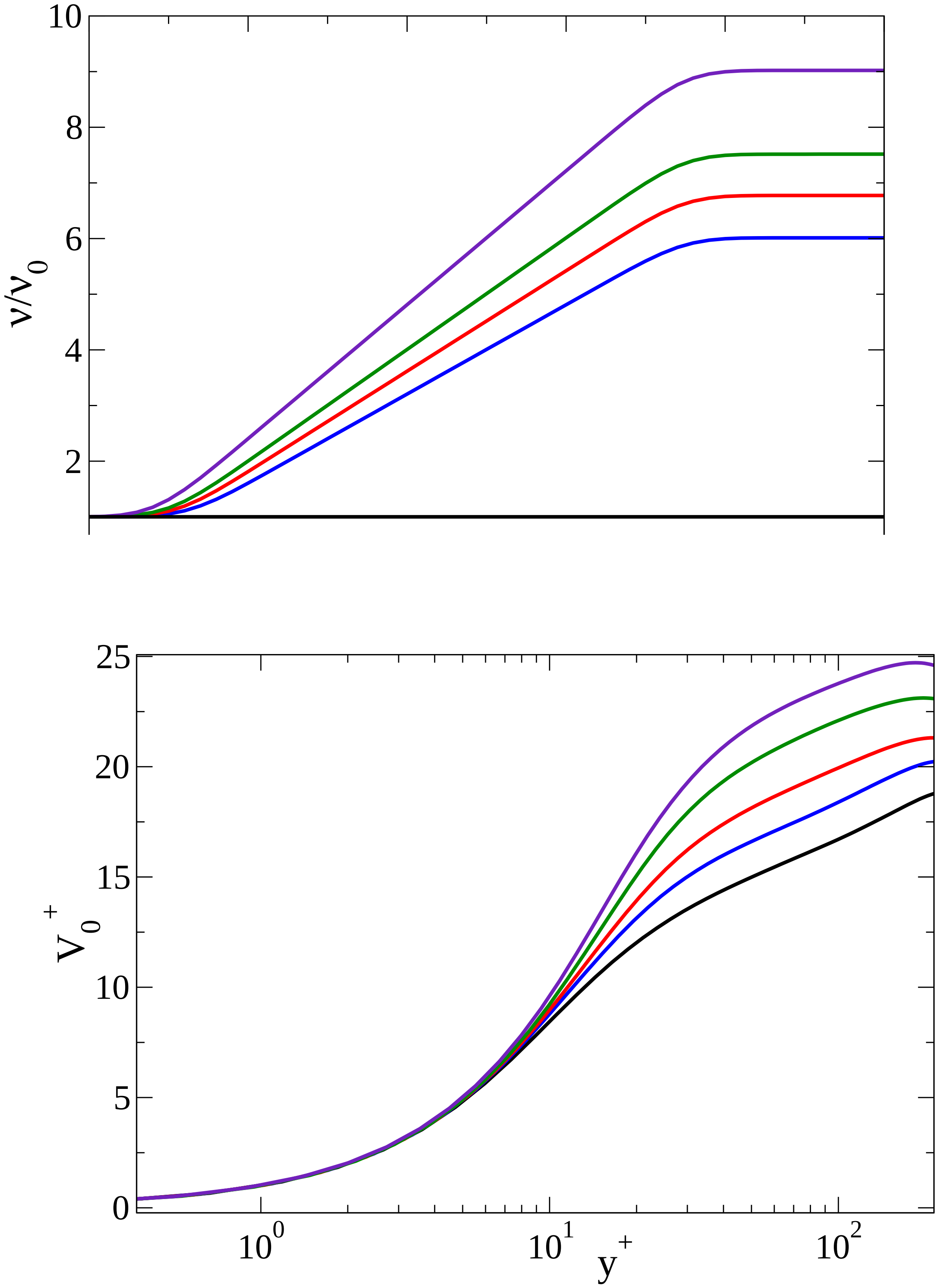

The viscosity (Left) & NSE-DNS mean velocity profiles (Right). $\mathcal{R}e = 6000$ (with centerline velocity). Solid black line — standard Newtonian flow. One sees a drag reduction in the scalar mean viscosity model.

- Comparison of **renormalized–NSE model** (Red line: – – –) and **full FENE-P model** (Blue circles: ∘∘∘∘) [Newtonian flow: —-] $\mathcal{R}e = 6000$ for velocity (down)

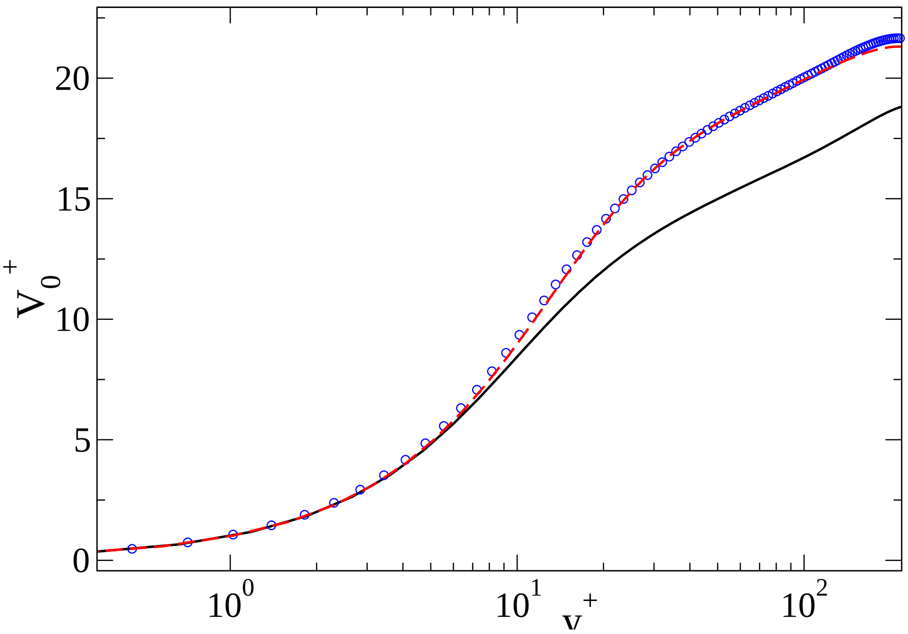

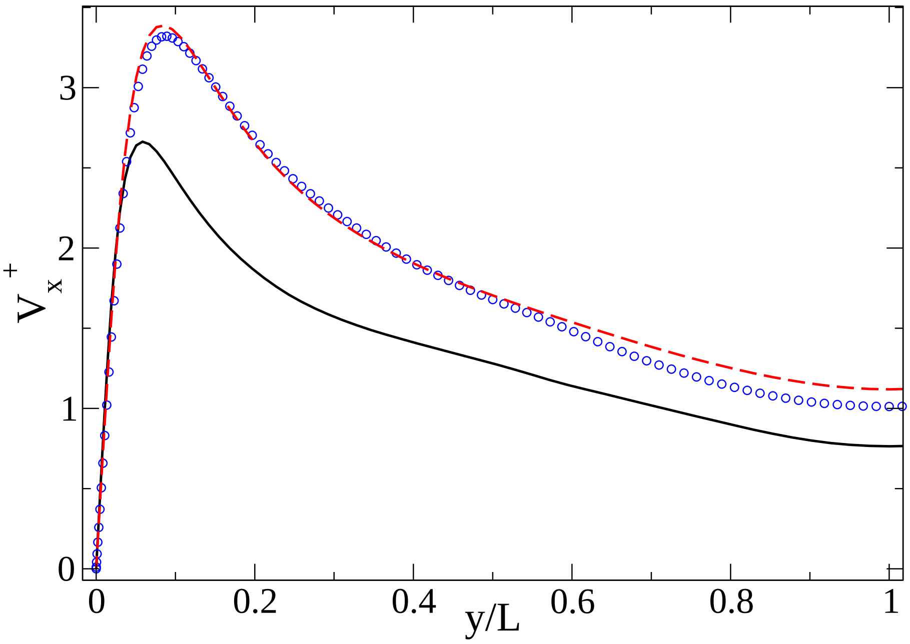

Conclusion: Suggested simple model of polymer suspension with self-consistent viscosity profile really demonstrates the drag reduction itself and its essentials: mean velocity, kinetic energy profiles not only in the MDR regime, but also for intermediate $\mathcal{R}e$.

- Riddle

Intuitively: effective polymeric viscosity ν_p should be proportional to the (thermodynamical) mean square polymeric extension $\mathcal{R} \equiv \overline{R^2}$, averaged over turbulent assemble, $\mathcal{R}_0 = \langle \mathcal{R} \rangle$:

$$\nu_\text{p} \propto \mathcal{R}_0(y) \ .$$

However, in the MDR regime in our model ν_p increases with the distance from the wall, $\nu_\text{p} \propto y$, while experimentally $\mathcal{R}(y)$ decreases.

- A way out

Instead of intuitive (and wrong) relationship $\nu_\text{p} \propto \mathcal{R}_0(y)$ one needs to find correct connection between ν_p and mean polymeric conformation tensor

$$\mathcal{R}_0^{ij} \equiv \left\langle \overline{R^i R^j} \right\rangle$$

. **This is a goal of**

Advanced approach: Elastic stress tensor Π & effective viscosity

Advanced approach: Elastic stress tensor Π & effective viscosity

Define:

- elastic stress $\Pi^{ij} \equiv \mathcal{R}^{ij}\, \nu_{0,\text{p}}/\tau_\text{p}$ &
- conformation $\mathcal{R}^{ij} \equiv \overline{R^i R^j}$ tensors,
- polymeric "laminar" viscosity $\nu_{0,\text{p}}$ and polymeric relaxation time τ_p ,
- $\boldsymbol{R} = \boldsymbol{r}/r_0$ – end-to-end distance, normalized by its equilibrium value

Write: Navier Stokes Equation (NSE) for dilute polymeric solutions:

$$\frac{\partial \vec{v}}{\partial t} + \left(\vec{v} \cdot \vec{\nabla}\right) \vec{v} = \nu_0 \Delta \vec{v} - \vec{\nabla} P + \vec{\nabla} \boldsymbol{\Pi} \,, \tag{17.12a}$$

together with the equation for the elastic stress tensor:

$$\frac{\partial \boldsymbol{\Pi}}{\partial t} + (\vec{v} \cdot \vec{\nabla}) \boldsymbol{\Pi} = \boldsymbol{S\Pi} + \boldsymbol{\Pi S}^\dagger - \frac{1}{\tau_\text{p}} (\boldsymbol{\Pi} - \boldsymbol{\Pi}_\text{eq}) \,, \tag{17.12b}$$

$$S^{ij} \equiv \partial v^i / \partial x^j ,$$

Averaging Eq. (17.12a) and $\int_0^y ...d\tilde{y}$ one has Eq. for $S(y) \equiv \langle \partial v^x/\partial y \rangle$:

$$\nu_0\, S(y) + \Pi_0^{xy}(y) + W(y) = p'\, L\,, \tag{17.13}$$

in which $\Pi_0^{xy}(y) \equiv \langle \Pi^{xy}(y) \rangle$ is the momentum flux, carried by polymers.

Averaging Eq. (17.12b), and taking $D/Dt = 0$ one gets stationary Eq. for $\mathbf{\Pi}_0$:

$$\mathbf{\Pi}_0 = \tau_\mathrm{p}\left(\boldsymbol{S}_0 \cdot \mathbf{\Pi}_0 + \mathbf{\Pi}_0 \cdot \boldsymbol{S}_0^\dagger + \boldsymbol{Q}\right)\,, \quad Q \equiv \tau_\mathrm{p}^{-1}\Pi_\mathrm{eq} + \left\langle s\cdot \pi + \boldsymbol{\pi}\cdot \boldsymbol{s}^\dagger \right\rangle\,. \tag{17.14a}$$

In the shear geometry $S_0 \cdot S_0 = 0$. This helps to find by the subsequent substitution of the RHS $\Rightarrow$ RHS of Eq. (**??**) its solution:

$$\mathbf{\Pi}_0 = 2\,\tau_\mathrm{p}^3\, S_0 \cdot \boldsymbol{Q} \cdot S_0^\dagger + \tau_\mathrm{p}^2\left(S_0 \cdot \boldsymbol{Q} + \boldsymbol{Q} \cdot S_0^\dagger\right) + \tau_\mathrm{p}\boldsymbol{Q}\ . \tag{17.14b}$$

At the onset of drag reduction Deborah number at the wall $\mathcal{D}e_0 \simeq 1$,
$\mathcal{D}e_0 = \mathcal{D}e(0)$, $\mathcal{D}e(y) \equiv \tau_\mathrm{p}\, S(y)$. In the MDR regime: $\mathcal{D}e(y) \gg 1$.
In the limit $\mathcal{D}e(y) \gg 1$, Eq. (17.14b) gives:

$$\Pi_0(y) = \Pi_0^{yy}(y)\begin{pmatrix} 2\,[\mathcal{D}e(y)]^2 & \mathcal{D}e(y) & 0 \\ \mathcal{D}e(y) & 1 & 0 \\ 0 & 0 & C \end{pmatrix}, \quad C = \frac{Q_{zz}}{Q_{yy}} \simeq 1\,. \tag{17.14c}$$

For $\mathcal{D}e(y) \gg 1$ tensorial structure of $\mathbf{\Pi}_0$ becomes universal. In particular:

$$\Pi_0^{xy}(y) = \mathcal{D}e(y)\ \Pi_0^{yy}(y)\ . \tag{17.14d}$$

Insertion (17.14d) into Eq. (17.14a) gives the model Eq:

$$\Big[\nu_0 + \nu_\mathrm{p}\Big]\ S(y) + W(y) = p'\, L\,, \tag{17.15}$$

where the polymeric viscosity is

$$\nu_\mathrm{p} \equiv \tau_p\ \Pi_0^{yy}(y) = \nu_{0,\mathrm{p}}\mathcal{R}^{yy} \tag{17.16}$$

Summary: Effective polymeric viscosity ν_p is proportional to yy component of the conformation (and elastic stress) tensor, not to its trace.

- Comparison of the theory with Direct Numerical Simulation

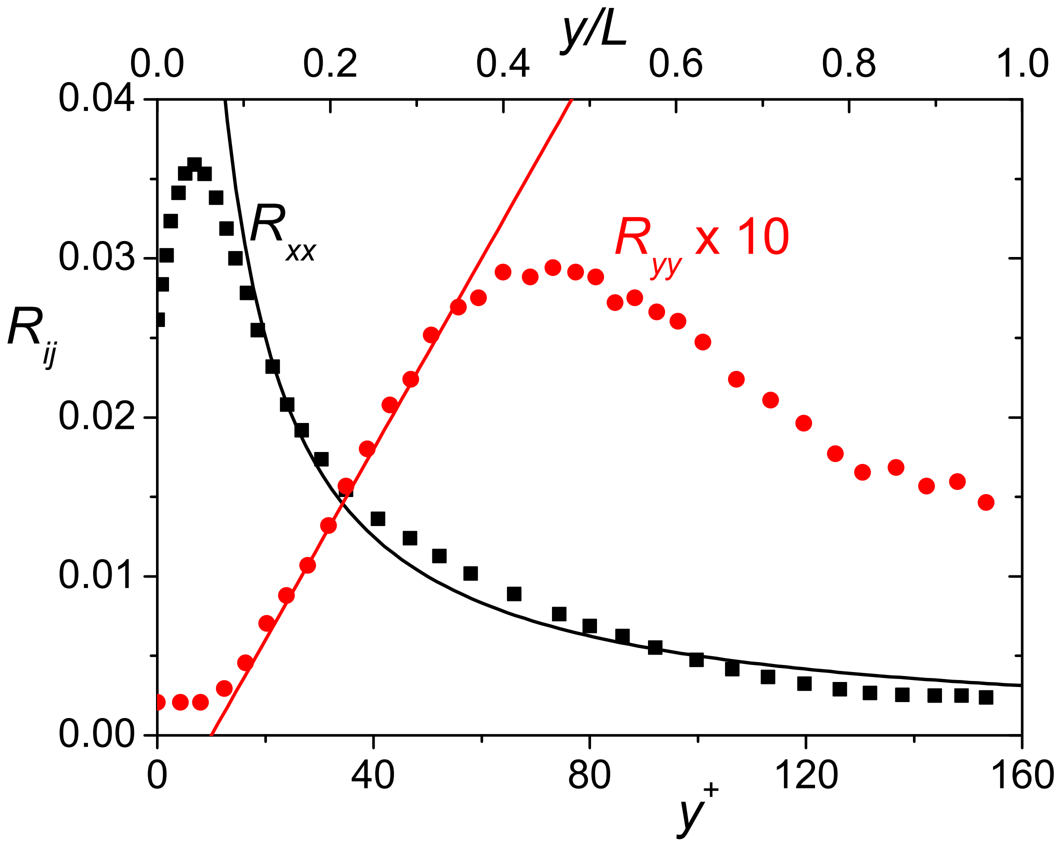

We found: In the MDR regime,

$$\nu_p(y) \propto \mathcal{R}_{yy}(y) \propto y\,,$$

while

$$S(y) \propto 1/y\,, \quad \mathcal{R}^{yy}(y) \propto y\,,$$

$$\mathcal{R}^{xx}(y) = 2S^2(y)\tau_{\rm p}^2\,\mathcal{R}^{yy}(y) \propto \frac{1}{y}\,.$$

DNS data for $\mathcal{R}^{yy}$ – red circles, for $\mathcal{R}^{xx}$ – black squares are fitted by red y and black $1/y$ lines.

Summary: Predicted spacial profiles of effective viscosity and polymeric extension are consistent with the DNS and experimental observations.

- Cross-over from the MDR asymptote to the Newtonian plug Model Eqs.

$$\Big[\nu_0 + \nu_{\rm p}\Big]\, S(y) + W(y) = p'\, L\,, \tag{17.17a}$$

$$\Big\{\Big[\nu_0 + \nu_{\rm p}\Big]\big(a/y\big)^2 + b\,\sqrt{K(y)}/y\Big]\Big\}K(y) = W(y)S(y)\,, \tag{17.17b}$$

$$W(y)\Big/K(y) = c_{\rm V}^2\,, \quad \tau_{\rm p}^2\, W(y) \simeq y^2\ . \tag{17.17c}$$

Reminder: In the MDR regime red-marked terms in Eqs. (17.17a), (17.17b) are small.

$\times$ -over of linearly extended polymers: Eq. (17.17a) $\Rightarrow$ $p'L \simeq W(y_\times) \Rightarrow$ with Eq. (17.17c):

$$p'\, L \simeq y_\times^2/\tau_{\rm p}^2 \quad \Rightarrow \quad y_\times \simeq \tau_{\rm p}\sqrt{p'L} \quad \Rightarrow \quad y_\times^+ \simeq \mathcal{D}e(0)\ . \tag{17.18}$$

$\times$ -over of finite extendable polymers: $\nu_{\rm p} \le \nu_{\rm p,max} \simeq \nu_0\, c_{\rm p}\, \big(a\, N_{\rm p}\big)^3$.

In the MDR: $\quad \nu_{\rm p}(y^+) \simeq \nu_0\, y^+ \quad \Rightarrow$

$$y_\times^+ \simeq c_{\rm p}\, \big(a\, N_{\rm p}\big)^3\ . \tag{17.19}$$

In general:

$$y_\times^+ \simeq \frac{\mathcal{D}e(0)\, c_{\rm p}\, \big(a\, N_{\rm p}\big)^3}{\mathcal{D}e(0) + c_{\rm p}\, \big(a\, N_{\rm p}\big)^3}\ . \tag{17.20}$$

Verification: $\times$ -over (17.18) is consistent with DNS of Yu et. al. (2001), $\times$ -over (17.19) is in agreement with DNA experiment of Choi et. al. (2002)

Summary of the results

• Essentials of the drag reduction by dilute elastic polymers can be understood within the suggested Effective Viscosity Approximation.

• For the NSE with the effective viscosity we have suggested an Algebraic Reynolds-stress model that describes relevant characteristics of the Newtonian and viscoelastic turbulent flows in agreement with available DNS and experimental data.

• The model allows one to clarify the origin of the universality of the maximum possible drag reduction and to calculate universal Virk's constants, that are are a good quantitative agreement with the experiments.

• The model predicts two mechanisms of $\times$- over MDR$\Rightarrow$ Newtonian plug in a qualitative agreement with DNS and experiment.

In short: Basic physics of drag reduction in polymeric solutions is under-stood and has reasonable simple and transparent description in the framework of developed theory. Further developments and detailing are possible

Lecture 18

Introduction to Fracture Theory

Outline

Basics of Linear Elasticity Theory

Let us consider a body in mechanical equilibrium and then displace each material point $\mathbf{r}$ by a small amount given by the vector field $\mathbf{u}(\mathbf{r})$. By applying the displacement field $\mathbf{u}(\mathbf{r})$ we did work on the body, thus we increased its energy content relative to its equilibrium state. Let us write down the most general energy functional for the body. First, we note that due to translational invariance the energy cannot directly depend on $\mathbf{u}(\mathbf{r})$, only on its derivatives. For that purpose we define the strain tensor

$$\epsilon_{ij} = \frac{1}{2}(\partial_i u_j + \partial_j u_i) \ . \tag{18.1}$$

For an isotropic material we should use only the invariants of the strain tensor ϵ_{ij}. Recalling that we restrict ourselves to small deformations, we can write down the most general second order energy functional

$$U = \frac{1}{2}\left[2\mu\, Tr(\epsilon_{ij}^2) + \lambda\, Tr^2(\epsilon_{ij})\right] \ , \tag{18.2}$$

where μ and λ are material constants known as Lame coefficients. The forces conjugate to the strain tensor ϵ_{ij} define the stress tensor σ_{ij} as

$$\sigma_{ij} = \frac{\partial U}{\partial \epsilon_{ij}} \ . \tag{18.3}$$

Using Eq. (18.2) we obtain the tensorial Hooke's law

$$\sigma_{ij} = 2\mu\epsilon_{ij} + \lambda\delta_{ij}\epsilon_{kk} \ . \tag{18.4}$$

Physically, σ_{ij} is the i^{th} component of the force acting on a unit area whose normal is in the j^{th} direction. The Lame coefficients μ and λ are related to the more familiar engineering constants Young's modulus E and Poisson's ratio ν by

$$\mu = \frac{E}{2(1+\nu)}, \qquad \lambda = \frac{E\nu}{(1+\nu)(1-2\nu)} \ . \tag{18.5}$$

E and ν are measured in a simple experiment in which a rod whose axis is along the z-axis is stretched by a uniaxial stress σ_{zz}. The longitudinal strain ϵ_{zz} gives E according to

$$\epsilon_{zz} = \sigma_{zz}/E \tag{18.6}$$

and the ratio of the transverse contraction ϵ_{xx} to the longitudinal elongation ϵ_{zz} gives ν according to

$$\epsilon_{xx} = -\nu\epsilon_{zz} \ . \tag{18.7}$$

In order to derive an equation of motion we write down Newton's second law for a volume element which yields

$$\frac{\partial \sigma_{ij}}{\partial x_j} = \rho\frac{\partial^2 u_i}{\partial t^2} \ , \tag{18.8}$$

where ρ is the material density that is regarded constant under the small deformations assumption. The final equation of motion for the fundamental field $\mathbf{u}(\mathbf{r})$ is obtained by substituting Eq. (18.4) in Eq. (18.8), resulting in

$$(\lambda+\mu)\nabla(\nabla\cdot\mathbf{u}) + \mu\nabla^2\mathbf{u} = \rho\frac{\partial^2\mathbf{u}}{\partial t^2} \ . \tag{18.9}$$

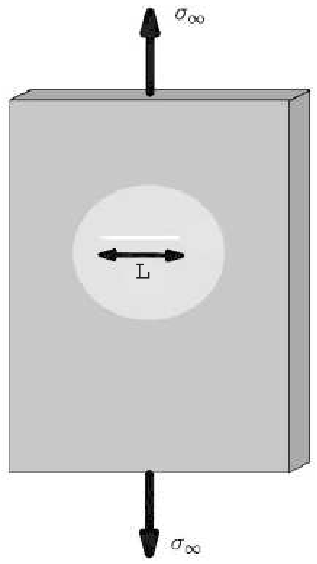

Figure 1: A material under the application of a uniform external stress σ_∞ at its far edges in the presence of a crack of length L that is cutting through the sample. The shaded region represents the typical area in which the potential energy density is changed relative to the uniform stress state.

Scaling Relations in Fracture

The modern development of the field of fracture as a scientific discipline initiated with the pioneering work of Griffith (1920) who identified the importance of defects in determining the strength of materials. These defects act as stress concentrators in the sense that the typical stress near the defect can be much higher than the applied stress. In that way the strength of materials is highly reduced, explaining the long lived conflict between theoretical strength estimations and experimental observations. In order to understand the way defects affect the failure of materials we first introduce a simple scaling argument in the framework of equilibrium thermodynamics. This means that for the sake of the present argument we ignore all irreversible processes that accompany crack formation and assume that cracks can form and disappear in agreement with global considerations.

In Fig. 1 we consider a material under the application of a uniform external stress σ_∞ at its far edges. In addition, the material contains a defect that is assumed here to be a crack of length L that is cutting through the material. A crack is defined as a region whose boundaries cannot support stress. In the absence of a crack the material is uniformly stressed with an associated elastic energy density U according to Eq. (18.2) (written in terms of stress instead of strain)

$$U \sim \frac{\sigma_\infty^2}{E} , \tag{18.10}$$

where E is Young's modulus and it is assumed that the material is linear elastic. The presence of a crack of length L releases the stresses in an area of the order of $\sim L^2$ (shaded area in Fig. 1), resulting in a reduction ΔU in the elastic energy per unit material width

$$\Delta U = -c\frac{\sigma_\infty^2 L^2}{E} , \tag{18.11}$$

where c is a dimensionless factor. On the other hand, the very existence of the crack is associated with free material surfaces. Assuming that the energy cost per unit area of free surfaces is Γ - the work of fracture, the generation of a crack of length L results in an energy increase ΔU_s per unit width by an amount,

$$\Delta U_s = \Gamma L . \tag{18.12}$$

The total energy change per unit width ΔU_t is given by

$$\Delta U_t = -c\frac{\sigma_\infty^2 L^2}{E} + \Gamma L . \tag{18.13}$$

This equation tells us that for small values of L the formation of a crack is costly ($\Delta U_t > 0$) whereas longer cracks are energetically favorable ($\Delta U_t < 0$). Actually, once a critical length is achieved the crack tends to increase indefinitely until the material completely fails. This non-equilibrium catastrophic crack propagation is at the essence of the failure of material. The two different regimes described above are separated by a Griffith critical length

$$L_G \sim \frac{E\Gamma}{\sigma_\infty^2} , \tag{18.14}$$

which is shown to be a combination of material properties (E and Γ) and external loading conditions (σ_∞).

The thermodynamic argument predicts that crack propagation should always be catastrophic once initiated. In fact, although fast crack propagation is common, there are many situations in which the crack evolves quasi-statically. The point to stress is that whatever is the mode of crack growth, the argument exemplifies the multi-scale nature of the phenomenon; the potential energy released from the large scales dissipates in a very localized region near the crack tip where new crack surfaces are generated.

At the continuum level of linear elasticity fracture mechanics, the crack is introduced as additional boundary conditions. As was mentioned before, a crack is a region whose boundaries are free surfaces. Denote the unit normal to the crack surface at any point by $\hat{\mathbf{n}}$; the boundary conditions on the crack surface are

$$\sigma_{ij} n_j = 0 \ . \tag{18.15}$$

These boundary conditions introduce non-linearities into the problem even if the field equations themselves are linear. This is a major source of mathematical difficulties.

The dissipation involved in the crack growth quantified by the phenomenological material function Γ expresses explicitly the irreversible nature of crack propagation and might include, in addition to the surface energy 2γ, additional sources of dissipation. It is important to note that dissipation Γ is assumed to be highly localized near the crack front. Therefore, one is interested in the near crack front fields. Within linear elasticity theory these are actually singular. To see this consider first a quasi-static infinitesimal extension δL of the crack. Denoting the stress field near the tip by $\sigma(r)$, the energy (per unit width) released from the linear elastic medium δU is

$$\delta U \sim \int_0^{\delta L} \frac{\sigma^2(r)}{E} \, r \, dr \ . \tag{18.16}$$

This amount of energy is invested in creating new crack surfaces whose energy cost (per unit width) is $\Gamma \delta L$. Therefore, we must have

$$\sigma(r) \sim \frac{1}{\sqrt{r}} \ . \tag{18.17}$$

The inverse square-root singularity seen in Eq. (18.17) exists also in the fully dynamic case and can be derived systematically using asymptotic expansion of the solution of Eq. (18.9) near the crack tip. To conclude this section, we summarize the basic properties of cracks:

1. Cracks act as stress concentrators (stress singularities). This result implies that strong non-linear processes near the crack tip regularize this unphysical singularity.

2. Dissipation is typically highly localized near the crack tip, while long range interactions due to elastic fields control the energy flow to the crack tip region. We thus observe that the problem couples very different scales.

3. Non-linearities are introduced by the cracks path and morphology.

Modes of Fracture and Asymptotic Fields

It is conventional to decompose the stress field under general loading conditions to three symmetry *modes* with respect to the fracture plane. These are illustrated in Fig. 2. In mode I the crack faces are displaced symmetrically in the normal direction relative to the fracture xz plane, by tension. In mode II, the crack faces are displaced anti-symmetrically relative to the fracture xz plane, in the x direction, by shear. In these two modes of fracture the deformation is in-plane (xy). In mode III, the crack faces are displaced anti-symmetrically relative to the fracture plane, in the z direction, by shear. This is an out-of-plane fracture mode.

In fact, by asymptotic expansion of the local stress tensor field near the crack front for a quasi-static crack (i.e. when the inertia term in the right hand side of Eq. (18.9) is neglected - physically this condition implies that the crack

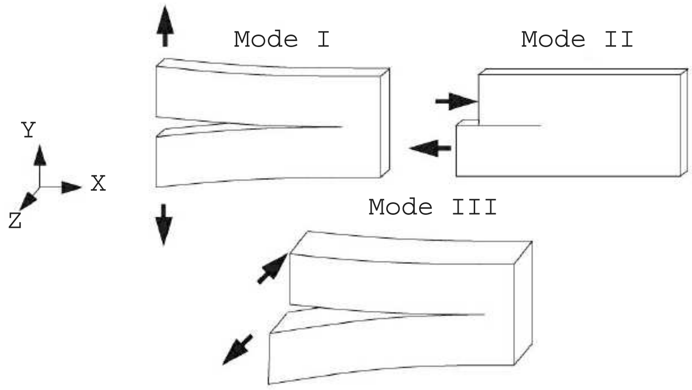

Figure 2: The typical symmetry modes of fracture, see text for more details.

propagation speed is much smaller than a typical sound speed of the material under consideration), it can be shown that the leading term is given by a sum of three contributions corresponding to the three modes of fracture

$$\sigma_{ij}(r,\theta,t) = K_{\text{I}}\frac{\Sigma^{\text{I}}_{ij}(\theta)}{\sqrt{2\pi r}} + K_{\text{II}}\frac{\Sigma^{\text{II}}_{ij}(\theta)}{\sqrt{2\pi r}} + K_{\text{III}}\frac{\Sigma^{\text{III}}_{ij}(\theta)}{\sqrt{2\pi r}} \; , \tag{18.18}$$

where (r,θ) are local polar coordinates system, $\Sigma^{(i)}(\theta)$ are universal and $K_{(i)}$ are the static stress intensity factors. The stress intensity factors are non-universal functionals of the loading conditions, sample geometry and crack history. The predicted singular behavior is, of course, not physical and there must exist mechanisms to cut off this apparent singularity. Nevertheless, there are many physical situations for which the size of the region where linear elasticity breaks down is small compared to other relevant lengths. Therefore, the stress intensity factors are very important physical quantities and the singularity may be retained in many models. This singularity is a source of mathematical difficulties and physical riddles. The stress concentration quantified by the stress intensity factors shows that the material near a crack front experiences extreme conditions; the response to these conditions is far from being well-understood.

Dynamic Fracture and the Micro-branching Instability

Up to now we limited the discussion to quasi-static situations in which the crack propagates at speeds much slower than a typical speed of sound of the medium. Nevertheless, when the a unit of crack advance releases more energy than is needed to create new free surfaces, the crack 'uses' the additional energy to accelerate its tip and thus to increase the kinetic energy of its surroundings. In that case the crack velocity can be comparable to the sound speed and dynamic effects should be taken in account. If we restrict the discussion to two space dimensions one can show that the resulting near tip stress tensor field is given by

$$\sigma_{ij}(r,\theta,v) = \frac{K_I\{t,...\}}{\sqrt{2\pi r}}\Sigma^I_{ij}(\theta,v) + \frac{K_{II}\{t,...\}}{\sqrt{2\pi r}}\Sigma^{II}_{ij}(\theta,v). \tag{18.19}$$

Here v is the instantaneous crack tip speed, Σ^I_{ij} and Σ^{II}_{ij} are universal functions that reduce to their static counterparts of Eq. (18.18) in the limit $v \to 0$ and $K_I\{t,...\}$ and $K_{II}\{t,...\}$ are the dynamic stress intensity factors corresponding to the two symmetry modes of fracture and are usually non-linear functionals of all the non-universal features of the problem. The term "universal" denotes the fact that a function is independent of the details of the applied loading or the configuration of the material under consideration. Mode I denotes the in-plane opening mode and Mode II denotes the in-plane shearing mode. The square root singularity is a universal feature of the stress tensor field. All the non-universal properties of a given problem, i.e. the history of crack propagation, the loading conditions and the geometry of the material, are expressed through the intensity of the universal singularity. Note that the angular dependence and the velocity dependence of the stress tensor field are universal. It is clear that no real material can sustain infinite stresses, so there must exist some scale r_c at which linear elasticity breaks down. It is assume that the scale in which linear elasticity is not valid is very small compared to any other length scale in a relevant problem. Below this scale all the dissipative processes are effective and the stress singularity is regularized. Therefore, the fundamental picture of linear elasticity fracture mechanics is that the tip of a crack is an energy sink that absorbs the elastic energy stored in the bulk material and dissipates it by some unspecified processes.

In order to write down an equation of motion for the crack tip one should be able to calculate the energy flux into the region near the tip. Consider a crack tip moving with the instantaneous speed v and a contour $\mathcal{S}$ that translates with it. We are interested in the instantaneous rate of energy flow through $\mathcal{S}$ toward the crack tip. The calculation can be performed in detail but the result can be constructed by physical intuition. The energy flux should be the sum of two contributions, one represents the work done on the material inside $\mathcal{S}$ by the forces acting on $\mathcal{S}$ and the other one represents the energy flux due to transport of material through $\mathcal{S}$, carrying an energy density $U + \mathcal{T}$. Here U is the strain energy density and $\mathcal{T}$ is the kinetic energy density. Therefore, we obtain

$$F(\mathcal{S}) = \int_{\mathcal{S}} \left[\sigma_{ij} n_j \frac{\partial u_i}{\partial t} + (U + \mathcal{T})\, v n_x \right] ds. \tag{18.20}$$

Here $\hat{\mathbf{n}}$ is the unit outward normal to $\mathcal{S}$, n_x is the direction of propagation, and s is the arclength measured along $\mathcal{S}$. For this integral to have a fundamental significance, its value should be path-independent. One can prove that if the contour of integration can be taken always within the universal singularity dominance region, the integral is indeed path-independent. Physically, this assumption corresponds to the condition that all the dissipative processes in the system take effect only very close to the crack tip. These processes dissipate energy per unit crack propagation in a rate $v\Gamma(v)$; $\Gamma(v)$ is a phenomenological quantity that measures the dissipation as a function of the crack speed, has the dimension of surface energy and is the dynamic counterpart of the dissipation function introduced previously in the quasi-static context. Therefore, from energy balance considerations, we can conclude that

$$\Gamma(v) = G = \lim_{\mathcal{S} \to 0} \left\{ \frac{F(\mathcal{S})}{v} \right\} , \tag{18.21}$$

where G is the so-called the energy release rate (though it is not really a rate, its dimensions are energy per unit area). Moreover, since the contour of integration is always within the universal singularity dominance region we can use Eq.(18.19) to calculate the integral. The obtained result is

$$G = \frac{A^I(v)K_I^2 + A^{II}(v)K_{II}^2}{E} \tag{18.22}$$

where $A^I(v)$ and $A^{II}(v)$ are two universal functions of the crack tip velocity.

A comment is in order. Eq. (18.21) is called an equation of motion for the crack tip, though actually it is not sufficient to fully describe the evolution of the crack tip. It is a scalar equation, as being derived from energy balance considerations, thus it cannot predict the trajectory of a crack. It must be supplemented by an additional dynamical law that will express the full vectorial nature of the propagation. To avoid this complication we consider a long straight crack under mode I loading conditions. In that case, it can be shown that

$$K_I\{t, ...\} = K_I(t, v = \dot{L}, L) \ , \tag{18.23}$$

where L is the crack length. Note that this is a non-trivial result; it claims that the stress intensity factor depends only on the local position and speed of the crack tip, but not on higher oredr time derivatives of the motion. In conjunction with Eqs. (18.21) and (18.22) we conclude that the crack tip equation of motion is a first order differential equation. This observation implies that the crack tip behaves as a massless particle that instantaneously adjusts its velocity to its length and loading conditions. Moreover, an explicit analysis of the equation of motion predicts that cracks accelerate smoothly to their limiting velocity that is bounded by the Rayleigh wave speed c_R, which is the speed in which waves propagate along a free surface. The typical stress field in the presence of a dynamic crack is shown in Fig. (3).

Is this prediction supported by experiments? Fig. (4) shows the velocity of a crack as a function of its length in a fracture experiment in PMMA. The figure shows explicitly that the crack speed saturates at a value much smaller than the theoretical prediction.

In order to understand better the failure of the theoretical prediction experimentalists scrutinized carefully the fracture process near the crack surfaces obtained

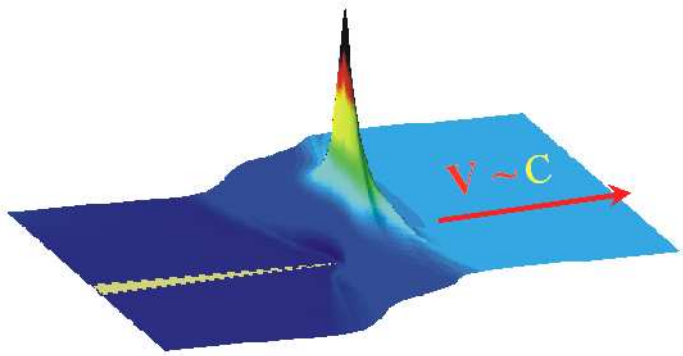

Figure 3: The typical stress field in the presence of a dynamic crack.

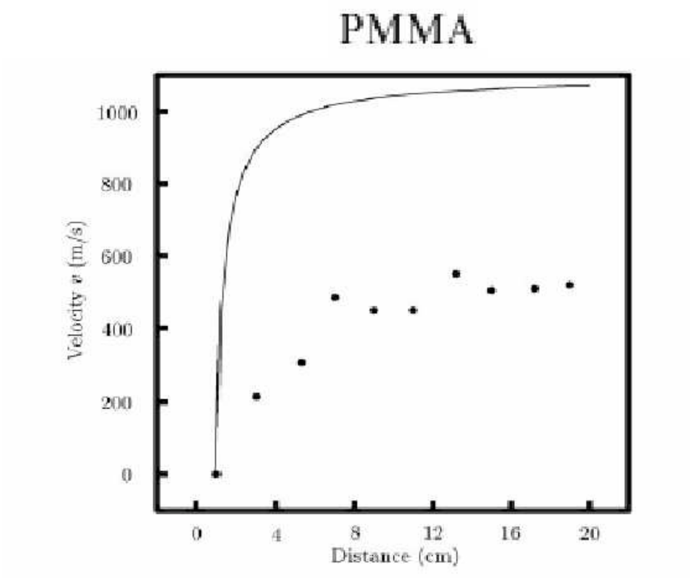

Figure 4: The velocity of a crack as a function of its length in fracture experiment in PMMA. It is seen explicitly that the crack speed saturates at a value much smaller than the theoretical prediction. Figure adapted from Fineberg and Marder (1999).

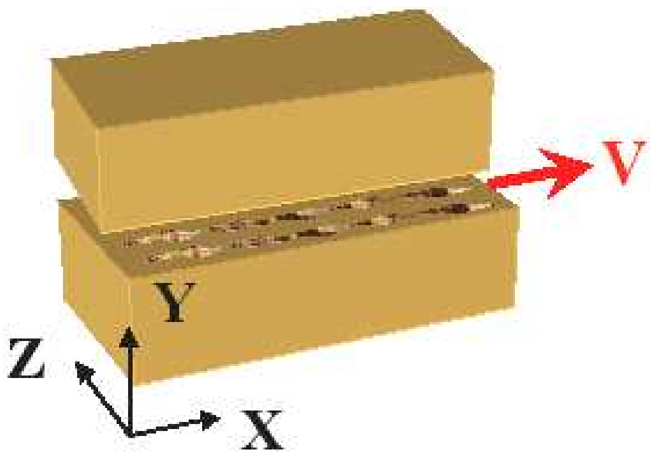

Figure 5: The typical geometry of a fracture experiment. x is the crack propagation direction, y is the direction of load application and z is the third direction.

in a typical fracture experiment depicted in Fig. (5).

The typical situation in the xy plane as a function of the velocity is shown in Fig. (6). It is observed that below a critical velocity v_c there is a single smooth crack and above v_c there is no single crack anymore, but an ensemble of cracks that emerged from the main crack accompany the propagation. These additional crack are called micro-sidebranches.

A similar picture can be obtained if one considers the surfaces of the crack. Fig. (7) shows the typical situation in the xz plane as a function of the crack tip velocity. It is observed that below a critical velocity v_c the crack surfaces are optically smooth while above v_c structure appear on the crack surfaces.

The full three-dimensional picture of the onset of micro-branching instability is shown in Fig. (8).

How this dynamic instability affects the crack velocity? As was explained earlier, when the a unit of crack advance releases more energy than is needed to create new free surfaces, the crack 'uses' the additional energy to accelerate its tip and thus to increase the kinetic energy of its surroundings. This is correct when the velocity is smaller than the critical velocity v_c. At v_c the physics changes qualitatively; instead of using the excess energy supplied to the crack tip for increasing the kinetic energy of the medium by acceleration, additional free surfaces are created per unit crack advance in the x-direction. At this stage of

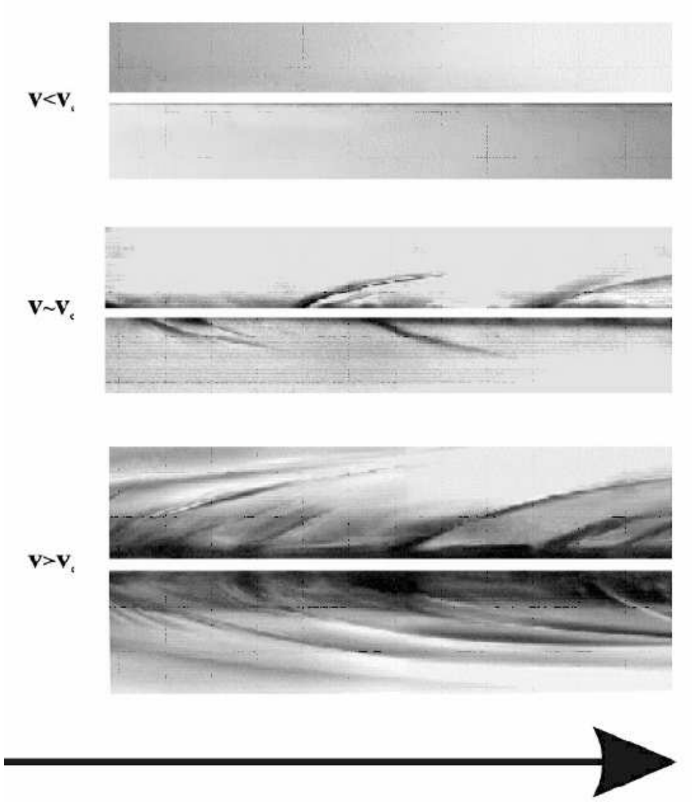

Figure 6: The typical situation in the xy plane as a function of the crack tip velocity. It is observed that below a critical velocity v_c there is a single smooth crack and above v_c there is no single crack anymore, but an ensemble of cracks that emerged from the main crack accompany the propagation. These additional crack are called micro-sidebranches. Figure adapted from Fineberg and Marder (1999).

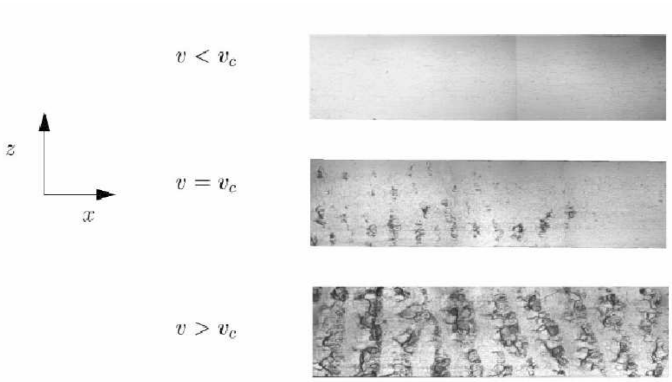

Figure 7: The typical situation in the $x - z$ plane as a function of the crack tip velocity. It is observed that below a critical velocity v_c the crack surfaces are optically smooth while above v_c structure appear on the crack surfaces. Figure adapted from Fineberg and Marder (1999).

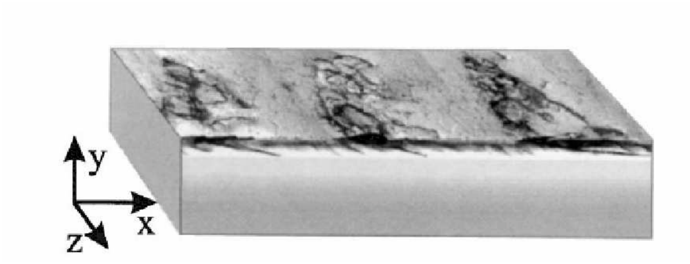

Figure 8: The full three-dimensional picture of the onset of micro-branching instability. Figure adapted from Fineberg and Marder (1999).

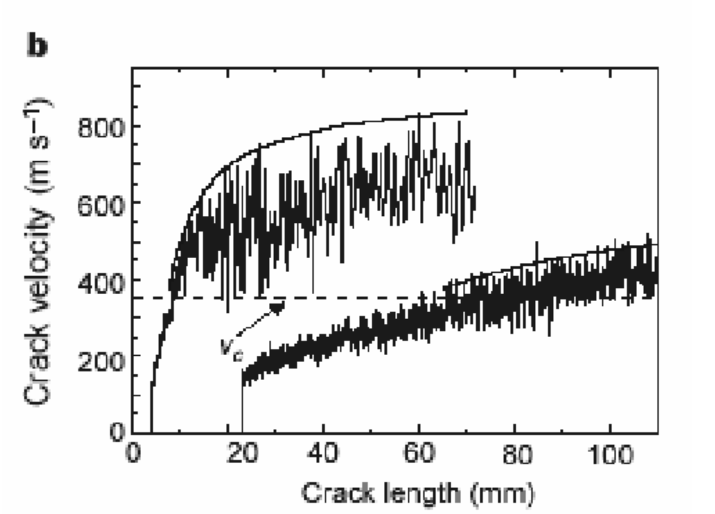

Figure 9: The velocity as a function of length for both glass and PMMA. The smooth envelope is the theoretical prediction. Figure adapted from Sharon and Fineberg (1999).

the dynamics, the assumption of a single straight crack breaks down!. In that case, the crack can even decelerate since now the higher energy dissipation due to the presence of sidebranches can support slower propagation. This is indeed the case, as shown in Fig. (9) showing the crack velocity as a function of the crack length for both glass and PMMA and compared with the theoretical prediction. It is observed that the crack tip velocity experiences strong fluctuations that were averaged out in the not detailed enough measurement shown in Fig. (4); there only the average value, that is much smaller than the predicted limiting velocity, is shown. Moreover, it was shown that the velocity fluctuations are perfectly correlated with the appearance of sidebranches. Indeed, the sidebranches formation results in crack tip deceleration.

Fig. (9) reveals another surprising aspect of the problem that is related to the theoretical crack tip equation of motion; there are isolated points where the velocity is identical to the theoretical prediction. These points correspond to instants where no sidebranches co-exist with the main crack and the assumptions of the theoretical equation of motion are restored. Since the crack tip has no inertia, it adjusts its velocity instantaneously according to the theoretical prediction. When a new sidebranch emerges, the velocity drops rapidly. In a sense, the theoretical prediction provides the envelope of the velocity dynamics.

A Short Bibliographic List

Here is a short bibliographic list of works cited in this lecture. Anyone who is interested in more references and guidance can contact me.

1. A. A. Griffith, Phil. Trans. Roy. Soc. (London) **A221**, 163 (1920).
2. L. D. Landau and E. M. Lifshitz, *Theory of Elasticity*, 3rd ed. (Pergamon, London, 1986).
3. L. B. Freund, *Dynamic Fracture Mechanics*, (Cambridge, 1998).
4. J. Fineberg and M. Marder, Phys. Rep. **313**, 1 (1999).
5. E. Sharon and J. Fineberg, Nature **397**, 333 (1999).